NIOZ - RAPPORT 1988 - 11

THE ECOSYSTEM OF THE WESTERN WADDEN SEA: FIELD RESEARCH AND MATHEMATICAL MODELLING

Nederlands Instituut voor Onderzoek der Zee

Ecologisch Onderzoek Noordzee en Waddenzee: EMOWAD II

Netherlands Institute for Sea Research
P.O. Box 59, 1790 AB Den Burg
Texel, The Netherlands

This is published as NIOZ - report 1988 - 11
This series was formerly called:
Interne Verslagen
Nederlands Instituut voor Onderzoek der Zee
Texel

cover design: H. Hobbelink

THE ECOSYSTEM OF THE WESTERN WADDEN SEA: FIELD RESEARCH AND MATHEMATICAL MODELLING

EON - projectgroep

This ecosystem research, which was carried out in 1984 - 1987, was commissioned by

the Ministry of Transport and Public Works,

the Ministry of Housing, Physical Planning and Environment,

the Ministry of Education and Science,

the Ministry of Agriculture and Fisheries.

NETHERLANDS INSTITUTE FOR SEA RESEARCH
ECOLOGICAL RESEARCH NORTH SEA AND WADDEN SEA

EMOWAD II
NIOZ - RAPPORT 1988 - 11

PREFACE

This report contains the results of the research project EMOWAD (Ecological Model Wadden Sea), which was carried out at the Netherlands Institute for Sea Research. Together with the Dutch report "Ecosysteemmodel van de westelijke Waddenzee" (NIOZ-rapport 1988-1) it constitutes the final report on the EMOWAD project. The aim of this project was to study the applicability to the western Dutch Wadden Sea of an ecosystem model developed by the same research group for the Ems estuary, published by Baretta & Ruardij (eds.) in a book entitled "Tidal Flat Estuaries. Simulation and analysis of the Ems Estuary" (Springer- Verlag, Berlin). First the existing biological submodels were combined with a new transport model which reflects the complex hydrography of this area. Differences between the western Wadden Sea and the Ems estuary made two major extensions of the model necessary. One was the modelling of the shallow subtidal regions and the second was the inclusion of nutrient regeneration. Furthermore, as the field data available at the Netherlands Institute for Sea Research had been collected over a long time in an ever-changing ecosystem, these data appeared to be incomplete and sometimes even inconsistent. Therefore, additional field and laboratory research was carried out in the period 1984-1987 to cope with the problems encountered during the construction of the model, including its validation. The papers in this report are partially based upon the modelling effort, and describe the scientific results of the field and laboratory research needed for modelling. The first article is a summary of the Dutch EMOWAD-I report.

The EMOWAD-project was part of the "Ecological Research Project North Sea and Wadden Sea" (EON), which was financed by four Dutch ministries and coordinated by the Ministry of Transport and Public Works.

The long-term purpose of the modelling effort is to create tools to help environmental managers in their decision-making. Although the present model still has several shortcomings, the first applications have demonstrated its usefulness.

The model formulation is available on microfiche from the Netherlands Institute for Sea Research.

H.J. Lindeboom.

ECOSYSTEM MODEL OF THE WESTERN WADDEN SEA

a summary

H.J. LINDEBOOM, W. VAN RAAPHORST, H. RIDDERINKHOF and H.W. VAN DER VEER
Netherlands Institute for Sea Research, P.O. Box 59, 1790 AB Den Burg, Texel, The Netherlands

1. INTRODUCTION

This article is a brief outline of the Dutch report "Ecosysteemmodel van de westelijke Waddenzee" (NIOZ rapport 1988-1), which together with the publications in this report forms the final report of the project "Ecological model research of the western Wadden Sea (EMOWAD)". The project, commissioned by four Dutch ministries, was carried out between 1984 and 1987 at the Netherlands Institute for Sea Research (NIOZ, Texel) and the department of Marine Biology at the State University of Groningen.

Two problems formed the central theme in the EMOWAD project: firstly the management of the Wadden Sea felt the need for an integration of the ecological studies which had been carried out in this area in the past; secondly, the managers felt that the existing knowledge was too inaccessible. Therefore, the aims of the project were the following:

— To gain insight into the structure and the functioning of the living communities in the western Wadden Sea, in order to get a qualitative and if possible quantitative description of the occurrence of and the connection between different groups of organisms in this ecosystem.

— To trace and describe the factors which on the one hand may lead to changes in the present structure and/or functioning of the ecosystem, and on the other hand can be influenced by human activity.

— To indicate on the basis of the knowledge described above to what extent specific human activities may influence the ecology of the western Wadden Sea.

These aims were to be achieved by putting to optimal use the knowledge on the area, collected by the NIOZ and by employing the knowledge and experience gained during the modelling research in the Ems-Dollard estuary (BARETTA & RUARDIJ, 1988).

Based upon this a mathematical ecosystem model was considered an important tool to meet the aims set above. The Ems-Dollard model was used as a basis for the EMOWAD-project, but some important changes were required: first, instead of a one-dimensional, a two-dimensional transport part of the model was needed; secondly, because of morphological differences, the model was expanded with a benthic and an epibenthic sublittoral part; and thirdly, nutrient regeneration (P and Si) was introduced into the model. In the different chapters of the EMOWAD I report, the successes and failures of these adaptations are described; applications of the model to management purposes are also given. The following sections summarize these chapters. This paper will be presented at the VIth International Wadden Sea Symposium on Sylt in October 1988.

2. ADJUSTMENTS AND EXTENSIONS TO THE ECOSYSTEM MODEL

The EMOWAD model is based on the ecosystem model which was originally developed for the Ems-Dollard estuary. An extensive discussion of the Ems-Dollard model has been given elsewhere (BARETTA & RUARDIJ, 1988). Therefore this chapter only summarizes the adjustments and extensions applied in converting this model to the western Dutch Wadden Sea.

The western Dutch Wadden Sea differs from the Ems-Dollard estuary mainly in that its geometry and morphology is more complex. An important morphological difference is that shallow subtidal regions cover more than 50 percent of the western Wadden Sea while the area of subtidal regions in the Ems-Dollard can be neglected. Furthermore, the benthic biomass in these subtidal areas forms a substantial part of the total biomass, so that a specific (epi)benthic submodel for this region has been included. Thus the EMOWAD model has a seperate submodel for simulating carbon flows in the (epi)benthic community of the subtidal. The structure of these new submodels is identical to the submodel for the (epi)benthic community on the tidal flats. Except for the benthic suspension feeders, the modelling of functional groups or state variables is also the same in both areas.

Another difference between the western Wadden Sea and the Ems-Dollard is the complexity of the geometry. The western Wadden Sea consists of two connected tidal basins and is therefore connected with the adjacent North Sea by two tidal inlets. Furthermore the channel systems in these basins are rather irregular and far from the "ideal" funnel shaped Ems-Dollard estuary. For these reasons the transport part of the model was made two-

dimensional. A direct consequence of this two-dimensionality is that parameters in this tidally averaged box-model cannot be computed from observed salinity distributions during stationary periods. A two-dimensional detailed hydrodynamical model (RIDDERINKHOF, 1988) has been used to determine these parameters, *e.g.* residual transports and exchange coefficients between the compartments of the EMOWAD model. Computations with the hydrodynamical model showed that there is a large-scale tidally driven residual flow through both basins, directed from the northern towards the southern inlet. For the EMOWAD model it has been assumed that the residual transport between these compartments is a combination of this tidally driven residual flow and the residual flow caused by the supply of fresh water from the IJsselmeer. Fig. 1 gives these total transports over a representative period.

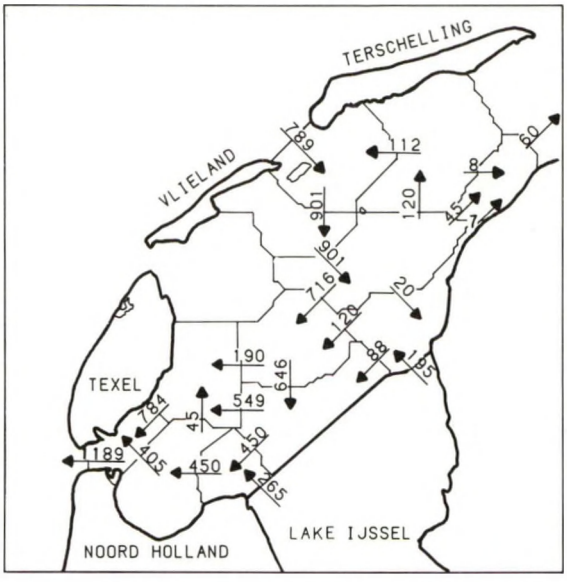

Fig. 1. Residual transport ($m^3 \cdot s^{-1}$) between the EMOWAD compartments during a period with a representative supply of fresh water from Lake IJssel.

Exchange coefficients, which are closely related to dispersion coefficients, have been determined by computing trajectories of watermasses in our detailed hydrodynamical model. The computed volume of water exchanged between adjacent compartments over a tidal period has been used for determining the different values of these parameters.

A general extension to the model is the explicit modelling of regeneration of Si and P. It has been assumed that the regeneration of Si is a relatively slow process which is only of importance in the benthic zone. Pelagic regeneration of P is simply modelled with a constant ratio between mineralised organic C and regenerated P.

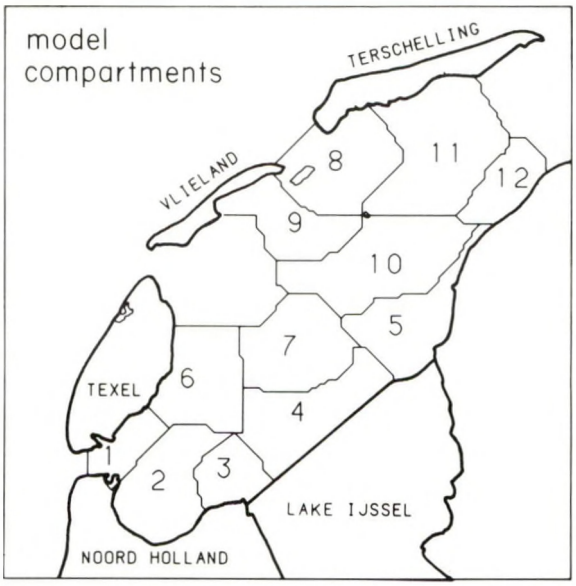

Fig. 2a. Model compartiments.

The formulation for benthic regeneration is based on the assumption of stationary chemical balances in the benthic anaerobic and aerobic layer. Expressions were derived for the flux of Si and P from the benthic to the pelagic zones. Some new state variables which are related to the explicit modelling of Si and P in the (an)aerobic layer(s) have been introduced. The value of parameters connected to this modelling of nutrient regeneration have been chosen such that fluxes of Si and P agree with reported measurements.

3. MODEL VALIDATION

A validation of the model has been performed by comparing the simulation results for 1986 with field-data of the same year. (For the calibration procedure simulations and data concerning 1979 and 1985 were used). For each variable to be evaluated three criteria were used for the validation. The first indicates whether the mean difference between the field data and the corresponding simulation points is acceptabel, *i.e.* when this difference is smaller than the mean value of the field data. The second criterion indicates to which extent the mean values of data and simulation points coincide, while the third gives information on the accuracy of the form of the simulation (seasonal pattern). The pelagic submodel was validated for 11 variables, usually in 7 compartments. For each variable the number of data-points per compartment ranged from 5 to 17. Examples are given in Figs 2 and 3 for Chl-a ($mg \cdot m^{-3}$) and the biological oxygen consumption, measured in 24 hrs incubation tests ($mg\ O_2 \cdot m^{-3}$). Based on all three criteria mentioned above, the Chl-a simulations are reasonable

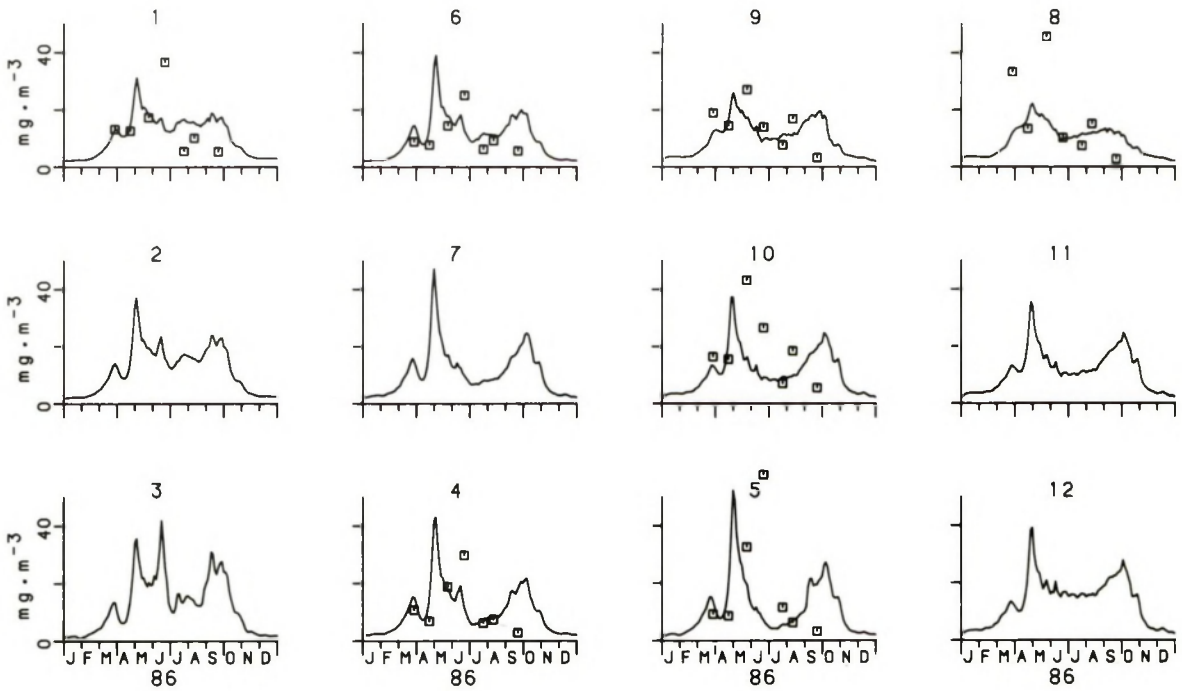

Fig. 2b. Chlorophyl-a concentrations ($mg \cdot m^{-3}$) according to the model simulations (———), and according to field data (□). The numbers refer to the different compartments (Fig. 2a).

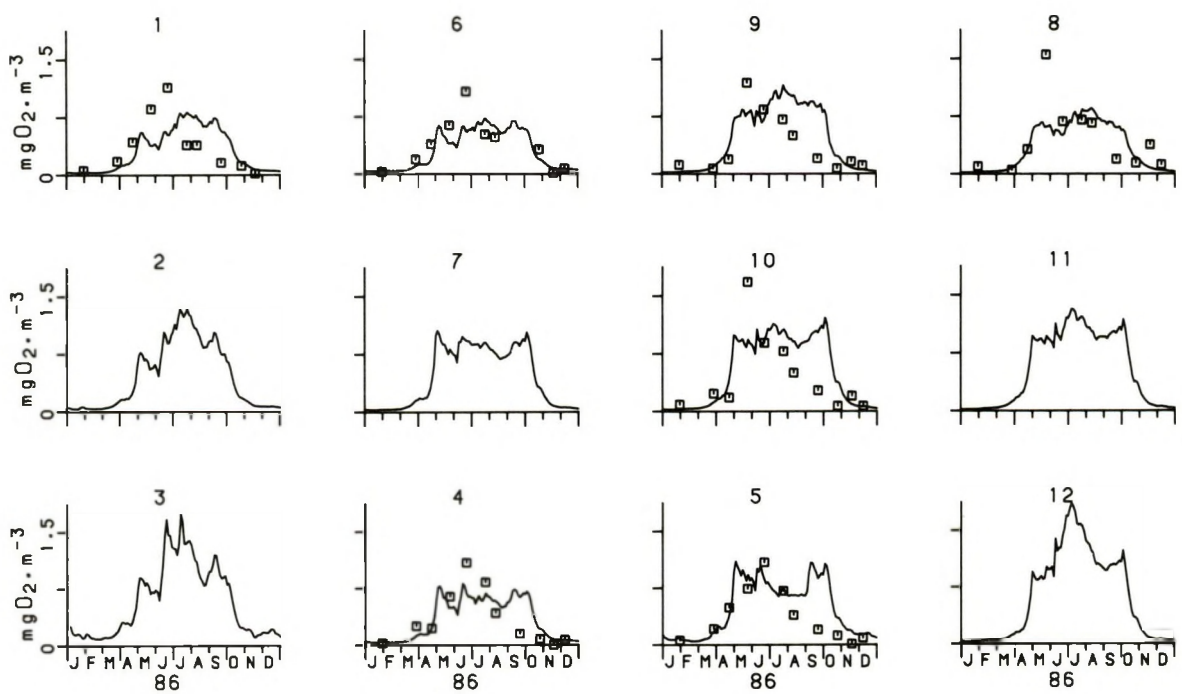

Fig. 3. Pelagic biological oxygen consumption integrated over 24 hrs ($mg \cdot O_2 \cdot m^{-3}$) according to the model simulations (———), and according to field data (□). The numbers refer to the different compartments (Fig. 2a).

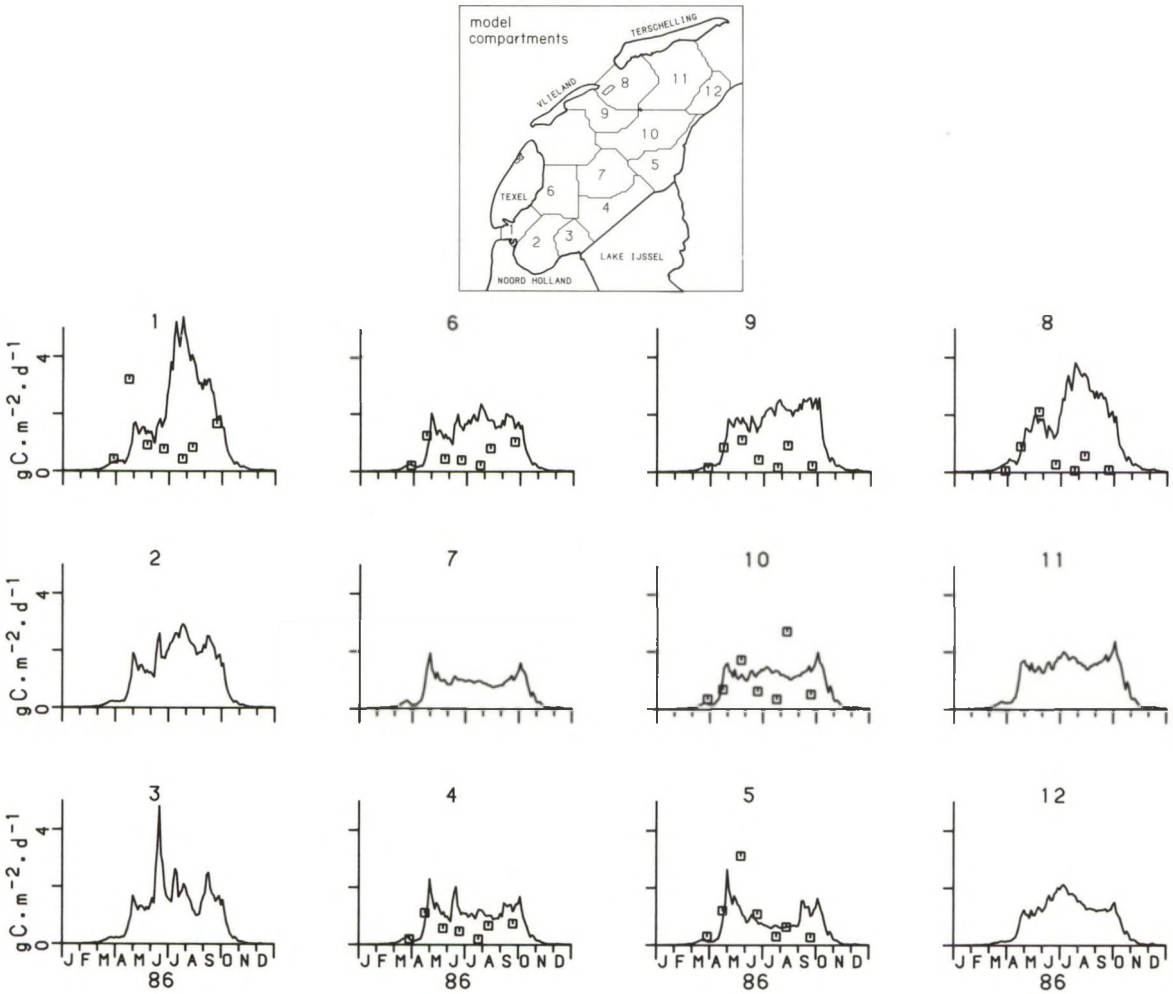

Fig. 4. Total pelagic primary production ($gC \cdot m^{-2} \cdot day^{-1}$) according to the model simulations (———), and according to field data (□).

for 2 compartments (6, 9) but for the others not very good, although the annual mean value of the simulation points is almost the same as that of the field data. The spring bloom is computed too early, while too high concentrations are simulated during the period June-September. On the other hand, the simulations of BOC1 fit the data points adequately. Only in late summer and autumn, oxygen consumptions are somewhat overestimated. The overall result of the validation of the pelagic submodel points to an adequate simulation of those components whose dynamics are largely determined by transport processes (*e.g.* phosphate, silicate). However, for almost all variables substantial discrepancies occur between field data and simulations during the second half of the summer-period. Most likely this is due to the absence of nitrogen components in the model, while there are indications that nitrogen is limiting primary production during the third quarter of the year. Most clearly this effect may be seen in the overestimation of the total pelagic primary production ($gC \cdot m^{-2} \cdot d^{-1}$; Fig. 4).

The benthic submodel is validated for 5 intertidal variables, but there were no field data at hand for the subtidal areas. The validation of this submodel is hampered by the low number of data. Actually only for 3 to 4 compartments, each having 2-6 data points, could the simulation results be evaluated. The total benthic community respiration on the tidal flats is simulated quite well, with typical maximum values of approximately 1 $gC \cdot m^{-2} \cdot day^{-1}$ in summer, and very low values in winter. The simulations of the higher trophic levels (meiofauna, macrobenthic deposit feeders and suspension feeders) do not agree well with the available field data. The reason for this is not very clear.

The submodel concerning the epibenthic processes and variables was validated for the biomass of the macro-epibenthos, for 7 compartments in the intertidal areas and for 5 compartments in the subtidal areas. The number of data points varied between 5 and 20 per compartment. The intertidal biomasses are simulated reasonably well, in some compartments quite well, in others poorly. The simulation of the subtidal macro-epibenthos does not agree with the field data; in all compartments the computed values are much too low. Actually, this is one of the results indicating that the model is not simulating the subtidal processes adequately.

To permit an evaluation of the overall modelling result, the organic carbon budget computed by the model has been compared with a budget obtained from literature data concerning external inputs, primary production, mineralization and sedimentation. It was not possible to estimate the carbon exchange of the western Wadden Sea with the North Sea directly. In the budget based on literature data, this transport term occurs as the closing entry. Consequently, this leads to a large level of uncertainty in the estimation of the transport via both tidal inlets. The conclusions based on the comparison of the two budgets are (Table 1):

1. The model computes a much larger pelagic primary production than the literature data suggest. On the other hand, the benthic primary production seems to be underestimated by the model;
2. According to the model, the pelagic mineralization is approximately 33% larger than the mineralization estimated from field data. The benthic mineralization, however, seems too small, most probably due to a strong underestimation of the carbon fluxes in the subtidal sediments;
3. Both budgets suggest a nett export of organic carbon from the estuary to the North Sea.

According to the budgets, there is a small difference between the total primary production and the total mineralization in the western Wadden Sea; external input and output seem to have a limited direct importance. In this view the model outcome agrees well with the literature data. The main discrepancies between the two budgets are the overestimation of the pelagic primary production, and the underestimation of the benthic mineralization. The absence of nitrogen as potentially limiting nutrient, and the disfunctioning of the model concerning the subtidal areas are most likely responsible for this lack of agreement. Future development of the EMOWAD model should therefore focus on these aspects.

4. MODEL APPLICATIONS

One of the goals of the EMOWAD project was to evaluate to what extent the effects of anthropogenic activities on the functioning of the ecosystem could be indicated with the EMOWAD model. However, it must be kept in mind that the model is not suited for an evaluation of all kind of activities. Its potential application is restricted to activities the model can deal with. Furthermore, all output generated by the model simulations is expressed in terms of energy, *i.e.* organic carbon, which means that only effects on the organic carbon fluxes in the system can be traced. For instance, effects on seal populations, pelagic fish and the accumulation of pollutants cannot yet be considered.

Although a wide range of anthropogenic activities occurs in the Wadden Sea, the examples chosen all deal with large-scale activities which are thought likely to interfere with the main processes. The anthropogenic activities discussed are:

1. Dredging activities;
2. Eutrophication;
3. Commercial mussel culture;
4. Oil spills.

Since the effects of changes in anthropogenic activities cannot be compared with actual field data, the model results are evaluated in an indirect way. For each anthropogenic activity a hypothesis is formulated about its impact upon the ecosystem.

TABLE 1

Organic carbon budget for the western Wadden Sea for 1986. All entries are expressed in 10^6 kg C. a: based on literature data, the transport to the north Sea is the closing entry; b: computed by the EMOWAD model, the term "rest" includes decrease in biomasses over the year, feeding by birds, etc.

Input and Production			*Export and Consumption*		
	a	b		a	b
Discharge L. IJssel	135 ± 5	133	Pelagic mineralization	270 ± 80	360
Pelagic pr. production	310 ± 95	483	Benthic mineralization	210 ± 95	129
Benthic pr. production	200 ± 100	54	Sedimentation	5 ± 5	31
Rest	-	16	Export to the North Sea	160 ± 185	166
Total	645 ± 135	686	Total	645 ± 135	686

Subsequently, the effects of different levels of the activity are simulated and the results are tested against the hypothesis. After a discussion of the effects of the 4 activities a general evaluation of the applicability of the EMOWAD model is made. Suggestions are formulated for further development of the model.

Dredging activities in the western Wadden Sea are sand extraction and spoil disposal of maintenance dredging of harbours and shipping channels throughout the area. Yearly about 3 million tons of sand (ANONYMOUS, 1981) are extracted and 1 million tons of spoil is disposed (VAN VEEN, 1988). Both activities affect the sediment load of the water, either by their overflow or by disposal of sediment, and as a result the turbidity of the water is increased, as was observed in the Ems-estuary (DE JONGE, 1983). This turbidity to a large extent determines the light penetration into the water column and hence the pelagic primary production. Since the relation between light penetration and turbidity is an inverse exponential one (DE WIT *et al.*, 1982), an increase in turbidity will result in only a slight decrease in the light penetration. On the other hand, a reduction in turbidity will have a much larger impact. These changes in light penetration might affect the primary production directly, but only during periods when light conditions are the limiting factor, *i.e.* in spring and autumn. During summer, when nutrient limitation is thought to occur, hardly any changes are expected. The results of the model simulations with a reduced and an increased sediment load of the water (normally between 25-80 $g \cdot m^{-3}$) (POSTMA, 1954; DE WIT *et al.*, 1982) show a good correspondence with the hypothesis (Fig. 5). Both the reduction and the increase in turbidity, (respectively to 0 and twice the natural concentration) affect the primary production but only in spring and autumn, *i.e.* the reduction in turbidity results in the largest changes. The maximum production during summer remains about the same in both cases.

Eutrophication of the western Wadden Sea occurs mainly by nutrient loadings originating from fresh water discharges of Lake IJssel. In the past these loadings increased considerably: for total P from 0.03 $kg \cdot sec^{-1}$ to about 0.16 $kg \cdot sec^{-1}$ and for total N from about 0.8 $kg \cdot sec^{-1}$ to about 2.3 $kg \cdot sec^{-1}$ (VAN DER VEER *et al.*, 1988). Some changes in the ecosystem have already been observed and suggestions have been made that they were the result of eutrophication, *e.g.*: locally low oxygen concentrations (TIJSSEN & VAN BENNEKOM, 1976 VAN DER VEER & BERGMAN, 1987), an increased bloom of the alga *Phaeocystis pouchetii* (CADÉE & HEGEMAN, 1986) and an increased biomass and recruitment of macrobenthic animals on the tidal flats (BEUKEMA & CADÉE, 1986). An overall analysis of the impact of eutrophication on the ecosystem is hampered by the fact that the model structure includes only P and Si and not N. Changes in nutrient loadings are thought to affect the primary production directly but only during periods of nutrient limitation, *i.e.* the summer period. Main effects are expected in case of a nutrient reduction, since this might prolong the period of nutrient limitation directly. An increase in the loadings will have less effect, since the period of limitation is restricted to 3-4 months in the present situation, and at high productions self-shadowing of the algae might become a feed-back mechanism. As a result of the changes in primary production, effects on the macrobenthic biomass might be expected. Since the loadings of P and N are largely in the form of organic compounds, a change in these discharges will also affect the input of organic matter. These changes are thought to be compensated for by alterations in the in- and export through the tidal inlets. The consequences of a reduced and an increased nutrient loading are illustrated in Fig. 6 for PO_4 and in Fig. 7 for the pelagic primary production. Effects on the PO_4 concentration in the Wadden Sea especially occur during the first month of the year.

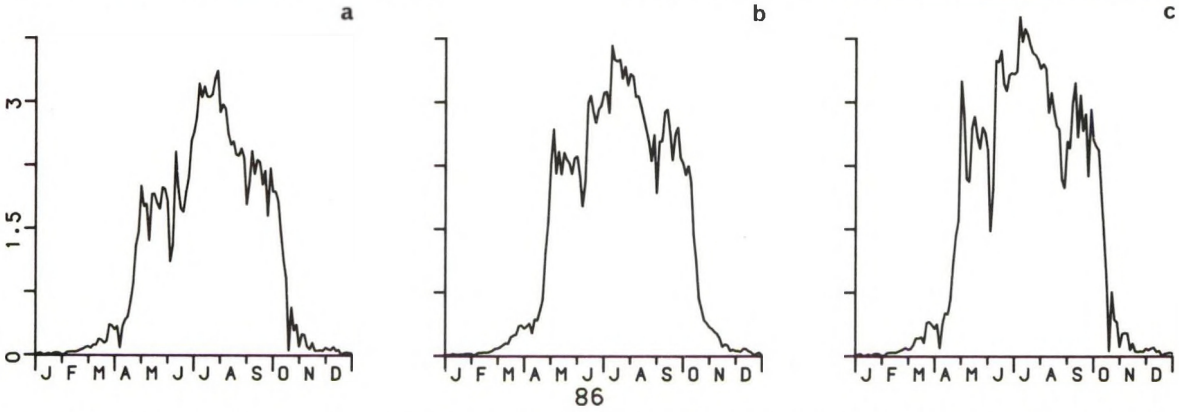

Fig. 5. Total pelagic primary production (10^6 kg C) according to the model simulations. a: reduced sediment load; b: standard situation; c: increased sediment load.

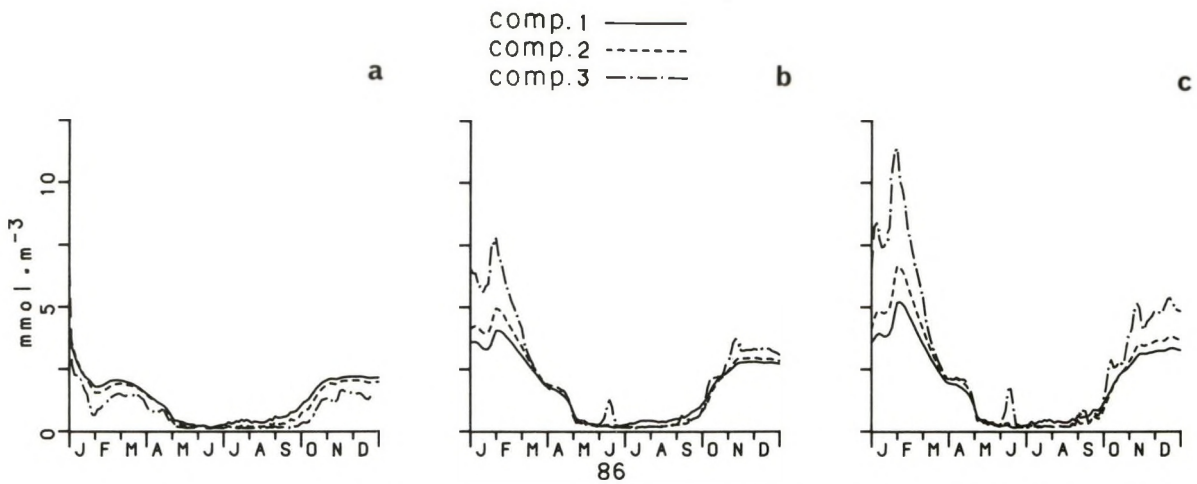

Fig. 6. Concentrations of dissolved reactive phosphate (mmol·m^{-3}) in the compartments 1, 2, 3 according to the model simulations. a: no discharge from Lake Ijssel; b: standard situation; c: discharges 1.5 times as large as in the standard situation.

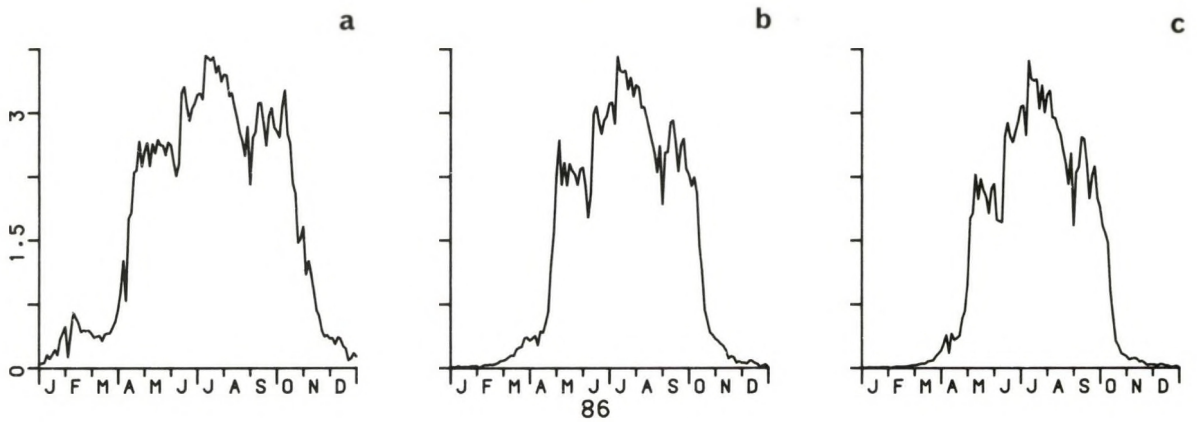

Fig. 7. Total pelagic primary production (10^6 kg C) simulated with a P and Si load from Lake IJssel equal to a: 0; b: the standard situation; c: 1.5 times as large as in the standard situation.

The impact on the primary production is visible especially between March and October, the period in which nutrient limitation might occur. Also effects on the benthic community can be observed; either a decrease or increase of macrobenthic animals (Fig. 8). The impact of eutrophication as simulated by the model seems to fit fairly well with the hypothesis formulated.

Mussel culture in the western Wadden Sea started in the 50s and rapidly increased to a commercial fishery with a yield of up to 100 million kg a year. Now mussel lots cover an area of about 80 km^2 distributed in the subtidal of the whole western Wadden Sea. The mussel *Mytilus edulis* is one of the dominant species in the subtidal of the Wadden Sea with a biomass of about 8 g AFDW·m^{-2} on mussel lots their biomass increases by a factor of 30-40 to about 260 g AFDW·m^{-2} (DEKKER, 1987).

At present, there is no insight in the impact of mussel culture on the ecosystem in the Wadden Sea. Recently VAN DER VEER (1988) postulated that under the assumption of a food limitation of the benthos in the Wadden Sea, the introduction of commercial mussel culture in the past might have resulted in a reduction of the other macrobenthic animals, especially at the tidal flat systems. In their present form, the model simulation result in a far too low macrobenthic biomass in the subtidal, compared with field data. Therefore, the impact of the mussel culture cannot be considered. An indirect approach for testing the hypothesis of VAN DER VEER (1988) is the introduction of extra biomass in the sublittoral and the analysis of the effects on the macrobenthic biomass in the intertidal zone. However, in the present model the sublittoral is functioning at too a low level. As a result the initial higher biomass values diminish to low levels again within a year (Fig. 9). Also the impact on the intertidal is too small to have

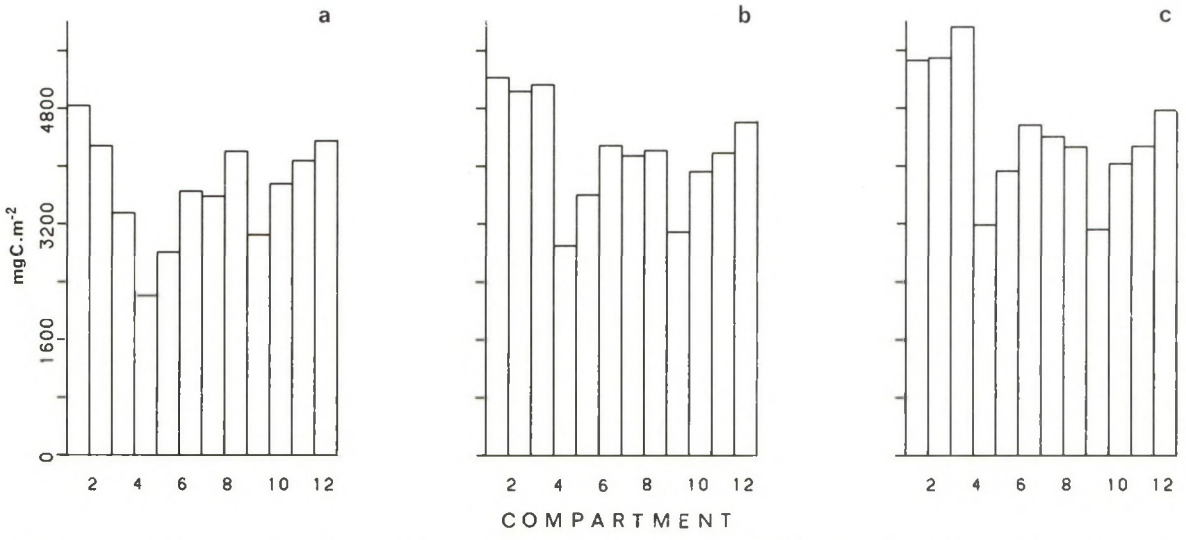

Fig. 8. Mean biomass of benthic suspension feeders in the intertidal ($mgC \cdot m^{-3}$) in the various compartments in April-September simulated with a P and Si load from Lake IJssel equal to a: 0 b: the standard situation; c: 1.5 times as large as in the standard situation.

any affect on the macrobenthos. Therefore the impact of mussel culture cannot adequately be evaluated at present.

Oil spills and other calamities in or near the Wadden Sea can result in a large-scale pollution of the area, especially of the benthic community in the intertidal. Since these macrobenthic animals are important as food source for wading birds (SMIT & WOLFF, 1983) and juvenile stages of commercially important fish species (ZIJLSTRA, 1972), such a calamity might have an enormous effect on the functioning of the area for fish and birds. In case of an elimination of the macrobenthic community, recolonization will occur either by new recruitment of juveniles or by immigration of adults. The time span necessary for recovery is thought to be fairly short, *i.e.* a few years (VAN DER VEER *et al.*, 1985). The exact initial response will depend on the time of occurrence, since recruitment is restricted to certain periods of the year. Therefore, the pattern of recolonization is examined for two situations: a reduction in January and one in May, during the period of recruitment. It is thought that in the latter case recolonization starts immediately, but at a lower rate due to the destruction of most animals during spawning. A reduction on 1 January results in fresh immigration before the period of recruitment and makes a larger recruitment possible. The above hypothesis is reflected in the model results, which in both situations show a recovery from May onwards. After a reduction on January 1, biomasses at first further decrease, following the natural seasonal pattern (Fig. 10). In both cases, recovery occurs within a

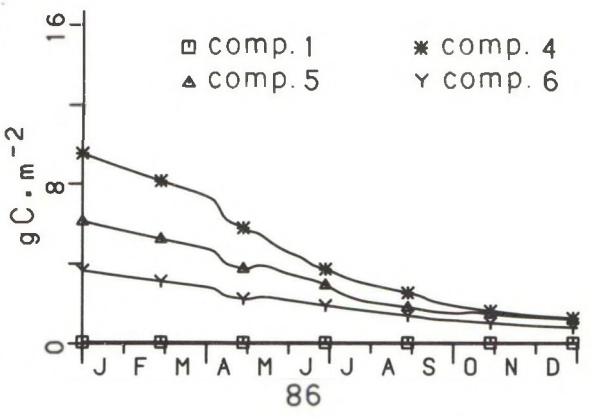

Fig. 9. Biomass of benthic suspension feeders in the subtidal ($gC \cdot m^{-2}$) in compartments 1, 4, 5 and 6 with increased initial values on Jan. 1.

year. Severe effects on the epibenthic predators are only observed after a reduction in May. These results fit fairly well with the expectations.

In conclusion it can be stated that the EMOWAD model in general is a useful tool in evaluating the impact of certain anthropogenic activities in the area. However, as soon as possible the functioning of the sublittoral part of the model should be improved and furthermore the model structure should be extended by an incorporation of the N cycle. Finally it must be kept in mind that the EMOWAD model, which gives a general description of the ecosystem, can never be applied to specific topics without exact definition of its specific processes.

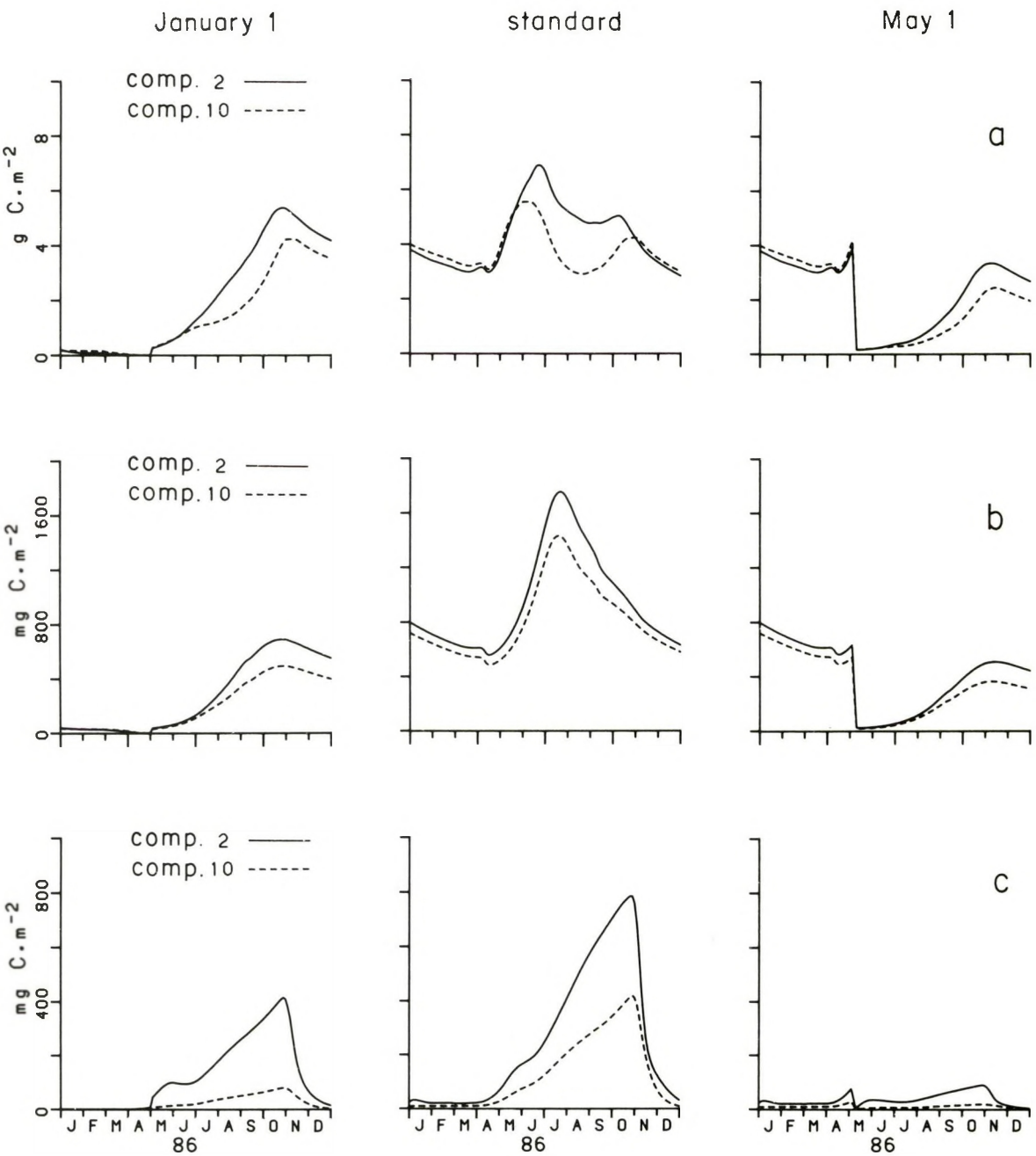

Fig. 10. Biomass in the intertidal in compartments 2 and 10 of A: benthic suspension feeders; B: benthic deposit feeders and C: epibenthic predators simulated with a reduction of the (epi)benthic system with 95% on Jan. 1 (left) and May 1 (right) compared with the standard model (middle).

5. CONCLUSIONS

The construction, validation and application of the EMOWAD model lead to the following conclusions:

— The use of a detailed hydrodynamical model in constructing the transport part of the ecological model gives good results.
— The model gives reasonable results for more than half of the variables validated.
— Probably due to the lack of a nitrogen module in the model, the pelagic primary production is overestimated. On the other hand, the benthic production is underestimated.
— The benthic and epibenthic system in the sublittoral functions insufficiently in the present model. However, a model version with higher food availability for benthic organisms in the sublittoral area shows an improvement.
— In principle the EMOWAD model is a useful tool in answering certain management questions.

Nevertheless, when further applications of the EMOWAD model are going to be made it is recommended to:

— Analyse the model formulation of the pelagic primary production, including limiting factors. When eutrophication problems are involved a nitrogen module should be constructed.
— Improve the functioning of the sublittoral model. Special attention should be paid to the possibility of including different amounts of mussel biomasses in different model runs in order to study the impact of these biomasses on the rest of the ecosystem.
— Create, in cooperation with the environmental management of the Wadden Sea, a discussion and working group around the model instrument to generate relevant management questions and to make the model more accessible to possible users. Because of the complexity of ecosystem models the latter can only be achieved by an active participation of the management in model building projects.

LITERATURE

ANONYMOUS, 1981. Zandwinning in de Waddenzee. Resultaten van een hydrografisch-sedimentologisch onderzoek. Werkgroep I. Rijkswaterstaat Directie Friesland, Leeuwarden: 1-48.

BARETTA, J.W. & P. RUARDIJ, 1988. Tidal flat estuaries (simulations and analysis of the Ems estuary). Springer Verlag Heidelberg, Ecological Studies, Vol. 71 (in press).

BEUKEMA, J.J. & G.C. CADÉE, 1986. Zoobenthos responses to eutrophication of the Dutch Wadden Sea.—Ophelia **26:** 55-64.

CADÉE, G.C. & J. HEGEMAN, 1986. Seasonal and annual variation in *Phaeocystis pouchetii* (Haptophyceae) in the westernmost inlet of the Wadden Sea during the 1973 to 1985 period.—Neth. J. Sea Res. **20:** 29-36.

DEKKER, R., 1987. The importance of the subtidal macrobenthos as food source for the Wadden Sea ecosystem. In: S. TONGAARD & S. ASBRIK. Proceedings of the 5th International Wadden Sea Symposium Esbjerg, Denmark Sept. 29th-Oct. 3, 1986. The National Forest and Nature Agency and The museum of Fishery and Shipping: 27-36.

EON-PROJECTGROEP, 1988. Ecosysteemmodel van de westelijke Waddenzee.—NIOZ-rapport 1988-1: 1-88.

JONGE, V.N. DE, 1983. Relations between yearly dredging activitities, suspended matter concentrations, and the development of the tidal regime in the Ems estuary.—Can. J. Fish. Aquat. Sci. **40:** 289- 300.

POSTMA, H., 1954. Hydrography of the Dutch Wadden Sea. Archs. néerl. Zool. **10:** 405-511.

RIDDERINKHOF, H., 1988. Tidal and residual flows in the western Dutch Wadden Sea. I. Numerical model results.—Neth. J. Sea Res. **22:** 1-21.

SMIT, C.J. & W.J. WOLFF, 1983. Birds of the Wadden Sea. Final report of the section Birds of the Wadden Sea Working Group. Report 6 of the Wadden Sea working Group. Balkema Press, Rotterdam: 1-308.

TIJSSEN, S.B. & A.J. VAN BENNEKOM, 1976. Lage zuurstofgehaltes in het water op het Balgzand. H_2O. **9:** 28-31.

VEEN, M. VAN, 1988. Inventarisatie baggeractiviteiten directie Friesland 1975-1987. Rijkswaterstaat Directie Friesland. Notitie ANW-8810.

VEER, H.W. VAN DER, 1988. Eutrophication and mussel culture in the western Dutch Wadden Sea: impact of the benthic ecosystem, a hypothesis. Proc. of the 6th International Wadden Sea Symposium Sylt, October 1988.

VEER, H.W. VAN DER & M.J.N. BERGMAN, 1987. Development of tidally related behaviour of a newly settled 0-group plaice (*Pleuronectes platessa*) population in the western Wadden Sea.—Mar. Ecol. Prog. Ser. **31:** 121-129.

VEER, H.W. VAN DER, M.J.N. BERGMAN & J.J. BEUKEMA, 1985. Dredging activities in the Dutch Wadden Sea: effects on macrobenthic infauna.—Neth. J. Sea Res. **19:** 183-190.

VEER, H.W. VAN DER, W. VAN RAAPHORST & M.J.N. BERGMAN, 1988. Eutrophication of the Dutch Wadden Sea: I. Nutrient loadings of the Marsdiep and Vliestroom basins. This report.

WIT, J.A.W. DE, F.M. SCHOTEL & L.E.J. BEKKERS, 1982. De waterkwaliteit van de Waddenzee 1971-1981. Rijkswaterstaat Rijksinstituut voor Zuivering van Afvalwater, Hoofdafdeling Oppervlaktewater Lelystad. Nota nr. 82065: 1-67.

ZIJLSTRA, J.J., 1972. On the importance of the Wadden Sea as a nursery area in relation to the conservation of the southern North Sea fishery resources.—Symp. zool. Soc. Lond. **29:** 233-258.

Netherlands Journal of Sea Research
22 (1): 1-21 (1988)

TIDAL AND RESIDUAL FLOWS IN THE WESTERN DUTCH WADDEN SEA I: NUMERICAL MODEL RESULTS*

H. RIDDERINKHOF

Netherlands Institute for Sea Research, P.O. Box 59, 1790 AB Den Burg, Texel, The Netherlands

ABSTRACT

A two-dimensional numerical model, which includes tidal basins in the western Dutch Wadden Sea and a part of the adjacent North Sea, is used to study tidal and tidally-driven residual flows and elevations. The model is verified by comparing observed and computed water elevations in some stations and transport rates through the tidal inlets. The consequence of topographical and geometrical differences for the terms in the governing equations is discussed by comparing the magnitude of these terms in some characteristic grid points, *viz.* the open sea, inlet and basin channel, in which all terms are decomposed along and perpendicular to the dominant current direction. Averaging over a tidal period shows that compared to the time-dependent equations an important shift takes place in the relative influence of the different terms, mainly caused by the increased influence of the advective term. The resulting tidally-driven residual flow field is interpreted as a combination of a constant volume transport (1 to 2% of the tidal transport in the tidal inlets) between connected tidal basins and isolated residual eddies (with velocities of 10 to 15% of the tidal velocity amplitude and a typical length scale of between 3 and 10 km). Observations confirm that the drop in residual elevations in tidal inlets and the rise in tidal basins are phenomena characteristic of all tidal basins.

1. INTRODUCTION

The western Dutch Wadden Sea consists of four more or less separated tidal basins drained by inlets between the islands. Global characteristics of tide and topography were described by POSTMA (1954) and ZIMMERMAN (1976) in their studies on the chemistry (POSTMA) and mixing processes (ZIMMERMAN) of this area. Observed salinity distributions and measurements of tidal velocities formed the basis of their studies on mixing time scales in the western Wadden Sea.

In the present study a detailed two-dimensional numerical model is used to study tidal and tidally-driven flows. In a later phase of the project the same numerical model will be used to study exchanges between the Wadden Sea and adjacent North Sea and mixing processes in the interior of the tidal basins. This first paper in a series presents the results of research on tidal and residual flows of the numerical model. In separate papers both the origin of the computed tidally-driven residual volume transport between two tidal basins and the isolated residual eddies will be discussed, as the residual current velocity field plays an important role in the displacement of dissolved matter.

Comparable modelling studies of tidal and/or residual flows in shallow seas and estuaries were performed by MADDOCK & PINGREE (1978), PRANDLE (1978), TEE (1976) and OEY *et al.* (1986). The present model is different in that its open boundaries are selected outside the sphere of influence of the tidal inlets. This makes it a model of large geographical coverage suitable for the study of internal tidally-driven residual volume transports between different basins.

Acknowledgements.—The author is much indebted to Rijkswaterstaat, Dienst Informatieverwerking, for the use of their computer

Publication no. 21 of the project "Ecological Reseach of the North Sea and Wadden Sea" (EON).

and the support in employing the extended system of computer programmes. The close cooperation with especially J. Dijkzeul of Rijkswaterstaat, Dienst Getijdewateren, was of great importance during the setting up and calibration of the numerical model.

2. NUMERICAL MODEL

2.1. INTRODUCTION

An extended system of computer programmes, the WAQUA system, developed and supported by the Dutch Ministry of Transport and Public Works, was used for two-dimensional simulation of tidal movements in the Wadden Sea. In the simulation programme the well-known shallow-water equations are solved numerically. These equations read:

$$\frac{\partial u}{\partial t} + u\frac{\partial u}{\partial x} + v\frac{\partial u}{\partial y} - fv =$$

$$= -g\frac{\partial \zeta}{\partial x} - g\frac{u\sqrt{(u^2+v^2)}}{C^2(H+\zeta)} + \nu\left(\frac{\partial^2 u}{\partial x^2} + \frac{\partial^2 u}{\partial y^2}\right) \quad (1)$$

$$\frac{\partial v}{\partial t} + u\frac{\partial v}{\partial x} + v\frac{\partial v}{\partial y} + fu =$$

$$= -g\frac{\partial \zeta}{\partial y} - g\frac{v\sqrt{(u^2+v^2)}}{C^2(H+\zeta)} + \nu\left(\frac{\partial^2 v}{\partial x^2} + \frac{\partial^2 v}{\partial y^2}\right) \quad (2)$$

$$\frac{\partial \zeta}{\partial t} + \frac{\partial (H+\zeta)u}{\partial x} + \frac{\partial (H+\zeta)v}{\partial y} = 0 \quad (3)$$

in which:

- u, v vertically averaged velocity components
- ζ water elevation relative to a reference plane
- H depth relative to a reference plane
- f coriolis parameter
- g acceleration of gravity
- ν horizontal eddy viscosity coefficient
- C bottom friction coefficient (Chezy coefficient)

These equations are solved numerically by employing a so-called ADI (Alternating Direction Implicit) method on a staggered grid. This method was developed by LEENDERTSE (1967) and has been applied successfully for tidal computations in several shallow seas and estuaries (LEENDERTSE *et al.*, 1981). STELLING (1984) recently revised the numerical approximations of the different terms in the shallow-water equations, changing the discretisations of the advective terms in the interior as well as along the boundaries into discretisations proved to be unconditionally stable. This version of the WAQUA system has been used for the computations discussed in this article. Earlier applications can be found in VOOGT, (1984) and KLATTER *et al.*, (1986).

2.2. MODEL DESCRIPTION

Boundary conditions for the small-scale model of the western Wadden Sea have been derived from a model which describes the tidal movement in the North Sea area to the north of the Wadden Sea (Fig. 1a). The latter model (grid size 3200 m) was constructed on the basis of data gathered during an extensive measurement campaign in May-June 1971 (STUDIEDIENST HOORN & DELFZIJL, 1973). During this campaign water-levels along the sea boundary were observed, from which boundary conditions were constructed for the 3200-m model. Filtering of the observed data showed that during the chosen simulation period (8 to 9 June 1971) the tidal water-levels along these boundaries could be described in three basic periodic bands (12.5, 6.25 and 4.16 h). The amplitude of the daily component, with a period of 25 h, was very small (less than 0.01 m) during these days. This simulation period, representative of average conditions during the neap-springtide cycle, was also chosen because of the simultaneous measurement of transport rates in the tidal inlets of the Wadden Sea basin. Furthermore, the influence of the wind could be neglected in this period (Dijkzeul, personal communication).

The aforementioned three basic periods are subsequently used in describing the water-levels along the open sea boundary of the smaller-scale model. The amplitude of the 12.5 h component increases from 0.67 m along the southern boundary to 0.90 m along the northern boundary, while the phase difference is about 4.0 h. The less important tidal components (overtides) with periods of 6.25 and 4.16 h are described with amplitudes of about 0.14 m and 0.08 m, respectively.

The location of the boundaries in the smaller-scale model (grid size 500 m), together with some

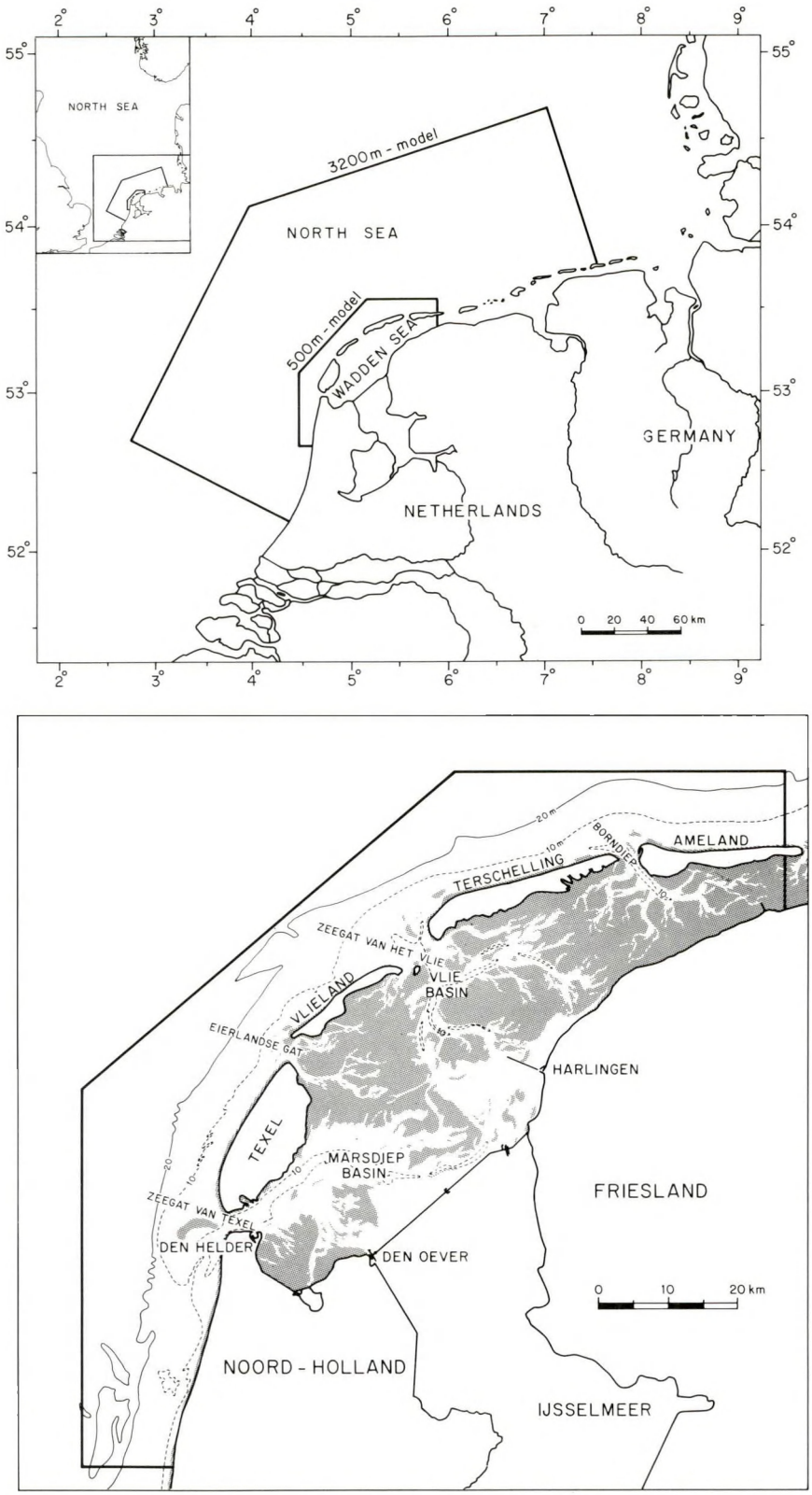

Fig. 1. (a) Location of the boundaries of the models with 3200 m and 500 m grid size. Results of the 500 m model are discussed in this article.

(b) Map showing the boundaries and some isobaths (10 m, 20 m) of the 500 m model. Shaded areas represent tidal flats.

isobaths is shown in more detail in an overall picture of the model area in Fig. 1b. The open boundaries at which water-levels are prescribed from the larger-scale model lie about 15 km off the coast, where the the inflow and outflow through the inlets between the islands have a negligible influence on the tidal movement. The north-eastern boundary between the island of Ameland and the mainland coincides with a tidal flat that separates two tidal basins. In the model this boundary has been schematized as a closed boundary.

The isobaths in Fig. 1b clearly show that the model area of the Wadden Sea is composed of four tidal basins drained by the inlets between the islands. Each of these basins can be subdivided into tidal channels and tidal flats, of which the latter are emersed during part of the tidal cycle. Most of these tidal flats form a separation between adjacent basins. An open connection exists only between the two major basins, the Marsdiep basin in the south, drained through the Zeegat van Texel, and the Vlie basin in the middle, drained through the Zeegat van het Vlie.

2.3. MODEL RESULTS

When a grid size of 500 m is used to schematize the area, sufficient resolution of the bottom topography is only expected for the larger tidal channels. Especially in the parts of the model where the water enters and leaves the tidal flats by way of narrow gullies, this grid size is too coarse to simulate the tidal movements in detail. So, although special procedures can simulate the emersion of tidal flats, no locally meaningful results in these areas can be expected. The main function of the tidal flats in this model is their capacity to store water. Model results are only compared with prototype measurements insensitive to such small-scale variations in bottom topography as volume transports through the deeper channels and water elevations along such channels.

Calibration of the model has been achieved by comparing observed and computed water-levels in different computations in which the bottom friction coefficient, being an important, but not well-known parameter, has been varied. Sufficiently accurate results were achieved by varying the Chezy coefficient, computed via the depth-dependent Manning's formulation,

$$C = \frac{1}{n} H^{\frac{1}{6}}$$

in which $n = 0.023$, from about 40 $m^{0.5}s^{-1}$ on tidal flats to 75 $m^{0.5}s^{-1}$ in the deeper channels. The less important coefficient for horizontal eddy viscosity, ν, is used to parametrize the lateral exchange of momentum on subgrid scale. The chosen value, $\nu = 7$ m^2s^{-1}, is based on modelling experience in the Eastern Scheldt (LEENDERTSE, 1984). The order of magnitude of this value is in agreement with dimensions and velocities of turbulent eddies observed in the Zeegat van Texel (VETH & ZIMMERMAN, 1981). This parameter has not been varied because the lateral stress term is only of minor importance to the computed volume transports and water-levels. Results of a sensitivity analysis for the parameter ν will be discussed in a subsequent paper, whose main subject will be the generation and dissipation of tidal and residual eddies.

In Figs 3a to d computed and observed water-levels are compared in some of the stations used for calibration (see Fig. 2 for their location). These Figs show that the agreement between the two is fairly good. The amplitude amplification and phase difference between the water elevation at the inlet (Den Helder, Fig. 3a) and the landward end of the Marsdiep basin (Harlingen, Fig. 3c) show that the tidal wave in the Wadden Sea can be seen as a combination of a standing and a propagating wave. This combined character stems from the relatively strong bottom friction in the tidal basin, which reduces the energy in

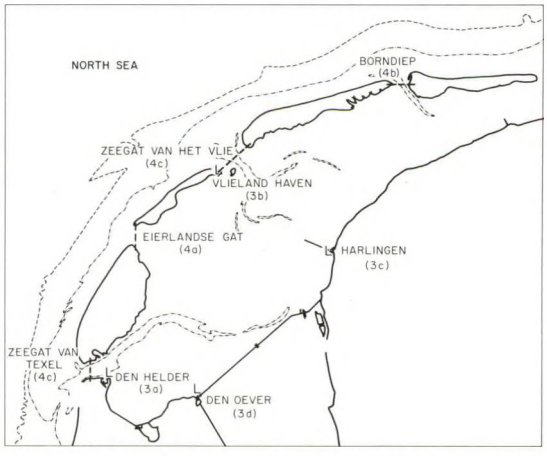

Fig. 2. Position of water-level stations (L) and transport crossections (----) used for calibration of the 500 m model.

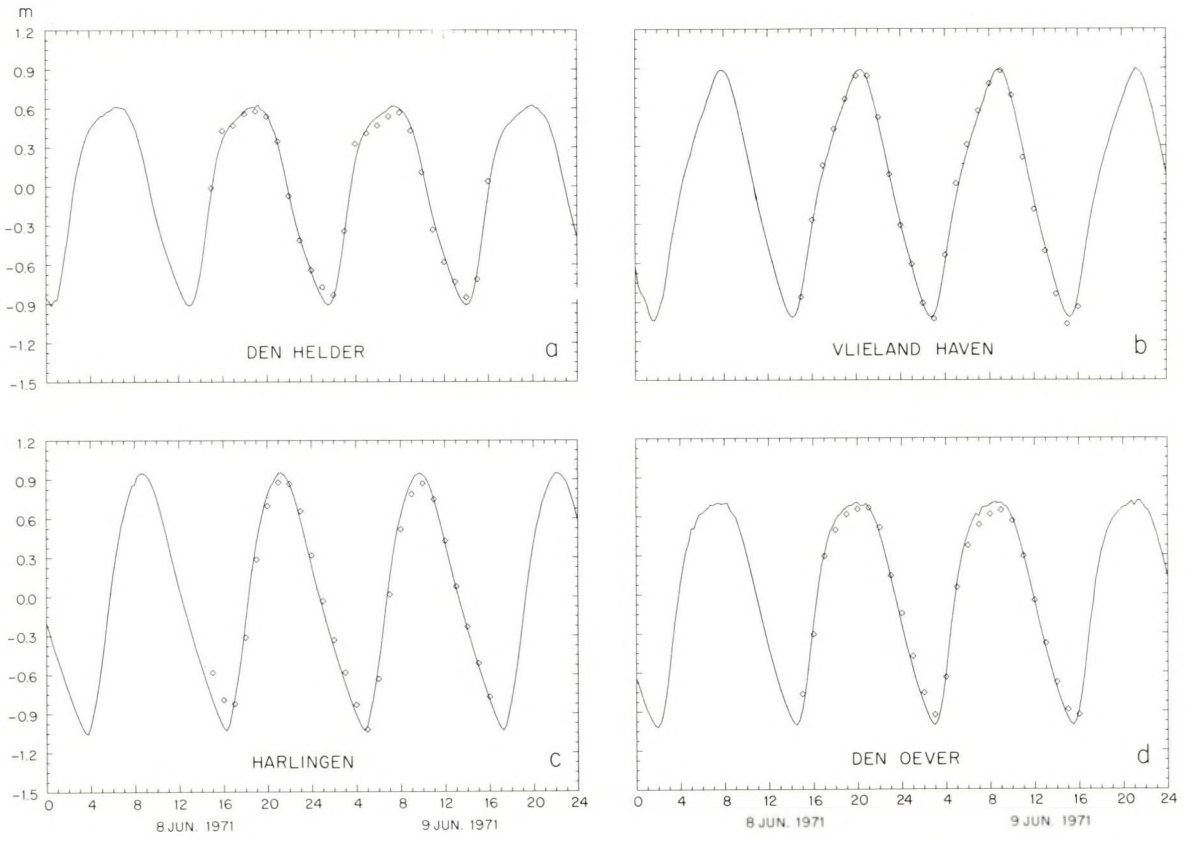

Fig. 3. Comparison of computed (——) and observed (□ □) water-levels. a) Den Helder; b) Vlieland Haven; c) Harlingen; d) Den Oever.

the incoming and reflected tidal wave. By this the amplitude of the reflected wave is very small near the tidal inlet. In this area the tidal wave can be characterized as a propagating wave, reflected in the phase difference between Figs 3a and c, while at the landward end near Harlingen it can be characterized as a standing wave. Figs 4a to d show a validation of the transport rates through the tidal inlets measured during the extensive campaign in 1971 (STUDIEDIENST HOORN & DELFZIJL, 1973). The differences in the dimensions of the tidal basins are clearly reflected in the amplitude of these transport rates. For the smaller inlets, Eierlandse Gat (Fig. 4a) and Borndiep (Fig. 4b), deviations can be recognized between observations and computations which can be explained by the use of rather too coarse a grid. For the greater part, these two basins are covered with tidal flats, poorly presented in the model, which causes perturbations in the transport rates. Model results and observations of the major inlets, the Zeegat van het Vlie (Fig. 4c), which drains the Vlie basin, and the Zeegat van Texel (Fig. 4d), which drains the Marsdiep basin, show that the tidal transport amplitudes through these inlets are nearly equal. The slightly better agreement of the transport rates through the Zeegat van Texel than of those of the Zeegat van het Vlie stems from the morphological differences between the two basins, the percentage of the tidal flats in the Vlie basin (40%) being much larger than in the Marsdiep basin (17%). However, small deviations can also be ascribed to the inaccuracy of the measurements.

Fig. 5 gives the two-dimensional velocity field in every fourth grid point one hour before the time of low water in Harlingen, near the landward end of the Marsdiep and Vlie basins. The 0.50 ms^{-1} velocity isoline indicates the location of the main basin channels. The dotted points are the grid points taken out of the computations as tidal flats are emerging at that moment. Such maps were compared with measurements of the

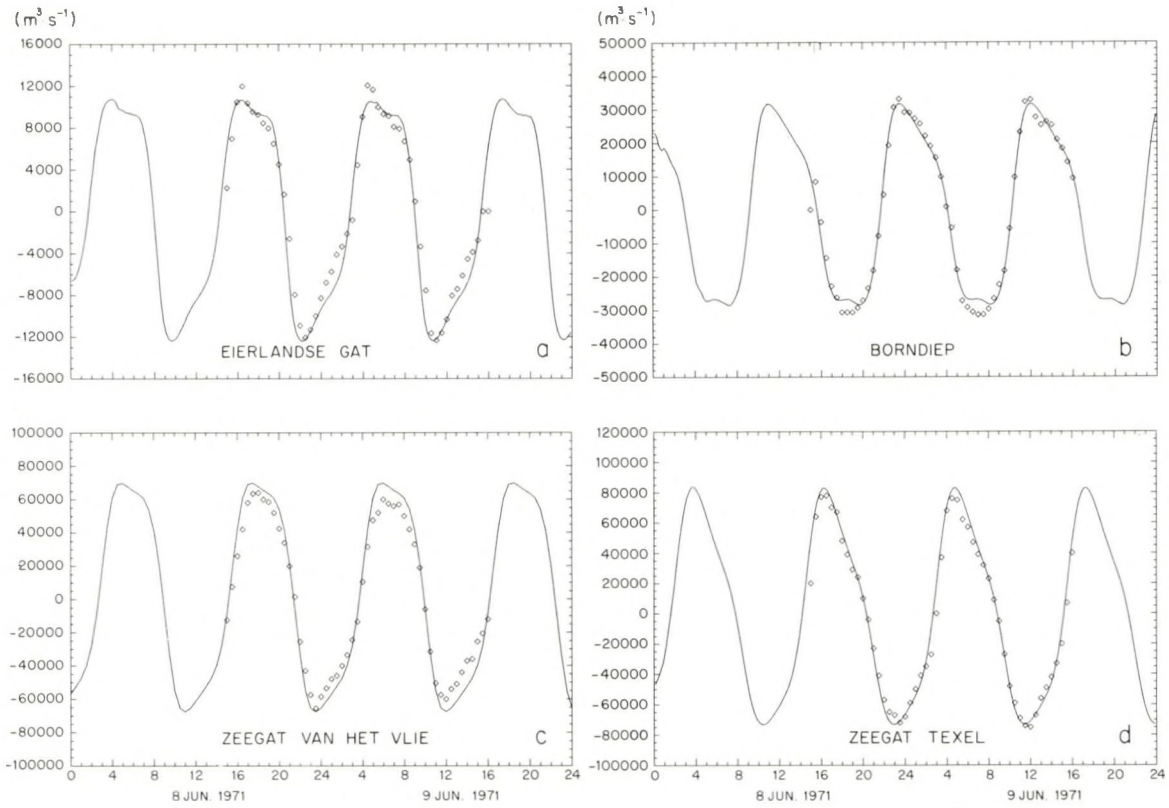

Fig. 4. Comparison of computed (——) and observed (□ □) transport rates through the inlets. a) Eierlandse Gat (between Texel and Vlieland); b) Borndiep (between Ameland and Terschelling); c) Zeegat van Vlie (between Vlieland and Terschelling); d) Zeegat van Texel (between Texel and the mainland).

global current velocity field and the location of emersed tidal flats (DE BOER *et al.*, 1984) to verify the large-scale results of the computations. A reasonable simulation of the emersion of the tidal flats was only to be achieved by excluding from the computations the grid points for which the water depth was less than 0.15 m. By this, an extreme growth of bottom friction term was prevented.

A plot showing the velocity vectors in every grid point at slack water before flood in a part of the model area near the Zeegat van Texel is given in Fig. 6. This map, in which the 5-m isobath is also indicated, demonstrates that a phenomenon like the time lag between the reversal of the tide in shallow and deeper parts of the basin is well simulated by the model.

2.4. INFLUENCE OF DIFFERENT TERMS IN THE TIDAL MOMENTUM EQUATIONS

The results of the numerical computations with the WAQUA programme, matrices of water-levels (ζ) and velocities (u, v) in staggered grid points, could only be stored at intervals of 30 min. due to limited storage facilities. These matrices have been used to compute the magnitude of the different terms in momentum equation. Although the same spatial differences were applied, the computed magnitude of these terms slightly differs from the magnitude in the numerical simulation. In the numerical simulation a time step is split up into two stages in which variables from different time levels are used by employing alternate implicit and explicit schemes (ADI method, STELLING, 1984), while in this section, as well as in section 3.4, all spatial differences are computed with variables (ζ, u, v) from the same time level. The difference hereby introduced is small and can be neglected. Furthermore, the consequence of a staggered grid is that water-levels, velocities and computed terms in the momentum equation are defined at different locations in one grid unit. Defining m as the position of the grid

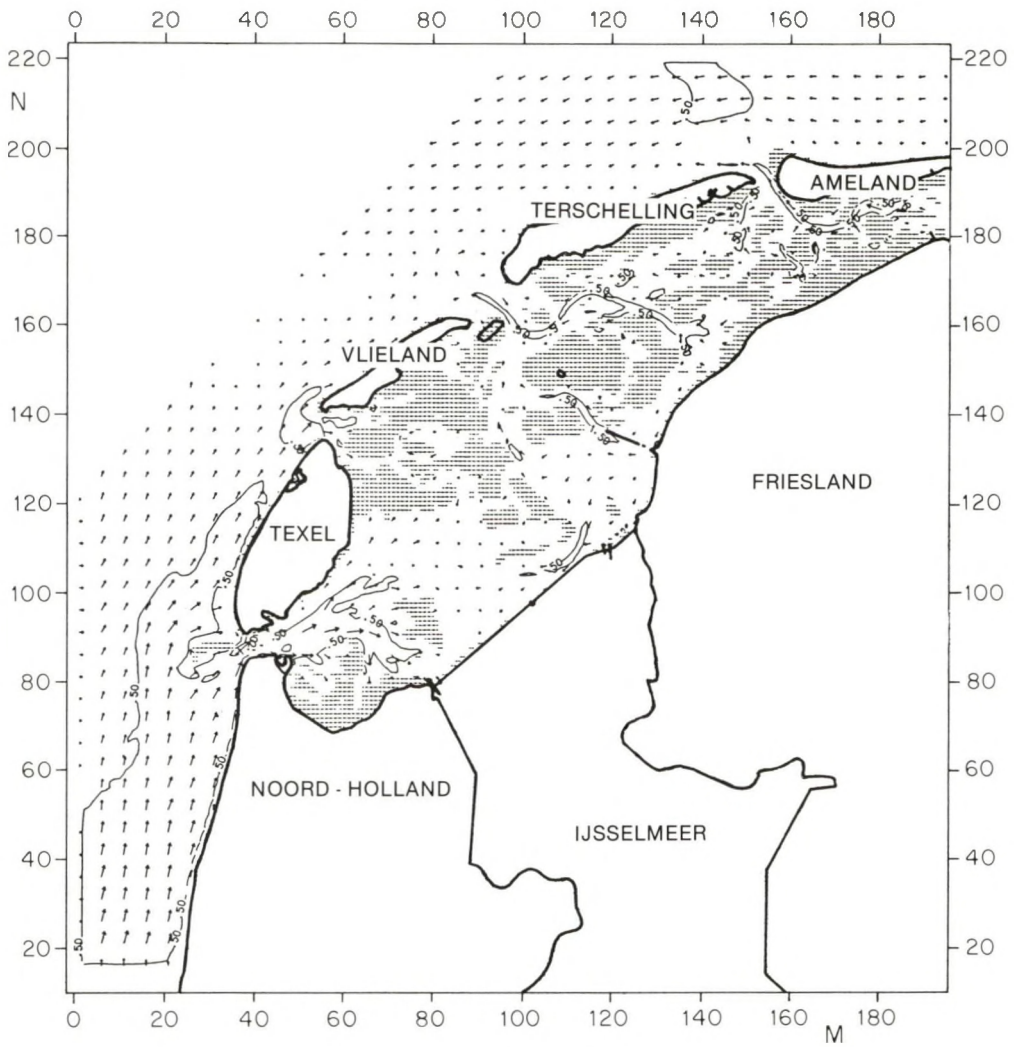

Fig. 5. Map of the two-dimensional velocity field in every fourth grid point one hour before the time of low water at Harlingen. The 0.50 ms^{-1} velocity isoline has been indicated, dotted points represent areas falling dry according the numerical model.

unit along the X-axis and *n* along the Y-axis, the water-levels are located at the integer values *m*, *n*, while the velocity variables and the terms in the momentum equation are located between the water-level points, in x-direction at $m + ½,n$ and in y-direction at $m,n + ½$. The magnitude and direction of a term in the momentum equation is therefore not known at one single position, which in principle prohibits a decomposition of these terms in an arbitrary direction. To enlighten the discussion in this section all terms and velocities are linearly interpolated towards the central water-level grid point (m,n) to be able to decompose these terms parallel and perpendicular to the local streamline:

$$X_{m,n} = ½(X_{m+½,n} + X_{m-½,n}) \quad (4)$$

$$Y_{m,n} = ½(Y_{m,n+½} + Y_{m,n-½}) \quad (5)$$

in which *X* and *Y* are velocities or terms in the x- and y-direction in the governing equations.

Fig. 7 shows isobaths in a part of the model near the Zeegat van het Vlie. This part encloses three different areas that are typical of the complete model and can be distinguished by their

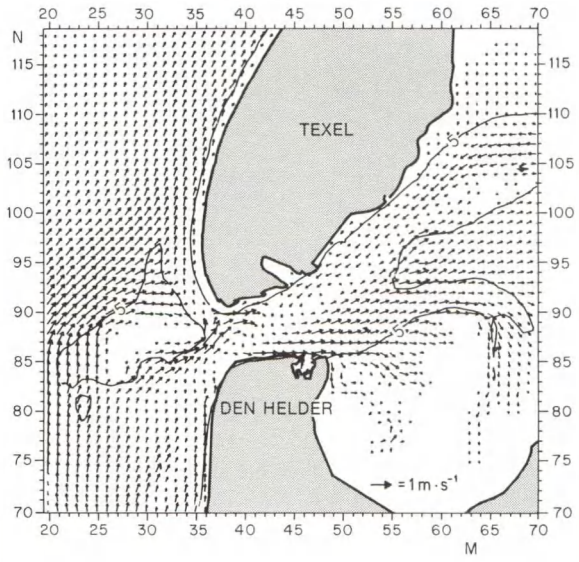

Fig. 6. Tidal velocities near the Zeegat van Texel at slack water, before flood, 1.5 hours after the time of low water at Den Helder, together with the 5 m isobath.

morphological properties: the open sea, the tidal inlet and the channels in the basin. The consequences of the topographical and geometrical differences for the magnitude of the different terms are discussed in detail for three characteristic grid points indicated in Fig. 7,

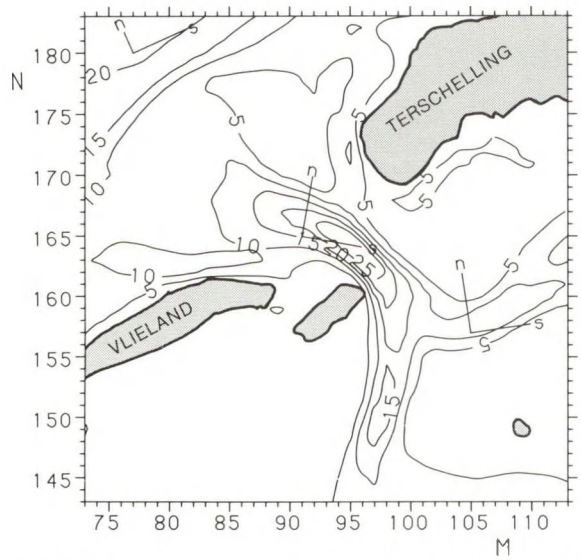

Fig. 7. Isobaths in a part of the model near the Zeegat van het Vlie (interval 5 m). The location of the characteristic grid points is given together with the local axes parallel (s) and perpendicular (n) to the dominant streamline.

while at two points of time during ebb and flood the magnitude of the most important terms are shown for the whole area of Fig. 7. First the dominant flow direction in the three characteristic model points has been determined by employing equation (6), which gives the angle between the dominant streamline and the x-axis:

$$\tan \varphi = \sum_{t=1}^{25} \left(\frac{v(t)}{u(t)} \right) \tag{6}$$

in which $(u(t), v(t))$ is the time-dependent velocity vector (the sign of both velocity components is reversed for negative $u(t)$) and φ is the angle between the x-axis and the dominant streamline. In the following the local s-axis is defined parallel and the n-axis perpendicular to that streamline in each grid point. For the chosen characteristic grid points both axes are indicated in Fig. 7. It clearly shows that the tidal current approximately flows along the local isobath.

In vector form the governing momentum equation reads:

$$\underset{\text{(a)}}{\frac{\partial \vec{u}}{\partial t}} + \underset{\text{(b)}}{\vec{u} \cdot \nabla \vec{u}} + \underset{\text{(c)}}{f(\vec{j} \times \vec{u})} + \underset{\text{(d)}}{g \nabla \zeta} + \underset{\text{(e)}}{\frac{g\vec{u}|\vec{u}|}{C^2(H+\zeta)}} - \underset{\text{(f)}}{\nu \nabla^2 \vec{u}} = \underset{\text{(g)}}{0} \tag{7}$$

where $\vec{j}$ is the vertical unit vector. Fig. 8 gives the average magnitude of the terms in equation (7) in the chosen grid points during the flood (solid lines) and ebb period (dashed lines). The sign of the velocity component in the local s-direction was used to separate the tidal cycle in a flood and ebb period. The average error caused by the approximations discussed above is indicated by a summation of all terms in equation (7). The magnitude of this error is also given in Fig. 8 ("term (g)") and appears to be negligible for the discussion in this section.

In general, Fig. 8 shows that the magnitude of all terms in grid point (79,180), in the open sea, is less than in both other grid points (note the different scales). Furthermore, advective terms (b) have a minor influence in this grid point. In both directions and in all grid points the relative influence of the viscosity term (f) is negligible.

The non-linear advective term (b) plays an important role in the grid points (91,165) and (105,157), especially in the direction perpen-

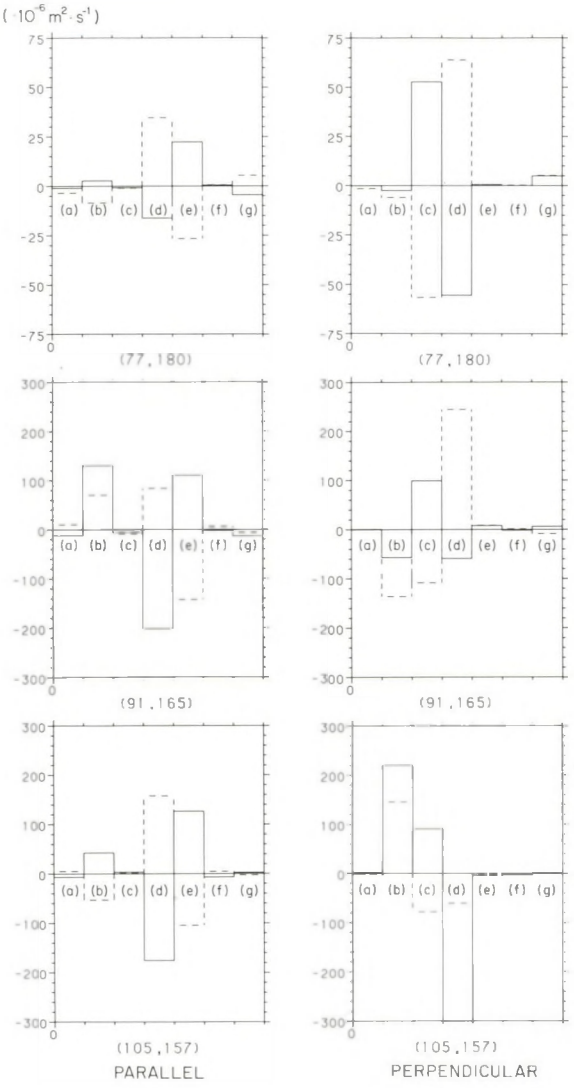

Fig. 8. Averaged magnitude of the terms (10^{-6}ms^{-2}) in equation (7) parallel (left-hand side) and perpendicular (right-hand side) to the dominant streamline in the characteristic grid points during the flood (solid) and ebb period (dashed).

dicular to the dominant streamline. LORENTZ (1926) showed that this term can be decomposed in a "Bernoulli acceleration" parallel and a "centrifugal acceleration" perpendicular to the local streamline:

$$(\vec{u} \cdot \nabla \vec{u})_s = \tfrac{1}{2} \frac{\partial}{\partial s} (u^2_s) \qquad \text{(s-direction)}$$

$$(\vec{u} \cdot \nabla \vec{u})_n = u_s \frac{\partial}{\partial s} (u_n) = \frac{u^2_s}{r} \qquad \text{(n-direction)} \qquad (8)$$

in which u_s and u_n are the velocity components in the local s-and n-direction and r is the radius of the local streamline. Such a decomposition shows that curves in the geometry of the coast and basin channels strongly influence the magnitude and direction of the centrifugal acceleration. This strong dependence on the local curvature of a streamline results in a large spatial variability in the magnitude as well as the direction in which this term acts. In the grid points in the tidal inlet and the channel the magnitude of the centrifugal acceleration about equals the coriolis acceleration while its sign does not differ between the ebb and flood periods. The consequence is that due to the rotation of the earth the magnitude of the counterbalancing water-level gradient perpendicular to the local streamline differs substantially between the ebb and flood periods.

The left-hand side of Fig. 8 shows that parallel to a streamline the bottom friction term (e) primarily balances the forcing water level gradient term (d). The advective term (b), interpreted as a Bernoulli acceleration in this direction and, together with term (d), forming the dynamic pressure gradient, plays a minor role compared to the role of the centrifugal acceleration in the n-direction. Spatial accelerations along a streamline, mainly caused by an increase/decrease in the channel cross section, determine the magnitude and relative influence of the Bernoulli term. This term has most influence at the tidal inlet grid point where the gradient in the magnitude of the flow cross section is relative large.

Term (a) in eq. 5 can be neglected at the ebb and flood phases when the tidal current reaches its maximum value. In a first approximation the governing momentum equation parallel and perpendicular to the local streamline then yields:

$$u_s \frac{\partial u_s}{\partial s} + g \frac{\partial \zeta}{\partial s} + \frac{g\, u_s |\vec{u}|}{C^2(H+\zeta)} = 0 \qquad \text{(s-direction)}$$

(b) (d) (e) (9)

$$\frac{u^2_s}{r} + f\, u_s + g \frac{\partial \zeta}{\partial n} = 0 \qquad \text{(n-direction)}$$

(b) (c) (d) (10)

At both tidal phases the spatial distribution of these terms in the area shown in Fig. 7 is given

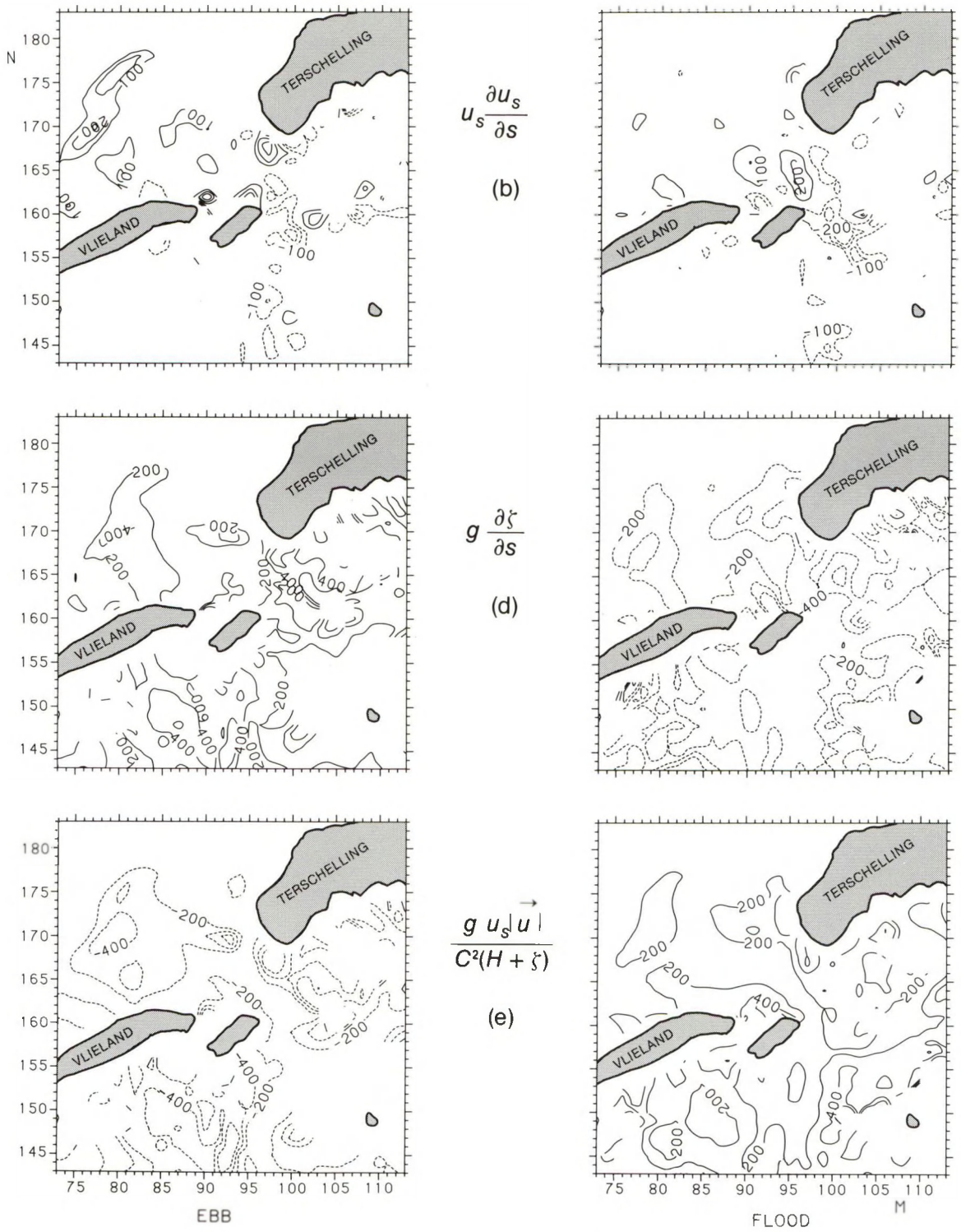

Fig. 9. (a) Isolines of the magnitude of terms b, d and e (10^{-6}ms^{-2}) in equation (9), parallel to the local momentary streamline. On the left-hand side at the time of maximum ebb, in which the positive s-axis has the same orientation as during the flood, and on the right-hand side at the time of maximum flood. Solid lines represent isolines with positive values; dashed lines represent the same range of negative values (see text).

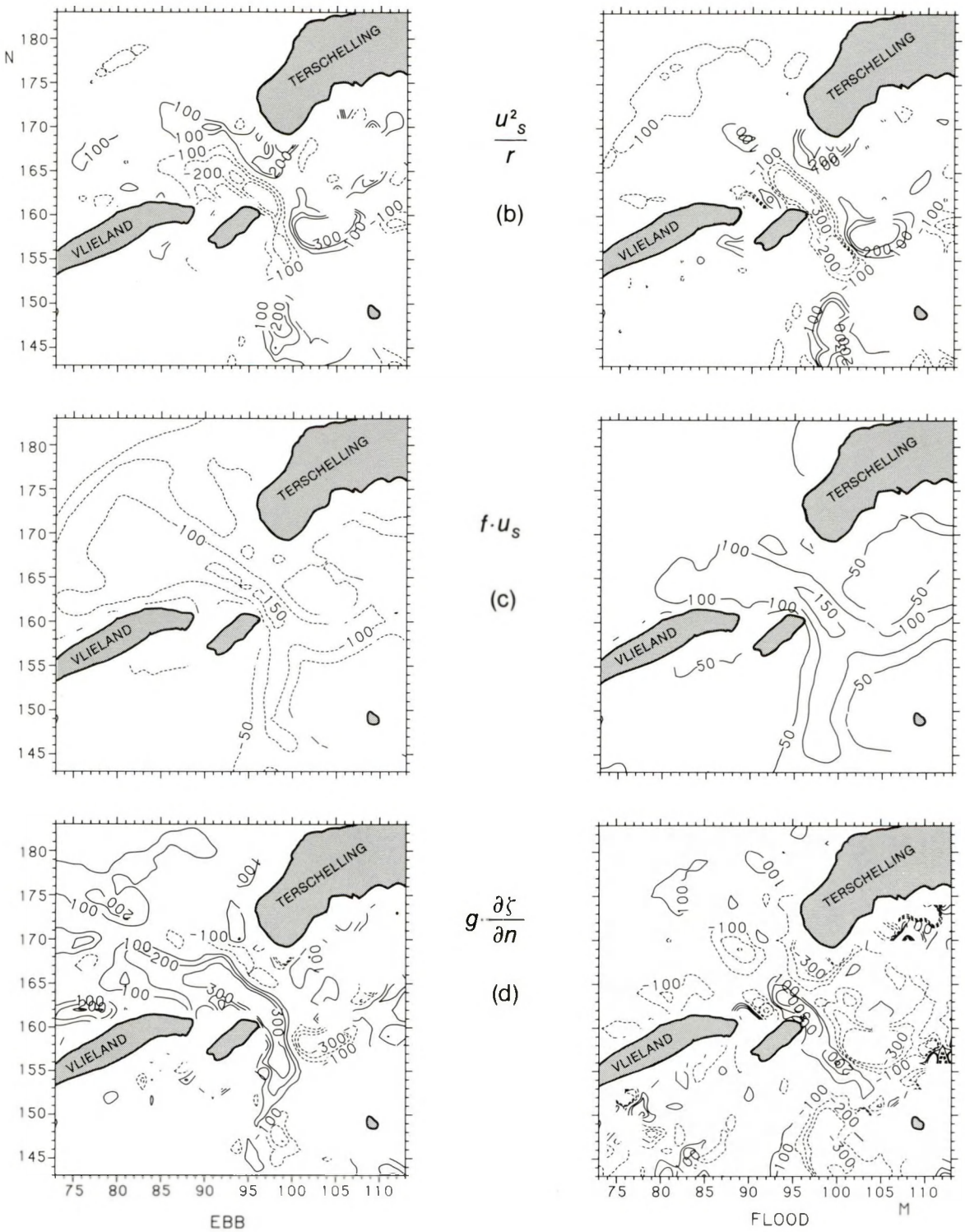

(b) Isolines of the magnitude of terms b, c and d ($10^{-6} ms^{-2}$) in equation (10), perpendicular to the local instantaneous streamline. On the left-hand side at the time of maximum ebb, in which the positive n-axis has the same orientation as during flood, and on the right-hand side at the time of maximum flood. Solid lines represent isolines with positive values; dashed lines represent the same range of negative values (see text).

in Figs 9a and b. Fig. 9a shows the isolines of the terms in equation (9) parallel to the local streamline, while Fig. 9b shows the isolines of the terms in equation (10) perpendicular to the local streamline. In both Figs the ebb phase is shown on the left-hand side. At the ebb phase the instantaneous positive s- and n-axes were chosen opposite to their computed direction to circumvent the problem of comparing terms that have been decomposed along oppositely orientated streamlines. Consequently, the difference between the local positive s- and n-axes at the ebb and flood phase is negligible. For each term solid lines represent the isolines with positive values; dashed lines represent the same range of isolines with negative values.

In Fig. 9a the intervals between the isolines for terms (d) and (e) ($2{\cdot}10^{-4}$ ms^{-2}) are greater than those for the isolines for term (b) (10^{-4}ms^{-2}). This Fig. shows that the terms (d) and (e) are the most important ones. The magnitude of these terms increases in the shallower parts. The less important Bernoulli acceleration (b) has most influence in the deeper channels, especially near the tidal inlet. Except for local deviations, the sign of the Bernoulli acceleration does not change between the ebb and flood periods. Therefore the influence of this term is relatively large in the tidally-averaged equations. The interval between the isolines of the most important terms in the n-direction, the advective term (b) and the water-level gradient term (d), is 10^{-4}ms^{-2} while the isolines for the coriolis term (c) have an interval of $0.5{\cdot}10^{-4}$ ms^{-2} between successive values (Fig. 9b). This Fig. shows that the geometry of the islands and channels causes the centrifugal acceleration (b) to be of great importance near the tidal inlet and the channel junctions. The changing curvature in a streamline is reflected in the large spatial variability in the direction in which this term acts. Furthermore, the orientation of the centrifugal acceleration does not differ between the ebb and flood periods. The water-level gradient in n-direction, term (d), balances the summation of terms (b) and (c), the centrifugal and coriolis acceleration. Depending on the local curvature of a streamline and the phase of the tide, the centrifugal and coriolis acceleration act in the same or opposite direction. In the tidal inlet the consequence is that during the ebb (flood) tide the cross inlet water-level gradient is composed of a relatively steep (small) gradient at the southern side and a relatively small (steep) gradient at the northern side. Also near channel junctions the centrifugal acceleration exceeds the coriolis acceleration so that the direction of the water-level gradient is the same during the ebb and flood periods. Only in the parts of the channel that have more or less straight streamlines does the coriolis term cause an alternating direction of the cross channel water-level gradient.

3. THE TIDAL MEAN FIELD

3.1. INTRODUCTION

In shallow seas and tidal lagoons (such as the Wadden Sea) the tidal flow generates a Eulerian residual flow pattern which can generally be regarded as a combination of isolated residual eddies and a constant flow through the sea or basin (ROBINSON, 1983). In many studies the only way to model the constant flow through the area is to impose residual boundary conditions at the open boundaries of the region under study, because a tidally-driven through-flow often depends on conditions outside the region of interest, which thus determine the open boundary conditions (PRANDLE, 1978). An important advantage of the Wadden Sea model in studying residual flows is that the open boundaries are located in the open sea, where the influence of the in and outflow through the tidal inlets is negligible. Because no residual elevations have been imposed on these open boundaries, constant flows through the inlets and between tidal basins are internally driven by the tide. Therefore special attention will be paid to this part of the residual flow field (and the residual surface elevation), even though the associated residual velocities are often one order of magnitude less than the residual eddy velocities.

3.2. DEFINITIONS

Tidal mean quantities are defined as follows:

mean water level

$$<\zeta> = \frac{1}{T} \int_{-\frac{1}{2}T}^{\frac{1}{2}T} \zeta(t)\, dt \qquad (11)$$

mean velocity

$$<\vec{u}> = \frac{1}{T} \int_{-\frac{1}{2}T}^{\frac{1}{2}T} \vec{u}(t)\, dt \qquad (12)$$

mean transport

$$\langle \vec{U} \rangle = \frac{1}{T} \int_{-\frac{1}{2}T}^{\frac{1}{2}T} \vec{u}(t) \cdot (H + \zeta(t))\, dt \qquad (13)$$

mean transport velocity

$$\langle \vec{u}_T \rangle = \frac{\langle \vec{U} \rangle}{\frac{1}{T} \int_{-\frac{1}{2}T}^{\frac{1}{2}T} (H + \zeta(t))\, dt} \qquad (14)$$

mean stream function $\Psi(m, n)$
in which:

$$\langle U(m, n) \rangle = \frac{\partial \Psi}{\partial y} \text{ and } \langle V(m, n) \rangle = -\frac{\partial \Psi}{\partial x} \qquad (15)$$

Averaging has been performed over a period of 12.5 h (T), the basic period in the boundary conditions. It should be stated here that all these residual quantities have been calculated in a Eulerian way, so that they cannot be used directly for Lagrangean interpretations such as residual transport of dissolved material. For instance, the mean transport velocity (14) is often interpreted as the Lagrangean residual velocity, while this is only the case for slowly varying one-dimensional velocity fields (ZIMMERMAN, 1979; VAN DE KREEKE & CHIU, 1981). In areas like the Wadden Sea, with a large spatial variability in the Eulerian velocity field, Lagrangean residual properties can only be determined by using the time-dependent velocity field to follow displacements of watermasses. This will be the subject of a subsequent paper.

3.3. RESULTS

3.3.1. MEAN WATER ELEVATION

Model results concerning mean water-levels on tidal flats are not physically meaningful because of the special treatment of these points during the simulation of their drying. The consequence is that residual water elevations are only presented for the channels in the model area.

In Figs 10a to c residual levels along the axis of the main channel of each tidal basin are drawn as a function of the distance along the channel axis. In Fig. 10c it was possible to combine in one picture the residual levels in the main chan-

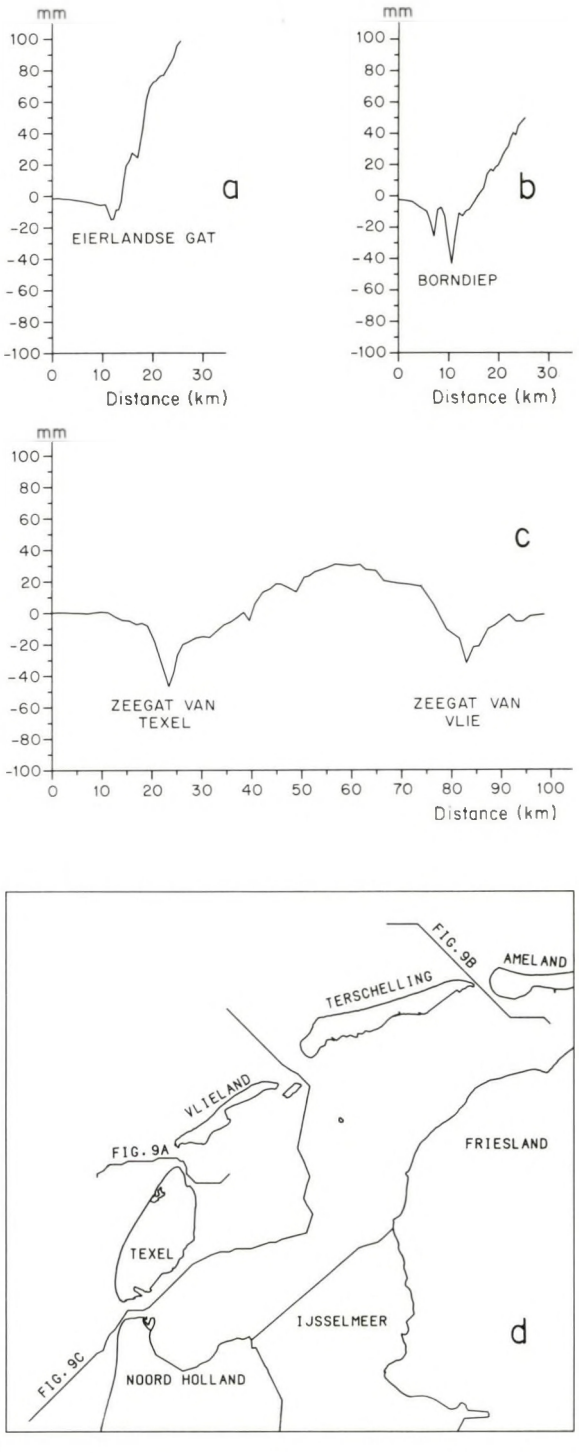

Fig. 10. Residual water elevations along the axes of the main basin channels in the tidal basins (mm) as a function of the distance from the seaward end of the inflow region. The locations of these axes are indicated in (d). (a) Eierlandse Gat; (b) Borndiep; (c) Marsdiep and Vlie basins.

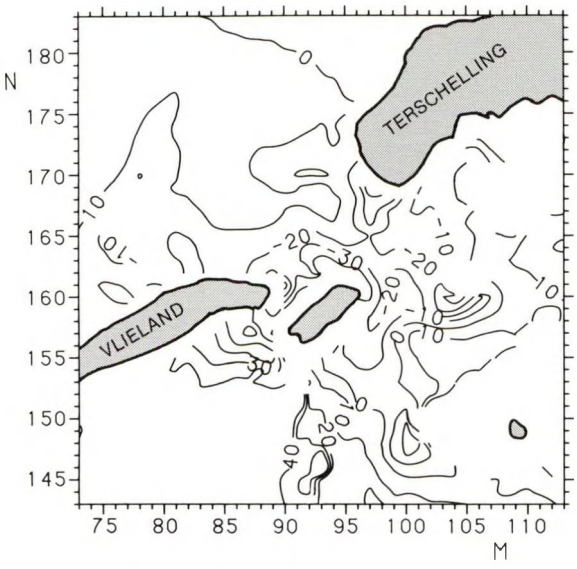

Fig. 11. Isolines of residual elevations in the area near the Zeegat van Vlie (intervals 10 mm).

nels of the Marsdiep and Vlie basin, because of the open connection between the two basins. The drop of the levels in the inflow area of all inlets and the rising in the basins, with larger gradients in the smaller basins, are characteristic features. Fig. 11 shows this phenomenon in more detail in a map of isolines of the residual level in the area near the Zeegat van Vlie (intervals of 10 mm). Two-dimensional characteristics of the distribution of mean water-levels are discussed in more detail in section 3.4.

The computed residuals at Den Helder (-3.9 cm) and Harlingen ($+1.8$ cm) agree with observations. In the "Getijatlas voor Nederland, 1986" residual levels of -3.9 cm and $+1.8$ cm, respectively, are mentioned for these stations. These levels have been determined by analysing 12 years' records of water-levels.

3.3.2. MEAN VELOCITIES

For spatial clarity only a ninth (every 3rd grid point in both directions) of the computed mean transport velocities, $<\vec{u}_T>$ (eq. 14), in the model area is mapped in Fig. 12. The mean transport velocities near the open boundaries are not physically meaningful because they are induced by the special treatment of the advective terms at the open boundaries (STELLING, 1984). Compared to results of modelling studies in other estuaries (OEY *et al.*, 1985; TEE, 1976), Fig. 12 gives qualitatively the same picture. Residual eddies dominate the residual current field in the channels and near the tidal inlets. The existence of many of these tide-induced residual eddies in this area is supported by field observations in the western Wadden Sea (ZIMMERMAN, 1976b; DE BOER *et al.*, 1986). A qualitative comparison of observations and computations shows that the orientation of all observed eddies agrees with the orientation of the computed eddies. These eddies are induced by pronounced variations in channel geometry and bottom topography, which, in the governing equations, increase the importance of the advective terms. OEY *et al.* (1985) have shown the strong effect on the residual flow pattern of omitting the advective terms.

Tidal mean velocities, $<\vec{u}>$ (eq. 12), in every grid point in the area near the Zeegat van het Vlie are shown in Fig. 13a. On average the magnitude of the residual velocity in these eddies varies from about 0.10 ms^{-1} in the tidal basin to 0.15 ms^{-1} in the tidal inlet. Fig. 13b gives the mean transport velocities, $<\vec{u}_T>$ (eq. 14), in the same region as in Fig. 13a. Solid lines indicate the isolines of the ratio between the absolute magnitude of the mean transport velocity (eq. 14) and the absolute magnitude of the mean velocity (eq. 12). At first sight, Figs 13a and b look the same due to the domination of the residual eddies in the mean field, which do not give much difference in the orientation and only slightly in the magnitude of the two velocities. The isolines of the ratio of the magnitude of the two velocities in Fig. 13b indicate, however, that especially outside these eddies, where the mean velocities are small, the difference between the two velocities can be considerable. For one-dimensional motion this difference is in a first approximation equal to the tidal mean of $u\zeta/H$ and is often referred to as the Stokes velocity (ZIMMERMAN, 1979; VAN DE KREEKE & CHIU, 1981). The magnitude of this Stokes velocity depends strongly on local water-depth and the phase difference between tidal water-levels and velocities.

3.3.3. MEAN TRANSPORTS

Isolines for the residual stream function in the interior of the Wadden Sea between the mainland and the islands, calculated from the mean transports (eq. 15), are shown in Fig. 14 with an interval between the isolines of 200 m^3s^{-1}. This map clearly shows that the residual transport

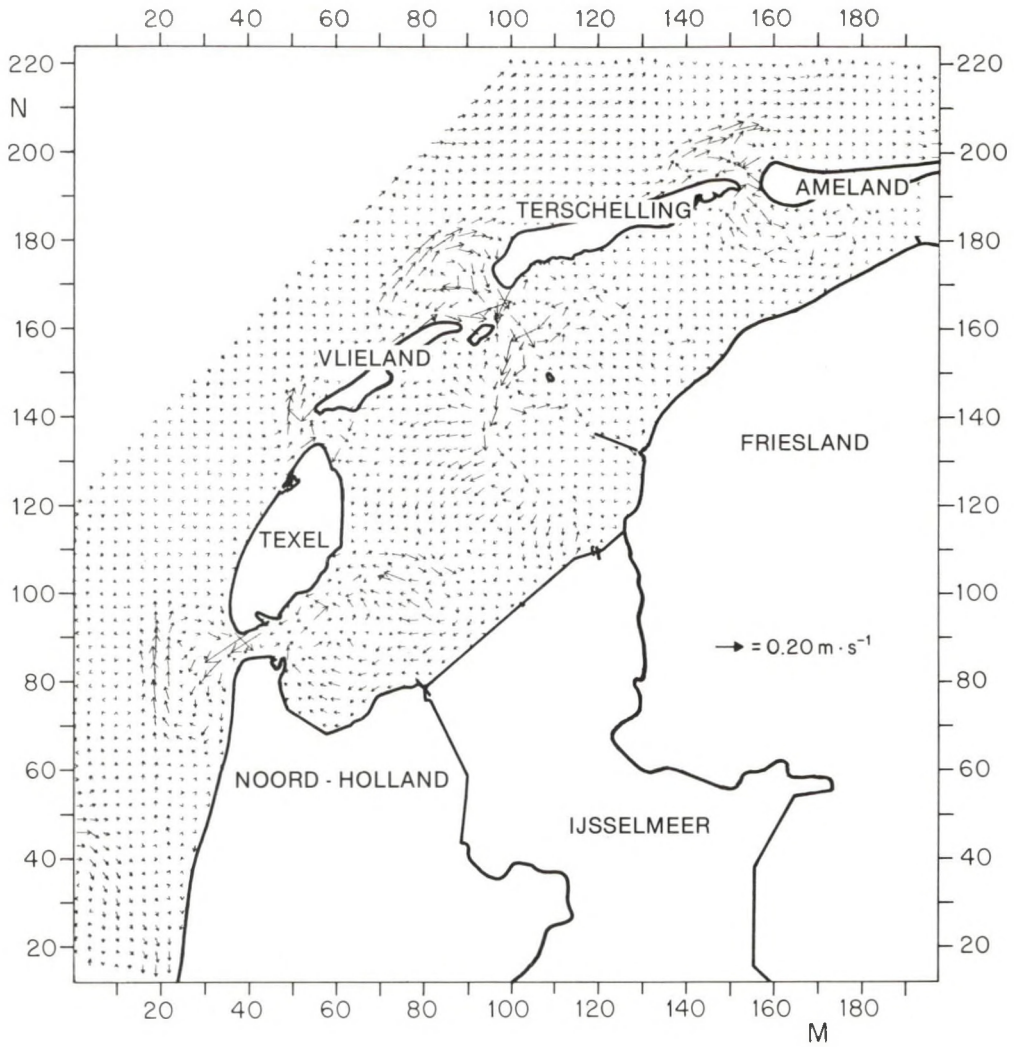

Fig. 12. Mean transport velocities, $<\vec{u}_T>$, in every 3rd grid points.

field in the Wadden Sea can be subdivided into isolated residual eddies and a constant flow through the basins. Fig. 15, which gives a picture of the area near the Zeegat van het Vlie with isoline intervals of 250 m^3s^{-1}, demonstrates this in more detail. The mean transports associated with the eddies are much larger (one order of magnitude) than the constant flow. The differences between the Ψ-values of the mainland and the islands, see Fig. 14, indicate the tidally-driven ebb and/or flood surplusses through the inlets. It shows that the largest through-going volume transport takes place between the two interconnected main basins, and is directed southwards from the Vlie basin towards the Marsdiep basin. The associated transport velocities are very small ($0(10^{-2}$ $ms^{-1})$) in comparison with the tidal velocity amplitude ($0(1$ $ms^{-1})$) as well as with the transport velocities associated with the residual eddies ($0(10^{-1}ms^{-1})$). Therefore it is difficult to support the computed ebb and flood surplusses with measurements. Furthermore, in reality a mean sea-level gradient in the North Sea, along the open boundaries of the model, may possibly influence the magnitude of the residual volume transport. This possible external forcing, combined with the dependence of the residual volume transport on the wind conditions, complicates the determination of the tidally-driven part of the residual volume transport. Analyses of a series of current measurements in the

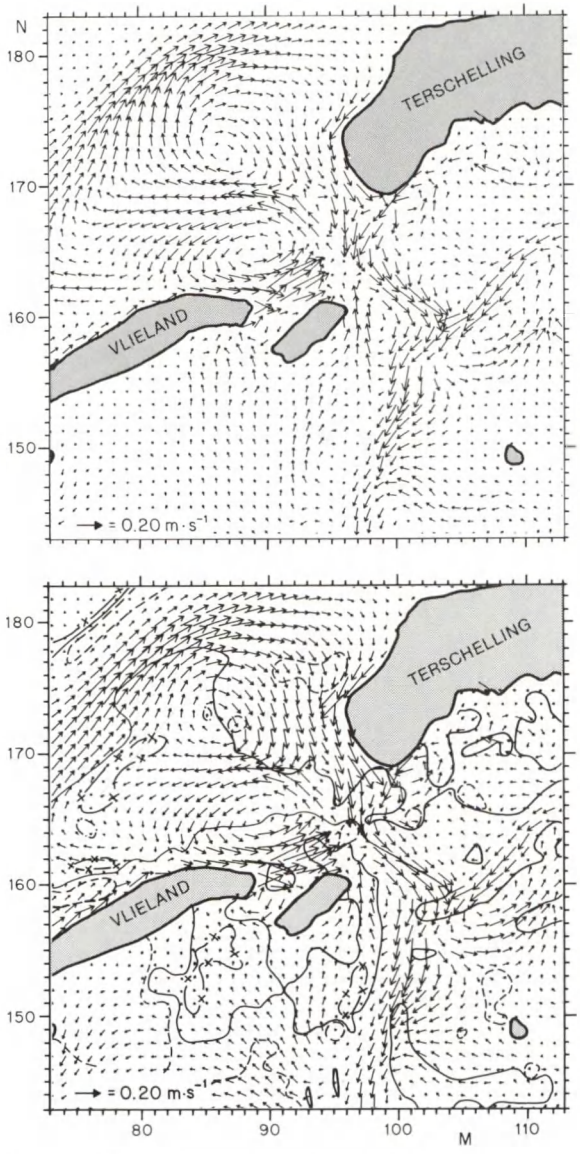

Fig. 13. (a) Mean velocities, $<\vec{u}>$, in the area near the Zeegat van Vlie.

(b) Mean transport velocities near the Zeegat van Vlie together with some isolines (0.5, 1. and 2.) of the ratio between the absolute values of the mean transport velocity and the mean velocity

$$\frac{|<\vec{u}_T>|}{|<\vec{u}>|}$$

The values of the isolines are 0.5 (---), 1.0 (———) and 2.0 (– x – x).

Zeegat van het Vlie (DE BOER *et al.*, 1986) indicate a strong variability in magnitude and direction of this part of the residual flow field and suggest that the total residual volume transport is composed of a wind-driven and a tidally-driven part. However, compared to the model results the same direction of the residual volume transport (southwards) is found during periods with weak winds.

3.3.4. INFLUENCE OF TERMS IN THE TIDALLY-AVERAGED MOMENTUM EQUATIONS

In vector form the governing tidally-averaged momentum equation reads:

$$<\vec{u}\cdot\nabla\vec{u}> + <f(\vec{j}\times\vec{u})> + <g\nabla\zeta> +$$

(b) (c) (d)

$$+ <\frac{g\vec{u}|\vec{u}|}{C^2(H+\zeta)}> - <\nu\nabla^2\vec{u}> = 0 \qquad (16)$$

(e) (f) (g)

in which as, in eqs. 11 to 15 < > stands for averaging over a tidal cycle. The magnitude and direction of a term in a specific grid point is determined in the same manner as described in section 2.4. Averaging over a tidal cycle is performed after decomposing all terms parallel and perpendicular to the dominant streamline at every available timelevel (interval 30 min.). In each grid point the dominant direction of the tidal flow is given by eq. (6); Fig. 7 gives the local s- and n-axes parallel and perpendicular to the dominant streamline in characteristic grid points in the neighbourhood of the Zeegat van het Vlie. In this section the same grid points are used to discuss the relative influence of all terms in the governing equation (16) while, as in section 2.4, the spatial distribution of the most important terms is shown for this area.

The error in the momentum balance, caused by the small differences between the computed magnitude of the terms and the magnitude in the numerical simulation (discussed in section 2.4), follows again from a summation of the terms in eq. (16). This error ("term (g)") is neglected in the discussion because it is only of importance in grid points where the magnitude of the dominating terms is relatively small.

The magnitude of all terms in equation (16) in the characteristic grid points is given in Fig. 16. A global comparison of Fig. 16 and Fig. 8, which

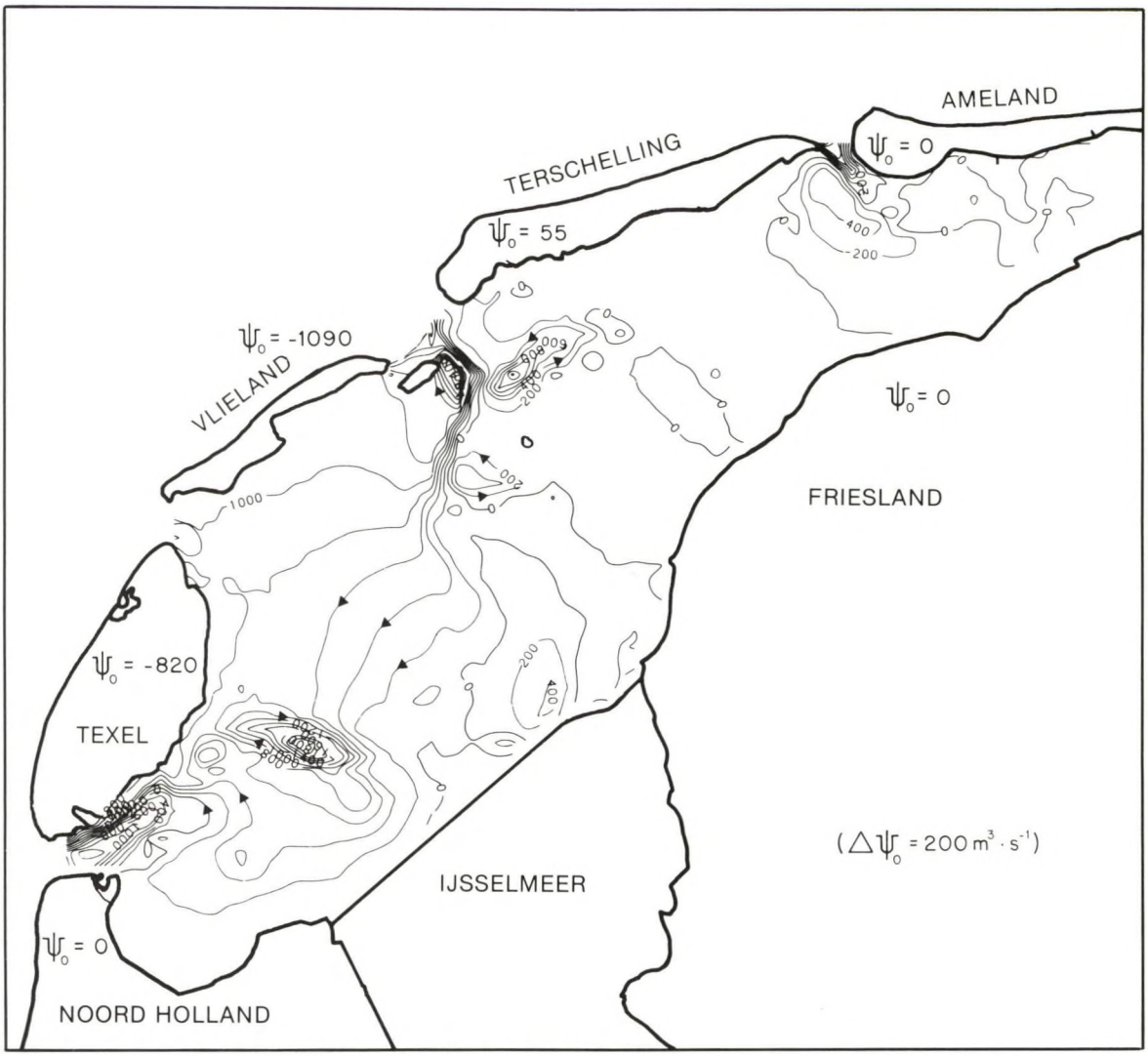

Fig. 14. Isolines of the residual stream function in the interior of the western Wadden Sea (interval 200 $m^3 s^{-1}$)

gives the average magnitude of the same terms during the ebb and flood periods, shows that there is a larger spatial variability in the magnitude of the dominant terms in the tidally-averaged equations.

Comparing the relative influence of the terms in one grid point in the tidal and tidally-averaged equations shows that parallel to the dominant streamline (s-axis) an important shift takes place: the role of the bottom friction term (e) decreases, while the role of the Bernoulli term (b) increases. Perpendicular to the streamline the relative influence of the coriolis term is diminished. Thus, in a first approximation, the non-linear term (b) is the forcing term in the mean state. This term is counterbalanced by the combination of a residual water-level gradient and a residual bottom-friction term. In the grid points shown term (d), due to a residual water-level gradient, is much larger than term (e), due to residual bottom friction.

Isolines for the magnitude of these terms are given in Fig. 17. In the left-side term, (b), (d) and (e), parallel to the dominant flow direction, are shown, in which solid lines represent the isolines ($0.5 \cdot 10^{-4} ms^{-2}$, $1 \cdot 10^{-4} ms^{-2}$ and $1.5 \cdot 10^{-4} ms^{-2}$) of terms that are positive in the local s-direction, determined according equation (6); and dashed lines represent the same range of isolines acting in the opposite direction. In general, the con-

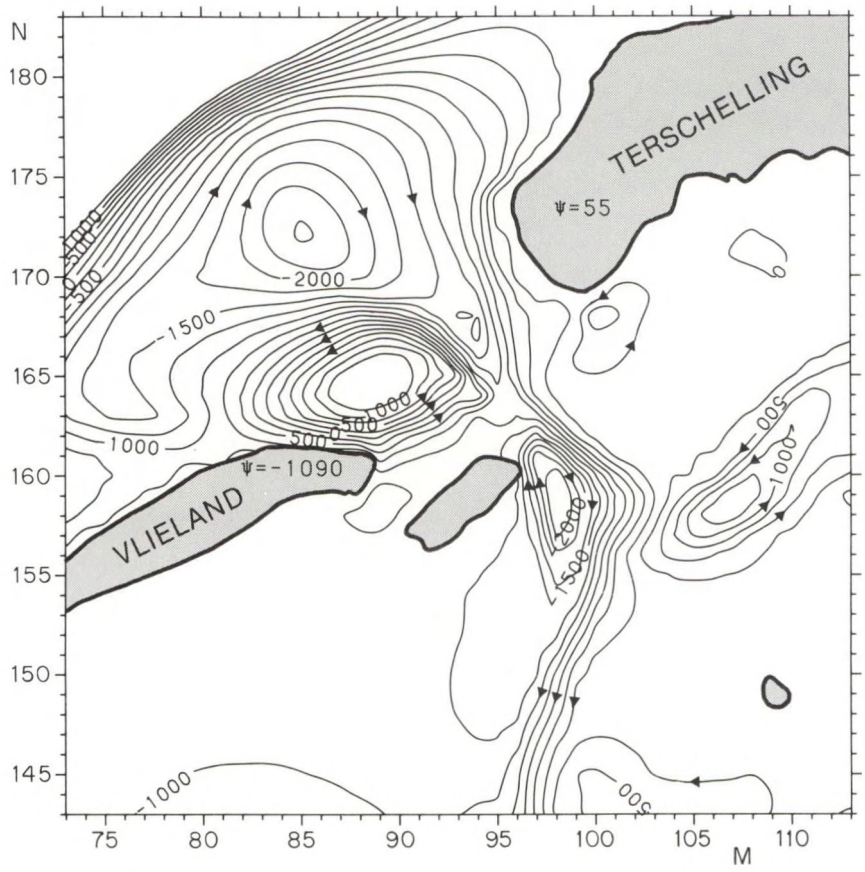

Fig. 15. Isolines of the residual stream function near the Zeegat van Vlie (interval 250 m^3s^{-1})

vergence of the tidal currents in the tidal inlet causes the Bernoulli term (b) to be positive in the inflow region of the tidal inlet and negative in the channels of the basin. The consequence is that the counterbalancing residual water-level gradient induces a drop in the residual water-level in the tidal inlet (see Fig. 10). The spatial distribution of the magnitude of the residual bottom-friction term combined with the spatial distribution of term (d) shows that in the shallower part of the area the main balance is formed by term (d) and (e), while in the deeper channels terms (b) and (d) dominate.

On the right-hand side of Fig. 17 the same terms perpendicular to the dominant streamline (in the local n-direction) are given. The range of the isolines for term (b) and (d) is greater; isolines are given for $1{\cdot}10^{-4}ms^{-2}$, $2{\cdot}10^{-4}ms^{-2}$ and $3{\cdot}10^{-4}ms^{-2}$, while term (e) has the same range of isolines as the range in the s-direction. It shows that in the n-direction the centrifugal term (b) has a large spatial variability, related to the geometry of the tidal inlet and the channels in the basin (see Fig. 7). This term is counterbalanced by a residual water-level gradient, resulting in a rising/lowering of the residual water-level in the outer/inner bend of a channel. The combined effect of the Bernoulli term and the centrifugal term on the residual levels in the tidal inlet is clearly reflected in Fig. 11. The Bernoulli term lowers the residual level in a relatively large region on both sides of the inlet and induces a drop in the centre of the inlet. A cross inlet gradient results from the more locally acting centrifugal term, which causes a further lowering of the residual levels near the islands.

Summarizing, it can be stated that in the mean state, compared to the time varying state, local geometry and bottom topography have more influence on the magnitude and spatial variability of the most important terms in the momentum equations. This is reflected in the increased in-

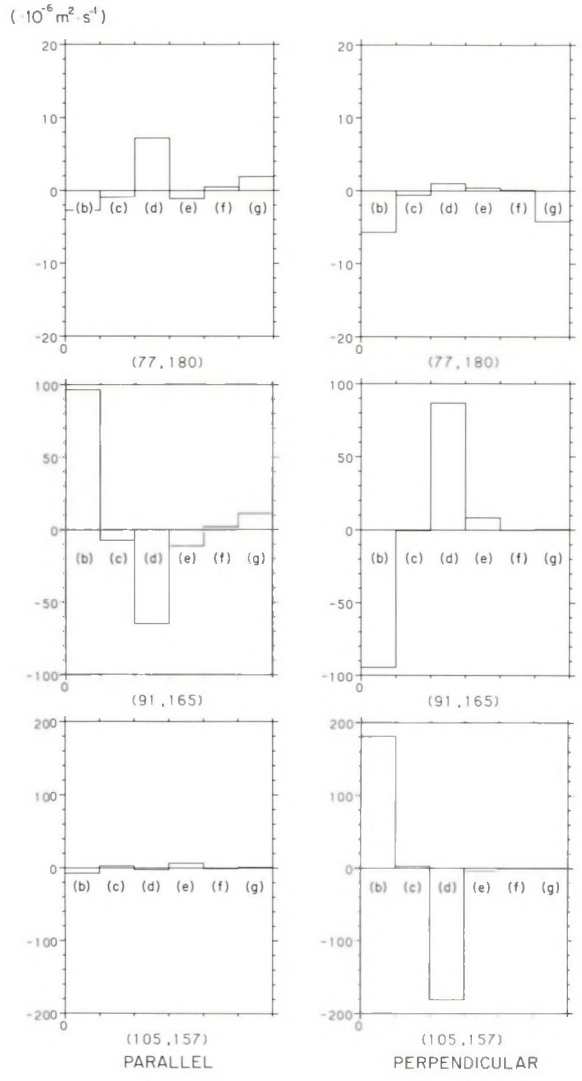

Fig. 16. Tidally averaged magnitude of the terms (in 10^{-6}ms^{-2}) in equation (16) parallel (left-hand side) and perpendicular (right-hand side) to the dominant streamline in the characteristic grid points.

fluence of the advective terms that drive the tidally averaged field.

4. CONCLUSIONS

Simulations with a two-dimensional numerical model of the western Dutch Wadden Sea, covering four tidal basins and a part of the adjacent North Sea, show a good agreement between observed and computed water elevations, transport rates through the tidal inlets, and, on a larger scale, between measured and computed global two-dimensional current fields and between the observed and simulated area of emersed tidal flats. Averaging the computed water-levels and current velocities over a tidal cycle shows that the tidally-driven residual current velocity field is composed of isolated residual eddies and a through-flow between different basins. In the tidal inlets the residual velocities associated with the eddies, of which the orientation is supported by measurements, are one order of magnitude larger than the residual velocities associated with the through-flow. A drop in the residual elevations in the inflow areas of tidal inlets and a rise in the interior of tidal basins are general features in all tidal basins.

Rewriting the governing momentum equations in directions parallel and perpendicular to the local dominant streamline and determining the magnitude of each term in some characteristic grid points show that morphological differences strongly influence the magnitude and relative importance of most of these terms. The advective term, decomposed in a Bernoulli acceleration parallel and a centrifugal acceleration perpendicular to the local streamline, is strongly increased by pronounced variations in channel and bottom geometry, which subsequently influence the magnitude of the other terms.

Averaging these terms over a tidal period shows that in the mean state the main balance is formed by the advective and water-level gradient term. Perpendicular to the dominant flow direction, the magnitude and spatial variability of both residual terms are larger than parallel to the dominant flow direction. This difference is caused by the high number of curves in the channels that cause a high spatial variability of the centrifugal term, while variations in the magnitude of the cross section of the tidal flow, responsible for a Bernoulli acceleration, are more gentle.

5. REFERENCES

BOER, M. DE, M.F. LIESHOUT, G. KOOL & R. PEEREBOOM, 1984. Waterbeweging westelijke Waddenzee: verloop natte en droge oppervlakten en kombergingen. Nota WWKZ-84.H009, Rijkswaterstaat, The Netherlands: 1-12.

BOER, M. DE, N. DE GRAAFF & C. VISSER, 1986. Het vermogen van het Zeegat van het Vlie. Nota ANW-86.H205, Rijkswaterstaat, The Netherlands: 1-20.

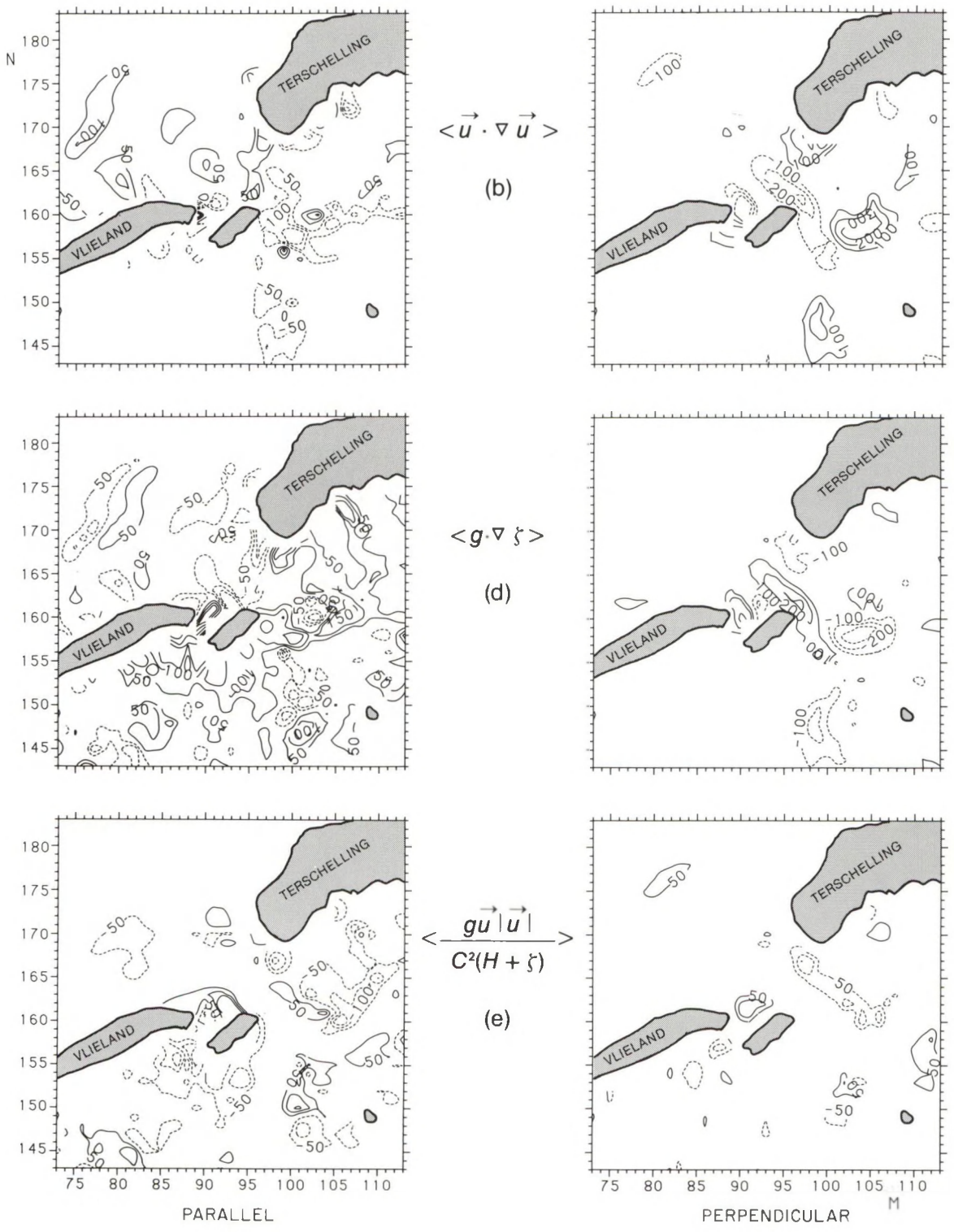

Fig. 17. Isolines of the tidally averaged magnitude of terms b, d and e (in $10^{-6} ms^{-2}$) in equation (16), parallel (left-hand side) and perpendicular (right-hand side) to the local dominant streamline. Solid lines represent isolines with positive values; dashed lines represent the same range of negative values (see text).

HEAPS, N.S., 1978. Linearized vertically integrated equations for residual circulation in coastal seas.—Dt. hydrogr. Z. **31:** 147-169.

KLATTER, H.E., J.M.C. DIJKZEUL, G. HARTSUIKER & L. BIJLSMA, 1986. Flow computations nearby a Storm Surge Barrier under Construction with Two-Dimensional Numerical Models.—Proc. Twentieth Coast. Eng. Conf., Taiwan.

KREEKE, J. VAN DE & S.S. CHIU, 1981. Tide-induced residual flow in shallow bays.—J. Hydraulic Res. **19:** 231-249.

LEENDERTSE, J.J., 1967. Aspects of a computational model for long period water wave propagation. Memorandum RM-5294-PR, Rand Corporation, Santa Monica, 1967: 1-116.

——, 1984. Verification of a Model of the Eastern Scheldt. Memorandum R-3108-NETH, Rand Corporation, Santa Monica, 1984: 1-31.

LEENDERTSE, J.J., A. LANGERAK & M.A.M. DE RAS, 1981. Two dimensional models for the Delta Works. In: H.B. FISCHER. Transport models for inland and coastal waters. Acad. Press, New York: 408-450.

LORENTZ, H.A., 1926. Verslag Staatscommissie Zuiderzee 1918-1926. Den Haag, 1926.

MADDOCK, L. & R.D. PINGREE, 1978. Numerical simulation of the Portland Tidal Eddies.—Est. Coast. Mar. Sci. **6:** 353-363.

OEY, L.Y., G.L. MELLOR & R.I. HIRES, 1985. Tidal modelling of the Hudson Raritan Estuary.—Estuar. coast. Shelf Sci. **20:** 511-527.

POSTMA, H., 1954. Hydrography of the Dutch Wadden Sea.—Archs néerl. Zool. **10:** 405-511.

PINGREE, R.D. & L. MADDOCK, 1977. Tidal eddies and coastal discharge.—J. mar. biol. Ass. U.K. **57:** 869-875.

PRANDLE, D., 1978. Residual flows and elevations in the Southern North Sea.—Proc. R. Soc. Lond. (A) **359:** 189-228.

ROBINSON, I.S., 1983. Tidally induced residual flow. In: B. JOHNS. Physical Oceanography of Coastal and Shelf Seas: 321-357.

STUDIEDIENST HOORN & DELFZIJL, 1973. De Noordzeemeting 1971. Nota W.73.1, Rijkswaterstaat, The Netherlands: 1-7.

STELLING, G.S., 1984. On the construction of computational methods for shallow water flow problems. Comm. no. 35, Rijkswaterstaat, The Netherlands: 1-226.

TEE, K.T., 1976. Tide induced residual current, a 2-d non linear numerical tidal model.—J. Mar. Res. **34:** 603-628.

VETH, C. & J.T.F. ZIMMERMAN, 1981. Observations of quasi-two-dimensional turbulence in tidal currents.—J. Phys. Oceanography **11:** 1425-1430.

VOOGT, L., 1985. Een getijmodel van de Noordzee gebaseerd op de JONSDAP-1976 meting. Nota WWKZ-84G006, Rijkswaterstaat, The Netherlands: 1-38.

ZIMMERMAN, J.T.F., 1976a. Mixing and flushing of tidal embayments in the western Dutch Wadden Sea, I: Distribution of salinity and calculation of mixing time scales.—Neth. J. Sea Res. **10:** 149-191.

——, 1976b. Mixing and flushing of tidal embayments in the western Dutch Wadden Sea, II: Analyses of mixing processes.—Neth. J. Sea Res. **10:** 397-439.

——, 1979. On the Euler-Lagrange transformation and the Stokes drift in the presence of oscillatory and residual currents. Deep-Sea Res. **26A:** 505-520.

(received 22 December 1987; revised 9 February 1988)

Netherlands Journal of Sea Research
22 (1): 23-36 (1988)

THE ASSESSMENT OF BENTHIC PHOSPHORUS REGENERATION IN AN ESTUARINE ECOSYSTEM MODEL*

W. VAN RAAPHORST[1], P. RUARDIJ[1] and A.G. BRINKMAN[2]

[1]*Netherlands Institute for Sea Research, P.O. Box 59, 1790 AB Den Burg, Texel, The Netherlands*
[2]*Twente University, Dept. of Chemical Technology, P.O. Box 217, 7500 AE Enschede, The Netherlands*

ABSTRACT

Benthic phosphorus regeneration is an important factor in eutrophication processes of shallow water systems. In any ecological modelling approach of such systems an adequate description of the sediment-water interactions is necessary. With this aim a fairly simple concept with a low number of variables and parameters has been formulated and analysed. The most important parameter regulating the benthic phosphorus fluxes is the Damköhler number (*Da*), which represents the combined effect of the aerobic first order adsorption/desorption rate *K* [T^{-1}], the oxygen penetration depth *H* [L] and the apparent diffusion coefficient *D* [$L^2 \cdot T^{-1}$]: $Da = K \cdot H^2 \cdot D^{-1}$. For $Da < 0.3$ anaerobic processes dominate P-fluxes across the sediment-water interface, for $Da > 12$ chemical transformations in the aerobic layer are the most important. The concept is applied to EMOWAD, an ecological model of the western part of the Dutch Wadden Sea.

In the subtidal sediments of this estuary, *Da* is estimated at 0.4 in summer and 5.8 in winter. For the intertidal areas these numbers are 3.9 and 23, respectively. According to the model, benthic phosphorus fluxes are almost absent in winter and reach values of up to 1.75 mmol·m^{-2}·d^{-1} in summer. Approximately 70% of the organic phosporus compounds reaching the sediments is regenerated within the same year. The model results suggest that organic phosphorus accumulated in the sediments during the winter and spring is released to the water column during the summer. Part of the phosphates produced by mineralization is retained temporarily in the sediment due to adsorption to the sediment particles.

1. INTRODUCTION

In shallow water systems the internal nutrient loading from the sediment is often an important factor in eutrophication processes. The favourable effects of the reduction of external nutrient inputs may be counteracted by benthic regeneration, particularly when the sediments have high nutrient contents. In most coastal and estuarine systems phosphorus does not limit primary production, but even then the sediment-water interaction may be an important process. RUTGERS VAN DER LOEFF (1980b) for example found that the P-input from the sea-floor of the Southern Bight of the North Sea was of the same order of magnitude as the contributions from other sources. BALZER (1984) in the Kiel Bight calculated that about 66% of the organic phosphorus reaching the sediments returned as inorganic phosphate to the water column, while HOPKINSON (1987) reported a 40% contribution of the benthic P-flux to the annual requirements of the pelagic primary producers in the nearshore zone of Georgia Bight. It is obvious that models concerning shallow water ecosystems must include an adequate description of benthic regeneration processes.

Sediment-water interactions and the processes involved have been discussed extensively. *In situ* studies with benthic chambers (ELDERFIELD *et al.*, 1981; KLUMP & MARTENS, 1981; RUTGERS VAN DER LOEFF *et al.*, 1981; CALLENDER & HAMMOND, 1982; FISHER *et al.*, 1982; HALL, 1984; SUNDBY *et al.*, 1986) as well as experiments

Publication no. 20 of the project "Ecological Research of the North Sea and Wadden Sea" (EON).

using undisturbed sediment cores (KAMP-NIELSEN, 1974, 1975; HOLDREN & ARMSTRONG, 1980; ELDERFIELD *et al.*, 1981; VAN LIERE & MUR, 1982; KELDERMAN, 1984; VAN RAAPHORST & BRINKMAN, 1984; QUIGLEY & ROBBINS, 1986) reveal that the actual P-regeneration is a function of the concentration in the overlying water, temperature, pH, oxygen penetration depth, mineralization rates, bioturbation and other mixing processes in the sediment, turbulence of the overlying water, and chemical characteristics of the sediment material. All these factors should to some extent be included in the model formulations.

In the literature many formulations for benthic fluxes may be found, ranging from purely empirical relationships (*e.g.* KAMP-NIELSEN, 1980) to formal and theoretical models (*e.g.* ALLER, 1980; BERNER, 1980; JAHNKE *et al.*, 1982). The first approach does not include any *a priori* knowledge of the processes affecting the actual fluxes. It leads to simple expressions, but feed-back mechanisms associated with the factors mentioned above are lacking. Moreover, by their nature the usefulness of these models is restricted to the specific situation for which they have been derived and calibrated. The second approach aims at completeness. All the relevant subprocesses are described explicitely, giving rise to a large number of state variables and parameters. Since for phosphorus there is a strong interaction between dissolved components and solid material, mass balances have to be set up for both phases. Generally this means that the resulting equations have to be solved numerically in a large number of thin sediment layers, mostly for small time-steps (KAMP-NIELSEN *et al.*, 1982). In an ecosystem model of which the benthic regeneration module is only a small part and where the period to be simulated is mostly in the order of months to years, both are undesirable features. Besides this drawback, appropriate data for the calibration of the models are absent in most cases, thus causing large uncertainties in the simulation results. Aggregation of the essential processes to a simpler approach is therefore necessary. In fact this may result in a conceptual model with a low number of state variables and parameters, in which only a limited amount of *a priori* knowledge of the processes dominating the benthic system is incorporated.

In this paper such a simple approach to assess the benthic P-regeneration is presented and analysed. The model, originally developed for the shallow eutrophic Lake Veluwe, the Netherlands (BRINKMAN & VAN RAAPHORST, 1986), is applied here with some modifications to EMOWAD, a complex estuarine ecosystem model of the western part of the Dutch Wadden Sea (henceforth called western Wadden Sea). For this application data from the literature are used to estimate the values of the various parameters. A more elaborate calibration will be presented elsewhere.

2. BASIC CONCEPTS

The objective of this modelling approach is to simulate benthic fluxes, rather than concentration gradients in the pore water or in the solid phase. An operational description of the diagenetic processes within the sediment may be sufficient for this purpose. The basic formula for the P-flux J_0 across the sediment-water interface we use is:

$$J_0 = \varphi \cdot K_m \cdot (C_0 - C_b) \qquad (1)$$

where J_0 has the dimension $M \cdot L^{-2} \cdot T^{-1}$, φ is the volumetric porosity just below the sediment-water interface $[-]$, K_m is an overall mass transfer coefficient $[L \cdot T^{-1}]$, C_0 is the concentration in the overlying water and C_b is a characteristic concentration in the interstitial water, both having the dimensions $M \cdot L^{-3}$. Eq.(1) is a general linear expression for fluxes across interfaces, well known from chemical engineering (*e.g.* BIRD *et al.*, 1960; LEVENSPIEL, 1962; ARIS, 1975).

The requirements to the model can be specified by stating that the parameters K_m and C_b have to be computed properly. The use of eq.(1) is justified by the experimental results of KELDERMAN (1984), VAN RAAPHORST & BRINKMAN (1984) and BRINKMAN & VAN RAAPHORST (1986), showing that P-fluxes from undisturbed sediment cores were linearly related to the concentration in the overlying water. To include the diagenetic phenomena mentioned in the introduction, eq.(1) should, however, be extended and further detailed.

For this purpose the sediment is, like in other regeneration models, (*e.g.* BILLEN, 1978; LIJKLEMA & HIELTJES, 1982; VAN ECK & SMITS, 1986; KLAPWIJK & SNODGRASS, 1986), schematized into distinct layers (Fig. 1), in which the transformations are aggregated to simple zero order or first

order reactions, and in which the parameters are treated as indifferent to depth. Obviously this simplification makes it impossible to compute the effects of vertical gradients of *e.g.* pH, porosity, *etc.* It is felt, however, that the possibility of defining different parameter values in the distinct layers is enough for the present purpose. Since the adsorption capacity of the bottom material for phosphate is dependent on the iron oxidation-state, the sediment is divided into an aerobic layer in which Fe(III) is present as strongly P-adsorbing Fe-oxyhydroxides, and an anaerobic layer in which Fe(II) is dominant. In the model a third layer is included to account for phosphorus definitely buried in the deeper sediment. The general diagenetic equation for dissolved phosphorus in each layer may be formulated as (BERNER, 1980):

$$\frac{\partial C}{\partial t} = \frac{\partial^2 C}{\partial x^2} - \omega \frac{\partial C}{\partial x} + \Sigma R \qquad (2)$$

where C is the concentration in the pore water [M·L^{-3}], t is time [T], D is the apparent diffusion or dispersion coefficient [L^2·T^{-1}], x is the depth relative to the sediment water interface [L], ω is an advection parameter [L·T^{-1}], and ΣR denotes the sum of all reactions and transformations affecting C [M·L^{-3}·T^{-1}]. To arrive at an equation equivalent to eq.(1), eq.(2) is solved analytically for the aerobic layer, while the concentration in the anaerobic layer (C_1, Fig. 1), needed as a boundary condition at the aerobic-anaerobic interface, is treated as depth independent within this layer. The flux of dissolved phosphorus across this interface (J_1, Fig. 1) is also calculated from the analytical solution of eq.(2) for the aerobic layer.

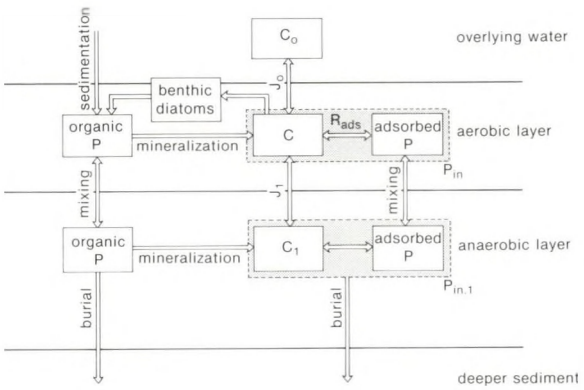

Fig. 1. Basic overview of the processes incorporated in the benthic phosphorus regeneration model. $P_{in} = C + Pads$. For further explanation see text.

In the aerobic zone the reaction term ΣR consists of phosphate production due to mineralization, reversible adsorption on the sediment particles, and of relatively slow precipitation/dissolution processes. Strictly speaking the P-uptake by benthic diatoms should also be included in ΣR. In the final application to EMOWAD, however, there is no direct interference between this uptake and the flux J_0. Benthic primary production is assumed to take place only on emerged intertidal flats. The P-flux across the sediment-water interface is assumed to be important only during submersion (Table 2). As a first approximation mineralization can be treated as a zero order process (*i.e.* independent of C) producing phosphate homogeneously over the entire layer. Adsorption is usually assumed to proceed at an infinite rate, thus leading to instantaneous equilibria (*cf.* BERNER, 1980). For the present purpose a dynamical formulation of the adsorption/desorption processes is more suitable (BRINKMAN & VAN RAAPHORST, 1986), a simple expression being (ARIS, 1975; DOMENICO, 1977):

$$R_{ads} = -K \cdot (C - C_{eq}) \qquad (3)$$

where R_{ads} denotes the contribution of reversible adsorption to ΣR [M·L^{-3}·T^{-1}], K is a first order rate-constant [T^{-1}] and C_{eq} is the adsorption equilibrium concentration [M·L^{-3}]. It should be noted that both K and C_{eq} depend on the phosphorus amount adsorbed on the solid surfaces, and will therefore vary in time and depth. For relatively thin layers, eq.(3) may still lead to acceptable results as long as in the actual model simulations C_{eq}, using a suitable isotherm, is computed each time-step from the total amount of inorganic phosphorus available for adsorption. In Fig. 1 this amount is represented by the variable P_{in} and $P_{in,1}$ for the aerobic and the anaerobic layer, respectively. Linear adsorption isotherms are used to calculate C_{eq} in the aerobic layer and the concentration C_1 [M·L^{-3}] in the anaerobic layer:

$$C_{eq} = P_{in} \cdot (1 + PC)^{-1};\ C_1 = P_{in,1} \cdot (1 + PC_1)^{-1} \qquad (4)$$

where PC and PC_1 are linear partition coefficients (dimensionless). In general $PC \gg PC_1$, leading to much higher concentrations in the

reduced zone than in the aerobic layer. Eq.(3) may also be used for the formulation of the precipitation-dissolution reactions, although in reality the kinetics of these are certainly more complex. Anyhow, these slow reactions likely do not dominate ΣR, and hence the use of eq.(3) for the overall chemical transformations is probably justified.

3. BENTHIC FLUXES J_0 AND J_1

In general the rates of the processes concerned and the concentration in the overlying water change slowly compared to the time needed to achieve steady state profiles in the pore water. This means that it is sufficient to solve eq.(2) for pseudo stationary conditions (supported further on). Assuming a zero order phosphate production due to mineralization P_m [$M \cdot L^{-3} \cdot T^{-1}$] and using eq.(3) for the chemical transformations, eq.(2) becomes:

$$0 = D\frac{\partial^2 C}{\partial x^2} - \omega\frac{\partial C}{\partial x} - K\,(C - C_{eq}) + P_m \qquad (5)$$

For convenience the equations are rendered dimensionless by setting $\Psi = C/C_0$ and $\lambda = x/H$, where H is the thickness of the aerobic layer, dimension L. The equations (1) and (5) thus become:

$$\Phi_0 = \varphi\cdot\frac{K_m\cdot H}{D}\cdot(1 - \Psi_b) = \varphi\cdot\alpha\cdot(1 - \Psi_b) \qquad (6)$$

$$0 = \frac{\partial^2\Psi}{\partial\lambda^2} - Pe\cdot\frac{\partial\Psi}{\partial\lambda} - Da\cdot(\Psi - \Psi_{eq}) + \Theta_a \qquad (7)$$

where the dimensionless flux $\Phi_0 = J_0\cdot H/(C_0\cdot D)$, the parameter α is defined in eq.(6), the Peclet number (Pe) is $\omega\cdot H/D$ and the Damköhler number (Da) is $K\cdot H^2/D$. The physical interpretation of these dimensionless numbers was discussed in detail by BIRD *et al.* (1960) and DOMENICO (1977). The term $\Theta_a = Pm\cdot H^2/(C_0\cdot D)$ denotes the dimensionless P-production due to mineralization, averaged over H, while the subscripts 0,*b* and *eq* have the same meaning as before. The link between eq.(6) and eq.(7) follows from Fick's first law :

$$\Phi_0 = -\varphi\cdot\left.\frac{\partial\Psi}{\partial\lambda}\right|_{\lambda=0} \qquad (8)$$

In most situations advection may be ignored (BERNER, 1980). With this assumption and the boundary conditions

$$\Psi(0) = 1,\ \Psi(1) = \Psi_1 \qquad (9)$$

the solution of eq.(7) and eq.(8) is:

$$\Phi_0 = \varphi\cdot\frac{\sqrt{Da}}{\tanh\sqrt{Da}}\cdot\left[1 - \Psi_{eq} - \frac{\Theta_a}{Da} + \frac{\Psi_{eq} + \frac{\Theta_a}{Da} - \Psi_1}{\cosh\sqrt{Da}}\right] \qquad (10)$$

Graphical examples of this solution are presented in Fig. 2. In eq.(10) two extremes can be distinguished. In the first Da is small, *i.e.* there is no substantial adsorption during the time period needed to diffuse over a distance H. In other words, the flux Φ_0 is merely determined by the production due to mineralization and the diffusion from the anaerobic layer. In the other extreme, Da is large and only a layer $\ll H$ just below the sediment-water interface is actually involved in the benthic flux. In this case the chemical reactions and the mineralization rate are controlling the benthic flux J_0, while the influence of the anaerobic layer is unimportant. Mathematically, both extremes read (Appendix 1, Fig. 2):

$Da < 0.3$: $\quad \Phi_0 \approx \varphi\cdot(1 - \tfrac{1}{2}\Theta_a - \Psi_1)$ (11a)

$Da > 12$: $\quad \Phi_0 \approx \varphi\cdot\sqrt{Da}\cdot\left(1 - \Psi_{eq} - \frac{\Theta_a}{Da}\right)$ (11b)

From the examples given in Fig. 2, it may be concluded that Φ_0 decreases at increasing values of Da. At $Da = 8$ to 15, however, Φ_0 increases again. The explanation of this is simple. The effect of the mineralization term Θ_a as well as the effect of the anaerobic layer on Φ_0 is most important at small Da-numbers. In Fig. 2 this can be seen by comparing the curves 1 with 2, 3 with 6, and 5 with 6. At increasing values of Da the absolute contribution of both effects to Φ_0 decreases, while the chemical transformations become more important. At large values of Da, Φ_0 is most sensitive to Ψ_{eq} (compare curves 1, 3 and 4). It should be noted that in case $\Psi_{eq} = 1$ (curve 4), Φ_0 approximates 0 for large values of Da. For $\Psi_{eq} < 1$, Φ_0 would turn into the opposite direction

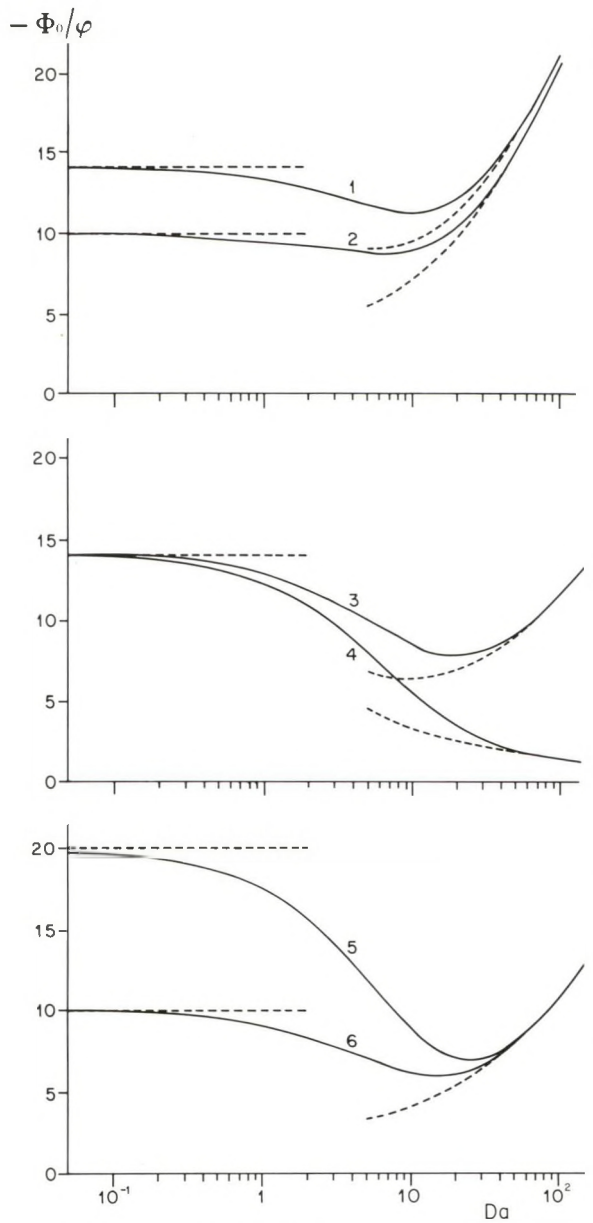

Fig. 2. Examples of the solution expressed in eq.(10), the dimensionless benthic flux $-\Phi_0/\varphi$ as a function of the *Da*number. The approximate solutions for extreme *Da*-numbers (eqs. 11 and 11b) are presented by the dashed lines.
curve 1: $\Psi_{eq}=3$, $\Theta_a=10$, $\Psi_1=10$; curve 2: $\Psi_{eq}=3$, $\Theta_a=2$, $\Psi_1=10$; curve 3: $\Psi_{eq}=2$, $\Theta_a=10$, $\Psi_1=10$; curve 4: $\Psi_{eq}=1$, $\Theta_a=10$, $\Psi_1=10$; curve 5: $\Psi_{eq}=2$, $\Theta_a=2$, $\Psi_1=20$; curve 6: $\Psi_{eq}=2$, $\Theta_a=2$, $\Psi_1=10$.

from the overlying water towards the sediment for large values of *Da*. From Appendix 1 it follows that eq.(11b) is the general solution of eq.(7) and eq.(8) in situations without an anaerobic layer. This means that the effects of the anaerobic layer on the flux can be identified by subtracting eq.(11b) from eq.(10). Thus, when eq.(10) is reformulated into:

$$\Phi_0=\varphi\cdot\sqrt{Da}\cdot(1-\Psi_{eq}-\frac{\Theta_a}{Da}-\Psi_{an}) \qquad (12)$$

Ψ_{an} comprises the effect of the anaerobic layer, and is given by:

$$\Psi_{an}=(1-\Psi_{eq}-\frac{\Theta_a}{Da})\cdot\frac{1-\tanh\sqrt{Da}}{\tanh\sqrt{Da}}+$$

$$+\frac{\Psi_{eq}+\frac{\Theta_a}{Da}-\Psi_1}{\sinh\sqrt{Da}} \qquad (13)$$

In eq.(12) the influence of the anaerobic layer is compressed into one term Ψ_{an}. This permits a direct comparison between this contribution and the chemical equilibrium term Ψ_{eq} and the effect of the mineralization processes Θ_a/Da. By taking the limit $Da\to\infty$ in eq.(13), it follows immediately that Ψ_{an} approximates 0 for large values of *Da*. Eq.(12) is equivalent to eq.(6) with $\alpha=\sqrt{Da}$ and $\Psi_b=\Psi_{eq}+\Theta_a/Da+\Psi_{an}$. This analysis shows that the Damköhler-number, expressing the combined effect of the reaction kinetics, diffusion and the oxygen penetration depth, determines the benthic flux Φ_0 to a large extent.

To set up a mass balance for inorganic phosphorus in the aerobic layer (P_{in}), the flux of dissolved P across the aerobic-anaerobic interface J_1 (Fig. 1) has to be calculated too. The expression for the dimensionless flux $\Phi_1=J_1\cdot H/(C_0\cdot D)$ is obtained by solving eq.(7) for the first derivative at $\lambda=1$:

$$\Phi_1=-\varphi\cdot\frac{\partial\Psi}{\partial\lambda}\Big|_{\lambda=1}=\frac{\varphi\cdot\sqrt{Da}}{\tanh\sqrt{Da}}\cdot$$

$$\cdot(\Psi_{eq}+\frac{\Theta_a}{Da}-\Psi_1+\frac{1-\Psi_{eq}-\frac{\Theta_a}{Da}}{\cosh\sqrt{Da}}) \qquad (14)$$

This equation is comparable to eq.(10). For small values of *Da*, eq. (14) is approximated by:

$$\Phi_1=\varphi\cdot(1+\tfrac{1}{2}\Theta_a-\Psi_1)$$

comparable to eq.(11a). In the other extreme, if *Da* is large

$$\Phi_1\approx\varphi\cdot\sqrt{Da}\cdot(\Psi_{eq}+\Theta_a/Da-\Psi_1),$$

comparable to eq.(11b). Also for Φ_1 it may be concluded that the *Da*-number is an important parameter.

4. ANALYSIS OF SOME MODEL ASSUMPTIONS

The most general assumptions underlying the above model equations are discussed in detail by BERNER (1980) and will not be treated here. To check quantitatively the validity of the more specific assumptions for applications to the western Wadden Sea, the relevant parameter values have to be estimated. In Table 1 the orders of magnitude are listed. It is obvious that the apparent diffusion coefficient D in the sediments of the western Wadden Sea is much larger than the molecular one (approximately $6 \cdot 10^{-10} m^2 \cdot s^{-1}$), bioturbation and dispersion due to bottom swell and tidal currents most likely being the major phenomena (RUTGERS VAN DER LOEFF, 1981). The value of H, estimated from ANDERSEN & HELDER (1987) is in accordance with other measurements in marine and estuarine sediments (*e.g.* SØRENSEN *et al.*, 1979 REVSBECH *et al.*, 1980; HELDER & BAKKER, 1985; JØRGENSEN & REVSBECH, 1985).

4.1. NEGLECTING ADVECTION

In Appendix 2 it is shown that advection can be ignored because:

$$\frac{Pe^2}{Da} = \omega^2 \cdot (K \cdot D)^{-1} \ll 4$$

According to the parameter values listed in Table 1 this requirement is fulfilled.

4.2. STEADY STATE ASSUMPTION

To check the validity of the steady state assumption eq.(2) has to be solved dynamically. From the solution in Appendix 3 it is concluded that the time t_a needed for the concentration profile in the aerobic layer to adapt itself to new conditions in the overlying water is given by:

$$t_a \approx \frac{3}{(K + \pi^2 \cdot D \cdot H^{-2})}$$

According to the parameter values listed in Table 1, t_a is in the order of minutes or hours (10^2 to 10^4 seconds), on average about half an hour. Although some fluctuations in C_0 may occur on the same time-scale or even faster, the time constants of the major variations are of the order of at least days. Moreover, the fast fluctuations will generally not be the main object of ecological models like EMOWAD. So the conclusion that the steady state is a valid assumption seems to be justified.

4.3. NEGLECTING TRANSFER RESISTANCE IN THE BENTHIC SUBLAYER

Strictly speaking, in eq.(1) C_0 is the concentration just at the sediment-water interface. Only if the resistance against mass-transfer in the sublayer above the bottom surface is low compared to the resistance within the sediment, may C_0 be approximated by the bulk concentration. However, many recent papers (SCHINK & GUINASSO, 1977; BOUDREAU & GUINASSO, 1982; SANTSCHI *et al.*, 1983; HALL, 1984; JØRGENSEN & REVSBECH, 1985; SUNDBY *et al.*, 1986) indicate

TABLE 1

Order of magnitude of the parameters in the basic concept.
*using the model outlined in the text and assuming $H = 5 \cdot 10^{-3}$ m.

parameter	*value*	*reference*
D	$10^{-9} - 10^{-8}$ $m^2 \cdot s^{-1}$	RUTGERS VAN DER LOEFF (1981)
K	$10^{-4} - 10^{-3}$ s^{-1}	BRINKMAN & VAN RAAPHORST (1986) KELDERMAN (1984) *
K_m	$10^{-6} - 10^{-5}$ $m \cdot s^{-1}$	BRINKMAN & VAN RAAPHORST (1986) KELDERMAN (1984) *
H	$10^{-3} - 10^{-2}$ m	ANDERSEN & HELDER (1987)
ω	$10^{-9} - 10^{-10}$ $m \cdot s^{-1}$	VAN DER GOES *et al.* (1980)
Pe	$10^{-5} - 10^{-3}$	——
Da	$10^{-1} - 10^{+1}$	——

that the resistance in the sublayer cannot always be ignored. Writing C_{ov} as the concentration in the overlying water far from the sediment-water interface [M·L^{-3}] and K_{ms} as the mass-transfer coefficient in the sublayer [L·T^{-1}], the flux across the sublayer becomes $K_{ms}\cdot(C_{ov} - C_0)$. By setting this flux equal to J_0 (eq.1) it can easily be shown that (*cf.* BIRD *et al.*, 1960; LEVENSPIEL, 1962):

$$J_0 = \frac{\varphi \cdot K_m \cdot K_{ms}}{\varphi \cdot K_m + K_{ms}} \cdot (C_{ov} - C_b) \qquad (15)$$

In case $K_{ms} \gg \varphi \cdot K_m$, eq.(14) is equivalent to eq.(1) with $C_0 = C_{ov}$, in the opposite $J_0 = K_{ms}\cdot(C_{ov} - C_b)$.

The transfer across the sublayer is a function of the hydrodynamics near the sediment surface. As in BOUDREAU & GUINASSO (1982) K_{ms} is estimated from:

$$K_{ms} \approx \gamma \cdot u_* \cdot Sc^{-0.67} \qquad (16)$$

in which the dimensionless constant $\gamma = 0.04 - 0.08$, the friction velocity u_* in shallow water $\approx 10^{-2}$ m·s^{-1} and the Schmidt-number Sc is estimated at 10^2 to 10^3. Hence K_{ms} is in the order of $8\cdot10^{-6}$ to $2\cdot10^{-5}$ m·s^{-1}. Assuming $\varphi = 0.5$ for sandy sediments, K_{ms} is approximately 10 times larger than $\varphi \cdot K_m$ (Table 1). The conclusion is that the resistance in the sublayer will have only a minor effect on the benthic P-fluxes, and hence eq.(1) may be applied with $C_0 = C_{ov}$.

5. APPLICATION TO EMOWAD

5.1. AREA DESCRIPTION

The western Wadden Sea is separated from the rest of the Wadden Sea by the tidal watershed south of the island of Terschelling (Fig. 3), and is connected to the North Sea by two major tidal inlets: Marsdiep south of the island of Texel and Vliestroom between the islands of Vlieland and Terschelling. The small inlet between Texel and Vlieland is separated from the main part of the western Wadden Sea by a tidal watershed, and is of minor importance to the system. The freshwater input from the adjacent Lake IJssel is mainly discharged into the North Sea via the Marsdiep. The area is divided into two major basins: the Marsdiep-basin in the west and the Vlie basin associated with the Vliestroom tidal inlet. The total surface area of the estuary is

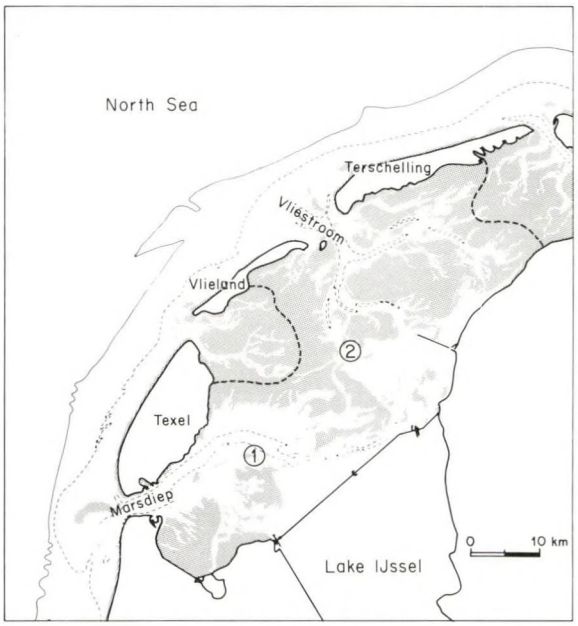

Fig. 3. Map of the western part of the Dutch Wadden Sea. 1: Marsdiep basin, 2: Vlie basin. ---- Tidal watershed.

$1415\cdot10^6$ m^2 (32% intertidal, 53% subtidal, 15% tidal channels). The mean depth is approximately 3.3 m.

5.2. RELEVANT CHARACTERISTICS OF EMOWAD

For the basic structure of EMOWAD, *i.e.* an extended form of an ecosystem model derived for the Ems Estuary, see BARETTA & RUARDIJ (1988). Principally the EMOWAD model expresses all biomasses and transformations in terms of organic carbon. Nutrients (P and Si; N is not included) are modelled only in so far as they affect primary production. The western Wadden Sea is divided into 12 compartments to permit the inclusion of lateral variations (see VAN DUYL & KOP (1988) and VELDHUIS *et al.* (1988)). In each compartment three different areas are distinguished: channel beds, subtidal areas, and intertidal flats (Table 2).

The benthic P-regeneration is computed according to the concept outlined in the previous sections. The lower boundary of the anaerobic layer (Fig. 1) is set at 0.3 m below the sediment-water interface. First, each time-step a mass balance is set up to calculate in both the aerobic and the

TABLE 2

Definitions and main properties of the benthic areas in the EMOWAD model.

channel beds	definition:	level >5 m below Mean Low Tide Level (MLTL)
	properties:	chemically and biologically inert, hence no P-regeneration
subtidal areas	definition:	MLTL >level ⩽5 m below MLTL
	properties:	submerged, no benthic primary production, P-regeneration 24h per day
intertidal flats	definition:	level ⩾ MLTL
	properties:	emerged during a part of the day, benthic primary production only while emerged, P-regeneration only while submerged

anaerobic layer the total amount of inorganic phosphorus available for adsorption/desorption (P_{in} and $P_{in,1}$ respectively). Next the P-flux across the sediment-water interface is calculated from eq.(12), see Appendix 4. The depth of the aerobic layer H, as well as the apparant diffusion coefficient D, is calculated each time-step. The main concepts on their calculation are listed in Table 3, for details see BARETTA & RUARDIJ (1988).

The order of magnitude of K is mentioned in the previous section: 10^{-3} to 10^{-4} s^{-1}, in EMOWAD $K = 3.5 \cdot 10^{-4}$ $s^{-1} = 30$ day^{-1} for both the subtidal and the intertidal sediments. Together with the typical values for the oxygen penetration depth H and for the diffusion coefficient D (listed in Table 3), this results in *Da*-numbers ranging from 0.4 and 3.9 in summer to 5.8 and 23 in winter for the subtidal and the intertidal areas, respectively. The partition coefficient PC is estimated at 750, again for both sediment types. This value is in accordance with the experimental results of BRINKMAN & VAN RAAPHORST (1986) for Lake Veluwe sediments. PC_1 is estimated at 2.5, in accordance with the data given by KROM & BERNER (1980).

5.3. RESULTS AND DISCUSSION

The model was run throughout 1986. In Fig. 4 some results are presented for compartment 10 in the central part of the Vlie basin. The tidal flats of this compartment are submerged for approximately 75% of the day; hence in these areas the daily averaged transfer coefficients and release rates are approximately a factor 0.75 lower than the momentary rates. The simulated fluxes are within the range that can be obtained from the references mentioned in the introduction. In comparable intertidal sediments of the Ems Estuary RUTGERS VAN DER LOEFF *et al.* (1981) measured fluxes between 0 and 1 $mmol \cdot m^{-2} \cdot d^{-1}$ in winter and summer, respectively. The simulated values of the mass transfer coefficient K_m (Fig. 4b) are in agreement with the

TABLE 3

Concepts and main properties of diffusion, oxygen penetration depth, and *Da*-numbers in the EMOWAD model.

concept	*properties*
apparent diffusion-coefficient D	Determined by storm-induced mixing, tidal pumping, bioturbation and bio-irrigation by deposit feeders, suspension feeders, meiobenthos and epibenthos. Typical values: 2.10^{-8} $m^{-2} \cdot s$ in summer 6.10^{-9} $m^{-2} \cdot s$ in winter
oxygen penetration depth H	Determined by oxygen production by benthic diatoms, consumption due to mineralization in the aerobic layer, by sulphide oxidation at the aerobic-anaerobic interface, and by the capacity to match the oxygen demand by diffusion across the sediment water interface. Typical values: 5.10^{-3} to 10.10^{-3} m (subtidal) 15.10^{-3} to $20.10.^{-3}$ m (intertidal) (summer and winter, respectively)
Da-numbers	subtidal: 0.4 (summer), 5.8 (winter) intertidal: 3.9 (summer), 23 (winter)

experimental data of BRINKMAN & VAN RAAPHORST (1986) for Lake Veluwe and those of KELDERMAN (1984) for Lake Grevelingen (0.02 to 0.10 m·d^{-1}). Unfortunately there are no data at hand to compare these simulation results with experimental data obtained in the Wadden Sea. The differences in the *Da*-numbers (Table 3) are directly reflected in the contributions to C_b (Fig. 4c). In winter *Da* is large and for the intertidal areas eq.(11b) applies. In this period C_{eq} is the dominating contribution to C_b. In summer the other factors become more important. In the subtidal sediments *Da* then becomes very small and consequently the contribution from the anaerobic layer is most important during this time of the year. At the end of March C_{eq} increases due to the mineralization of organic phosphorus compounds accumulated in the sediments during the preceding months. In early summer there is a strong decrease in C_{eq}, and hence also in P_{in}. This means that phosphorus accumulated in winter and spring is released in summer. The simulation results suggest a net loading of the sediments with phosphorus in winter and a net release to the water column in June and July. This pattern is in agreement with the data of POSTMA (1954) and DE JONGE & POSTMA (1974). From the occurrence of spring minima and summer maxima in the concentrations of phosphorus components in the water column of the Wadden Sea, they concluded that organic phosphorus is mineralized and released as inorganic phosphates during the summer. The model results suggest that part of these phosphates are adsorbed to the sediment particles, and thus are retained temporarily within the sediment.

The characteristic benthic concentration $C_b = C_{eq} + P_m/K + C_{an}$ (eq.(A8), Appendix 4) averaged over the period October-March is computed by the model at 3.4 and 3.1 mmol·m^{-3} for the subtidal and intertidal areas, respectively. The corresponding values for spring and summer (April to September) are 9.3 and 4.5 mmol·m^{-3} respectively. These results are in fairly good agreement with the data of RUTGERS VAN DER LOEFF (1980a). In the upper cm of the sediment of subtidal area in the western Wadden Sea he observed P-concentrations in the pore water < 10 mmol·m^{-3}. Only during August and September did he measure concentrations between 10 and 20 mmol·m^{-3}. Data from 4 other locations in the western Wadden Sea (VAN RAAPHORST & KLOOSTERHUIS, unpublished results for 1987) in-

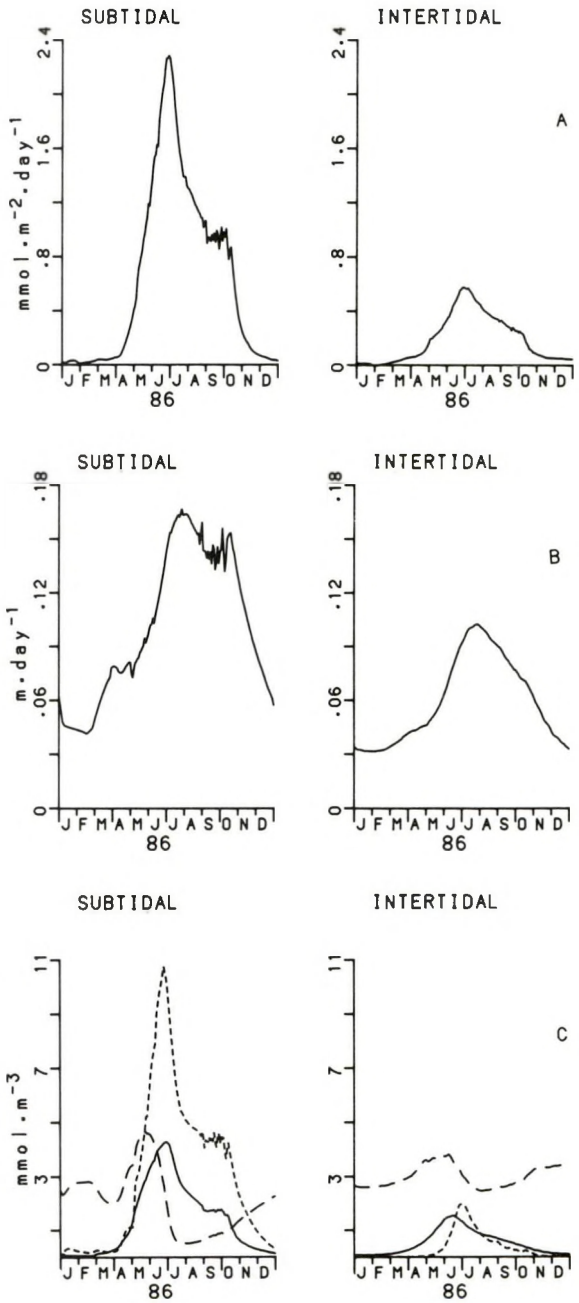

Fig. 4. Results of the standard simulation for compartment 10 in the Vlie basin. A: flux $= p \cdot J_0$ (mmol·m^{-2}·d^{-1}), B: transfer coefficient $p \cdot \varphi \cdot Km$ (m·d^{-1}), C: contributions to the characteristic benthic concentration C_{eq} (mmol·m^{-3}): chemical equilibrium concentration C_{eq} (——), mineralization term Pm/K (____) and the contribution from the anaerobic layer C_{an} (·····). The factor p denotes the fraction of the day the areas are submerged. Subtidal: $p = 1$, intertidal: $p = 0.75$.

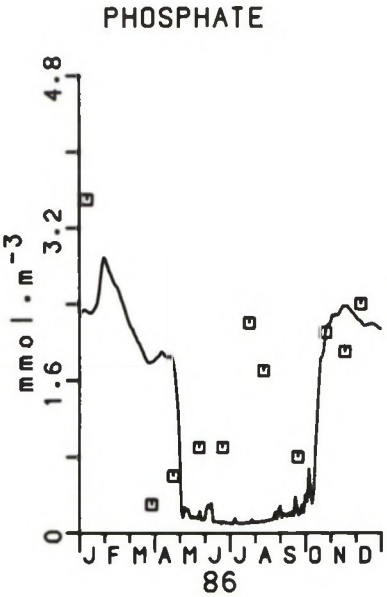

Fig. 5. Dissolved phosphate concentrations in compartment 10 of the Vlie basin (1986). (——) simulation; (□) field observations (data obtained from VELDHUIS *et al.*, 1988).

dicate phosphate concentrations in the pore water of the upper 5 mm of intertidal sediments between 1 and 3 mmol·m^{-3} in winter, and between 2 and 5 mmol·m^{-3} in summer, respectively.

The model predicts too low phosphate concentrations in the overlying water (Fig. 5). Consequently, the flux driving force $C_b - C_0$ is too large, leading to too large fluxes. The discrepancy between field data and simulations is probably due to the absence of another nutrient than P or Si potentially limiting primary production in the EMOWAD model. For instance, inorganic nitrogen concentrations are low from June to September (VELDHUIS *et al.*, 1988) and may limit primary production during that period. Fig. 6 shows the impact of benthic regeneration on three ecological variables of compartment 2 in the Marsdiep basin and compartment 10 in the

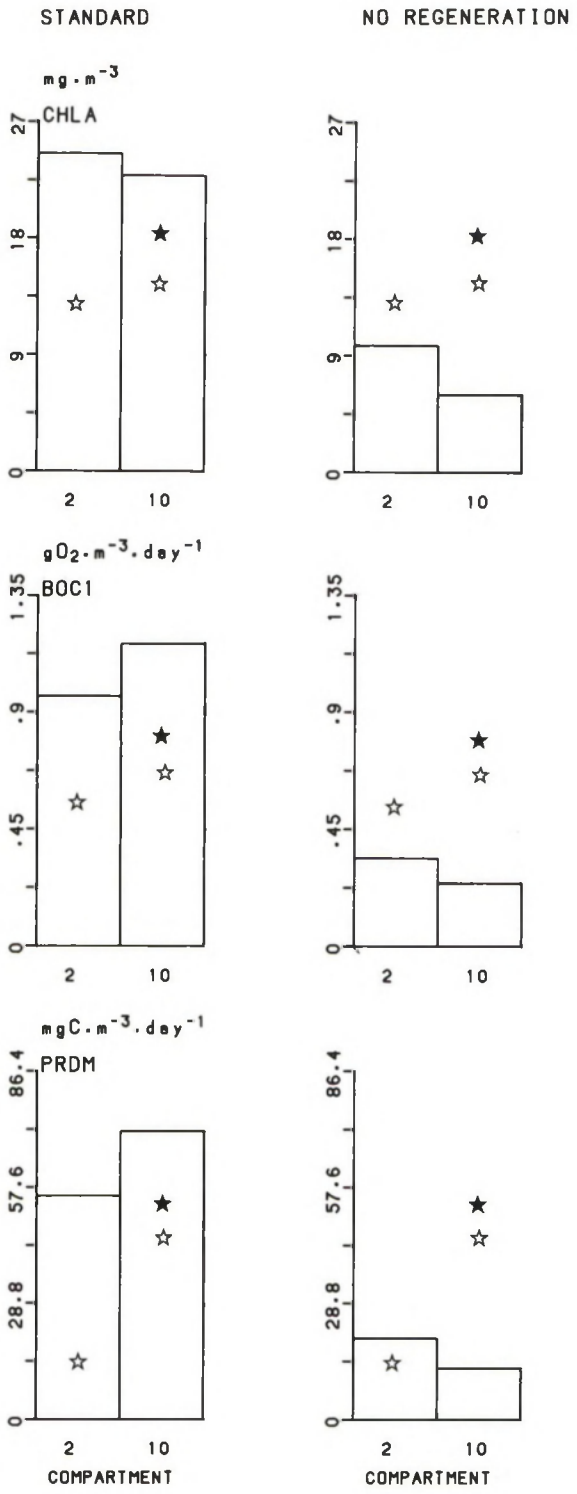

Fig. 6. April-September averaged values separately for compartments 2 and 10 of (top) Chl-*a* (mg·m^{-3}), (middle) pelagic Biological Oxygen Consumption (BOC, $gO_2 \cdot m^{-3} \cdot d^{-1}$) and (bottom) pelagic bacterial production (PRDM, $mgC \cdot m^{-3} \cdot d^{-1}$). (left): simulation including benthic regeneration, (right): simulation without benthic regeneration. Bars denote simulation results. (☆☆) indicate mean field observations in the two total basins, (★★) for compartment 10 in the Vlie basin (1986). Chl-*a* from VELDHUIS *et al.* (1988), BOC and PRDM from VAN DUYL & KOP (1988).

Vlie basin. In Fig. 6a simulations are shown for the standard model including benthic regeneration. The results presented in Fig. 6b are obtained by switching off the regeneration module. Field observations from both basins are given for comparison. Regeneration almost doubles the simulated summer averaged Chl-*a* concentrations, as well as the pelagic Biological Oxygen Consumption (BOC) and the pelagic bacterial production (PRDM). As with the findings of RUTGERS VAN DER LOEFF (1980b), BALZER (1984) and HOPKINSON (1987) for other areas, the conclusion seems justified that benthic regeneration plays an important role in the western Wadden Sea too.

The model computes a yearly averaged flux of approximately 0.6 and 0.2 mmol·m^{-2}·day^{-1} for intertidal and subtidal sediments, respectively. Taking into account the total surface areas, the corresponding gross internal loadings for the western Wadden Sea may be estimated at 90 and 435 kmol·d^{-1}. The model also calculates that on average 134 kmol·day^{-1} are deposited on the tidal flats as organic phosphorus, while 573 kmol·d^{-1} reach the subtidal sediments. The annual mean benthic regeneration efficiency is approximately 70% in both intertidal and subtidal areas. This efficiency does not differ much from that mentioned by BALZER (1984) for the Kiel Bight. In 1986 the total phosphorus input from the freshwater sources to the estuary was 350 kmol·d^{-1}. The total benthic regeneration as computed by the model is of the same order of magnitude (525 kmol·d^{-1}). The net accumulation in the sediments being 182 kmol·d^{-1}, the average output to the North Sea becomes 350 – 182 = 168 kmol·day^{-1}. Hence according to the model, accumulation and output to the North Sea are of equal importance. These figures again demonstrate the potential impact of benthic exchange processes on the phosphorus budget of the western Wadden Sea.

6. CONCLUSIONS

The simple model based on eq.(1), eq.(2) and eq.(3) permits the assessment of the phosphorus regeneration in a complex ecosystem model like EMOWAD. In the model the *Da*-number is the most important parameter. In systems where *Da* is large (>12), chemical processes in the aerobic layer dominate over mineralization and diffusive transport from the anaerobic zone. If *Da* is small (<0.3), adsorption of phosphorus to the sediment particles is less important and mineralization and diffusion from the anaerobic layer determine the benthic P-flux. In the sediments of the western Wadden Sea *Da* varies between 0.5 in the subtidal areas in summer, and 23 in the intertidal areas in winter.

Application of the model to EMOWAD reveals that approximately 70% of the annual amount of phosphorus reaching the sediments is regenerated and released to the overlying water. According to the model, organic phosphorus components accumulated in the sediments during the winter and spring are mineralized and released to the water column during the summer. A part of the inorganic phosphate produced by mineralization is retained temporarily in the sediments due to adsorption processes. The internal loading of the western Wadden Sea is of the same order of magnitude as the external phosphorus inputs.

7. REFERENCES

ALLER, R.C., 1980. Diagenetic processes near the sediment-water interface of Long Island Sound. I. Decomposition and nutrient element geochemistry (S, N, P). In: B. SALTZMAN. Estuarine physics and chemistry: studies in Long Island Sound. Advances in Geophysics **22**, Academic Press, New York: 237-350.

ANDERSEN, F.Ø. & W. HELDER, 1987. Comparison of oxygen microgradients, oxygen flux rates and electron transport system activity in coastal marine sediments.—Mar. Ecol. Prog. Ser. **37:** 259-264.

ARIS, R., 1975. The mathematical theory of diffusion and reaction in permeable catalysts. Vol.1: the theory of the steady state. Clarendon, Oxford: 1-444.

BALZER, W., 1984. Organic matter degradation and biogenic element cycling in a nearshore sediment (Kiel Bight).—Limnol. Oceanogr. **29:** 1231-1246.

BARETTA, J.W. & P. RUARDIJ, 1988. The ecosystem of a tidal flat estuary (simulation and analysis of the Ems estuary). Ecological Studies 70. Springer, Berlin (in press).

BERNER, R.A., 1980. Early diagenesis: A theoretical approach. Princeton Univ. Press, Princeton: 1-241.

BILLEN, G., 1978. A budget of nitrogen recycling in North Sea sediments off the Belgian coast.—Estuar. Coast. Shelf Sci. **7:** 127-146.

BIRD, R.B., W.E. STEWART & E.N. LIGHTFOOT, 1960. Transport phenomena. Wiley, New York: 1-780.

BOUDREAU, B.P. & N.L. GUINASSO JR., 1982. The influence of a diffusive sublayer on accretion, dissolution and diagenesis at the sea floor. In: K.A. FANNING & F.T. MANHEIM. The dynamic environment of the ocean floor. Lexington books, Lexington: 115-146.

BRINKMAN, A.G & W. VAN RAAPHORST, 1986. De fosfaathuishouding in het Veluwemeer (The phosphorus cycle in Lake Veluwe). Ph.D. thesis, Twente Univ. Technology, Enschede: 1-481.

CALLENDER, E. & D.E. HAMMOND, 1982. Nutrient exchange across the sediment water interface in the Potomac river estuary.—Estuar. Coast. Shelf Sci. **15:** 395-413.

DOMENICO, P.A., 1977. Transport phenomena in chemical rate processes in sediments.—Ann. Rev. Earth Planet. Sci. **5:** 287-317.

DUYL, F.C. VAN & A.J. KOP, 1988. Temporal and lateral fluctuations in production and biomass of bacterioplankton in the western Dutch Wadden Sea.—Neth. J. Sea Res. **22:** 51-68.

ECK, G.TH.M. & J.G.C. SMITS, 1986. Calculation of nutrient fluxes across the sediment-water interface in shallow lakes. In: P.G. SLY. Sediments and water interactions. Springer, New York: 289-301.

ELDERFIELD, H., N. LUEDKTKE, R.J. MCCAFFREY & M. BENDER, 1981. Benthic fluxes studies in Narragansett Bay.—Am. J. Sci. **281:** 768-787.

FISHER, T.R., P.R. CARLSON & R.T. BARBER, 1982. Sediment nutrient regeneration in three North Carolina Estuaries.—Estuar. coast. Shelf Sci. **14:** 101-116.

GOES, E.R.F. VAN DER, H. RUNDBERG & G.C. VISSER, 1980. Erosie en sedimentatie in de westelijke Waddenzee. (Erosion and sedimentation in the western part of the Dutch Wadden Sea). Rijkswaterstaat, Studiedienst Hoorn, rapport nr. 79.H002.

HALL, P.O.J., 1984. Chemical fluxes at the sediment-water interface *in situ*; investigations with benthic chambers. Ph.D. Thesis, Univ. Gothenburg, Gothenburg: 1-183.

HELDER, W. & J.F. BAKKER, 1985. Shipboard comparison of micro- and minielectrodes for measuring oxygen distribution in marine sediments.—Limnol. Oceanogr. **30:** 1106-1109.

HOLDREN, G.C. & D.E. ARMSTRONG, 1980. Factors affecting phosphorus release from intact lake sediment cores.—Environm. Sci. Technol. **14:** 79-87.

HOPKINSON JR, C.S., 1987. Nutrient regeneration in shallow-water sediments of the estuarine plume region of the nearshore Georgia Bight, USA.—Mar. Biol. **94:** 127-142.

JAHNKE, R., D. HEGGIE, S. EMERSON & V. GRUNDMANIS, 1982. Pore waters of the central Pacific Ocean: nutrient results.—Earth Planet. Sci. Letters **61:** 233-256.

JONGE, V.N. DE & H. POSTMA, 1974. Phosphorus compounds in the Dutch Wadden Sea.—Neth. J. Sea Res. **8:** 139-153.

JØRGENSEN, B.B. & N.P. REVSBECH, 1985. Diffusive boundary layers and the oxygen uptake of sediments and detritus.—Limnol. Oceanogr. **30:** 111-122.

KAMP-NIELSEN, L., 1974. Mud-water exchange of phosphate and other ions in undisturbed sediment cores and factors affecting the exchange rates.—Arch. Hydrobiol. **73:** 218-237.

——, 1975. Seasonal variation in sediment-water exchange of nutrients in Lake Esrom.—Verh. Int. Ver. Limnol. **19:** 1057-1065.

——, 1980. The influence of sediments on changed phosphorus loading to hypertrophic L. Glumsø. In: J. BARICA & L.R. MUR. Hypertrophic ecosystems. Developments in hydrobiology 2. Junk, The Hague: 29-36.

KAMP-NIELSEN, L., H. MEJER & S.E. JØRGENSEN, 1982. Modelling the influence of bioturbation on the vertical distribution of sedimentary phosphorus in L. Esrom.—Hydrobiologia **91:** 197-206.

KELDERMAN, P., 1984. Sediment-water exchange in Lake Grevelingen under different environmental conditions.—Neth. J. Sea Res. **18:** 286-311.

KLAPWIJK, A. & W.J. SNODGRASS, 1986. Lake oxygen model 3: Simulation of ammonia, nitrate and oxygen in Hamilton Harbor (1977-1978). In: P.G. SLY. Sediments and water interactions. Springer, New York: 265-288.

KLUMP, J.V. & C.S. MARTENS, 1981. Biochemical cycling in an organic rich coastal marine basin. II. Nutrient sediment-water exchange processes.—Geochim. Cosmochim. Acta **45:** 101-121.

KROM, M.D. & R.A. BERNER, 1980. Adsorption of phosphate in anoxic marine sediments.—Limnol. Oceanogr. **25:** 797-806.

LEVENSPIEL, O., 1962. Chemical reactor engineering. An introduction to the design of chemical reactors. Wiley, New York: 1-501.

LIERE, L. VAN & L.R. MUR, 1982. The influence of simulated groundwater-movement on the phosphorus release from sediments, as measured in a continuous flow system.—Hydrobiologia **92:** 511-518.

LIJKLEMA, L. & A.H.M. HIELTJES, 1982. A dynamic phosphate budget model for a eutrophic lake.—Hydrobiologia **91:** 227-233.

POSTMA, H., 1954. Hydrography of the Dutch Wadden Sea.—Archs néerl. Zool. **10:** 405-511.

QUIGLEY, M.A. & J.A. ROBBINS, 1986. Phosphorus release processes in nearshore southern Lake Michigan.—Can. J. Fish. Aquat. Sci. **43:** 1201-1207.

RAAPHORST, W. VAN & A.G. BRINKMAN, 1984. The calculation of transport coefficients of phosphate and calcium fluxes across the sediment-water interface, from experiments with undisturbed sediment cores.—Wat. Sci. Technol. **17:** 941-951.

REVSBECH, N.P., J. SØRENSEN, TH.H. BLACKBURN & J.P LOMHOLT, 1980. Distribution of oxygen in marine sediments measured with micro-electrodes.—Limnol. Oceanogr. **25:** 403-411.

RUTGERS VAN DER LOEFF, M.M., 1980a. Time variation in interstitial nutrient concentrations at an exposed subtidal station in the Dutch Wadden Sea.—Neth. J. Sea Res. **14:** 123-143.

——, 1980b. Nutrients in the interstitial waters of the Southern Bight of the North Sea.—Neth. J. Sea Res. **14:** 144-171.

——, 1981. Wave effects on sediment water exchange in a submerged sand bed.—Neth. J. Sea Res. **15:** 100-112.

RUTGERS VAN DER LOEFF, M.M., F.B. VAN ES, W. HELDER & R.T.P. DE VRIES, 1981. Sediment water ex-

changes of nutrients and oxygen on tidal flats in the Ems-Dollard Estuary.—Neth. J. Sea Res. **15:** 113-129.

SANTSCHI, P.H., P. BOWER, U.P. NYFFELER, A. AZEVEDO & W.S. BROECKER, 1983. Estimates of the resistance to chemical tranport posed by the deep-sea boundary layer.—Limnol. Oceanogr. **28:** 899-912.

SCHINK, D.R. & N.L. GUINASSO, 1977. Modelling the influence of bioturbation and other processes on calcium carbonate dissolution at the sea floor. In: N.R. ANDERSEN & A. MALAHOFF. The fate of fossil fuel CO_2in the oceans, Plenum, New York: 455-478.

SØRENSEN, J., B.B. JØRGENSEN & N.F. REVSBECH, 1979. A comparison of oxygen, nitrate and sulfate respiration in coastal marine sediments.—Microbial Ecol. **5:** 105-115.

SUNDBY, B., L.G. ANDERSON, P.O.J. HALL, A. IVERFELDT, M.M. RUTGERS VAN DER LOEFF & S.T.G. WESTERLUND, 1986. The effect of oxygen on release and uptake of cobalt, manganese, iron and phosphate at the sediment-water interface.—Geochim. Cosmochim. Acta **50:** 1281- 1288.

VELDHUIS, M.J.W., F. COLIJN, L.A.H. VENEKAMP & L. VILLERIUS, 1988. Phytoplankton primary production and biomass in the western Wadden Sea (The Netherlands); A comparison with an ecosystem model.—Neth. J. Sea Res. **22:** 37-49.

(received 22 December 1987; revised 29 February 1988)

APPENDIX 1.
Solutions for extreme *Da*-numbers.

In case of small *Da*-numbers the first order term in eq.(7) may be neglected. Neglecting the advection term too, eq.(7) becomes:

$$0 = \frac{\partial^2 \Psi}{\partial \lambda^2} + \Theta_a \qquad \text{(A1)}$$

With the boundary conditions given in eq.(9) the solution of eq.(8) and eq.(A1) is:

$$\Phi_0 = \varphi \cdot (1 - \tfrac{1}{2} \Theta_a \cdot \Psi_1) \qquad \text{(A2)}$$

In fact this is the solution to the situation without any (first order) chemical reaction. The expression for the other extreme (*Da* large), given in eq.(11b), can be obtained directly from eq.(10) taking the extreme limit $Da \rightarrow \sim$. This extreme may be interpreted as the solution to situations without an anaerobic layer, which may be demonstrated by taking

$$\Phi(0) = 1;\ \lambda \rightarrow \infty: \frac{\partial \Psi}{\partial \lambda} \rightarrow 0 \qquad \text{(A3)}$$

as boundary conditions instead of eq.(9), and subsequently solving eq.(7) and eq.(8).

APPENDIX 2.
Neglecting advection.

The general solution of eq.(7) is

$$\Psi = \Psi_{eq} + \frac{\Theta_a}{Da} + A \cdot e^{\mu_1 \lambda} + B \cdot e^{\mu_2 \lambda} \qquad \text{(A4)}$$

where

$$\mu_{1,2} = \frac{Pe \pm \sqrt{(Pe^2 + 4Da)}}{2}$$

and where *A*, *B* are integration constants. From the expression for $\mu_{1,2}$ it immediately follows that *Pe* may be ignored if $\frac{Pe^2}{Da} \ll 4$.

APPENDIX 3.
Adaptation time.

Writing the dimensionless time $\tau = \frac{t \cdot D}{H^2}$, ignoring advection, and substituting

$\xi = \Psi - \Psi_{eq} - \frac{\Theta_a}{Da}$, eq.(2) becomes:

$$\frac{\partial \xi}{\partial \tau} = \frac{\partial^2 \xi}{\partial \lambda^2} - Da \cdot \xi \tag{A5}$$

If the steady state solution of eq.(7) is taken as the initial condition, say $f(\lambda)$, and if $g(\lambda)$ is the new profile after changing the boundary condition at $\tau = 0$, the solution of eq.(A5) takes the form:

$$\xi(\lambda, \tau) = g(\lambda) + \sum_{n=1}^{\infty} b_n \cdot exp[-(Da + n^2 \cdot \pi^2) \cdot \tau] \cdot \sin(n \cdot \pi \cdot \lambda) \tag{A6a}$$

and

$$b_n = \int_0^1 [f(\lambda) - g(\lambda)] \cdot \sin(n \cdot \pi \cdot \lambda) \cdot d\lambda \tag{A6b}$$

The second term in eq.(A6a) fully describes the transient state of ξ and thus of Ψ and C. The dynamics are determined by the exponential terms. The time needed for the concentration profile to adapt to the new conditions is defined by $\xi(\lambda, \tau_a) \leq 0.05\ \xi(\lambda, 0)$. Taking as criterion the first term in the series of eq.(A6a), it follows that $\tau_a \approx 3/(Da + \pi^2)$. Again two extreme cases are possible. If $Da \gg \pi^2$, $\tau_a \approx 3/Da$ and hence, by substituting the definitions of Da and τ, the "real-time" constant for adaptation $t_a \approx 3/K$. In this situation diffusion does not affect t_a. On the other hand, if $Da \ll \pi^2$: $\tau_a \approx 3 \cdot \pi^{-2}$ and $\tau_a \approx 0.3 \cdot H^2/D$, independent of K. In the intermediate situation

$$t_a = \frac{3}{(K + \pi^2 \cdot D \cdot H^{-2})}$$

APPENDIX 4.
Input to simulations.

In eq.(12) the P-flux across the sediment-water interface is given in dimensionless form. In the actual model eq.(1) is used. From the definitions of the various dimensionless terms it follows that eq.(1) is equivalent to eq.(12) with:

$$J_0 = \Phi_0 \cdot D \cdot C_0 \cdot H^{-1} \tag{A7}$$

Analogously, $J_1 = \Phi_1 \cdot D \cdot C_0 \cdot H^{-1}$. All concentrations follow from multiplication of Φ with C_0:

$$C_b = (\Psi_{eq} + \frac{\Theta_a}{Da} + \Psi_{an})\ C_0 = C_{eq} + \frac{P_m}{K} + C_{an} \tag{A8}$$

It should be noted that the contribution of the mineralization rate P_m to the concentration C_b is given by the ratio between this rate and the first order adsorption rate K.

Netherlands Journal of Sea Research
22 (1): 37-49 (1988)

PHYTOPLANKTON PRIMARY PRODUCTION AND BIOMASS IN THE WESTERN WADDEN SEA (THE NETHERLANDS); A COMPARISON WITH AN ECOSYSTEM MODEL*

M.J.W. VELDHUIS[1, 2], F. COLIJN[3], L.A.H. VENEKAMP[1, 2] and L. VILLERIUS[2, 1]

[1]*Netherlands Institute for Sea Research, P.O. Box 59, 1790 AB Den Burg, Texel, The Netherlands*

[2]*Department of Marine Biology, University of Groningen, P.O. Box 14, 9750 AA Haren, The Netherlands*

[3]*Tidal Water Division (DGW), Ministry of Transport and Public Works, P.O. Box 20904, 2500 EX Den Haag, The Netherlands*

ABSTRACT

Dissolved nutrient concentrations (Si, P, N), algal biomass (separated into diatoms and microflagellates), and total primary production were determined in 1986 during 7 cruises in both the inner and outer parts of the estuary of the western Wadden Sea. The biomass data, obtained after converting cell biovolume and cell counts into carbon, were compared with those simulated by a two-dimensional multitrophic ecosystem model.

The general pattern of the succession of algal species was the same for all compartments: a bloom of diatoms in early spring followed by one of microflagellates, predominantly the colonial alga *Phaeocystis pouchetii*. Throughout the year the biomass of the two algal groups differed between inner and outer compartments of the estuary. In spring the carbon biomass of the microflagellates in the compartments bordering on the North Sea exceeded that of the inner compartments by a factor of 2. The reverse was found for the diatoms in summer.

A reasonable fit between the field data and simulated data was only obtained in spring; large differences were found for the summer period. During that period an extensive diatom population characterized by a low primary production was observed, which did not correspond with the model simulation.

Possible factors causing the differences between observed and simulated data, such as nutrient regeneration, were analysed.

1. INTRODUCTION

The Dutch Wadden Sea is characterized by a complex tidal system (Fig. 1). It consists of various basins separated by shallow areas and each with a different input of freshwater and seawater. One of the systems, the Ems-Dollard estuary, has been the subject of a detailed study resulting in a multitrophic ecosystem model of this area (BARETTA *et al.*, 1988). This model enables us to combine and improve our knowledge of the partitioning of carbon over various state variables and of the carbon flow between various trophic levels of the food web.

Since the Ems-Dollard is only a part of the Wadden Sea, it was of interest to investigate whether or not this model could be used, with or without adaptation, for another area such as the western Wadden Sea. A restriction was that modifications of the original Ems-Dollard model should be kept at a minimum. Nevertheless several adaptations were necessary because of spatial differentiation and different morphological parameters. In contrast to the Ems-Dollard estuary, the western Wadden Sea has different freshwater sources and two main seawater inlets (Fig. 1). A more detailed description of this area is given by RIDDERINKHOF (1988).

The phytoplankton primary production and species composition of the western Wadden Sea has been the subject of a detailed long-term study. The Marsdiep area, one of the tidal inlets from the North Sea, has been studied intensively over the last two decades by CADÉE (1986a and

Publication no. 23 of the project "Ecological Research of the North Sea and Wadden Sea" (EON).

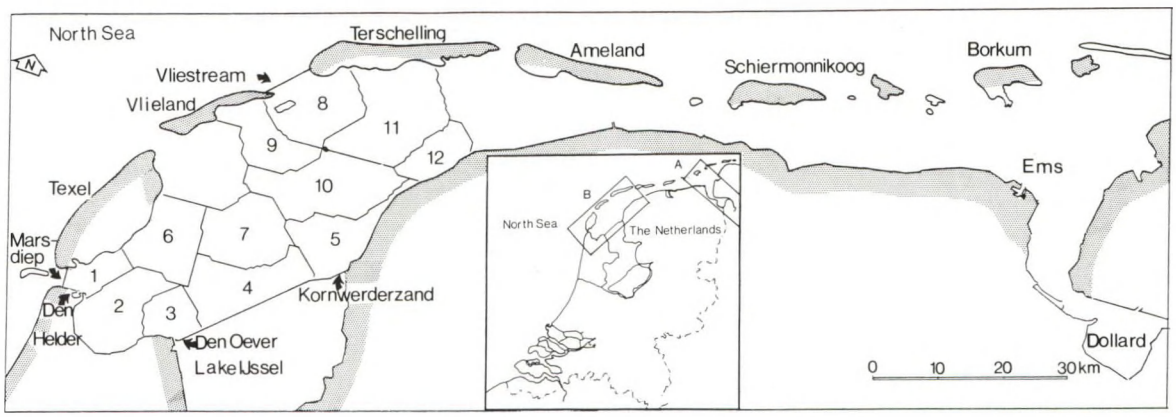

Fig. 1. Location of Ems-Dollard (A) and western Wadden Sea (B) estuary in the northern part of the Netherlands: Map of the western Wadden Sea, location of the compartments, of tidal inlets and freshwater inlets.

b). He showed that the increasing eutrophication of the coastal North Sea zone resulted in a considerable increase in phytoplankton cell numbers and consequently primary production. This increase in the biomass of phytoplankton appeared to be the result of a selective increase in the density of microflagellates. In contrast, cell numbers of the diatoms remained more or less constant (CADÉE, 1986b).

Detailed data for other parts of the western Wadden Sea are not available. This raised the question whether the phytoplankton dynamics in the Marsdiep inlet are representative of the whole western Wadden Sea. This question was examined by comparing new data sets of various parameters, including phytoplankton primary production and composition, of several locations in the western Wadden Sea. These field data were also compared with those generated by the primary producers of an ecosystem model of the western Wadden Sea.

Acknowledgements.—The authors wish to thank W.W.C. Gieskes for his comments on earlier drafts and R. Jalink for drawing some of the figures.

2. MATERIAL AND METHODS

2.1. DESCRIPTION OF THE AREA

A detailed description of the morphology of the western Wadden Sea is given by RIDDERINKHOF (1988). The area is characterized by the presence of two main channel systems for each basin, each with its own seawater inlet (Fig. 1.). The average tidal range is ~1.5 m. On the southern side the western Wadden Sea is bordered by a dyke with two sluices that allow fresh water to enter from Lake IJssel (Kornwerderzand and Den Oever). Most of the water of Lake IJssel originates from the nutrient-rich river Rhine. As a result of this freshwater discharge the salinity ranges from 30 at the seaside down to 10 near the freshwater inlets.

For the model, the Marsdiep basin was divided into 7 compartments (nos. 1-7), while the Vliestream basin had 5 compartments (nos. 8-12). The average water volume of the Marsdiep area is ~1.5 times larger than that of the Vliestream basin. On the other hand, the surface of tidal flats in the latter area is ~40% of the surface, while for the Marsdiep this is only 16%.

2.2. WATER SAMPLING AND CHEMICAL MEASUREMENTS

A total of 7 cruises were carried out during 1986 with the R.V. "Heffesant". Samples were taken at fixed positions in the following compartments: 1, 4, 5, 6, 8, 9, and 10. On two later occasions, in April and June 1987, the tidal variation of several parameters was investigated at a fixed anchor-station in compartment 10. Furthermore, three cruises were made in 1987 with the R.V. "Holland" in the North Sea, in an area bordering on the tidal inlets of the western Wadden Sea, to compare the nutrient dynamics in the two areas. For all chemical and primary production measurements water samples were collected with either a membrane pump or a bottle (30 dm^3) at a depth of ~1.5 m. Subsamples for

pigment-analysis were filtered over Whatman GF/C; these filters were immediately frozen until analysis in the laboratory by means of the HPLC technique. The method used is based on those of MANTOURA & LLEWELLYN (1983) and GIESKES & KRAAY (1986).

Unfiltered samples and filtrates (0.45 μm membrane filters) were collected for nutrient analysis. These samples were analysed with a Technicon Auto Analyzer for inorganic phosphate, ammonia, nitrate and silicate according to standard methods as used by the Tidal Waters Division (DGW) in their monitoring programme.

Samples for the identification of phytoplankton species composition were preserved with Lugols solution buffered with Na$^-$ acetate. Cell counts were carried out after sedimentation, as described by VELDHUIS *et al.* (1986). Phytoplankton biomass was determined by estimating cell number and cell biovolume of the dominant species in preserved samples for each sampling date.

The carbon content of diatoms and other phytoplankton (predominantly microflagellates) was estimated by the following equations (EPPLEY *et al.*, 1970).

$$^{10}\log C = 0.76\ (^{10}\log V) - 0.352 \quad \text{(for diatoms)}$$

$$^{10}\log C = 0.94\ (^{10}\log V) - 0.60 \quad \text{(for microflagellates)}$$

In which
V = mean volume of each species in μm^3
C = mean carbon content of each species in pg per cell.

2.3. ALKALINE PHOSPHATASE ACTIVITY

Assays on the alkaline phosphatase activity (APA) of the phytoplankton were carried out as described in VELDHUIS *et al.* (1987). These measurements were conducted only in 1987 to investigate whether phytoplankton was phosphorus limited in certain parts of the North Sea or western Wadden Sea.

2.4. PRIMARY PRODUCTION

Phytoplankton primary production was measured according to the method used by CADÉE & HEGEMAN (1974). This enables us to make a direct comparison with earlier data from the same area. Triplicate 60 cm^3 subsamples in screw-cap bottles, 2 light and 1 dark, were incubated in a rotating water-cooled incubator for ~3 h. To each bottle 2.5 μCi of $NaH^{14}CO_3$ was added. The samples were incubated at ambient temperature $\pm 1°C$. Light was provided by fluorescent lamps (Philips TLF no. 33) with an irradiance of 0.23 $J \cdot cm^{-2} \cdot s^{-1}$. Filtration and counting procedures were the same as described earlier by VELDHUIS *et al.* (1986). The daily primary production was calculated by the following empirical formula: (after CADÉE & HEGEMAN, 1974, *cf.* COLIJN *et al.*, 1983).

$$P = \tfrac{1}{2}\ P_i \cdot E \cdot D\ (mgC \cdot m^{-2} \cdot d^{-1})$$

P_i = mean incubator primary production (in mg $C \cdot m^{-3} \cdot h^{-1}$)
E = depth of euphotic zone, taken as 3 times the Secchi disc depth (in m)
D = daily light period (in $h \cdot d^{-1}$)

2.5. PHYTOPLANKTON CARBON MODEL

The mathematical ecosystem model used in this study to compare our data set of primary production and carbon content of the phytoplankton is a modification of the Ems-Dollard ecosystem model (BARETTA *et al.*, 1988). The current state variables and the fluxes of the pelagic part of the model are partly described by COLIJN *et al.* (1987). Except for the conversion of the original one-dimensional Ems-Dollard model into a two-dimensional version, the section of the model describing primary producers has not been changed essentially.

3. RESULTS

3.1. ANNUAL VARIATION IN NUTRIENT CONCENTRATION, ALGAL BIOMASS AND PRIMARY PRODUCTION

Fig. 2 shows the annual variation of the mean water temperature and daily irradiance (measured at Den Helder, Fig. 1). During the winter of 1986 considerable parts of the tidal flats were covered with ice, resulting in low water temperatures in February. The total discharge of nutrients (silicate and phosphate) varies with the season, with low values in summer (VAN DER VEER *et al.*, unpubl. ms.). All but the entire discharge of fresh water enters the Marsdiep basin (RIDDERINKHOF, 1988). Mixing and transport processes distribute the freshwater nutrient load

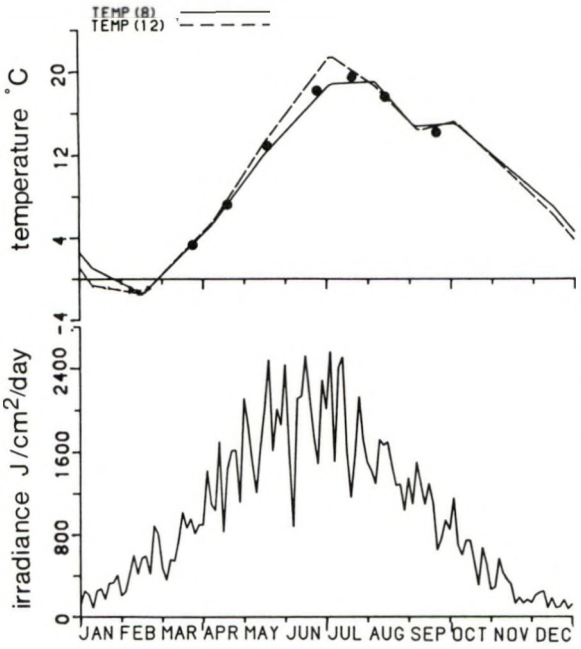

Fig. 2. Model simulations (lines) and measured data (symbols, mean of compartments visited) of annual changes in temperature (top) and measured daily irradiance (bottom).

over the entire Marsdiep basin. An effect of this nutrient-rich freshwater discharge is that the nutrient levels of the compartments bordering on the freshwater inlets (compartments 4 and 5) were slightly higher (Fig. 3) than in those adjacent to the North Sea (compartments 1 and 6).

In spring the silicate and phosphate concentrations, measurements as well as model simulations, declined concurrently (Fig. 3a and b). This decrease was accompanied by an increase in algal biomass (Fig. 4, 5). In contrast, the decrease in inorganic nitrogen seemed somewhat delayed (Fig. 3c). The observed and simulated data for silicate matched not only in spring but also in summer (Fig. 3b). In contrast, from June onwards the measured data of phosphate were much higher than the model simulations (Fig 3b). In the following autumn and winter, data matched again.

Figs 4 and 5 show several measured and simulated phytoplankton parameters of the inner and outer compartments of the Marsdiep and Vliestream basin. The highest measured values in chlorophyll *a* were observed in May/June. In contrast to the Vliestream basin, for many compartments in the Marsdiep basin these high chlorophyll *a* values were related to the presence of diatoms. Microflagellate blooms were always found after the diatom blooms.

Inner and outer compartments differed in the observed carbon biomass of both algal groups over the seasons. A first difference was found for the microflagellate population in spring when the carbon biomass values in the outer compartments exceeded those of the inner compartments considerably (Figs 4c, 5c). A second difference was found in May and June (Figs 4b, 5b); during that period the carbon biomass values of diatoms in the inner compartments were higher than those of the outer compartments.

A comparison of field data with model simulations shows that they were not always in agreement. The most distinct difference was found in summer when field observations showed the presence of a dense diatom bloom in all compartments, which was not simulated by the model.

Measured values for phytoplankton primary production and those predicted by the model were only similar in spring. Values measured in summer were always lower than the simulated production rates: slightly lower for the inner compartments, but up to 8 times lower for the outer

TABLE 1

Annual primary production of the Marsdiep area, in g $C \cdot m^{-2} \cdot y^{-1}$.

Year	*Prim. prod.*	*Reference*	*Remarks*
1963/65	170	POSTMA & ROMMETS, 1970	
1972/73	200	CADÉE & HEGEMAN, 1974	
1974	145	CADÉE & HEGEMAN, 1979	
1981/82	260-340	CADÉE, 1986a	lower value after discarding extreme (high) value in August
1986	303	this study	measurements, extrapolated over the year (Fig. 4D).
1986	453	this study	model simulation.

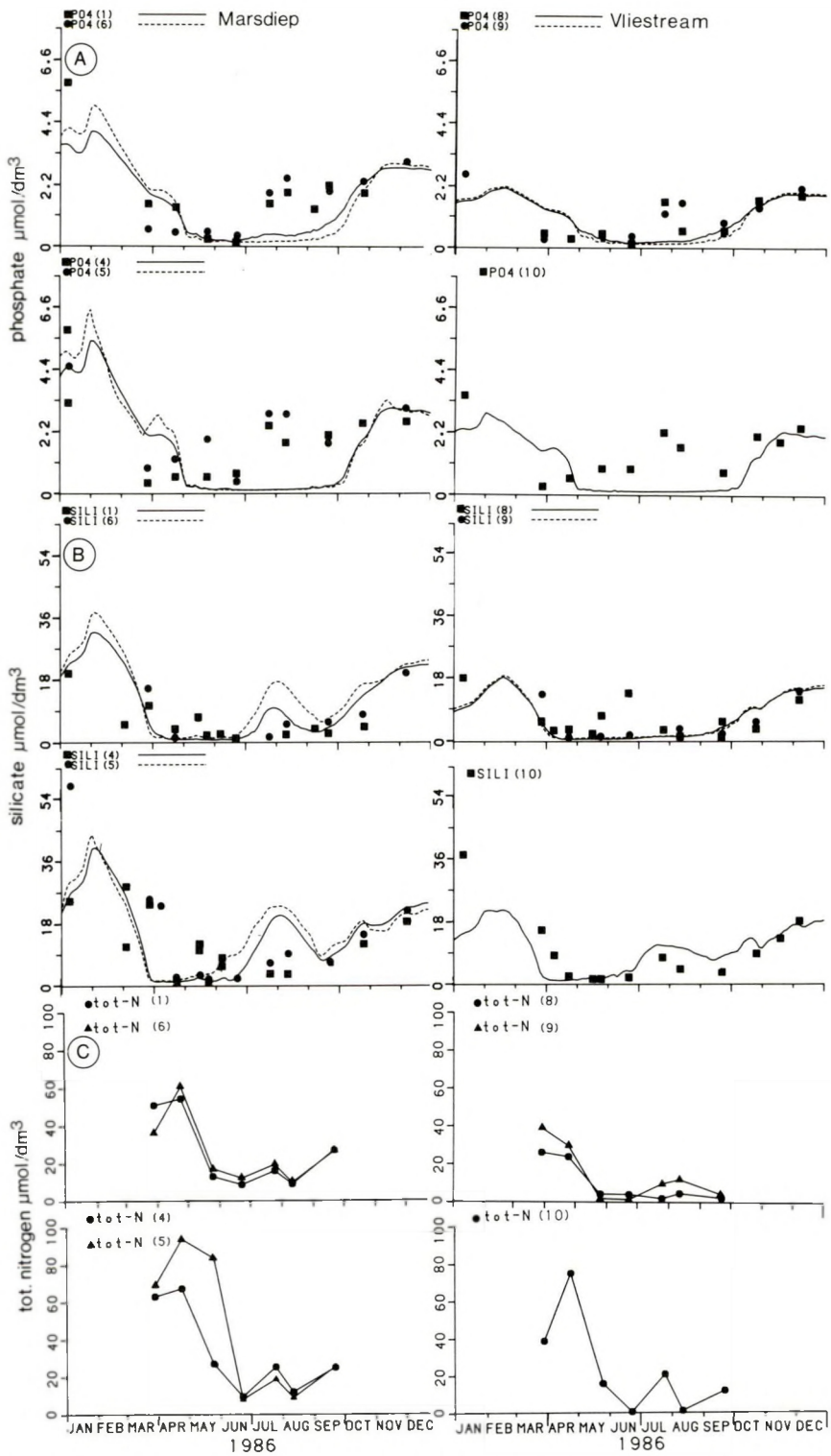

Fig. 3. Model simulation (lines) and measured concentrations (symbols) of (A) inorganic phosphate, (B) silicate and (C) nitrogen (NO_3 + NO_2, only measured data) of a series of selected compartments representing the inner and outer compartments of the Marsdiep and Vliestream basins. Compartment numbers are indicated in brackets (see Fig. 1).

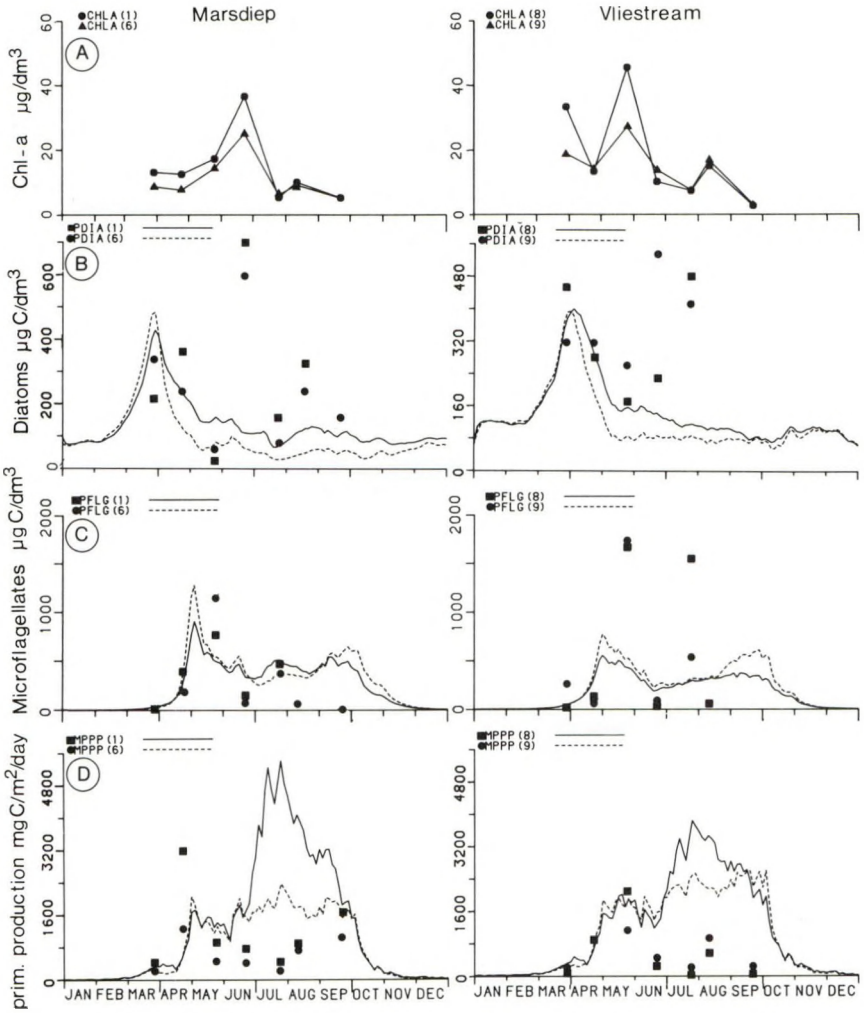

Fig. 4. Annual distribution of (A) Chl. *a* (only measured data), model simulations (lines) and measured data (symbols) of carbon content of (B) diatoms, (C) microflagellates and (D) phytoplankton primary production for the outer compartments of Marsdiep and Vliestream basins. Compartment numbers are indicated in brackets (see Fig. 1).

compartments. Consequently, for most of the compartments the measured annual primary production values were lower than those simulated by the model (Fig. 6). Model simulations demonstrated a decreasing trend from the outer towards the inner compartments of both basins. However, the measurements did not completely confirm this trend.

A comparison with earlier observations in the tidal inlet of the Marsdiep area shows that the measured annual primary production in 1986 was not different from the one calculated for 1981/82 (CADÉE, 1986a, Table 1). On the other hand, the annual primary production generated by the model for 1986 indicated an enhancement in the production by ~50% compared with 1981/82.

3.2. TIDAL VARIATION IN ALGAL BIOMASS AND PRIMARY PRODUCTION

Fig. 7 shows that nutrient concentration and several parameters related to the phytoplankton varied considerably over the tide. Especially in June the variation in phosphate and nitrogen concentration was large, with nutrient levels ranging from limiting to non-limiting conditions for the phytoplankton within one tide. Primary production varied concurrently with the algal cell

numbers. The variation of these parameters amounted to a factor of 2 to 3. Differences in the variation in cell numbers of both algal groups, diatoms (with a cell biovolume of 1000 μm^3 or less) and microflagellates (predominantly *Phaeocystis*) appeared to be remarkably small. To be precise, the measurements of algal biomass and primary production should be corrected for the tide (the model simulates a mean value during half tide). The current observations over 2 complete tidal cycles indicate that in an extreme case the field data of 1986 would vary at most by a factor of 2.

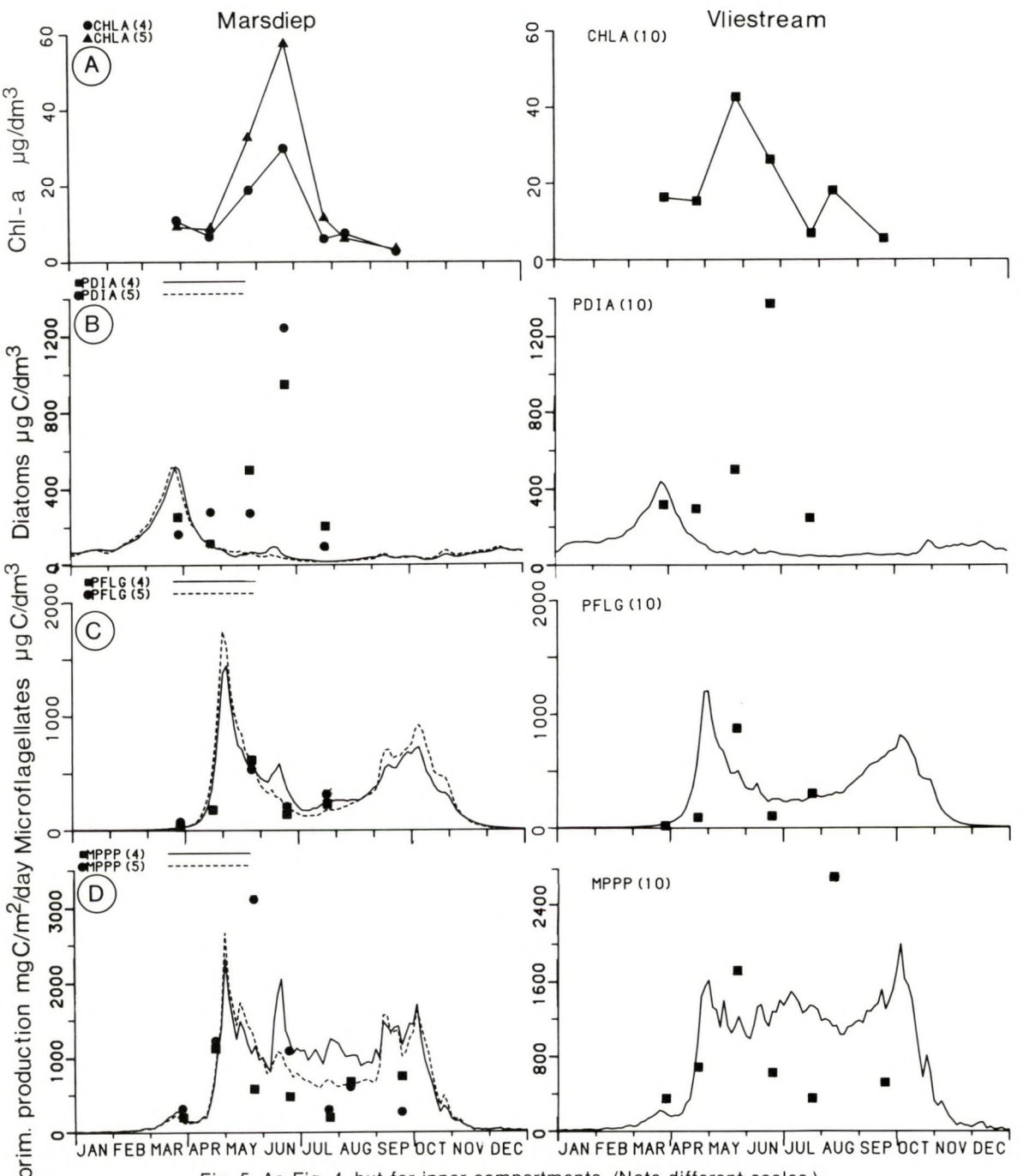

Fig. 5. As Fig. 4, but for inner compartments. (Note different scales.)

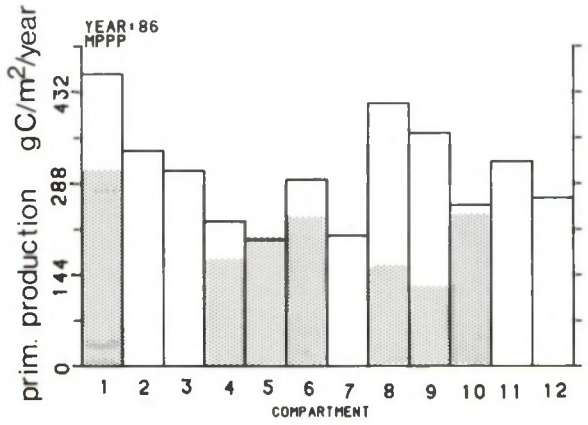

Fig. 6. Model simulations and measurements (shaded) of the annual phytoplankton primary production for all compartments (in g $C \cdot m^{-2} \cdot y^{-1}$).

4. DISCUSSION

By use of a multitrophic ecosystem model, complex relations and fluxes between parts of the marine coastal foodweb can be studied. Models have also received considerable attention as possible tools for improved management and environmental protection. As the results of the simulations of the ecosystem model have been discussed in various papers (VAN DUYL & KOP, 1988; VAN RAAPHORST *et al.*, 1988), we will concentrate on a few details of phytoplankton, primary production and species composition. Special emphasis will be placed on the absence of the summer diatom population, the low primary production of these algae as well as the apparent absence of nutrient limitation.

4.1. FACTORS AFFECTING PHYTOPLANKTON BIOMASS AND PRIMARY PRODUCTION

In a recent paper CADÉE (1986a) summarized the recurrent succession of diatoms and microflagellates (2 to 3 times a year) of the tidal inlet of the Marsdiep basin (compartment 1), over a 16-year period. The year-to-year variation in cell numbers can be considerable. The model simulation (Fig. 8) of the carbon biomass of diatoms (PDIA) and microflagellates (PFLG) shows a pattern rather similar to that for cell numbers of CADÉE (1986a), except for the absence of a summer peak of diatoms. Our field data showed a similar trend, but also with the exception of the high summer values. Minor differences between field data and model simulation in peak values of biomass or onset of growth may be partly due to sampling frequency. Since this was only once a month and phytoplankton peaks can be very sharp (CADÉE, 1986b), the actual onset or true peak values are not known precisely. However, as far as the summer situation is concerned the current state of the model largely underestimates phytoplankton biomass.

Different parameters can be used to estimate phytoplankton biomass (Fig. 9). A direct conversion of chlorophyll *a* or cell number into phytoplankton carbon biomass highly depends on the cellular carbon or chlorophyll *a* content, which must be constant over the whole growing season. High values of chlorophyll *a* often corresponded only with high numbers of diatoms. This implies that the cellular chlorophyll *a* content of both algal groups (diatoms and microflagellates) varies. Therefore, the use of this parameter to estimate the phytoplankton carbon biomass of mixed algal populations, as in our case, would not be reliable. Moreover, while the average cellular biovolume of the flagellates remains more or less constant, that of the diatoms changes considerably over the season. Hence, the use of a single value for the conversion of cell number into carbon biomass will also result in either an over or underestimation of the phytoplankton carbon biomass (*cf.* BANSE, 1977). The present method to estimate phytoplankton carbon biomass solves these problems and is probably more accurate because it includes the variability in cellular carbon content caused by differences in cell size of the various species at each sampling. However, this method is time-consuming and limits the number of samples that can be inspected.

4.2. DISCREPANCIES BETWEEN FIELD DATA AND MODEL SIMULATION

The reasons for the absence of a summer diatom population in the model simulation may be diverse, *e.g.* a high grazing pressure by (micro)zooplankton or the reduction of growth rate as a result of the simulated nutrient limitation in summer (Fig. 3). The effect of nutrient stress (MINU) on the carbon assimilation rate of phytoplankton in the model is shown in Fig. 10. This factor (MINU always $\leqslant 1$) expresses the reduction of the carbon assimilation rate, due to nutrient stress, as compared with non-limited conditions. In microflagellates (PFLG) this MINU

factor is only the effect of phosphate (MIPO4) shortage. In diatoms (PDIA) there is an extra effect of silicate (MISI) limitation. Fig. 10 indicates that in summer the reduction of the model simulation of the carbon assimilation rate is predominantly due to phosphate shortage. The assimilation rate of diatoms, however, is further reduced as a result of silicate limitation; moreover, their photosynthetic response is lower at the high summer temperatures. A further dif-

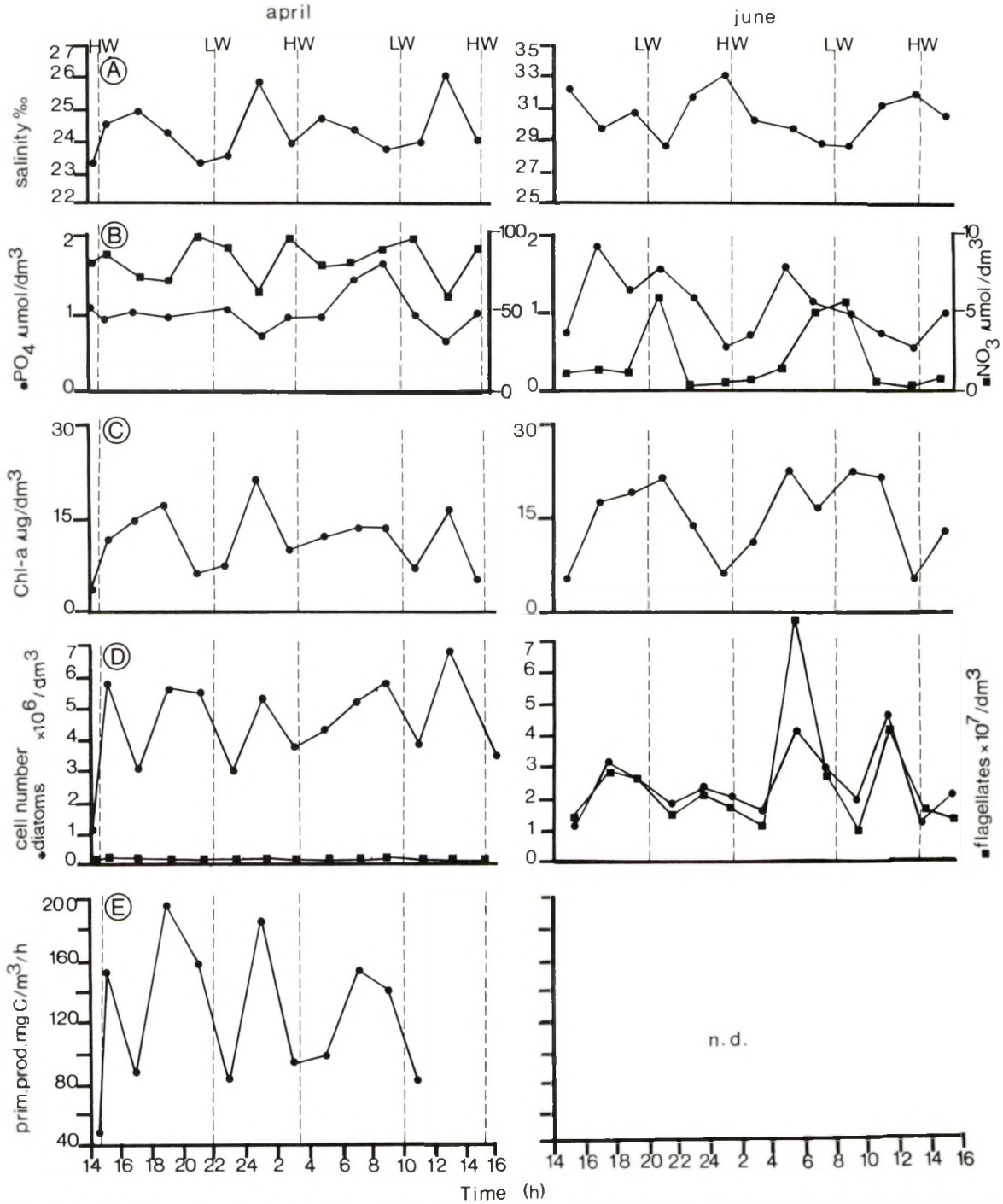

Fig. 7. Daily variation in (A) salinity, (B) nutrient concentrations (phosphate and nitrate), (C) Chl. *a*, (D) total cell number and (E) primary production, at an anchored station in compartment 10. (Note diffent scales for N.)

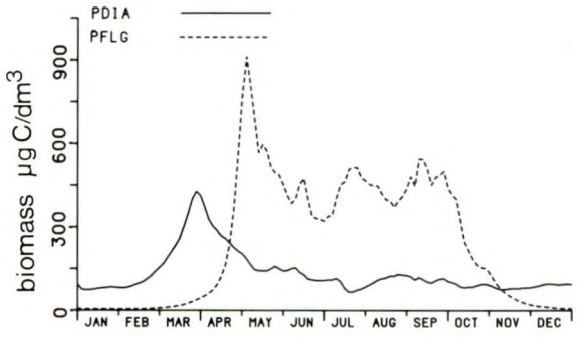

Fig. 8. Model simulation of annual variation of biomass of diatoms (PDIA, full line) and microflagellates (PFLG, interrupted line) for 1986.

ference between the two algal groups is the loss of newly produced phytoplankton caused by predation. In the current state of the model the grazing pressure by microzooplankton on diatoms is relatively high. Ultimately, the overall effect of all selective losses is that the increase in diatom biomass is too low to produce a second bloom in summer. Further study must focus on the simulation of the growth characteristics of summer diatoms, as opposed to spring diatoms, as well as on the regeneration of nutrients during that period.

The actually observed summer values of inorganic phosphate (Fig. 3) suggest that this nutrient does not limit phytoplankton growth. To study the limiting effect of phosphate, the alkaline phosphatase activity (APA) of phytoplankton in the western Wadden Sea and in the North Sea was assessed in the spring and early summer of 1987 (Fig. 11, Table 2). A high APA is an indication of phosphate shortage (PERRY, 1972; CEMBELLA *et al.*, 1983; RIVKIN & SWIFT, 1985; VELDHUIS *et al.*, 1987). Table 2 shows

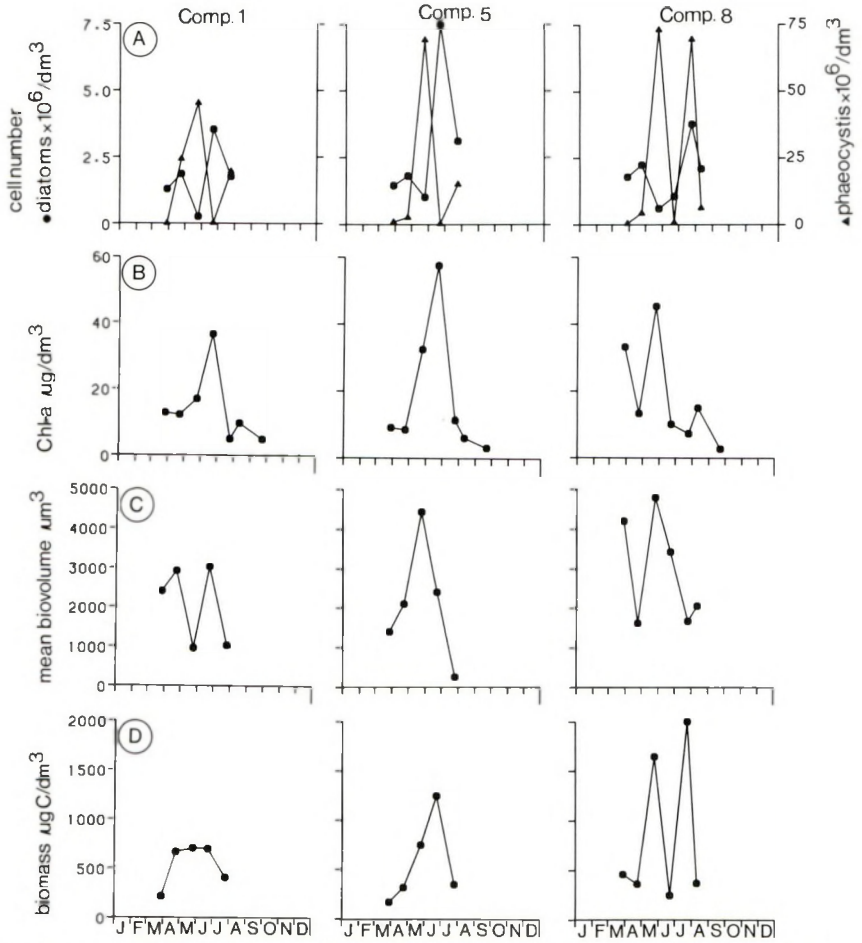

Fig. 9. Comparison of seasonal variation in (A) cell numbers, (B) chl. *a*, (C) mean cell biovolume (only diatoms) and (D) cellular biomass (calculated by using cell number and cell biovolume) for compartments 1, 5 and 8.

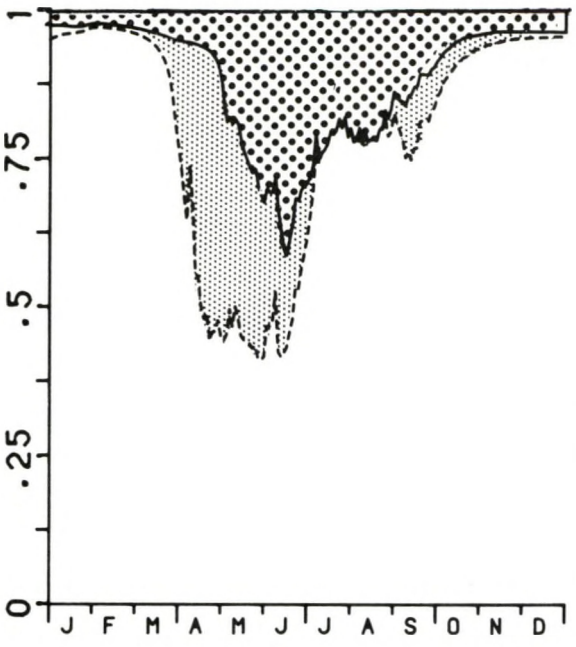

Fig. 10. Phytoplankton carbon assimilation reducing factor MIPO4 (coarse shading): effect of phosphate limitation; MISI (fine shading): effect of silicate limitation. Actual carbon assimilation rate = potential carbon assimilation rate· (MIPO4 + MISI).

Fig. 11. Map showing location of sampling stations in North Sea, near tidal water inlets and position of station in compartment 10 of the western Wadden Sea.

that few trends are clear. The APA of phytoplankton in the North Sea adjacent to tidal inlets is high throughout the summer (*cf.* VELDHUIS *et al.*, 1987). In contrast, phytoplankton in compartment 10 of the western Wadden Sea hardly exhibits APA, confirming earlier studies carried out in compartments 1, 2 and 3 between March and July 1985 (Admiraal, pers. comm.). Table 2 shows that phytoplankton in the western Wadden Sea was not phosphate limited that summer. Therefore, the simulated phosphate limitation by the model does not reflect the actual summer situation in the field. But then the model does not include nitrogen, and concentrations of this nutrient are sometimes relatively low and possibly limiting.

The origin of the high summer values for phosphate is still a matter of controversy (POSTMA, 1954; 1981; VAN DER VEER *et al.*, 1988). The discharge of nutrient-rich fresh water from Lake IJssel seems to be a factor of importance (Fig. 2), but predominantly for the Marsdiep basin (RIDDERINKHOF, 1988). However, this discharge of nutrients by the sluices is included in the model.

In situ regeneration of nutrients in the pelagic and benthic systems may be a major source of

TABLE 2

Chlorophyll *a* concentrations (in $\mu g \cdot dm^{-3}$), PO_4 concentration (in μM) and alkaline phosphatase activity (APA, in nM-P·μg Chl.a·h) of two stations near tidal inlet of the Marsdiep, three near Vliestream inlet and of an anchored station in compartment 10; * highest and lowest value over 24-h measurement.

Date	*station no.*				
23/24 Febr 1987	*26*	*27*	*28*	*29*	*30*
Chl *a*	0.21	0.40	0.10	2.38	1.63
PO_4	0.61	1.45	1.35	1.94	0.96
APA	<0.02	<0.02	<0.02	<0.02	<0.02
18/19 May 1987					
Chl *a*	1.28	13.22	22.21	64.93	11.36
PO_4	0.16	0.13	0.35	0.16	0.19
APA	1.74	5.45	2.34	0.89	3.18
20/21 Juli 1987					
Chl *a*	2.47	3.27	11.70	14.18	9.97
PO_4	0.35	0.35	0.64	1.16	1.00
APA	7.65	0.76	0.18	0.06	0.08
Compartment 10					
6/7 April 1987					
Chl *a*	4.2 - 19.9*				
PO_4	0.6 - 1.42*				
APA	<0.02*				
1/2 June 1987					
Chl *a*	4.3 - 21.1*				
PO_4	0.4 - 1.92*				
APA	0.08 - 0.12*				

nutrients for phytoplankton (HELDER *et al.*, 1983; YAMATA & D'ELIA, 1984; DEGOBBIS *et al.*, 1986; HOPKINSON, 1987). On an annual base sediment effluxes are found to exceed the allochtonous supply of nutrients, up to a factor of 2 to 7.5 (YAMATA & D'ELIA, 1984). HOPKINSON (1987) estimated that the benthic efflux of phosphate can contribute up to 40% of the annual phosphate load. Recent estimates show that this percentage is ~70 for the western Wadden Sea (VAN RAAPHORST *et al.*, 1988). The model does not include this apparently important phosphate source in summer. This may be the explanation of the differences between measured and simulated data during that period.

In summer phytoplankton seems to be characterized by a low assimilation rate (low P/B ratio). Possible artifacts that might affect primary production (SHARP, 1977; MAGUE *et al.*, 1980) have been reduced as much as possible. Also, increased excretion due to nutrient stress, which can account for up to 60% of the total carbon fixed (SHARP, 1977; LANCELOT, 1983), is unlikely. Excretion percentages of ~25 have been estimated for another part of the Wadden Sea, the Ems-Dollard estuary (COLIJN, 1983) and coastal zone of the adjacent North Sea (VELDHUIS *et al.*, 1986). Microscopic observation may explain this low P/B ratio. In freshly collected material 5% of the dominant diatom species (*Rhizosolenia delicatula*) was infected with a parasitic dinoflagellate, but after ~24 h up to 80% showed an infection. Because incubation facilities were not present on board, the incubation experiments were carried out on shore, 12 to 24 h after sampling. Although the role of this infection in phytoplankton assimilation rates is unknown, it might occasionally result in a significant reduction of particulate carbon fixation.

In conclusion: the ecosystem model in its current state gives a fair description of the phytoplankton state variables and primary production in spring. Great improvement of the model is desired for summer conditions. Discrepancies between measurements and simulation are not only due to artifacts of the measurements but also the mathematical description of nutrient regeneration needs to be improved.

5. REFERENCES

BANSE, K., 1977. Determining the carbon-to-chlorophyll ratio of natural phytoplankton.—Mar. Biol. **41:** 199-212.

BARETTA, J.W., P. RUARDIJ, H.G.J. SCHRÖDER, W. ADMIRAAL, M.A. VAN ARKEL, J.G. BARETTA-BEKKER, F. COLIJN, W. EBENHÖH, V.N. DE JONGE, R.W.P.M. LAANE & A. STAM, 1988. The ecosystem of a tidal flat estuary (Simulation and analysis of the Ems estuary); Ecological Studies. Springer, Berlin, Heidelberg: in press.

CADÉE, G.C., 1986a. Increased phytoplankton primary production in the Marsdiep area (western Dutch Wadden Sea).—Neth. J. Sea Res. **20:** 285-290.

——, 1986b. Recurrent and changing seasonal patterns in phytoplankton of westernmost inlet of the Dutch Wadden Sea from 1969 to 1985.—Mar. Biol. **93:** 281-289.

CADÉE, G.C. & J. HEGEMAN, 1974. Primary production of phytoplankton in the Dutch Wadden Sea.—Neth. J. Sea Res. **8:** 240-259.

——, 1979. Phytoplankton primary production, chlorophyll and composition in an inlet of the western Wadden Sea (Marsdiep).—Neth. J. Sea Res. **13:** 224-241.

CEMBELLA, A.D., N.J. ANTIA & P.J. HARRISON, 1983. The utilization of inorganic and organic phosphorus compounds as nutrients by eukaryotic microalgae: a multidisciplinary perspective: Part 1.—Crit. Rev. Microbiol. **10:** 317-391.

COLIJN, F., 1983. Primary production in the Ems-Dollard estuary. Thesis, University of Groningen: 1-123.

COLIJN, F., G.C. CADÉE & J. HEGEMAN, 1983. Comparison between a laboratory incubator technique and *in situ* measurements: measurements of marine phytoplankton. In: F. COLIJN, W.W.C. GIESKES & W. ZEVENBOOM. Problems with the measurement of primary production; conclusions and recommendations.—Hydrobiol. Bull. **17:** 29-51.

COLIJN, F., W. ADMIRAAL, J.W. BARETTA & P. RUARDIJ, 1987. Primary production in a turbid estuary, the Ems-Dollard: field and model studies.—Cont. Shelf Res. **7:** 1405-1409.

DEGOBBIS, D., E. HOMME-MASLOWSHA, A.A. ORIO, R. DONAZZOLA & B. PAVENI, 1986. The role of alkaline phosphatase in the sediments of Venice Lagoon on nutrient regeneration.—Estuar. coast. Shelf Sci. **22:** 425-437.

DUYL, F.C. VAN & A.J. KOP, 1988. Temporal and lateral fluctuations in production and biomass of bacterioplankton in the western Dutch Wadden Sea.—Neth. J. Sea Res. **22:** 51-68.

EPPLEY, R.W., F.M.H. REID & J.D.H. STRICKLAND, 1970. The ecology of the plankton off La Jolla, California in the period through September 1967. Part III. Estimates of phytoplankton crop size, growth rate and primary production.—Bull. Scripps Inst. Oceanogr. **17:** 33-42.

GIESKES, W.W.C. & G.W. KRAAY, 1986. Analysis of phytoplankton pigments by HPLC before, during and after mass occurrence of the microflagellate *Corymbellus aureus* Green during the spring bloom in the open northern North Sea.—Mar. Biol. **92:** 45-52.

HELDER, W., R.T.P. DE VRIES & M.M. RUTGERS VAN DER LOEFF, 1983. Behaviour of nitrogen nutrients and

dissolved silica in the Ems-Dollard Estuary.—Can. J. Fish. aquat. Sci. **40:** 188-200.

HOPKINSON JR., C.S., 1987. Nutrient regeneration in shallow-water sediments of the estuarine plume of the nearshore Georgia Bight, USA.—Mar. Biol. **94:** 127-142.

LANCELOT, C., 1983. Factors affecting phytoplankton extracellular release in the Southern Bight of the North Sea.—Mar. Ecol. Progr. Ser. **12:** 115-121.

MANTOURA, R.F.C. & C.A. LLEWELLYN, 1983. The rapid determination of algal chlorophyll and carotenoid pigments and their breakdown products in natural waters by reverse-phase high-performance liquid chromatography.—Anal. chim. Acta. **151:** 297-314.

MAGUE, T.H., E. FRIBERG, D.J. HUGHES & I. MORRIS, 1980. Extracellular release of carbon by marine phytoplankton: a physiological approach.—Limnol. Oceanogr. **25:** 262-279.

PERRY, M.J., 1972. Alkaline phosphatase activity in subtropical Central North Pacific waters using a sensitive fluorometric method.—Mar. Biol. **15:** 113-119.

POSTMA, H., 1954. Hydrography of the Dutch Wadden Sea.—Archs néerl. Zool. **12:** 319-349.

——, 1981. Exchange of materials between the North Sea and the Wadden Sea.—Mar. Geol. **40:** 199-213.

POSTMA, H. & J.W. ROMMETS, 1970. Primary production in the Wadden Sea.—Neth. J. Sea Res. **4:** 470-493.

RAAPHORST, W. VAN, P. RUARDIJ & A.G. BRINKMAN, 1988. The assessment of benthic phosphate regeneration in an estuarine ecosystem model.—Neth. J. Sea Res. **22:** 23-36.

RIDDERINKHOF, H., 1988. Tidal and residual flows in the western Dutch Wadden Sea I.: numerical model results.—Neth. J. Sea Res. **22:** 1-21.

RIVKIN, R.B. & E. SWIFT, 1985. Phosphorus metabolism of oceanic dinoflagellates: phosphate uptake, chemical composition and growth of *Pyrocystis noctiluca*.—Mar. Biol. **88:** 189-198.

SHARP, J.H., 1977. Excretion of organic matter by marine phytoplankton. Do healthy cells do it ?—Limnol. Oceanogr. **22:** 381-399.

VEER, H.W. VAN DER, W. VAN RAAPHORST & M.J.N. BERGMAN, unpublished manuscript. Eutrophication of the Dutch Wadden Sea. I. Nutrient loadings of the Marsdiep and Vliestroom basin.

VELDHUIS, M.J.W., F. COLIJN & L.A.H. VENEKAMP, 1986. The spring bloom of *Phaeocystis pouchetii* (Haptophyceae) in Dutch coastal waters.—Neth. J. Sea Res. **20:** 37-48.

VELDHUIS, M.J.W., L.A.H. VENEKAMP & T. IETSWAART, 1987. Availability of phosphorus sources for blooms of *Phaeocystis pouchetii* (Haptophyceae) in the North Sea: impact of the river Rhine.—Neth. J. Sea Res. **21:** 219-229.

YAMATA, S.S. & C.F. D'ELIA, 1984. Silicic acid regeneration form estuarine sediment cores.—Mar. Ecol. Progr. Ser. **18:** 113-118.

(received 9 December 1987; revised 21 January 1988)

Netherlands Journal of Sea Research
22 (1): 51-68 (1988)

TEMPORAL AND LATERAL FLUCTUATIONS IN PRODUCTION AND BIOMASS OF BACTERIOPLANKTON IN THE WESTERN DUTCH WADDEN SEA*

F.C. VAN DUYL and A.J. KOP
Netherlands Institute for Sea Research, P.O. Box 59, 1790 AB Den Burg, Texel, The Netherlands

ABSTRACT

To contribute to the validation of a recently developed ecosystem model of the western Wadden Sea (EON, 1988), data on bacterial biomass and production were acquired. Seven field stations, spread over the two main basins of the estuarine system, were sampled monthly in 1986. Between these basins significant differences were found in counts, biovolume, biomass and production of bacteria (measured by the ^{3}H-thymidine method) with consistently higher mean values of bacterial variables in the Vlie basin. Bacterial production rates of 2 to 175 mg C· m^{-3}· d^{-1} were obtained for the Vlie basin, with an annual production of 10 to 11 g C· m^{-3}, while the production in the Marsdiep basin did not exceed 45 mg C·m^{-3} ·d^{-1}, with an annual production of 3 g C·m^{-3}. Bacterial biomass varied over the year from 2 to 140 mg C·m^{-3} in the study area, with a mean biomass of 39 mg C·m^{-3} in the Vlie basin and 23 mg C·m^{-3} in the Marsdiep basin. Blooms of bacteria occurred in May and July-August. Spatial and temporal fluctuations in bacterial variables are discussed, taking into account different environmental factors and the availability of food for bacteria in relation to transport and exchange of water masses between the two basins and the North Sea. Results are compared with the results as simulated by the ecosystem model.

1. INTRODUCTION

Though the Dutch Wadden Sea has been, and still is, the subject of extensive biological studies (for a review see WOLFF, 1983), little research has been done on the distribution and role of bacteria in the system. Attempts to quantify microbial processes and mineralization rates in the Wadden Sea were made on the basis of ATP and ETS measurements (VOSJAN, 1982; VOSJAN & THYSSEN, 1978), sulphate reduction estimates (GROENENDAAL, 1975) and oxygen consumption (VAN ES, 1982; DE WILDE & BEUKEMA, 1984; VOSJAN, 1987). However, relations between these measurements and bacterial activities are still unclear. Improvements in microscopy and chemical techniques have resulted in bacteria-specific methods for measuring biomass of bacteria and production of heterotrophic bacterial populations. The direct-count technique for the determination of biomass (*e.g.* HOBBIE *et al.*, 1977) has already found wide application (VAN ES & MEYER-REIL, 1982), and it is generally recognized that this method now renders the most realistic estimate of numbers and biovolumes of bacteria in natural environments (FUHRMAN, 1981). With methods for measuring production of bacteria more scepticism is justified. Most widely used and already thoroughly tested is the ^{3}H-thymidine method (FUHRMAN & AZAM, 1980, 1982). Conversion factors as well as the degree of participation of the ^{3}H-thymidine in the incorporation of bacterial DNA have been the subject of ample discussions (MORIARTY & POLLARD, 1981; BELL *et al.*, 1983; MORIARTY, 1984; POLLARD & MORIARTY, 1984; RIEMANN & SØNDERGAARD, 1984; BELL, 1986; ROBARTS *et al.*, 1986 BELL & AHLGREN, 1987; RIEMANN *et al.*, 1987). It is generally agreed upon that for every new environment the method should be submitted to a number of tests before standard measurements are made. Provided such conditions are met, the thymidine method is at present the best method available for deter-

Publication no. 27 of the project "Ecological Research of the North Sea and Wadden Sea" (EON).

mining bacterial production (MORIARTY, 1986) and was accordingly adopted in the present study.

The aim of the study was to map regions of the western Wadden Sea with respect to distributional and seasonal patterns of bacterial biomass and production, and to gain insight into the role of bacteria in the system. Data were required for the validation of a recently developed ecosystem model of the western Wadden Sea. To assess the quality of the ecosystem model in predicting bacterioplankton dynamics, field data are compared with simulated values.

Acknowledgements.—We express our thanks to the crew of the MS "Heffesant" (Rijkswaterstaat, Harlingen) for our pleasant stay on board and for their contribution to the smooth progress of the fieldwork. Thanks are due to H.J. Lindeboom, H.W. van der Veer, M.J.W. Veldhuis and J.H. Vosjan for critically reading the manuscript.

2. MATERIAL AND METHODS

2.1. AREA DESCRIPTION

The western Wadden Sea is arbitrarily bordered in the NE by the tidal watershed between the island of Terschelling and the mainland. Two main tidal basins are distinguished, the Marsdiep basin in the west and the Vlie basin in the northeast. These basins are connected by "deep" tidal channels. A third basin, associated with the tidal inlet between the islands of Texel and Vlieland, is separated from the latter basins by tidal watersheds. Consequently, it is of limited importance in the water exchange between these basins and the North Sea and was therefore excluded in this study.

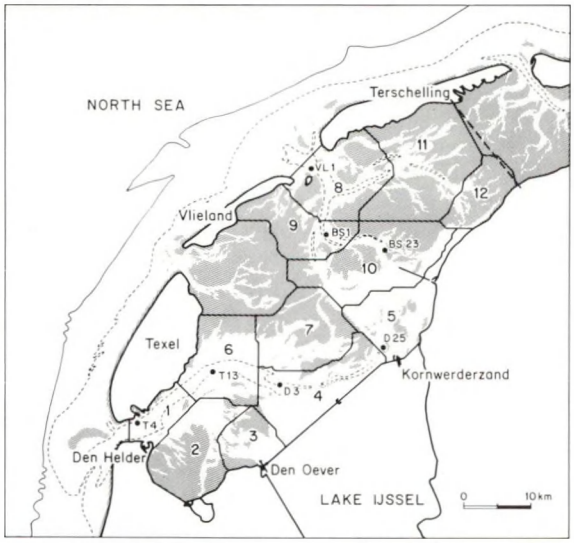

Fig. 1. Map of the western Dutch Wadden Sea with compartment division and location of field stations.

The surface areas of the Marsdiep basin amount to $742.5 \cdot 10^6$ m^2 and $672 \cdot 10^6$ m^2 for the Vlie basin, with water volumes of $2893 \cdot 10^6$ m^3 and $1771 \cdot 10^6$ m^3 and mean depths of 3.9 and 2.6 m, respectively. The main source of freshwater discharge in the western Wadden Sea is Lake IJssel. In 1986 a total of $15524 \cdot 10^6$ m^3 was discharged, *viz.* $6037 \cdot 10^6$ m^3 at Kornwerderzand and $9487 \cdot 10^6$ m^3 at Den Oever. The location of sluices and the division of the western Wadden Sea into compartments as used in the ecosystem model are given in Fig. 1. Compartments 1 to 7 belong to the Marsdiep basin and 8 to 12 to the Vlie basin (EON, 1988).

2.2. SAMPLING

Seven sampling stations (4 in the Marsdiep basin: T4, T13, D3 and D25; 3 in the Vlie basin: VL1, BS1 and B23) were selected in the study area and it was assumed that they represented the various water masses in the headwaters in accordance with area coverages in the two basins (see Fig. 1). All stations were sampled once a month (February excepted). Each sample consisted of surface water pumped into a 30-dm^3 glass jar with a membrane pump over a distance of ~200 m. In this way mixed water samples were obtained. The samples were stirred and subsamples were taken immediately. Samples in the Vlie basin were always taken during the flood tide and in the Marsdiep basin during the ebb tide or at HW. Each month the consecutive sampling stations were sampled at approximately similar tidal phases.

From January to August samples for bacterial production measurement were kept on ice in 5-dm^3 glass jars in darkness for up to 8 h, because there were no facilities on board to work with radioactive isotopes. After August we incubated samples on board. Parallel measurements were then carried out to assess the effect of conservation on ice on bacterial production rates. Besides samples for bacterial biomass and production, water samples were taken for measuring biological oxygen consumption (BOC_1), temperature, salinity and suspended matter.

2.3. BACTERIAL BIOMASS

Numbers and biovolume of bacteria were determined by epifluorescence microscopy of acridine orange-stained samples, collected on 0.2 μm polycarbonate filters (HOBBIE *et al.*, 1977; ZIMMERMAN *et al.*, 1978). Counting and measuring were carried out with a Zeiss epifluorescene microscope fitted with objective Plan Apochromat *63/1.4, oculars of *10 and Optovar *2. Ten to twenty randomly chosen fields containing together ~200 cells were counted. Approximately 100 cells per filter were sorted into 13 size classes and equivalent volumes were calculated. To convert biovolume into bacterial carbon, a factor of $1 \cdot 10^{-13}$ g C·μm^{-3} was used according to RUBLEE *et al.* (1978).

2.4. BACTERIAL PRODUCTION

The incorporation of ^{3}H-thymidine into cold TCA-precipitated material was measured essentially according to FUHRMAN & AZAM (1980, 1982). Samples of 65 cm^3 water were incubated in 100-cm^3 serum bottles in the dark at *in situ* temperature with 5 nmol·dm^{-3} of ^{3}H-thymidine with a specific activity of 40 to 60 Ci·mmol^{-1} (Amersham). This concentration maximally labelled the macromolecules in an incorporation experiment with various concentrations of tritiated thymidine (Fig. 2). Incubation times ranged from 10 to 60 min and time courses were performed routinely to check linearity. Subsamples of 10 cm^3 were taken and stopped at 0, 10, 20, 30, 40 and 60 min, respectively. Duplicate incubations generally showed identical rates of ^{3}H-thymidine incorporation. The rate of thymidine incorporation into TCA-precipitated material was converted into bacterial production by assuming that $1.7 \cdot 10^{18}$ cells were produced per mole thymidine incorporated according to FUHRMAN & AZAM (1980). This conversion factor was verified by ADMIRAAL *et al.* (1985) in the Ems estuary (part of the eastern Dutch Wadden Sea) and as such applied for this study.

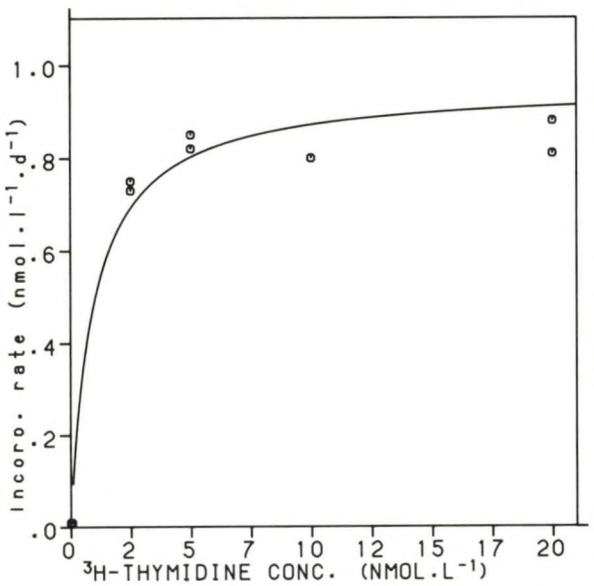

Fig. 2. Effect of increasing ^{3}H-thymidine concentration on the rate of ^{3}H-thymidine incorporation.

2.5. OXYGEN CONSUMPTION

As an index of overall heterotrophic activity oxygen consumption was measured. Four calibrated oxygen bottles of ca. 100 cm^3 were filled with water; 2 bottles were immediately fixed and 2 bottles incubated in the dark for 24 h at *in situ* temperature before fixation. Oxygen concentrations were determined by Winkler titration according to STRICKLAND & PARSON (1972). A carbon:oxygen ratio of 0.30 was applied, an intermediate value between the ratios of SEPERS (1981) of 0.29 and of HARGRAVE (1973) of 0.32. The activity respiration of bacteria was derived from the production as measured with ^{3}H-thymidine. A bacterial assimilation efficiency of 30% was assumed with a growth efficiency of 25%. These are reasonable mean annual values, considering the efficiencies determined in Dutch and Belgian coastal waters (ADMIRAAL *et al.*, 1985; LAANBROEK *et al.*, 1985; LAANBROEK & VERPLANKE, 1986; BILLEN & FONTIGNY, 1987).

2.6. SUSPENDED MATTER

Suspended matter in the water column was determined by filtering a known quantity of water over a preweighed 0.45-μm membrane filter (Sartorius). After washing with distilled water, filters were dried and weighed. The difference in weight is attributed to suspended matter representing organic and inorganic matter >0.45 μm.

2.7. ECOSYSTEM MODEL

A system-wide ecological model has recently been developed for the western Dutch Wadden Sea (EON, 1988). It is a deterministic compartment model with 12 spatially divided compart-

ments (Fig. 1) describing in equations the circulation of components and the biological processes in terms of carbon in the western Dutch Wadden Sea. The model consists of several submodels such as the pelagic, epibenthic and benthic submodels. Its structure was adopted from the Ems estuary ecosystem model extensively described by BARETTA & RUARDIJ (1988) and extended where necessary to meet hydrographical conditions in the western Dutch Wadden Sea (EON, 1988) different from those of the Ems estuary. For the western Dutch Wadden Sea the model was extended with a subtidal submodel and nutrient recycling (EON, 1988; VAN RAAPHORST *et al.*, 1988). The exchange coefficients between compartments were calculated from the results of a 2-dimensional numerical transport model (RIDDERINKHOF, 1988).

In the pelagic submodel 7 groups of organisms are distinguished. For each group growth, consumption, respiration, excretion and mortality are modelled. In SCHRÖDER *et al.* (1988) the bacterial part of this model is explained. They discuss the different equations representing the state and rate variables of pelagic bacteria one by one. The most important equation is repeated below, with which bacterial biomass is calculated in time steps of one day:

$$\frac{\delta PBAC}{\delta t} =$$

$$PBAC + mM - rsM - fIME - fIMD - fIM3 - fIM8,$$

in which

δ PBAC = change in bacterial biomass in mg $C \cdot m^{-3}$
mM = uptake of organic matter in mg $C \cdot m^{-3}$
rsM = respiration in mg $C \cdot m^{-3}$
f1ME = consumption by microzooplankton in mg $C \cdot m^{-3}$
fIMD = mortality including excretion in mg $C \cdot m^{-3}$
fIM3 = sedimentation of pelagic bacteria becoming benthic bacteria in mg $C \cdot m^{-3}$
fIM8 = sedimentation of pelagic bacteria becoming organic matter in mg $C \cdot m^{-3}$

The different components in the equation are further elucidated by SCHRÖDER *et al.* (1988), where they discuss the availability of food to bacteria in relation to maximum growth rates. In additon, they tested the sensitivity of the Ems estuary model to changes in assimilation efficiencies of bacteria and in food supply. The model gave a satisfactory simulation of the role of bacteria in this system as known at present; hence the bacterial part was applied unchanged for the ecosystem model of the western Dutch Wadden Sea.

The model was run for 1986 with the proper boundary conditions to compare the values simulated by the model in the western Dutch Wadden Sea with field data collected in 1986 and to assess the usefulness of the model in carbon budget studies. In addition, the model was used to calculate the primary production in the water column.

3. RESULTS

3.1. TIDE TEMPERATURE AND SALINITY

Field data were not corrected to mean tidal conditions. Tidal variations in bacterial variables measured in September 1986 and April-June 1987 in the Vlie basin did not show similar tidal patterns. Patterns appear to vary seasonally (own observations). For this study it is assumed that on a whole-year basis the flood current on a particular location is as rich and productive in bacterial variables as the HW turn of the tide and the ebb current.

The mean water temperature curve of the western Wadden Sea for 1986 is given in Fig. 3. The temperature range covered by the different stations on consecutive sampling dates is also shown. In February the cruise was cancelled due

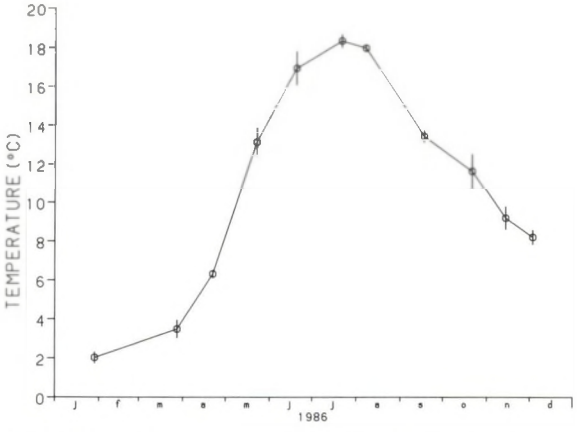

Fig. 3. Changes in the mean water temperature of the western Dutch Wadden Sea in 1986. Temperature range of the stations visited is given by a vertical bar.

to ice formation in the Wadden Sea. Water temperatures of 0 to −1.5°C occurred (not indicated in Fig. 3).

Salinities at the sampling stations varied from 31.5 in the tidal inlets to 18.0 at the onshore ends of the transects, with the Vlie basin more saline than the Marsdiep basin. The lowest salinities in both basins are related to maxima in freshwater discharge through the sluice at Kornwerderzand in January. The stations here demonstrated the largest amplitudes in salinity (BS23: 18.2 to 32.2; D25: 18.0 to 27.7). The salinities at the other stations generally did not drop below 24.

3.2. BACTERIOPLANKTON

Bacterial abundance varied between $0.2 \cdot 10^9$ and $9.4 \cdot 10^9$ cells·dm^{-3} and showed the greatest amplitude in the tidal inlets (Fig. 4). Deeper in the estuary moderate seasonal fluctuations were found in numbers of bacteria. Two separate bacterial blooms occurred in the Marsdiep basin and in the Vlie basin: in May and July-August. In the tidal inlets the spring bloom was most conspicuous, while the summer maxima were relatively more pronounced deeper in the estuary. In the Marsdiep basin the spring peak appeared in a later phase than in the Vlie basin. The mean number of bacteria·dm^{-3} was higher in the Vlie basin than in the Marsdiep basin (Sign test, $p = 0.033$).

Cell volumes of bacteria in the western Wadden Sea varied between 0.06 and 0.17 μm^3, with a tendency towards larger cell volumes in March and May-June than in the rest of the year (Fig. 5). The mean cell volume in the Vlie basin was larger than in the Marsdiep basin (Sign test, $p = 0.033$). The total biomass of the population of bacteria varied between 2 and 140 mg C·m^{-3}, with a mean biomass in the Vlie basin of 39 mg C·m^{-3} and 23 mg C·m^{-3} in the Marsdiep basin (Fig. 6). The seasonal pattern roughly reflected fluctua-

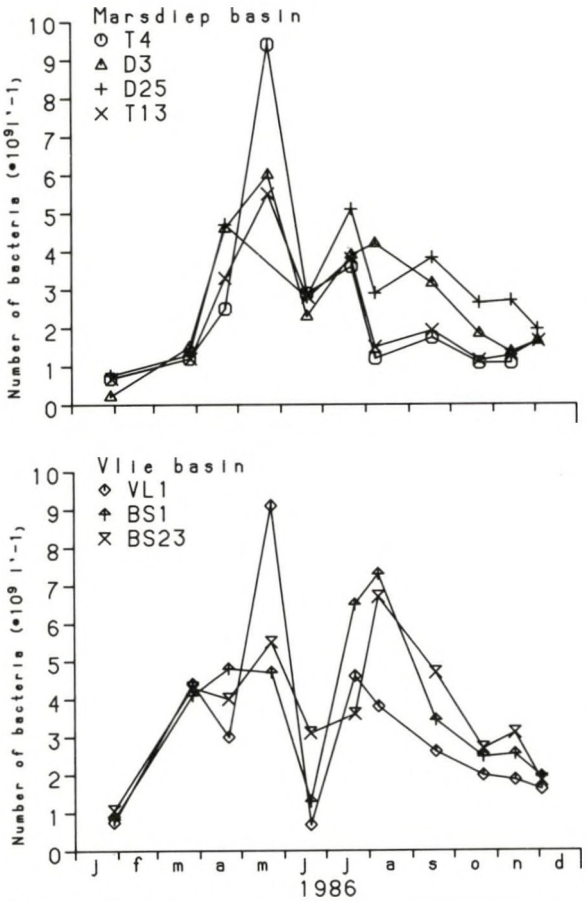

Fig. 4. Variation in abundance of bacterioplankton (in $10^9 \cdot dm^{-3}$) during 1986 in the Marsdiep basin (top), Vlie-basin (bottom).

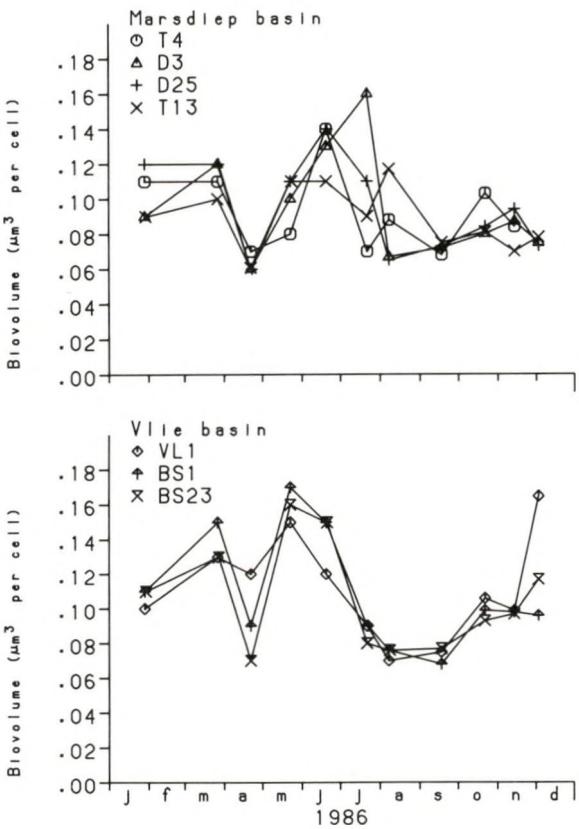

Fig. 5. Variation in biovolume (in μm^3) per cell during 1986 in the Marsdiep basin (top), Vlie-basin (bottom).

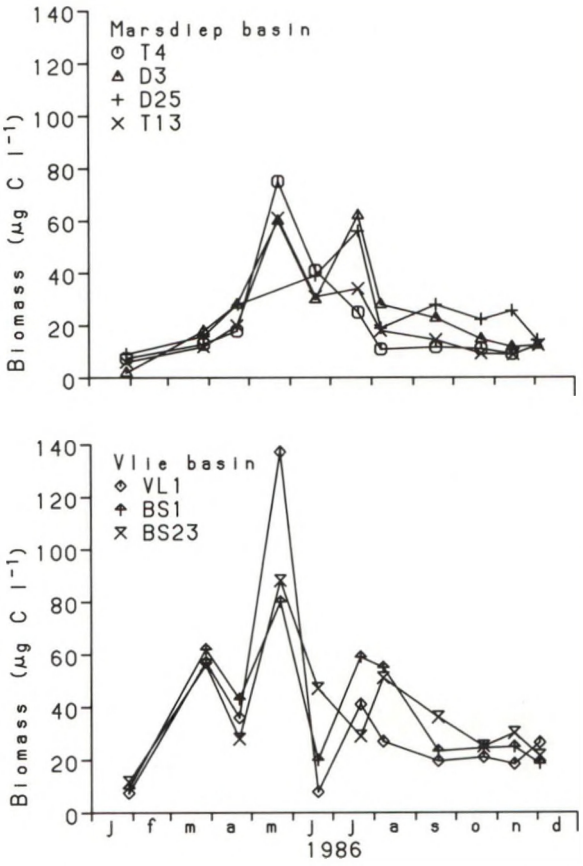

Fig. 6. Variation in bacterial biomass (in μg C $\cdot dm^{-3}$) during 1986 in the Marsdiep basin (top), Vlie basin (bottom), using a conversion factor of $1 \cdot 10^{-13}$ g C $\cdot \mu m^{-3}$.

tions of the bacterial numbers in spring and early summer (the May peak in the tidal inlet of the Marsdiep basin excepted), but from then onwards patterns were different (Figs 4 and 6). Mean cell volumes were relatively small in this period and depressed the biomass to values only 2 to 3 times higher than winter values. Mean biomass was significantly higher in the Vlie basin than in the Marsdiep basin (Sign test, $p = 0.033$).

Conservation of water samples on ice for longer than 4 h reduced the thymidine incorporation rate by approximately 35% ($\pm$ 15%). This factor was derived from parallel measurements of incorporation rates conducted from September through December in samples kept on ice for 1 to 8 h and from direct incubations. Where applicable, data were corrected accordingly.

The rate of ^{3}H-thymidine incorporation in cold TCA-insoluble material showed a conspicuous amplitude (0.1 to 7 nmol thymidine $\cdot dm^{-3} \cdot d^{-1}$) in the Vlie basin (Fig. 7). Starting at insignificant winter values an abrupt increase in the rate to maxima in May was recorded, with the highest value in the Vlie basin tidal inlet (VL1) and gradually lower maxima deeper in the estuary. The opposite pattern was found for the data collected in August. In general, values in the Marsdiep basin stayed well below the values recorded in the Vlie basin, but still showed a 30-fold variation in incorporation rates of 0.07 to 2 nmol thymidine $\cdot dm^{-3} \cdot d^{-1}$. Mean values per sampling date of the Vlie basin were significantly higher than those of the Marsdiep basin (Sign test, $p = 0.006$). Furthermore, in both basins significant correlations were found between bacterial abundance and ^{3}H-thymidine incorporation (Spearman rank correlation coefficient, denoted as r_s : $r_s = +0.56$, $n = 42$, $p < 0.01$, Marsdiep basin; $r_s = +0.36$, $n = 33$, $p < 0.05$, Vlie basin).

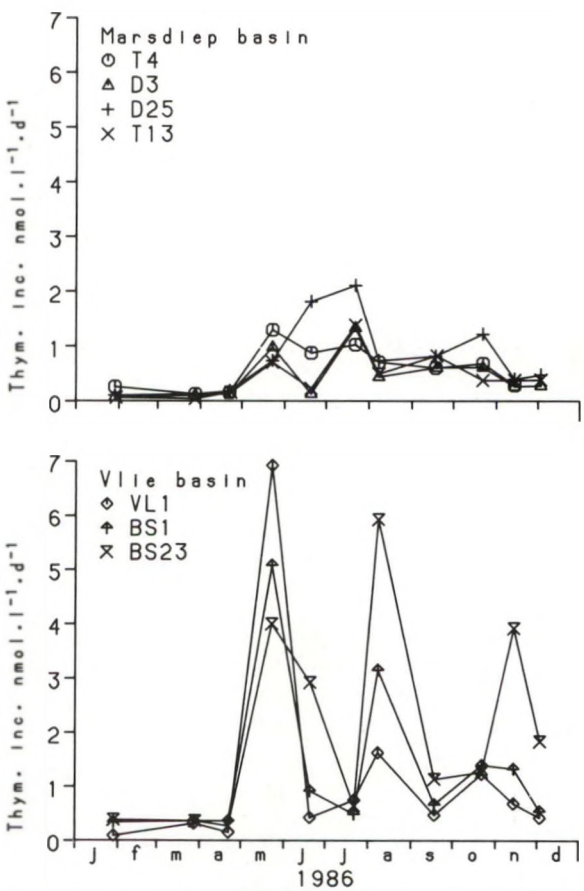

Fig. 7. Variation in the rate of ^{3}H-thymidine incorporation (in nmol $\cdot dm^{-3} \cdot d^{-1}$) during 1986 in the Marsdiep basin (top), Vlie basin (bottom).

Disagreements in the patterns of thymidine incorporation rate and production are due to variations in mean biovolume per cell. The production varied between 2 and 175 mg $C \cdot m^{-3} \cdot d^{-1}$ in the Vlie basin and between 2 and 45 mg $C \cdot m^{-3} \cdot d^{-1}$ in the Marsdiep basin (Fig. 8), with annual productions of 10 and 3 g $C \cdot m^{-3} \cdot y^{-1}$, respectively. The production in the Vlie basin was significantly higher than in the Marsdiep basin (Sign test, $p = 0.006$). Bacterial biomass was significantly correlated with production in both basins ($r_s = +0.54$, $n = 42$, $p < 0.01$, Marsdiep basin; $r_s = +0.38$, $n = 33$, $p < 0.05$, Vlie basin).

3.3. OXYGEN CONSUMPTION

Variations in dark oxygen consumption broadly followed the temperature curve. Maxima in oxygen consumption were measured in May in the Vlie basin (1.68 mg $O_2 \cdot dm^{-3} \cdot d^{-1}$) and in June in the Marsdiep basin (1.14 mg $O_2 \cdot dm^{-3} \cdot d^{-1}$) and coincided with peaks in the phytoplankton density (see VELDHUIS *et al.*, 1988).

The activity respiration of bacteria varied roughly between 2 and 500% of the total respiration, but was nevertheless significantly correlated with the oxygen consumption ($r_s = +0.46$, $n = 75$, $p < 0.01$). In May and June respectively, the activity respiration amounted to ca. 16 and 12% in the Marsdiep basin and to 70 and 36% in the Vlie basin. Scores exceeding 100% occurred predominantly in October, November and December.

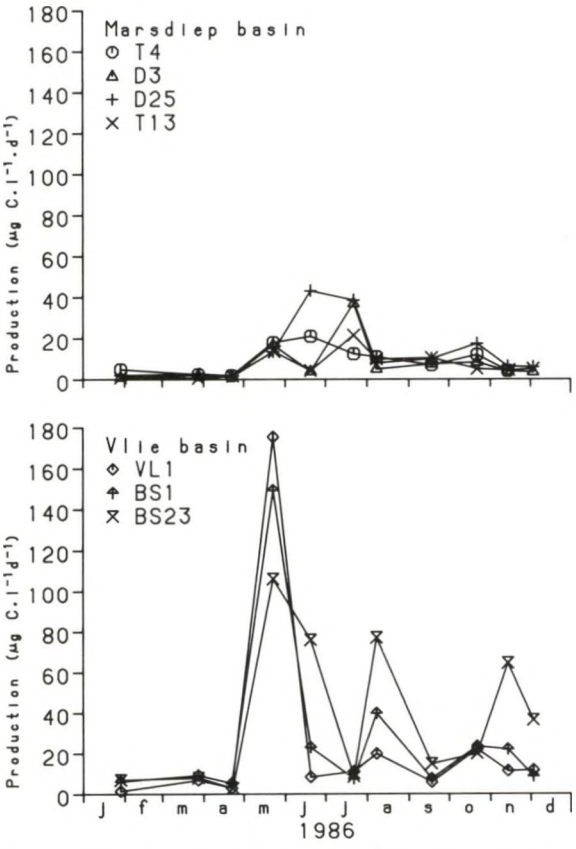

Fig. 8. Variation in the rate of bacterial production (in μg $C \cdot dm^{-3} \cdot d^{-1}$) during 1986 in the Marsdiep basin (top), Vlie basin (bottom).

3.4. SUSPENDED MATTER

Suspended matter loads were measured at different times in the tide at the consecutive sampling stations. Because tidal variations in suspended matter are often large in the Wadden Sea (POSTMA, 1982; CADÉE, 1982), values of different stations cannot be compared quantitatively. In the Vlie basin 10 to 280 mg $DW \cdot dm^{-3}$ was measured during the flood, with maxima in the tidal inlet in March and deeper in the estuary in August, October and December. Resuspension of sand grains probably contributed to these high values. No correlations were found between suspended matter and bacterial parameters in the Vlie basin. In the Marsdiep basin values ranged from 10 to 100 mg $DW \cdot dm^{-3}$ during high tide and the ebb. Maxima were recorded in January and March. Suspended matter was found to be negatively correlated with bacterial abundance, biomass, and production, respectively, ($r_s = -0.38$ to -0.41, $n = 42$; $p < 0.02$).

3.5. VALIDATION OF THE ECOSYSTEM MODEL OF THE WESTERN DUTCH WADDEN SEA

Results of the ecological model (Figs 9, 10 and 11) of the western Wadden Sea are compared with field data of biomass, production of bacterioplankton and measured BOC_1 values. The results are given only of the compartments for which field data are available. Field data and simulated graphs of respective compartments are plotted. The degree of fit of the simulation and the field data is expressed in C-values, the average value of 2 differently calculated deviation values and a value of correlation (STROO, 1986). C-values grade linearly from 1 to 10, with a better fit as C-values are higher.

Field data of bacterial variables and BOC_1

broadly matched the model simulations (C-values varied between 5.6 and 7.2 for bacterial variables, see Figs 9 and 10; and between 7.1 and 8.5 for BOC_1, Fig. 11). The simulated onsets of bacterial blooms and BOC_1 in spring agreed with field data but the declines set in too late (October). The large fluctuations in bacterial variables measured from March until September were not reflected by the model. The model did not accurately simulate oscillations in the small food web, which can be considerable in eutrophic coastal waters (ANDERSON & SØRENSEN, 1986).

The mean order of magnitude of simulations compared to field data was generally good. It was slightly better in the Vlie basin than in the Marsdiep basin, though with larger disagreements between field data and corresponding simulated values per sampling date (Figs 9, 10 and 11).

The quality of the model with respect to the seasonal patterns of bacterial variables and BOC_1 is judged on the basis of the correlation coefficient r and slope component SC (STROO, 1986). Overall annual patterns in biomass were best simulated in the compartments 1, 4, 5 and 6 ($r = 0.70$, 0.73, 0.65, 0.79, respectively) and parallelled by patterns in the bacterial production with best fits in the same compartments ($r = 0.75$, 0.81, 0.79, 0.90, respectively).

Simulated mean annual values of biomass, production and BOC_1 are shown for all compartments separately in Fig. 12a, b and c, with the annual means based on field measurements plotted in. Higher mean annual values were generally found deeper in the estuary, in which

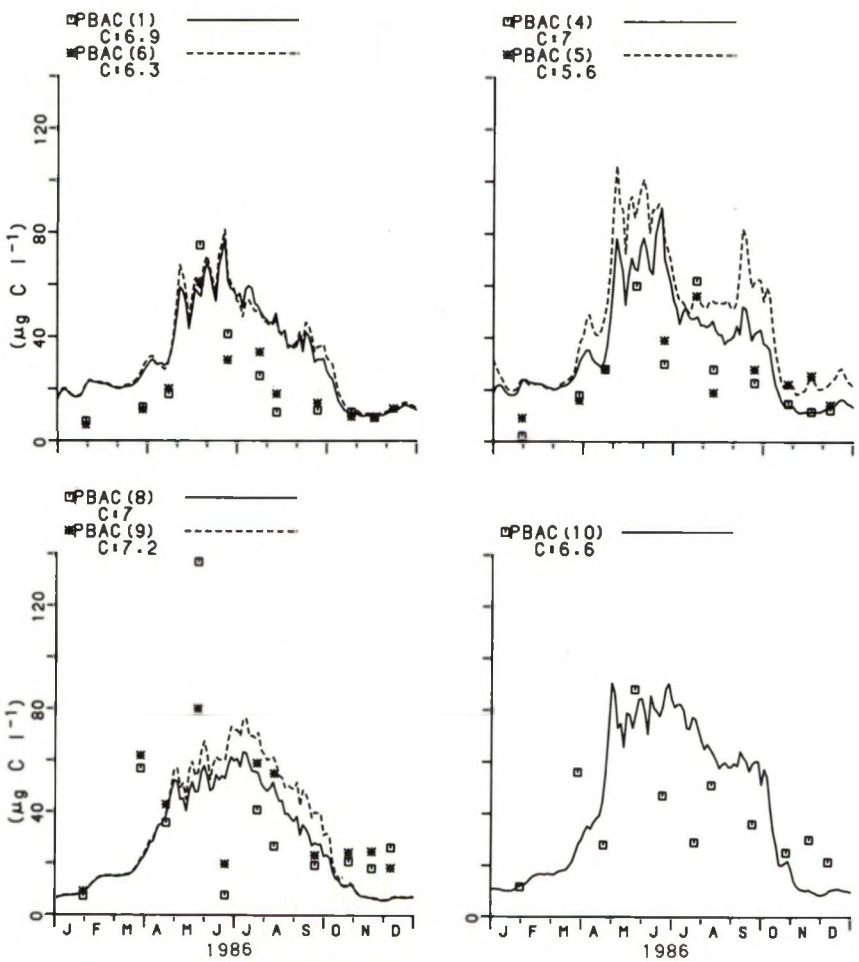

Fig. 9. Model simulations of the biomass of bacterioplankton (PBAC) in each of the 7 compartments 1, 4, 5, 6, 8, 9, 10 (lines) and field data (symbols) in µg C·dm^{-3} in 1986.

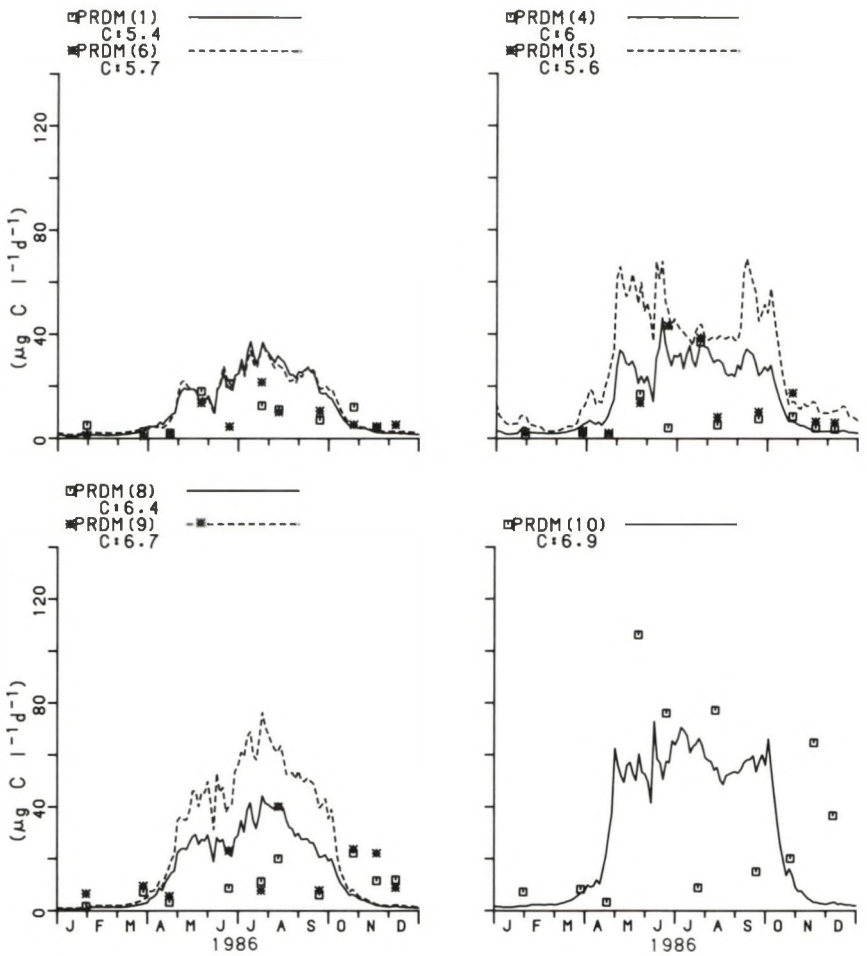

Fig. 10. Model simulations of the bacterial production of heterotrophic bacteria (PRDM) in each of the 7 compartments 1, 4, 5, 6, 8, 9, 10 (lines) and field data (symbols) in µg C·dm^{-3}·d^{-1} in 1986.

respect the simulation is in accordance with the measured data. But the simulated values of bacterial biomass and production in the Marsdiep basin (Fig. 12a and b) have been overestimated by the model, ~1.5- and 2-fold, respectively. In Table 1, model outputs on an annual basis are shown with measured data and give a survey of the discrepancy in field data and simulated data.

4. DISCUSSION

4.1. METHODOLOGICAL CONSIDERATIONS

At present, several dilemmas are faced by microbial ecologists, who require absolute values of bacterial parameters in C-flux studies, as to which conversion factors are to be used. Biovolume-to-biomass conversion factors of bacteria vary in the literature from 0.87 to $5.6 \cdot 10^{-13}$ g C·µm^{-3} (FERGUSON & RUBLEE, 1976; BRATBAK, 1985). Recently an increasing amount of evidence has been published that conversion factors have been underestimated in the past by at least 3 times (BRATBAK & DUNDAS, 1984; BRATBAK, 1985; BJØRNSEN, 1986; LEE & FUHRMAN, 1987). In this light the value of the biovolume-to-biomass conversion used in this study is conservative, $1 \cdot 10^{-13}$ g C·µm^{-3} (RUBLEE *et al.*, 1978). However, NAGATA (1986) determined the C-content of natural planktonic bacteria by a different method and arrived at values comparable to the value we applied.

The thymidine conversion factor we used, $1.7 \cdot 10^{18}$ bacterial cells formed after incorporation of 1 Mol thymidine in cold TCA insoluble

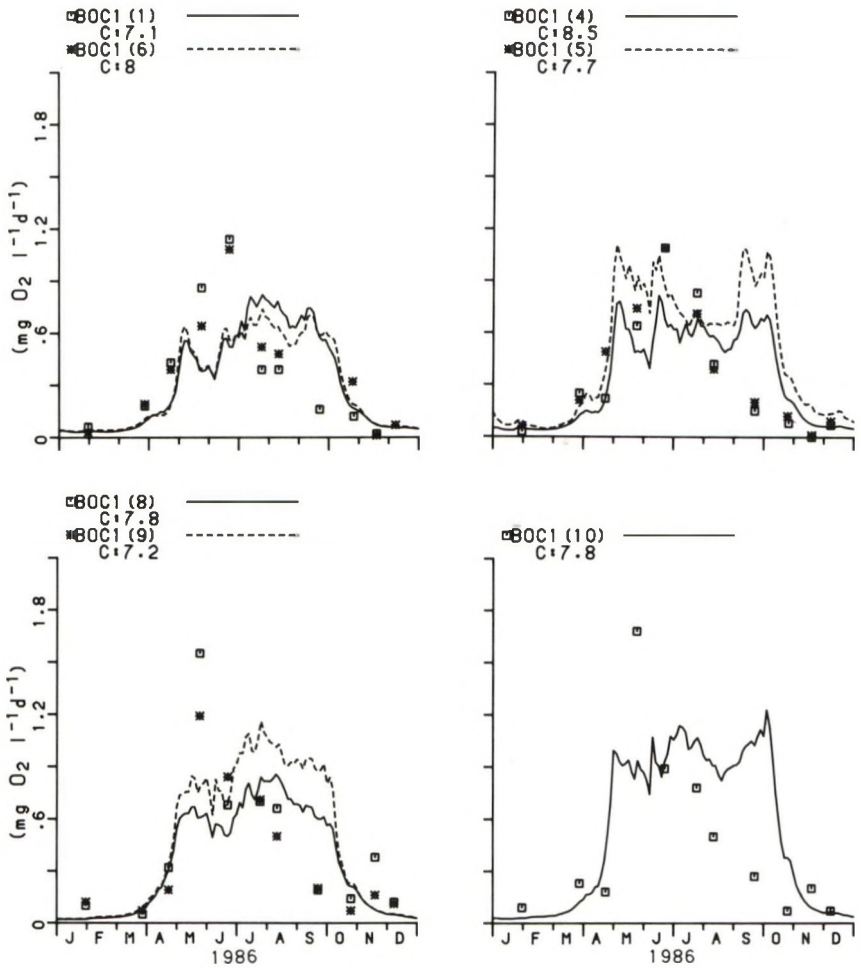

Fig. 11. Model simulations of the oxygen consumption (BOC_1) of the water column in each of the 7 compartments 1, 4, 5, 6, 8, 9, 10 (lines) and field data (symbols) in mg $O_2 \cdot dm^{-3} \cdot d^{-1}$ in 1986.

material, has been determined only once with a bacterial population from the tidal inlet of the Ems estuary (ADMIRAAL *et al.*, 1985). A similar conversion factor was derived by BILLEN & FONTIGNY (1987) in the Southern Bight of the North Sea. This factor also fits in the range of 1.1 to $10 \cdot 10^{18}$ determined on the basis of an array of experiments with marine bacterial populations of the North Sea, which demonstrated the consistency of this factor with different mediums, temperatures or generation times (1 to 200 h) (RIEMANN *et al.*, 1987).

4.2. SEASONAL VARIATIONS

The microbial distribution and dynamics in the western Wadden Sea exhibited similarities to the Ems estuary in the eastern Dutch Wadden Sea. Particularly the seasonal pattern of bacterial abundance and biomass agreed with patterns found in the headwater of the Ems (ADMIRAAL *et al.*, 1985). The seasonal variation of bacteria in the western Wadden Sea was characterized by a sequence of bacterial blooms from March until September, represented by considerable fluctuations in bacterial abundance (0.7 to $9.4 \cdot 10^9$ cells$\cdot dm^{-3}$) and biomass (0.8 to 137 μg C$\cdot dm^{-3}$). Prominent peaks occurred in May and July-August, which coincided with maxima in ^{3}H-thymidine incorporation rates (up to 7 nmol$\cdot dm^{-3} \cdot d^{-1}$) and production (up to 175 μg C$\cdot dm^{-3} \cdot d^{-1}$), with generation times of ~ 12 to 20 h in the Vlie basin. Production maxima in the Marsdiep basin occurred in June-July (2 nmol

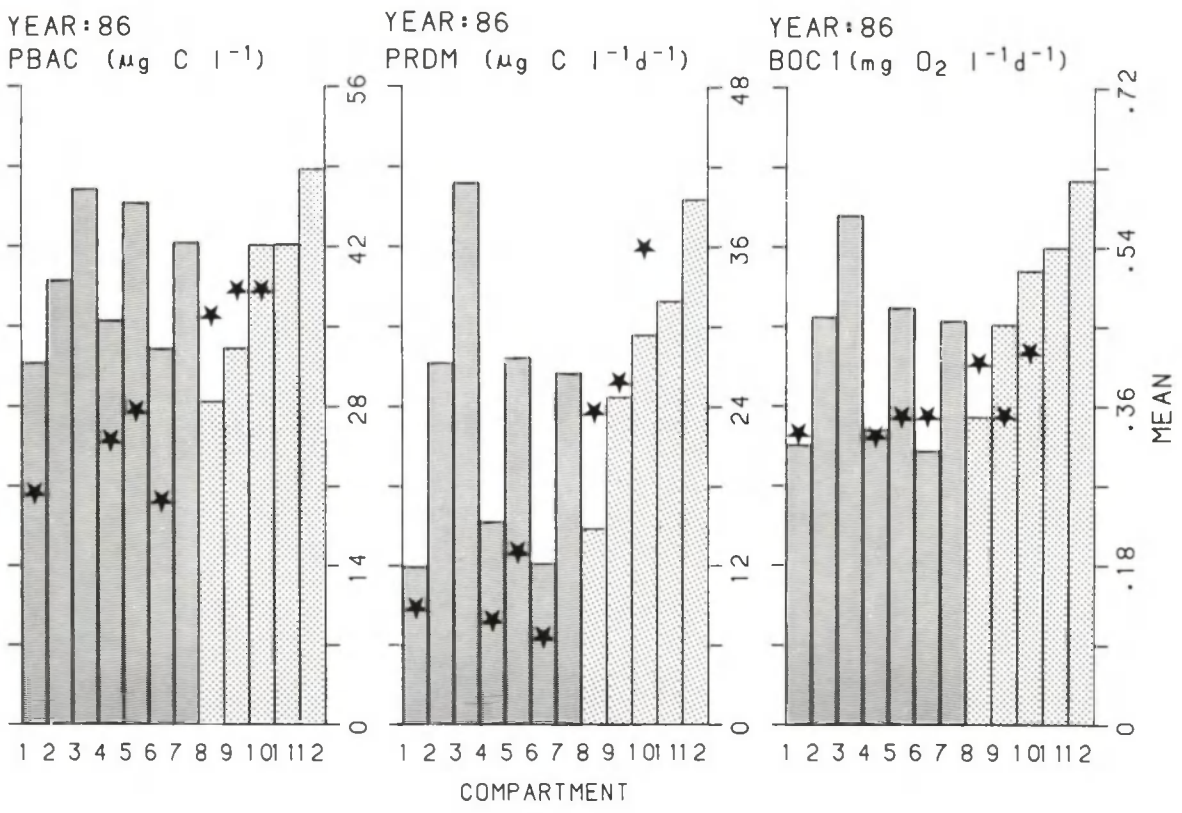

Fig. 12. Simulated mean annual bacterial biomass in μg C·dm^{-3} (left), production in μg C·dm^{-3}·d^{-1} (middle) and BOC_1 in mg O_2·dm^{-3}·d^{-1} (right) in the compartments 1 to 12, respectively in 1986. Mean annual values of field data are also given (symbols).

thymidine·dm^{-3}·d^{-1}; 45 mg C·dm^{-3}·d^{-1}), with generation times of ~20 to 50 h.

The range of bacterial numbers (0.23 to 9.4·10^9 cells·dm^{-3}) and biomass (2.1 to 137 μg C·dm^{-3}) in the western Wadden Sea is comparable to that found in the Ems estuary (ADMIRAAL *et al.*, 1985), though with maximum production rates twice as high. The mean annual production measured in the Vlie basin (10 to 11 g C·m^{-3}·y^{-1}) was practically equal to what was measured in the Ems-Dollard in 1982 (9 g C·m^{-3}·y^{-1}) (*ibid*). This is more than 3 times higher than the annual production measured in the Marsdiep basin (3 g C·m^{-3}·y^{-1}). Our ^{3}H-thymidine incorporation rates compare favourably with those reported by DUCKLOW (1982), FUHRMAN & AZAM (1982), NEWELL & FALLON (1982) and RUBLEE (1984) in coastal and estuarine waters. In contrast, our maximum values were up to 12 times higher than those recorded by LAANBROEK *et al.* (1985) in the Dutch Eastern Scheldt basin.

4.3. LATERAL VARIATIONS

Seasonal patterns of bacterial parameters varied by station. Along the onshore-offshore transect in headwaters, large and systematic lateral variations in bacterial abundance, biomass and production were found in the western Wadden Sea. Stations deeper in the estuary showed maxima in spring and summer. Pronounced summer maxima were restricted to the onshore end of the transects and were absent in the tidal inlets. During the summer, food supply to bacteria was apparently greater here than in the tidal inlets. This cannot be directly related to the discharge of organic matter as this is negligible during the summer months. We suggest that higher summer temperatures enhance the bacterial activity, which results in higher production rates. This process is supposed to play a more important role at the onshore ends of the transects, where sedimentation generally overrides erosion (due

TABLE 1

Synoptic view of the simulated values by the model and the field data. Mean values of field data are calculated for the compartments 1, 4, 5, 6, 8, 9, 10 and not extrapolated to the total surface area of the western Wadden Sea. The % respired of the gross primary production is added to column B. The % of the total respiration which is respired by bacterioplankton (..%) and the total uptake by bacteria of the primary production (-..-%) is added to column C (assimilation efficiency of 30%; growth efficiency of 25%; restrespiration of bacterial biomass and the contribution of allochthonous organic matter to bacterial biomass production are neglected in the calculation). Mean depths of the defined areas are also given.

*Total dark respiration = $BOC_1 \cdot 0.30$,

[1]*Derived from VELDHUIS *et al.* (1988) and increased with 25% to include exudates (Veldhuis, pers. comm.).

[2]*Biovolume-to-biomass conversion factor $1 \cdot 10^{-13}$g C·μm^{-3} (RUBLEE *et al.*, 1978).

[3]*Biovolume-to-biomass conversion factor $3.8 \cdot 10^{-13}$g C·μm^{-3} (LEE & FUHRMAN, 1987).

	A. Gross primary production g C·m^{-2}·y^{-1}		B. Total dark respiration* g C·m^{-2}·y^{-1}		C. Bacterial biomass production g C·m^{-2}·y^{-1}			Mean annual bacterial biomass mg C·m^{-2}		
	simulated	measured 1*	simulated	measured	simulated	measured 2*	measured 3*	simulated	measured 2*	measured 3*
western Wadden Sea (d = 3.30 m)	341	253	156 (46%)	186 (74%)	26.2 (47%) -31%-	26.4 (40%) -42%-	100.3 (151%) -159%-	127	130	494
Marsdiep-basin (d = 3.90 m)	330	281	166 (50%)	205 (73%)	26.9 (45%) -33%-	16.5 (23%) -23%-	62.7 (86%) -89%-	148	122	464
Vlie-basin (d = 2.64 m)	354	215	145 (41%)	165 (77%)	25.2 (49%) -29%-	36.8 (62%) -68%-	139.8 (237%) -261%-	104	137	521

to lower current velocities), than at the tidal inlet.

Mean annual values of bacterial abundance, biomass and production were higher deeper in the estuary than in the tidal inlets. This is also correctly simulated by the model (see Fig. 12a and b). In the tidal inlets conspicuous maxima in bacterial abundance and biomass were restricted to the spring. The May blooms of bacteria in the tidal inlets exceeded those deeper in the estuary. Comparable gradients have been found in the Ems estuary (ADMIRAAL *et al.*, 1985). The instigation of the bacterial spring bloom in the estuary might be related to phytoplankton blooms, which come from the North Sea and spread up the estuary. Arguments to support this view are presented by VELDHUIS *et al.* (1986), who found a strong increase in the bacterial abundance in the Dutch coastal waters in April 1984. Its peak occurred in May (2 to $10 \cdot 10^9$ cells·dm^{-3}) shortly after the increase and maximum of the chlorophyll *a* concentration, predominantly represented by the haptophycean phytoplankton alga *Phaeocystis pouchetii*. The association of phytoplankton and bacteria implicates that bacterial blooms, analogous to phytoplankton blooms (COLIJN, 1983; GIESKES & KRAAY, 1975; CADÉE, 1986), develop earlier in clearer offshore waters of the North Sea than in the more turbid estuarine waters of the Wadden Sea. Consequently, in spring bacterial blooms appear later in the estuarine waters than in the North Sea (shortly after the drop in suspended matter in April).

In the Vlie basin chlorophyll *a* (measured synchronously from March to September, see VELDHUIS *et al.*, 1988) was found to be significantly correlated with bacterial abundance ($r_s = +0.47$, $n = 21$, $p < 0.05$), biomass ($r_s = +0.75$, $n = 21$, $p < 0.01$), and production ($r_s = +0.53$, $n = 21$, $p < 0.02$) respectively. These correlations emphasize the close relation which apparently existed between bacteria and phytoplankton in the Vlie basin. Close coupling of bacterial parameters and phytoplankton has

also been demonstrated in the Southern Bight of the North Sea (LANCELOT & BILLEN, 1984; BILLEN & FONTIGNY, 1987) and in the Eastern Scheldt (LAANBROEK *et al.*, 1985) as well as in other aquatic environments (FUHRMAN *et al.*, 1980; MALONE *et al.*, 1986; SIMON & TILZER, 1987). More and more evidence is coming up that such correlations are to be attributed to the rapid consumption by bacteria of algal exudates and organic compounds released during the lysis of algal cells (LAANBROEK *et al.*, 1985; BILLEN & FONTIGNY, 1987; FUHRMAN, 1987). In the Marsdiep basin chlorophyll *a* was not found to be significantly correlated ($p > 0.05$) with bacterial abundance ($r_s = -0.05$, $n = 27$), biomass ($r_s = +0.36$, $n = 27$), ^{3}H-thymidine incorporation rate ($r_s = -0.01$, $n = 28$) and production ($r_s = +0.19$, $n = 28$), respectively. The high numbers of bacteria recorded in the Marsdiep basin in May ($9.4 \cdot 10^9$ cells·dm^{-3}) did not coincide with high bacterial production rates and were possibly imported from the North Sea. In Dutch coastal waters near the Marsdiep, on May 15 1984, Admiraal (unpubl. results) found $6.4 \cdot 10^9$ cells·dm^{-3} with a production of ~75 μg C·dm^{-3}·d^{-1} in the *Phaeocystis pouchetii* phytoplankton spring bloom. Possibly, bacterial production in the Marsdiep tidal inlet was only recently uncoupled from chlorophyll *a* due to antibacterial agents (such as acrylic acid), which are associated with *Phaeocystis* blooms and inhibit bacterial production (EBERLEIN *et al.*, 1985).

Absence of couplings between bacterial parameters and phytoplankton has also been observed in other estuarine environments (ALBRIGHT, 1983; DUCKLOW & KIRCHMAN, 1983). Allochtonous organic matter supply can override such a coupling and provide the prominent food supply for the bacteria.

4.4. DISSIMILARITIES BETWEEN THE MARSDIEP BASIN AND THE VLIE BASIN

The difference in the dynamics and distribution of bacteria between the two basins is remarkable. In the Vlie basin significantly higher mean values for bacterial parameters were recorded than in the Marsdiep basin (Sign tests, $0.006 \leq p < 0.033$). The bacterial production in the Vlie basin was, on most sampling dates, 2 to 10 times higher than the production in the Marsdiep basin. Particularly the drop in production between the stations BS 1 or BS23 and D25 in May and August was spectacular (149.3 μg C·dm^{-3}·d^{-1} and 106.2 μg C·dm^{-3}·d^{-1} at BS1 and BS23 in the Vlie basin, respectively, to 13.5 μg C·dm^{-3}·d^{-1} at D25 in the Marsdiep basin).

These differences are too large to be ascribed to the different tidal phases in which measurements were conducted. Tidal variations in bacterial activity were found to be considerable, particularly when bacterial activity was high. However, standard deviations of mean tidal bacterial productivity did not exceed 50% in the Vlie basin (own observations). We expect tidal variations in the headwater of the Marsdiep basin to be smaller than in the Vlie basin, because intertidal flats are less extensive here and are located at greater distances from the sampling stations. As a consequence, resuspension of bottom sediments will play a more restricted role in the surface waters, also due to the greater mean depth of the compartments in the Marsdiep basin than in the Vlie basin.

The much higher overall bacterial production in the headwaters of the Vlie basin was not expected, considering the import of large amounts of organic matter ($133 \cdot 10^9$ g C·y^{-1} in 1986; ANONYMUS, 1986a and b) and nutrients (VAN DER VEER *et al.*, 1988) from Lake IJssel into the Marsdiep basin. In addition, the advective transport from the Marsdiep basin into the Vlie basin is limited by the purported rest transport of water from the Vlie basin to the Marsdiep basin (RIDDERINKHOF, 1988). This implicates that practically all material discharged from Lake IJssel is contained in the Marsdiep basin, so we assumed that this allochtonous C source would result in an enhanced production of bacteria in the Marsdiep basin. However, no positive correlations were found ($p > 0.05$) between the discharge of labile organic C (LOC) (Fig. 13) at Den Oever and Kornwerderzand and bacterial parameters (bacterial abundance, biomass, ^{3}H-thymidine incorporation and production at stations D3, D25 and BS1 and BS23 ($-0.70 \leq r_s \leq +0.10$, $n = 10$ or 11)). The fraction of the total organic matter discharge consisting of labile organic C was derived from EON (1988), where it is defined as consisting predominantly of easily degradable DOM released by freshwater organisms supposed to desintegrate shortly after being introduced into the saline Wadden Sea. Apparently the direct availability of this organic matter to the bacteria at the field stations is limited.

Given the large discrepancy in production between the two basins, it is remarkable that bacterial abundance and biomass in the

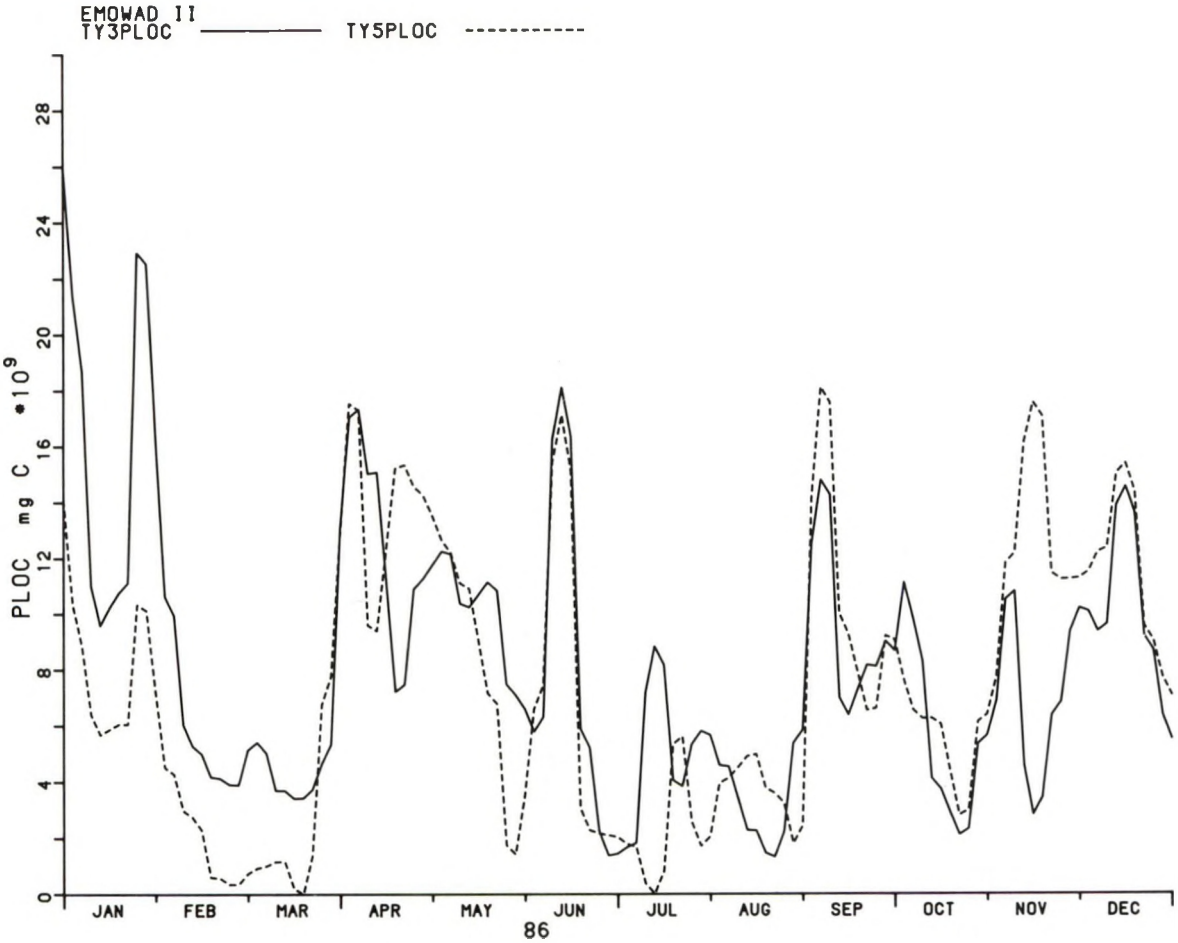

Fig. 13. Variations in total discharge of labile organic carbon (PLOC) in 1986 at Den Oever (TY3PLOC) and at Kornwerderzand (TY5PLOC) in mg C, based on measurements.

Marsdiep basin were only slightly lower in mean values than in the Vlie basin with broadly similar seasonal fluctuations. Apparently only the share of thymidine-active bacteria in the population dropped. This drop might be caused by a considerable dilution of productive waters with less productive waters and/or by the food supply to bacteria declining from the Vlie basin towards the Marsdiep basin.

—a. Dilution hypothesis:

The cumulated annual freshwater discharge in 1986 into the Marsdiep basin was 5 times larger than the volume of this basin. The largest discharges took place from November through January and in April. It was tested by comparing bacterial parameters with the discharge regime how the dilution of Wadden Sea water with fresh water discharged through the sluices at Kornwerderzand and Den Oever on the day preceding the sampling date affected the sampling stations D3, D25, BS1 and BS23. The bacterial production at D25 and D3 was negatively correlated with the discharge regime of the sluice at Kornwerderzand (D25: $r_s = -0.74$, $n = 10$, $p < 0.01$ and D3: $r_s = -0.58$, $n = 11$, $p < 0.1$). Such strong and significant correlations were not found for the other stations (BS23: $r_s = -0.42$, $n = 11$, $p > 0.1$; BS1: $r_s = -0.35$, $n = 11$, $p > 0.1$). The discharge might dilute the food supply of bacteria at D25 and D3 directly or reduce it indirectly by negatively affecting the *in situ* production of bacterial food (due to lowered salinities). On the other hand, bacterial abundance was not significantly diluted at these stations by the discharge (D25: $r_s = -0.43$, $n = 11$, $p > 0.1$ and D3: $r_s = -0.05$, $n = 11$, $p > 0.1$). This might be explain-

ed by assuming that part of the bacteria imported into the Wadden Sea from Lake IJssel remained intact, but were metabolically inactive and as such only contributed to the abundance and not to the production of bacteria. It is well known that bacteria present in domestic sewage can survive the salinity shock after introduction in the marine environment but refrain from producing.

—b. Food depletion hypothesis:
The rest transport from the Vliegat to the Marsdiep exceeds the annual freshwater discharge by ~2 times in the absence of wind-driven water transport (RIDDERINKHOF, 1988). This means that up to 800 $m^3 \cdot s^{-1}$ (dependent on the amount of freshwater discharge) is transported from the Vlie basin into the Marsdiep basin. With the transport, bacteria and phytoplankters are washed into the Marsdiep basin, which explains the similar seasonal patterns in bacterial abundance of basins. However, the close coupling of bacteria and phytoplankton disappeared in the Marsdiep basin. It is possible that phytoplankters sink out on the threshold of basins and in the broader tidal channels in the Marsdiep basin and/or are heavily cropped over the extensive mussel cultures (*Mytilis edulis*) present in the inner compartments of the Marsdiep basin (DE WILDE & BEUKEMA, 1984). CADÉE & HEGEMAN (1974) suggested that the conspicuous drop in chorophyll *a* in the water column they found over a mussel culture in the western Wadden Sea could be attributed to consumption by mussels. It should be investigated, however, if mussels in the western Wadden Sea compete for food with bacterioplankton, indirectly via the intake of phytoplankton and directly via the intake of DOM (SIEBERS & WINKLER, 1984), and if consumption of bacterioplankton by mussels in the western Wadden Sea plays a role of significance.

On the basis of the present knowledge of the role of bacteria in the ecosystem no decisive answer can be given for the differences observed between Marsdiep and Vlie basins. More research is required to solve this enigma.

4.5. MODEL VALIDATIONS

In the model, biomass and production of bacteria are deterministically calculated from the amount of C available for uptake and the amount of C already fixed in bacterial biomass with a constant assimilation efficiency of 30%, a growth restriction by setting a maximum uptake rate which is temperature dependent and a 20% mortality (SCHRÖDER *et al.*, 1988). This implies that bacterial biomass and production in the model are determined independent of biovolume-to-biomass and thymidine conversion factors, which makes our field data pre-eminently suitable for validation. The initial values of biomass and production in January 1986 have been generated by a 6-year run of the model preceding 1986.

Simulated values broadly corresponded with field data of bacterial biomass, production and BOC_1. In the Marsdiep basin patterns were better simulated than in the Vlie basin, where the March peak of bacterial biomass was missed by the model. The increase of discharged labile organic matter in September/October from Kornwerderzand and Den Oever (Fig. 13) contributed to the conspicuous peaks simulated in the compartments 4, 5 and 10 (Figs 9, 10 and 11), but was not reflected by the field data of bacterial variables and BOC_1. The fate of allochtonous material in the estuary is still poorly understood. The order of magnitude of simulations of bacterial variables was quite good with the C conversion factor of $1 \cdot 10^{-13}$ g $C \cdot \mu m^{-3}$ applied in this research. This implicates that the simulations would have been ~3.5 times too low if biomass and production rates had been calculated according to biovolume-to-biomass conversion factors now in use (*e.g.* $3.8 \cdot 10^{-13}$ g $C.\mu m^{-3}$; LEE & FUHRMAN, 1987). If so, the role of bacteria in the model is underestimated and should receive more attention. However, with this conversion factor the activity respiration of bacteria in the water column exceeds the total dark respiration and the total uptake of organic matter by bacteria exceeds primary production (Table 1). Mean assimilation and growth efficiencies of pelagic bacteria might be higher than 30 and 25%, respectively. Growth efficiencies as high as 80% have been reported by among others HOPPE (1978), BILLEN (1984) and WILLIAMS (1984).

The dissimilarities in bacterial variables between the compartments and the two basins were not reflected by the model (see Fig. 12a and b and Table 1). The model overestimates bacterial biomass and production in the Marsdiep basin. The input of allochtonous C in the Marsdiep basin was assumed to enhance the bacterial production and increase the biomass in this basin, but apparently this does not happen. The fate of this material in the western Wadden

Sea needs further research. In the Vlie basin the model slightly underestimates the bacterial variables (Fig. 12a and b), particularly the bacterial production in the compartments 8 and 10. This might be traced back to underestimation of the carbon flow from phytoplankton to bacteria. In the model the bacteria consume ~30% of the gross primary production while in the Vlie basin (field data) this was more than twice as much (68%, Table 1). The close coupling between Chl-*a* and bacterial variables found in this basin might be an indication of enhanced transfer of energy from phytoplankton to bacteria as compared to a situation in which this coupling is absent, such as in the Marsdiep basin. The model results emphasize our poor understanding ot the dynamics in and the nature of the trophic relationships between bacteria and phytoplankton.

5. CONCLUSIONS

The Marsdiep basin differs considerably from the Vlie basin particularly in bacterial activity, with a significantly lower productivity in the Marsdiep basin than in the Vlie basin. The bacterial distribution and dynamics in the Vlie basin were more strongly influenced by the North Sea than in the Marsdiep basin, particularly in spring. A close coupling of bacteria and chlorophyll *a* existed in the Vlie basin but was absent in the Marsdiep basin. Allochtonous organic matter originating from Lake IJssel was not directly available to bacterioplankton in the headwaters. The ecosystem model produced fair simulations of the oxygen consumption rate and its seasonal variations. The quality of the model in simulating bacterial variables is reasonable considering the main trend in the seasonal pattern, but it fails to simulate the proper timing and amplitude of separate major fluctuations. According to biovolume-to-biomass conversion factors now in use the model underestimates the flow of organic carbon to bacteria and their standing stock. Improvements of the model should concern a reconsideration of the trophic relations between phytoplankton and bacteria, and an adjustment of the availability of allochthonous organic carbon from Lake IJssel for pelagic bacteria.

6. REFERENCES

ADMIRAAL, W., J. BEUKEMA & F.B. VAN ES, 1985. Seasonal fluctuations in the biomass and metabolic activity of bacterioplankton and phytoplankton in a well-mixed estuary: the Ems-Dollard (Wadden Sea).—J. Plankton Res. **7:** 877-890.

ALBRIGHT, L.J., 1983. Influence of river-ocean plumes upon bacterioplankton production of the Strait of Georgia, British Columbia.—Mar. Ecol. Prog. Ser. **12:** 107-113.

ANDERSEN, P. & H.M. SØRENSEN, 1986. Population dynamics and trophic coupling in pelagic microorganisms in eutrophic coastal waters.—Mar. Ecol. Prog. Ser. **33:** 99-109.

ANONYMUS, 1986a. Kwaliteitsonderzoek in de Rijkswateren. Verslag van de resultaten over het eerste, tweede, derde en vierde kwartaal 1986. Rijkswaterstaat. Rijksinstituut voor Volksgezondheid en Milieuhygiëne.

——, 1986b. Spuistaten Zuiderzeewerken 1986. Rijkswaterstaat. Directie Zuiderzeewerken, Lelystad.

BARETTA, J.W. & P. RUARDIJ, 1988. Tidal flat estuaries (simulation and analysis of the Ems estuary). Springer Verlag Heidelberg **70:** (in press)

BELL, R.T., 1986. Further verification of the isotope dilution approach for estimating the degree of participation of [^{3}H] thymidine in DNA synthesis in studies of aquatic bacterial production.—Appl. Environ. Microbiol. **52:** 1212- 1214.

BELL, R.T. & I. AHLGREN, 1987. Thymidine incorporation and microbial respiration in the surface sediment of a hypereutrophic lake.—Limnol. Oceanogr. **32:** 476-482.

BELL, R.T., G.M. AHLGREN & I. AHLGREN, 1983. Estimating bacterioplankton production by measuring ^{3}H thymidine incorporation in a eutrophic Swedish lake.—Appl. Environ. Microbiol. **45:** 1709-1721.

BILLEN, G., 1984. Heterotrophic utilization and regeneration of nitrogen. In: J.E. HOBBIE & P.J.LEB. WILLIAMS. Heterotrophic activity in the Sea. NATO Conference Series. Series IV. Marine Sciences, Plenum Press, New York: 313-355.

BILLEN, G. & A. FONTIGNY, 1987. Dynamics of a *Phaeocystis*-dominated spring bloom in Belgium coastal waters. II. Bacterioplankton dynamics.—Mar. Ecol. Prog. Ser. **37:** 259- 264.

BJØRNSEN, P.K., 1986. Automatic determination of bacterioplankton biomass by image analysis.—Appl. Environ. Microbiol. **33:** 1229-1232.

BRATBAK, G., 1985. Bacterial biovolume and biomass estimations.—Appl. Environ. Microbiol. **49:** 1488-1493.

BRATBAK, G. & I. DUNDAS, 1984. Bacterial dry matter content and biomass estimations.—Appl. Environ. Microbiol. **48:** 755-757.

CADÉE, G.C., 1982. Tidal and seasonal variation in particulate and dissolved organic carbon in the western Dutch Wadden Sea and Marsdiep tidal inlet.—Neth. J. Sea Res. **15:** 228-249.

——, 1986. Recurrent and changing seasonal patterns in phytoplankton of the westernmost inlet of the Dutch Wadden Sea from 1969 to 1985.—Mar. Biol. **93:** 281-289.

CADÉE, G.C. & J. HEGEMAN, 1974. Primary production of the benthic microflora living on tidal flats in the Dutch wadden Sea.—Neth. J. Sea Res. **8:** 260-291.

COLIJN, F., 1983. Primary production in the Ems-Dollard estuary. Ph. D. thesis, State University Groningen, The Netherlands: 1-123.

DUCKLOW, H.W., 1982. Chesapeake Bay nutrient and plankton dynamics. I. Bacterial biomass and production during spring tidal destratification in the York River, Virginia estuary.—Limnol. Oceanogr. **27:** 651-659.

DUCKLOW, H.W. & D.L. KIRCHMAN, 1983. Bacterial dynamics and distribution during a spring bloom in the Hudson River plume, U.S.A.—J. Plankton Res. **5:** 333-355.

EBERLEIN, K., M.T. LEAL, K.D. HAMMER & W. HICKEL, 1985. Dissolved organic substances during a *Phaeocystis* bloom in the German Bight.—Mar. Biol. **89:** 311-316.

EON, 1988. Ecosysteem model van de westelijke Waddenzee. (Opzet, resultaten en toepassingen). NIOZ-rapport 1988-1: 1-88.

ES, F.B. VAN, 1982. Some aspects of the flow of oxygen and organic carbon in the Ems-Dollard estuary. Boede Publications 5. Ph. D thesis, State University, Groningen, The Netherlands: 1-121.

ES, F.B. VAN & L.A. MEYER-REIL, 1982. Biomass and metabolic activity of heterotrophic marine bacteria. In: K.C. MARSHALL.—Adv. Microb. Ecol. **6:** 111-170.

FERGUSON, R.L. & P. RUBLEE, 1976. Contribution of bacteria to standing crop of coastal plankton.—Limnol. Oceanogr. **21:** 141-145.

FUHRMAN, J.A., 1981. Influence of method on the apparent size distribution of bacterioplankton cells: Epifluorescence microscopy compared to scanning electron microscopy.—Mar. Ecol. Prog. Ser. **5:** 103-106.

——, 1987. Close coupling between release and uptake of dissolved free amino acids in seawater studied by an isotope dilution approach.—Mar. Ecol. Prog. Ser. **37:** 45-52.

FUHRMAN, J.A. & F. AZAM, 1980. Bacterioplankton secondary production estimates for coastal waters of British Columbia, Antarctica and California.—Appl. Environ. Microbiol. **39:** 1085-1095.

——, 1982. Thymidine incorporation as a measure of heterotrophic bacterioplankton production in marine surface waters: Evaluation and field results.—Mar. Biol. **66:** 109-120.

GIESKES, W.W.C. & G.W. KRAAY, 1975. The phytoplankton spring bloom in Dutch coastal waters of the North Sea.—Neth. J. Sea Res. **9:** 166-196.

GROENEDAAL, M.M., 1975. Bacteriële sulfaatreduktie in de wadbodem. Netherlands Institute for Sea Research, unpublished report, 1975-15: 1-32.

HARGRAVE, B.T., 1973. Coupling carbon flow through some pelagic and benthic communities.—J. Fish. Res. Bd Can. **30:** 1317-1326.

HOBBIE, J.E., R.J. DALEY & S. JASPER, 1977. Use of Nuclepore filters for counting bacteria by fluorescence microscopy.—Appl. Environ. Microbiol. **33:** 1225-1228.

HOPPE, H.G., 1978. Relations between active bacteria and heterotrophic potential in the sea.—Neth. J. Sea Res. **12:** 78-98.

LAANBROEK, H.J. & J.C. VERPLANKE, 1986. Seasonal changes in percentages of attached bacteria enumerated in a tidal and stagnant coastal basin: relation to bacterioplankton productivity.—FEMS Microb. Ecol. **38:** 87-98.

LAANBROEK, H.J., J.C. VERPLANKE, P.R.M. DE VISSCHER & R. DE VUYST, 1985. Distribution of phyto- and bacterioplankton growth and biomass parameters, dissolved inorganic nutrients and free amino acids during a spring bloom in the Oosterschelde basin, The Netherlands.—Mar. Ecol. Prog. Ser. **25:** 1-11.

LANCELOT, C. & G. BILLEN, 1984. Activity of heterotrophic bacteria and its coupling to primary production during the spring phytoplankton bloom in the southern bight of the North Sea.—Limnol. Oceanogr. **29:** 721-730.

LEE, S. & J.A. FUHRMAN, 1987. Relationships between biovolume and biomass of naturally derived marine bacterioplankton.—Appl. Environ. Microbiol. **53:** 1298-1303.

MALONE, T.C., W.M. KEMP, H.W. DUCKLOW, W.R. BOYNTON, J.H. TUTTLE & R.B. JONAS, 1986. Lateral variation in the production and fate of phytoplankton in a partially stratified estuary.—Mar. Ecol. Prog. Ser. **32:** 149-160.

MORIARTY, D.J.W., 1984. Measurements of bacterial growth rates in some marine systems using the incorporation of tritiated thymidine into DNA. In: J.E. HOBBIE & P.J.I. WILLIAMS. Heterotrophic activity in the sea. NATO Conference Series. Series IV: Marine Sciences: 217-231.

——, 1986. Measurement of bacterial growth rates in aquatic systems from rates of nucleic acid synthesis. In: K.C. MARSHALL.—Adv. Microb. Ecology **9:** 245-292.

MORIARTY, D.J.W., & P.C. POLLARD, 1981. DNA synthesis as a measure of bacterial productivity in seagrass sediments.—Mar. Ecol. Prog. Ser. **5:** 151-156.

NAGATA, T., 1986. Carbon and nitrogen content of natural planktonic bacteria.—Appl. Environ. Microbiol. **52:** 28-32.

NEWELL, S.Y. & R.D. FALLON, 1982. Bacterial productivity in the watercolumn and sediments of the Georgia (USA) coastal zone: estimates via direct counting and parallel measurements of thymidine incorporation.—Microb. Ecol. **8:** 33-46.

POLLARD, P.C. & D.J.W. MORIARTY, 1984. Validity of the tritiated thymidine method for estimating bacterial growth rates: The measurement of isotope dilution during DNA synthesis.—Appl. Environ. Microbiol. **48:** 1076-1083.

POSTMA, H., 1982. Hydrography of the Wadden Sea: Movements and properties of water and particulate matter. Reports of the Wadden Sea Working Group. Balkema, Rotterdam, Report 2.

RAAPHORST, W. VAN, P. RUARDIJ & A.G. BRINKMAN, 1988.

The assessment of benthic phosphorus regeneration in an estuarine ecosystem model. —Neth. J. Sea Res. **22:**23-36.

RIEMANN, B., P.K. BJØRNSEN, S.Y. NEWELL & R.D. FALLON, 1987. Calculation of cell production of coastal marine bacteria based on measured incorporation of ^{3}H thymidine.—Limnol. Oceanogr. **32:** 471-476.

RIEMANN, B. & M. SØNDERGAARD, 1984. Measurements of diel rates of bacterial secondary production in aquatic environments.—Appl. Environ. Microbiol. **47:** 632-638.

RIDDERINKHOF, H., 1988. Tidal and residual flows in the western Dutch Wadden Sea. I. Numerical model results.—Neth. J. Sea Res. **22:** 1-21.

ROBARTS, R.D., R.J. WICKS & L.M. SEPHTON, 1986. Spatial and temporal variations in bacterial macromolecule labeling with [methyl-^{3}H] thymidine in a hypertrophic lake.—Appl. Environ. Microbiol. **52:** 1368-1373.

RUBLEE, P.A., S.M. MERKEL, M.A. FAUST & J. MIKLAS, 1984. Distribution and activity of bacteria in the headwaters of the Rhode River Estuary, Maryland, USA.—Microb. Ecology **10:** 243-255.

RUBLEE, R., L. CAMMEN & J. HOBBIE, 1978. Bacteria in a North Carolina Salt Marsh: standing crop and importance in decomposition of Spartina altiflora.—UNC Sea Grant Publication UNC-SG-78-11: 1-79.

SCHRÖDER, H.G.J., A.J. KOP & H.J. LINDEBOOM, 1988. Modelling of pelagic microbial activities in the carbon cycle of an estuarine ecosystem.—Arch. Hydrobiol. Beih. Ergebn. Limnol. **31:** 115-131.

SEPERS, A.B.J., 1981. Diversity of ammonifying bacteria.—Hydrobiologica **83:** 343-350.

SIEBERS, D. & A. WINKLER, 1984. Amino-acid uptake by mussels, *Mytilus edulis*, from natural sea water in a flow-through system.— Helgoländer Meersunters. **38:** 189-199.

SIMON, M. & M.M. TILZER, 1987. Bacterial response to seasonal changes in primary production and phytoplankton biomass in Lake Constance.—J. Plankton Res. **9:** 535-552.

STRICKLAND, J.D.H. & T.R. PARSONS, 1972. A practical handbook of seawater analysis.—J. Fish. Res. Board Can. **167:** 1-310.

STROO, D., 1986. A method for validation. Internal Publication EON, 1986-1.

VEER, H.W. VAN DER, W. VAN RAAPHORST, M.J.N. BERGMAN, 1988. Eutrophication of the Dutch Wadden Sea. I. External nutrient loadings of the Marsdiep and Vliestroom basin. NIOZ-rapport (in prep.).

VELDHUIS, M.J.W., F. COLIJN & L.A.H. VENEKAMP, 1986. The spring bloom of *Phaeocystis pouchetii* (Haptophyceae) in Dutch coastal waters.—Neth. J. Sea Res. **20:** 37-48.

VELDHUIS, M.J.W., F. COLIJN, L.A.H. VENEKAMP & L. VILLERIUS, 1988. Phytoplankton primary production and biomass in the western Wadden Sea (The Netherlands); A comparison with an ecosystem model.—Neth. J. Sea Res. **22:** 37-49.

VOSJAN, J.H., 1982. Sauerstoffaufnahmegeschwindigkeit und ETS-Aktivität im Niederländischen Wattenmeer. In: I. Daubner. III. Internationales Hydromikrobiologisches Symposium, Smolenice, 3-6 Juni 1980. Verlag der Slowakischen Akademie der Wissenschaften, Bratislawa: 355-367.

——, 1987. A sketchy outline of the fate of organic matter in the Dutch Wadden Sea.—Hydrobiol. Bull. **21:** 127-132.

VOSJAN, J.H. & S.B. TIJSSEN, 1978. Respiratory electron transport system (ETS) activity variations in a tidal area during one tidal period.—Oceanol. Acta **1:** 181-186.

WILDE, P.A.W.J. DE & J.J. BEUKEMA, 1984. The role of zoobenthos in the consumption of organic matter in the Dutch Wadden Sea. In: R.W.P.M. LAANE & W.J. WOLFF. The role of organic matter in the Wadden Sea, 145-158. Neth. Inst. Sea Res. Publ. Ser. 10.

WILLLIAMS, P.J. LEB., 1984. A review of measurements of respiration rates of marine plankton populations. In: J.E. HOBBIE & P.J. LEB. WILLIAMS. Heterotrophic activity in the Sea. NATO Conference Series. Series IV. Marine Sciences: 357-389.

WOLFF, W.J., 1983. Ecology of the Wadden Sea. Reports of the Wadden Sea Working Group. Balkema, Rotterdam, Vols 1-3: 2066 pp.

ZIMMERMAN, R., R. ITURRIAGA & J. BECKER-BIRK, 1978. Simultaneous determination of the total number of aquatic bacteria and the number thereof involved in respiration.—Appl. Environ. Microbiol. **36:** 926-935.

(received 1 November 1987; revised 22 January 1988)

Netherlands Journal of Sea Research
22 (1): 69-81 (1988)

DISTRIBUTION AND ABUNDANCE OF THE ZOOPLANKTON OF THE EMS ESTUARY (NORTH SEA)*

J.W. BARETTA and J.F.P. MALSCHAERT
Netherlands Institute for Sea Research, P.O. Box 59, 1790 AB Den Burg, Texel, The Netherlands

ABSTRACT

From 1974 to 1977 a study was made of the abundance and the distribution of the zooplankton species of the Ems estuary (The Netherlands and the Federal Republic of Germany), an area of about 500 km^2 with extensive tidal flats.

The most important component of the zooplankton consisted of holoplanktonic calanoid copepods with, during the summer, a significant contribution of meroplankton, mainly consisting of polychaete and cirripede larvae. Zooplankton abundance showed a marked seasonality, with a pronounced spring peak and a smaller late summer/autumn peak. In the low salinity area the spring bloom was dominated by *Eurytemora affinis*, which persisted in the salinities below S=5 upriver during the whole year. In the polyhaline area *Acartia bifilosa* was the main component of the spring bloom. The late summer maximum from August to October was dominated by *Acartia tonsa* in the meso- and polyhaline area and by *A. discaudata* and *Centropages hamatus* in the euhaline part of the estuary bordering on the Wadden Sea proper. The number of abundant (>1000 ind·m^{-3}) species increased from the inner, fresher part of the estuary towards the Wadden Sea but, except for April, average zooplankton density in salinities <18 was similar (2768 ind·m^{-3}) to the density in salinities >18 (2817 ind·m^{-3}).

The distribution patterns show that there are only a few autochthonous species and that the majority of species is allochthonous and penetrates more or less deeply into the estuary from the Wadden Sea and North Sea, varying with species and season.

1. INTRODUCTION

This study describes the abundance and the distribution of the most common zooplankton populations in the Ems Estuary on the border of the Netherlands and the Federal Republic of Germany (Fig. 1). A global description of the ecosystem of the estuary is given in GORDON & BARETTA (1982).

The zooplankton of the Ems estuary had not been studied extensively before. STOCK & DE VOS (1960) took a number of samples during the summer of 1954 and enumerated the species found. KÜHL & MANN (1968) surveyed the plankton in 1951, using a Helgoland egg-net. They did not distinguish between the different copepod species but gave relative abundances of a number of zooplankton groups along the longitudinal axis of the estuary.

The present study is the first quantitative examination of zooplankton in the Ems Estuary. The zooplankton of other estuaries bordering the German and the Southern Bights of the North Sea has received more attention. BAKKER & DE PAUW (1975) compared the zooplankton assemblages of Lake Veere and the Western Scheldt estuary. KÜHL & MANN (1968) gave data on the plankton of the Ems estuary, and HICKEL (1975) studied species composition and biomass of the mesozooplankton near Sylt. VON VAUPEL-KLEIN & WEBER (1975) studied the distribution of *Eurytemora affinis* in the western Wadden Sea in relation to salinity. REDEKE (1934) discussed seasonal succession of *Acartia tonsa and A. bifilosa* in Dutch brackish waters. WIBAUT-ISEBREE MOENS (1954) described the changes in plankton composition following the transformation of the brac-

*Publication no. 15 of the project "Ecological Research North Sea and Wadden Sea" (EON).

kish Zuiderzee into a freshwater lake, Lake IJssel.

Many authors (*e.g.* KETCHUM, 1954; JEFFRIES, 1962; ROGERS, 1940; BARLOW, 1955) have stressed the importance of estuarine circulation in determining distribution and abundance of the zooplankton within an estuary. The spatial distribution of planktonic organisms in an estuary is to a large extent determined by physical processes, such as mixing and flushing. RUARDIJ (1981) calculated an average residence time of 38 days at the average summer discharge of the Ems River of 56 $m^3 \cdot s^{-1}$. Seasonal variations in the freshwater discharge from the Ems and the Westerwoldsche Aa change both the flushing rate and the salinity distribution throughout the estuary. In general, isohalines lie further out in winter and spring (Fig. 1b), when freshwater discharge is high, and further inwards with the lower discharges of summer and autumn (Fig. 1a). It is difficult to describe plankton composition and distribution in terms of geographical location because of the continuous movement of the estuarine water masses, which is mainly tidal, but also has components due to seasonal variations in freshwater discharge and an irregular component due to stormy weather. We therefore tried to find a more suitable frame of reference which does not depend on location but on the composition of the water mass surrounding the planktonic organisms. Because estuarine water is a mixture of freshwater and seawater, salinity reflects the relative contents of both components. It is a conservative property and governs the distribution of estuarine species (GUNTER, 1961), so it should be a useful descriptor of spatial distribution patterns of estuarine plankton.

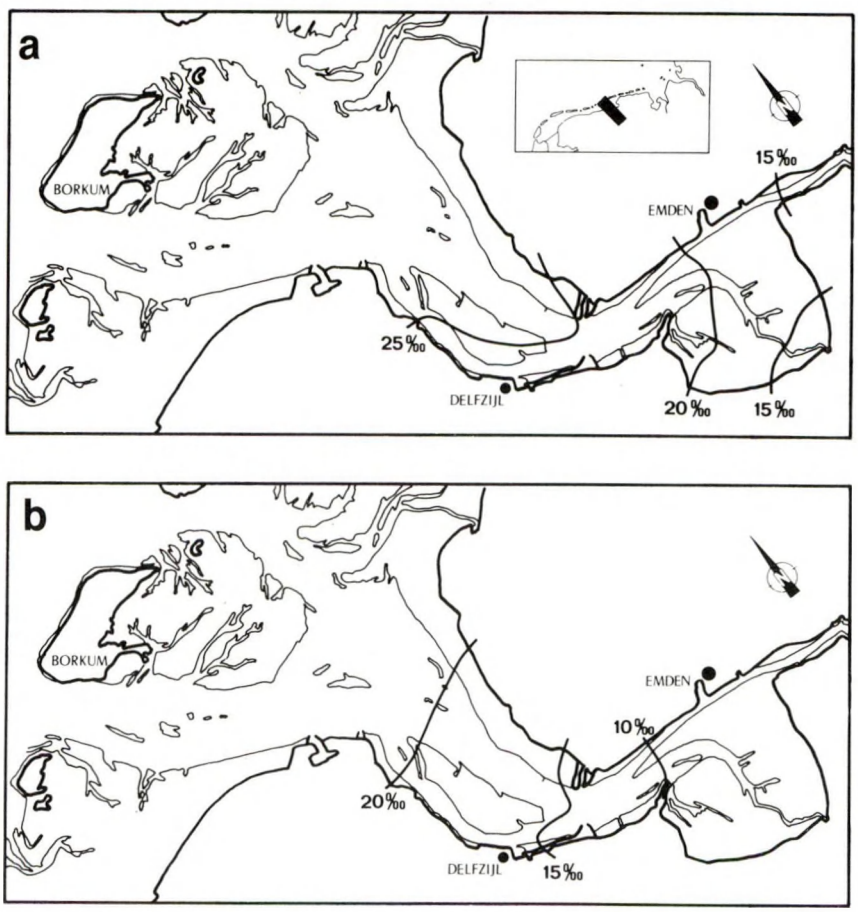

Fig. 1. Map of the Ems estuary, with inset indicating its location in the Wadden Sea. The isohalines in (a) indicate the salinity distribution in the estuary in a period of low freshwater discharge (summer) at high water. In (b) the salinity distribution in a period with high freshwater discharge is indicated.

Acknowledgements.—Thanks are due to the crew of the R.V. "Ephyra" for their help in all seasons, as well as to Wilma Lewis, Henk Pelleboer and Paul Busschots, who did the majority of the plankton counts.

2. MATERIAL AND METHODS

2.1. THE EMS ESTUARY

The estuary investigated occupies an area of about 500 km^2. The estuary has a tidal amplitude ranging from 2.25 m near the island of Borkum in the outermost part of the estuary to 3 m at Nieuw Statenzijl in the inner part (Fig. 1). Maximum current velocity in the channels is about 1.5 $m \cdot s^{-1}$ and the tidal excursion is some 10 km. DORRESTEIN (1960) gave a detailed treatment of the hydrographical features.

The main freshwater source of the estuary is the river Ems, which has a mean discharge of 70 $m^3 \cdot s^{-1}$, with monthly means ranging from 114 $m^3 \cdot s^{-1}$ in February to 34 $m^3 \cdot s^{-1}$ in September. A secondary freshwater source located at Nieuw Statenzijl has a long-term mean discharge of about 10 $m^3 \cdot s^{-1}$, with monthly means ranging from 30 $m^3 \cdot s^{-1}$ in winter to 4 $m^3 \cdot s^{-1}$ in summer. This source only discharges during low tide, being a canal-lock with self-closing doors. The Ems estuary is well-mixed, showing no significant stratification even in extreme summer conditions. However, the inner part of the estuary, the Dollard, should possibly be considered partially mixed (HELDER & RUARDIJ, 1982).

2.1.1. SAMPLING

During a three-year period quantitative zooplankton samples were taken throughout the Ems estuary with high speed plankton samplers. The shallow areas of the estuary were sampled at high tide with a small high-speed plankton sampler, to establish whether the plankton over the tidal flats is different from the plankton in the channels. Sampling in the channels was done with a modified Gulf-III plankton torpedo (GEHRINGER, 1962) with a mouth-diameter of 19 cm. Directly behind the mouth a General Oceanics 2030 flowmeter was mounted. A Monodur cylindrical net with 200 μm meshes was used. The sampler used in the shallow water over the tidal flats had a mouth-diameter of 7 cm, a 200 μm net and was fitted with a General Oceanics 2030 flowmeter too.

To permit direct calculation of the sampled volume from the flowmeter readings, the intake tube of the Gulf-III was modified by extending it inwards, so that it ended right in front of the flowmeter, which was mounted centrally in the net. This way the flowmeter was in the main flow without obstructing it. The volume thus sampled is equal to the surface area of the intake times the length of the water column drawn through the intake (which is given by the flowmeter reading). For the small sampler it was not possible to calculate the sampled volume directly because of the different geometry of the intake and the relative position of the flowmeter in the sampler. Instead, the small sampler was calibrated indirectly by mounting it on the large one and taking a number of samples ($n = 15$) with this combination. Since detritus can be expected to have no avoidance behaviour, and the amount of detritus is assumed to be representative of the volume sampled by the small sampler, we were able to calculate the relation between flowmeter reading and sampled volume for the small sampler with the amount of detritus taken by both samplers as unit of comparison. If this calculation of volume sampled (based on the correspondence between the amount of detritus and the volume sampled) was correct, there should be no significant difference in zooplankton densities between the large and the small sampler for these paired samples. According to a paired T-test (SOKAL & ROHLF, 1981) the null hypothesis of no difference between the large and small samplers could not be rejected ($P = 0.22$). A detailed comparison of samples from over the tidal flats with samples from the nearest tidal channels showed that the zooplankton composition was not significantly different (VAN SPLUNDER, 1976). Therefore, the samples from the two areas were pooled.

Both the sampling in the channels and over the tidal flats was done at approximately mid-depth, with a towing speed of 2.5 $m \cdot s^{-1}$ (5 knots) and a duration of about 10 min. This method was adopted because the winch available at the start of the sampling programme did not allow taking double-oblique hauls. However, the Ems-Dollard being a well-mixed estuary, this method was expected to yield samples representative of the whole water column. During the survey period, from 1974 to 1977, 376 samples were taken throughout the estuary, including the river Ems, at intervals of about five weeks. Because the large sampler had a depressor extending 1 m

below the intake, it was not possible to sample within 1 m of the bottom.

2.1.2. ABIOTIC PARAMETERS

During the sampling the following parameters were measured:
—pH, with an Orion 601 pH meter with automatic temperature compensation and an accuracy of 0.05 pH units.
—Salinity, with a Switchgear SW5 conductivity-meter having an accuracy of 0.1 S.
—Temperature, with the coupled thermistor of the same Switchgear meter having an accuracy of 0.1°C.
—Duration of haul, in seconds. Because of the constant ship's speed through the water, this enabled us to check the sensitivity of the flowmeter readings to clogging of the nets.
—Water depth in m. Geographical location: channel name, nearest buoy.
—Date and time of day.

2.1.3. TREATMENT OF THE SAMPLES

Samples were preserved in a 4% $CaCO_3$-buffered formaldehyde solution. Due to the high detritus content of the samples (usually about ten times as much detrital material as plankton), it was necessary to separate the two fractions. We did this with a modified version of the separation method of DE JONGE & BOUWMAN (1977). The whole sample was pre-rinsed with demineralized water to remove salts and formaldehyde. Then the samples were put in 600 cm^3 centrifuging beakers containing a solution of 25% Ludox-TM, a silicasol, and centrifuged at 2000 rpm for 10 min in a Heraeus Christ Macrofuge. This resulted in a separation of the detritus/sediment fraction and the planktonic fraction, the detritus sinking to the bottom, the plankton floating on top. The plankton was then siphoned off and rinsed with fresh water to remove Ludox. The percentage of recovery of the zooplankton fraction was dependent on the dominant type of detritus present. If this was filamentous material, recovery was reduced to about 70%. In those cases, repeatedly centrifuging smaller amounts of sample resulted in increases in recovery to satisfactory values of about 90%. The recovery was determined by counting the zooplankters in the detritus fraction of a number of samples. Comparison of species composition and numbers of individuals with those of the clean zooplankton fraction of the same samples showed that recovery ranged between 90% and 99% of the total present. There were no significant differences in composition between the plankton retained in the detrital fraction and the plankton fraction itself. Therefore, any plankton retained in the detritus results in lowering the calculated abundance, but does not influence the frequency distribution of the species.

2.1.4. SUBSAMPLING AND COUNTING

After centrifuging and rinsing, the samples were sieved over a 2 mm mesh sieve to separate mysids, shrimps, larval fishes, amphipods, ctenophores etc. from the smaller zooplankton. This large fraction was counted under a dissecting microscope (Zeiss 4B). The remaining, smaller fraction was put into a measuring cylinder and left to settle for 24 h. After settling, settled volume was noted and total volume in the cylinder adjusted to 4 times settled volume. From this volume a subsample of 0.1 cm^3 was taken with an Eppendorf pipette under continuous stirring. The adjustment to four times settled volume of the sample was chosen to obtain a number of around 50 zooplankters in the subsample. This number was chosen to reach a compromise between counting effort and ability to detect rarer species. Counting was done on a Projectina BK-13 projecting microscope.

To gain insight into the errors inherent to the subsampling and counting procedures, a number of samples were subsampled and counted by different people and the results compared. The differences between results from the same subsamples were on average around 2% and never larger than 3%. To test subsampling error, the counters were asked to count different samples which were actually subsamples from the same source. Differences between these counts were again around 2.5%. Subsampling and counting errors were, therefore, in the worst case approximately 5%.

3. RESULTS

3.1. ORGANISMS ENCOUNTERED

Within the holoplankton the most abundant groups were the Copepoda, calanoid and harpacticoid, followed by the Mysidacea. Meroplankton

mainly occurred as polychaete and cirripede larvae.

Table 1 gives the average monthly abundance of each species or taxonomical group in salinities below 18. Table 2 gives these values for the salinities above 18. This division has been chosen because it is the division between mesohalinicum and polyhalinicum as given by REDEKE (1932) and makes good sense biologically, as is shown for this estuary in BARETTA (1981).

In Tables 3 and 4 the samples have been aggregated in salinity groups of 5 S units each and according to sampling month, resulting in 12 (months) times 7 (salinity groups) cells in each of the tables. Table 3 gives the number of samples contained in each cell. Tables 4a to n give the distribution of the frequently occurring taxonomical units along the salinity gradient throughout the year. Abundance has been expressed as the base ten logarithm of the sum total of adults and copepodites III to V, averaged over all samples in each cell.

3.1.1. COPEPODA CALANOIDA

Of the calanoid copepods the genus *Acartia* is the most strongly represented with four species: *A. bifilosa, A. clausi, A. discaudata* and *A. tonsa*. Of these 4 species *A. bifilosa* and *A. tonsa* contribute most in terms of numerical abundance. The following genera are only represented by one species each: *Centropages hamatus, Eurytemora affinis, Paracalanus parvus, Pseudocalanus* sp. and *Temora longicornis*.

—*Eurytemora affinis* Poppe, 1880 is perennial in the salinity range 0-15 (Table 4a). It is most abundant in winter and spring. In winter it occurs throughout the salinity range 0-30. As the season progresses the occurrence of *E. affinis* gradually becomes more restricted to lower salinities until it is almost totally confined to salinities below 15 in summer. From November on, *E. affinis* again expands into the higher salinities.

—*Acartia tonsa* Dana, 1848, occurs during most of the year at salinities between 20-25 (Table 4b).

TABLE 1

Abundance (ind·m^{-3}) of zooplankton in the Ems estuary in salinities below 18. Numbers rounded to nearest integer. Abundances between 0 and 0.5 given as +

Month	*Jan*	*Feb*	*Mar*	*Apr*	*May*	*Jun*	*Jul*	*Aug*	*Sep*	*Oct*	*Nov*	*Dec*
No. of samples→	*14*	*10*	*25*	*30*	*4*	*14*	*9*	*2*	*10*	*3*	*15*	*4*
Species name↓												
Eurytemora affinis	4682	3220	2093	10948	1489	3720	160	158	2223	56	1164	462
Acartia tonsa	0	0	0	290	+	10	53	2578	1815	32	6	6
Acartia bifilosa	18	63	623	3861	273	143	176	0	0	0	1	0
Acartia discaudata	0	0	3	1	0	0	0	0	98	0	+	0
Acartia clausi	0	0	0	0	16	0	0	0	0	0	0	0
Acartia spec.	211	56	124	969	+	33	16	645	94	2	12	+
Centropages hamatus	0	1	1	64	0	+	3	0	9	1	4	3
Pseudocalanus spec.	4	37	23	112	0	0	0	0	0	0	+	5
Temora longicornis	0	5	0	32	0	115	0	0	1	0	25	6
Paracalanus parvus	5	0	9	9	0	0	0	0	0	0	+	0
Harpacticoida	63	37	19	409	40	47	29	822	166	4	280	0
Neomysis integer	2	+	3	+	0	42	13	0	9	0	6	0
Mesopodopsis slabberi	0	+	+	3	74	32	7	20	78	0	0	0
Praunus flexuosus	0	0	0	0	+	+	0	0	0	0	0	0
Larval mysids	0	0	0	0	40	24	8	0	25	1	0	0
Cirripeda nauplii	0	4	17	220	0	46	26	0	0	75	42	0
Cirripeda cyprids	0	0	4	13	0	14	947	63	77	0	176	0
Carcinus larvae	0	0	0	+	+	0	5	0	0	0	0	0
Amphipoda	+	+	+	5	0	5	9	0	0	0	3	0
Cumacea	0	0	0	0	0	0	0	0	0	5	0	0
Polychaeta larvae	0	90	21	1094	28	70	4	0	12	0	85	4
Lanice spec. larvae	0	0	0	17	0	0	6	0	0	0	0	0
Nematoda	0	0	0	30	0	0	68	63	12	0	249	0
Ctenophora	0	0	0	0	+	+	2	0	0	0	0	0
Sagitta setosa	0	0	1	5	+	+	4	0	0	0	+	0
Pisces juveniles	0	0	0	+	+	+	+	0	0	0	0	0

TABLE 2

Abundance (ind·m^{-3}) of zooplankton in the Ems estuary in salinities over 18. Numbers rounded to nearest integer. Abundances between 0 and 0.5 given as +

Month	*Jan*	*Feb*	*Mar*	*Apr*	*May*	*Jun*	*Jul*	*Aug*	*Sep*	*Oct*	*Nov*	*Dec*
No. of samples →	*5*	*12*	*13*	*25*	*13*	*8*	*36*	*10*	*32*	*32*	*22*	*11*
Species name ↓												
Eurytemora affinis	1211	83	99	67	23	5	36	6	7	9	96	35
Acartia tonsa	0	13	13	263	11	3	240	281	1373	146	62	31
Acartia bifilosa	314	528	2322	3388	3288	107	21	74	+	21	189	225
Acartia discaudata	0	3	0	18	3	0	+	174	248	973	5	1
Acartia clausi	0	+	0	100	19	126	434	21	15	49	49	+
Acartia spec.	46	113	318	454	14	76	271	198	141	272	115	33
Centropages hamatus	14	11	11	106	132	91	190	219	143	641	87	5
Pseudocalanus spec.	300	117	119	457	19	0	0	40	+	1	151	11
Temora longicornis	29	41	8	240	337	55	567	4	77	18	389	14
Paracalanus parvus	0	8	1	28	137	4	7	48	17	103	120	0
Harpacticoida	182	6	5	220	47	3	9	557	475	2843	143	60
Neomysis integer	1	+	+	0	5	+	23	3	1	1	+	0
Mesopodopsis slabberi	1	+	1	+	+	12	14	18	52	8	1	0
Praunus flexuosus	1	+	1	+	+	0	+	+	+	2	+	0
Larval mysids	0	0	+	0	5	1	2	21	61	1	0	+
Cirripeda nauplii	0	0	15	288	403	1427	929	96	3	274	0	0
Cirripeda cyprids	0	6	0	27	20	1938	0	177	600	671	0	0
Carcinus larvae	0	0	0	0	3	1	0	1	1	4	0	0
Amphipoda	0	0	0	0	1	330	5	3	3	3	0	0
Cumacea	0	0	0	0	14	0	0	0	0	0	0	0
Polychaeta larvae	0	85	126	238	310	220	51	59	39	236	0	5
Lanice spec. larvae	0	0	0	8	+	95	0	+	0	28	0	0
Nematoda	0	+	2	0	0	71	0	5	0	0	0	0
Ctenophora	0	0	0	+	0	4	1	0	+	2	0	0
Sagitta setosa	0	0	1	+	+	4	0	2	2	3	0	0
Pisces juveniles	0	0	0	0	1	1	0	2	+	+	0	0

Maximum abundance occurs during September, when it is common throughout the estuary. Its main period of abundance is in summer and autumn.

—*Acartia bifilosa* (Giesbrecht, 1884) is a typical winter-spring species occuring in all salinities between 0 and 35 during this period (Table 4c). In summer its occurrence is restricted to salinities between 15 and 30. It does not occur at all in September. From October on, it re-establishes itself, starting from outside the estuary and slowly penetrating further inward.

—*Acartia discaudata* (Giesbrecht, 1882) is an autumn species that is most successful in salinities over 30 (Table 4d). It penetrates farthest into the lower salinities in September. It remains in the estuary into December at salinities over 30.

—*Acartia clausi* Giesbrecht, 1892 in this area is a summer- autumn species (Table 4e). It is not very common in the Ems estuary, only reaching densities >1000 m^{-3} in July at salinities >30. In July it also penetrates furthest into lower salinities.

—*Centropages hamatus* (Lilljeborg, 1853) only infrequently occurs in salinities <20 (Table 4f). At higher salinities it is perennial, with low abundances in winter and early spring. It does not show any pronounced abundance maximum, except for a small peak in October.

—*Pseudocalanus* sp. is a winter/spring species in this area (Table 4g). It does penetrate to low salinities occasionally, especially in winter, but disappears almost totally from the estuary during the summer.

—*Temora longicornis* (O. F. Mueller, 1785) is probably perennial in salinities >20 but reaches maximal abundance in salinities >30 (Table 4h). It shows three abundance peaks: in April, July and November, but only rarely penetrates to salinities <15.

3.1.2. COPEPODA HARPACTICOIDA

All species of harpacticoids encountered have been lumped into one category (Table 4i). A major part of the catches of harpacticoids consisted of *Euterpina acutifrons*, a pelagic species.

TABLE 3
Number of samples taken in each salinity group

month → *Sal. range in S units↓*	*Jan*	*Feb*	*Mar*	*Apr*	*May*	*Jun*	*Jul*	*Aug*	*Sep*	*Oct*	*Nov*	*Dec*
0 - 5	1	2	1	5	1	6	1	0	4	1	5	1
5 - 10	5	2	6	2	1	1	2	1	2	1	6	0
10 - 15	6	4	13	17	2	2	1	0	2	0	1	0
15 - 20	5	3	10	14	2	7	9	1	4	1	9	4
20 - 25	1	5	4	7	2	5	7	5	12	6	6	5
25 - 30	1	4	4	8	9	1	18	4	13	10	6	2
30 - 35	0	2	0	2	1	0	7	1	5	16	4	3

This group shows abundance maxima in summer and autumn at salinities >20.

3.1.3. MYSIDACEA

Seven different species have been identified, of which only *Neomysis integer* and *Mesopodopsis slabberi* occurred frequently enough for an analysis to be made of their distribution. The other 5 species were: *Gastrosaccus spinifer, Praunus flexuosus, Schistomysis kervillei, S. ornata* and *S. spiritus*. As we could not sample very close to the bottom (see 2.1.1.), where mysids occur most frequently (Stam, pers. comm.), the abundance of mysids given in Table 1 is probably an underestimate of true abundance; however there are no indications that this sampling bias has distorted the distribution given in Table 4k and l, the bias being systematic.

Neomysis integer (Leach, 1815) (Table 4k) occurs mainly from June to December, with an abundance peak in June. Its occurrence is confined to salinities <25, indicating that it is an autochthonous species in the estuary.

Mesopodopsis slabberi (van Beneden, 1861) (Table 4l). The distribution pattern of *M. slabberi* in summer reveals a slow shift towards higher salinities, with a sudden reversal in September, when this species occurs at all salinities. In October, however, the trend of occurring at higher salinities resumes again. *M. slabberi* has abundance peaks in May and September.

3.2. CIRRIPEDE LARVAE

The nauplii and cyprids of the Cirripedes occurring in the estuary were counted (Table 4m), but no attempt has been made to identify them down to species level. Species known to be present (KÜHL & MANN, 1968) are: *Balanus improvisus, B. crenatus, B. balanoides* and *Elminius modestus*. This group mainly occurs at salinities above 15, with the exception of *B. improvisus*, which is a typical brackish-water species. They are abundant from April to November.

3.3. POLYCHAETE LARVAE

Table 4n. Due to the difficulty of quickly identifying these organisms down to species level in routine plankton counting, we have only counted them as such on occurrence in our samples, with the exception of *Lanice* sp. The polychaete larvae show an abundance peak in April. Their occurrence is concentrated in the first half of the year but at higher salinities there apparently also is some autumn spawning.

3.4. OTHER GROUPS

Occasionally the samples contained Nematoda (often attached to detrital material), Ctenophora (mainly *Pleurobrachia pileus*), Amphipoda, Isopoda, Cumacea Chaetognatha (*Sagitta setosa*), Zoea stages of *Carcinus* and juvenile shrimps (*Crangon*). The abundance of these organisms is given in Tables 1 and 2.

4. DISCUSSION

4.1. ABUNDANCE

Comparison of Table 1 and 2 permits the following conclusions: the number of species (3) at lower salinities (Table 1) that occurs in densities of >1000 ind·m^{-3} is lower than the number of species (5) that occurs in such densities at higher salinities (Table 2). Moreover, the number of abundant species is more variable from month to month at low salinities than at higher.

Average total density is about 30% higher at lower salinities, but this is entirely due to the ex-

tremely high April value; when the April values are removed from both Tables, the average total densities are almost identical: 2768 m^{-3} for salinities <18 (Table 1) versus 2817 m^{-3} for salinities >18 (Table 2). The changes in numerical abundance from month to month are much more abrupt in the low-salinity samples than in the high-salinity ones. Also, the range in abundance between maximum and minimum values in the high-salinity samples is only a fifth of the range in the low-salinity ones. These differences indicate that the low salinity environment is rather extreme and only suitable for a few species. These species can and do become

TABLE 4

The figures given are abundances expressed as the base 10 logarithm of the average abundance of each cell. Blanc = not sampled; – = not present; + = present in very low densities

4a	*Eurytemora affinis*											
month → *sal. range in S units↓*	*Jan*	*Feb*	*Mar*	*Apr*	*May*	*Jun*	*Jul*	*Aug*	*Sep*	*Oct*	*Nov*	*Dec*
0 - 5	4	3	-	4	3	3	2		3	-	2	3
5 - 10	3	3	3	3	2	3	+	2	2	2	3	
10 - 15	3	3	3	3	2	3	2		1		1	
15 - 20	3	2	2	2	+	2	1	-	-	+	2	1
20 - 25	2	2	1	+	-	+	-	+	1	+	2	1
25 - 30	1	1	+	+	1	-	+	+	+	-	+	2
30 - 35		-		-	-		2	-	+	1	1	-

4b	*Acartia tonsa*											
month → *Sal. range in S units↓*	*Jan*	*Feb*	*Mar*	*Apr*	*May*	*Jun*	*Jul*	*Aug*	*Sep*	*Oct*	*Nov*	*Dec*
0 - 5	-	-	-	-	-	1	+		1	-	-	-
5 - 10	-	-	-	-	-	-	1	3	3	1	1	
10 - 15	-	-	-	2	+	-	2		2		-	
15 - 20	-	-	-	1	1	+	2	2	3	1	1	1
20 - 25	-	1	1	1	1	+	1	2	3	2	2	1
25 - 30	-	-	+	2	+	-	1	2	3	2	1	+
30 - 35		-		-	-		-	1	2	1	1	+

4c	*Acartia bifilosa*											
month → *Sal. range in S units↓*	*Jan*	*Feb*	*Mar*	*Apr*	*May*	*Jun*	*Jul*	*Aug*	*Sep*	*Oct*	*Nov*	*Dec*
0 - 5	-	1	3	2	-	1	-		-	-	-	-
5 - 10	1	-	2	-	2	2	-	-	-	-	-	
10 - 15	1	1	2	3	2	-	-		-		-	
15 - 20	1	2	3	3	2	2	2	-	-	-	1	2
20 - 25	3	2	3	3	+	2	+	2	-	1	2	2
25 - 30	1	2	2	3	3	-	+	1	-	1	2	1
30 - 35		2		2	2		-	-	-	1	2	-

4d	*Acartia discaudata*											
month → *Sal. range in S units↓*	*Jan*	*Feb*	*Mar*	*Apr*	*May*	*Jun*	*Jul*	*Aug*	*Sep*	*Oct*	*Nov*	*Dec*
0 - 5	-	-	-	-	-	-	-		-	-	-	-
5 - 10	-	-	-	-	-	-	-	-	-	-	-	
10 - 15	-	-	-	-	-	-	-		-		-	
15 - 20	-	-	-	-	-	-	-	-	2	-	-	-
20 - 25	-	-	-	1	-	-	1	2	1	1	-	
25 - 30	-	+	-	1	+	-	-	2	2	2	+	-
30 - 35		-		-	-		-	2	2	3	1	+

4e *Acartia clausi*

month→ Sal. range in S units↓	Jan	Feb	Mar	Apr	May	Jun	Jul	Aug	Sep	Oct	Nov	Dec
0 - 5	-	-	-	-	-	-	-		-	-	-	-
5 - 10	-	-	-	-	-	-	-	-	-	-	-	
10 - 15	-	-	-	-	1	-	-		-		-	
15 - 20	-	-	-	-	-	-	2	-	-	-	+	-
20 - 25	-	-	-	-	-	2	1	1	+	1	-	-
25 - 30	-	-	-	2	1	-	2	+	1	+	2	-
30 - 35		-		-	-		3	-	+	1	2	+

4f *Centropages hamatus*

month→ Sal. range in S units↓	Jan	Feb	Mar	Apr	May	Jun	Jul	Aug	Sep	Oct	Nov	Dec
0 - 5	-	-	-	-	-	-	-		-	-	-	-
5 - 10	-	-	-	-	-	-	-	-	-	-	-	
10 - 15	-	+	-	2	-	-	-		1		-	
15 - 20	-	-	1	1	-	+	1	-	1	-	1	+
20 - 25	1	+	1	2	1	2	1	1	1	1	1	+
25 - 30	1	1	+	2	2	2	2	2	2	2	1	1
30 - 35		+		2	1		2	2	2	3	2	+

4g *Pseudocalanus spec.*

month→ Sal. range in S units↓	Jan	Feb	Mar	Apr	May	Jun	Jul	Aug	Sep	Oct	Nov	Dec
0 - 5	-	-	-	-	-	-	-		-	-	-	-
5 - 10	+	-	-	-	-	-	-	-	-	-	-	
10 - 15	+	1	+	1	-	-	-		-		-	
15 - 20	1	1	1	2	-	-	-	-	-	-	+	+
20 - 25	2	2	1	2	-	-	-	1	-	-	+	+
25 - 30	2	1	2	2	+	-	-	1	+	-	2	1
30 - 35		2		3	2		-	2	-	+	2	+

4h *Temora longicornis*

month→ Sal.range in S units↓	Jan	Feb	Mar	Apr	May	Jun	Jul	Aug	Sep	Oct	Nov	Dec
0 - 5	-	-	-	2	-	2	-		-	-	-	-
5 - 10	-	-	-	-	-	-	-	-	+	-	1	
10 - 15	-	1	-	+	-	-	-				-	
15 - 20	+	+	+	1	+	1	1	-	+	-	1	+
20 - 25	2	1	+	1	1	1	+	+	+	+	1	1
25 - 30	1	1	1	2	2	1	2	-	1	1	2	1
30 - 35		1		3	2		3	-	2	1	3	1

4i *Copepoda harpacticoida*

month→ Sal. range in S units↓	Jan	Feb	Mar	Apr	May	Jun	Jul	Aug	Sep	Oct	Nov	Dec
0 - 5	-	1	-	1	2	1	-		-	-	2	-
5 - 10	1	1	1	2	-	-	+	2	1	+	2	
10 - 15	1	1	1	2	-	-	2		2		1	
15 - 20	2	1	+	2	-	1	1	2	2	+	1	1
20 - 25	2	1	-	2	1	+	-	3	2	2	+	1
25 - 30	1	-	1	2	1	-	+	3	2	2	2	2
30 - 35		-		-	-		1	3	+	3	2	+

4k *Neomysis integer*

month→ / Sal. range in S units↓	Jan	Feb	Mar	Apr	May	Jun	Jul	Aug	Sep	Oct	Nov	Dec
0 -5	+	-	-	-	-	1	1		+	-	-	-
5 - 10	+	-	+	-	-	2	+	-	+	-	1	
10 - 15	-	-	+	-	-	1	+		-		+	
15 - 20	+	-	-	-	-	+	+	-	1	-	+	-
20 - 25	-	-	-	-	-	-	+	+	+	+	+	-
25 - 30	-	-	-	-	-	-	-	-	-	-	-	-
30 - 35		-		-	-		-	-	-	-	-	

4l *Mesopodopsis slabberi*

month→ / Sal. range in S units↓	Jan	Feb	Mar	Apr	May	Jun	Jul	Aug	Sep	Oct	Nov	Dec
0 -5	-	-	-	-	-	-	-		2	-	-	+
5 - 10	-	-	-	-	-	+	+	-	1	-	-	
10 - 15	-	-	-	+	2	1	+		1		-	
15 - 20	-	-	+	+	-	1	1	1	1	-	-	-
20 - 25	-	-	+	-	-	-	1	+	1	1	-	-
25 - 30	-	-	-	-	-	-	+	1	1	+	+	-
30 - 35		-		-	-		-	-	+	+	+	

4m Polychaete larvae

month→ / Sal. range in S units↓	Jan	Feb	Mar	Apr	May	Jun	Jul	Aug	Sep	Oct	Nov	Dec
0 -5	-	-	-	2	-	1	1		1	-	-	-
5 - 10	-	1	-	-	-	-	-	-	-	-	2	
10 - 15	-	2	1	3	1	-	-		1		+	
15 - 20	-	1	1	2	1	1	+	-	-	-	-	+
20 - 25	-	2	2	2	2	2	+	1	+	1	-	+
25 - 30	-	+	-	1	2	2	1	1	1	1	-	+
30 - 35		1		-	1		2	2	1	2	-	-

4n Cirripede nauplii + cyprids

month→ / Sal. range in S units↓	Jan	Feb	Mar	Apr	May	Jun	Jul	Aug	Sep	Oct	Nov	Dec
0 -5	-	1	-	-	-	1	-		-	2	1	-
5 - 10	-	-	1	-	-	-	-	2	-	-	2	
10 - 15	-	-	1	2	-	-	-		1		1	
15 - 20	-	-	1	1	-	2	3	-	2	-	-	-
20 - 25	-	-	1	2	1	3	2	2	2	2	-	-
25 - 30	-	1	-	2	2	2	2	2	3	2	-	-
30 - 35		-		2	2		3	3	2	3	-	-

very successful, but apparently not for very long periods. Hence the strong fluctuations in abundance from month to month.

There also is a marked difference in the relative importance of meroplanktonic organisms between the low-salinity and the high-salinity series. In the low-salinity set meroplankton usually contributes less than 10% to total abundance. Only Polychaete larvae reach a monthly average abundance of over 1000 per m^3 in April and even then only make up some 6% of total abundance. In the high-salinity samples on the other hand, meroplankton sometimes constitutes over 50% of total numbers (June) and consistently contributes more than 10% to total abundance. Consequently, copepods numerically dominate the zooplankton in the low-salinity area to a larger extent than they do in the high-salinity area. The bulk of the standing stock at low salinities consists of *E. affinis*, except for the

period July to September, when *A. tonsa* contributes more. The only other calanoid copepod of any importance at low salinities is *A. bifilosa* and then only from March to July.

4.2. DISTRIBUTION

When a sampling programme extends over several years we have to allow for year-to-year variations in abundance, which can be up to an order of magnitude. In establishing distribution patterns for planktonic species we may, in the abundances of any species, find wide variations that we are unable to relate with anything whatever. This of course makes it very difficult to indicate what is a significant difference in abundance. We have, arbitrarily, set the difference in abundance we consider to be significant at one order of magnitude, which seems fairly conservative, since the abundances given in Table 4 are average monthly abundances. Tables 4a to h show which copepod species should be considered autochthonous to the estuary (*E. affinis, A. bifilosa, A. tonsa*) or allochthonous (*T. longicornis, A. clausi, A. discaudata, C. hamatus, Paracalanus parvus, Pseudocalanus* sp.). Those species are considered to be allochthonous that show decreasing abundance with decreasing salinity. This decrease indicates that, at best, reproduction by these species is reduced at reduced salinities, although they are able to survive at lower-than- preferred salinities for some time. The autochthonous species do reproduce in the estuary and hence show a quite different distribution pattern from the allochthonous ones. The abundance maximum is always found in salinities below 30. In the salinity range of its maximal abundance a species usually also persists longest. Our conclusion is obvious: in this (preferred) salinity range reproduction is maximal and continues longest. For *E. affinis* this occurs in salinities from 5 to 10, whereas *A. bifilosa* and *A. tonsa* reach their maximal period of occurrence in salinities from 20 to 25.

E. affinis shows a very curious seasonal distribution (Table 4a). In autumn and winter it extends its presence into almost all salinities, up to almost full strength seawater. In spring it reaches very high densities at lower salinities but rapidly disappears from higher salinities. In summer and early autumn it only occurs in large numbers at low salinities. The explanation of this distribution pattern might be a temperature-dependent salinity tolerance, but VON VAUPEL-KLEIN & WEBER (1975) found no indications of this.

The observation that in summer and autumn *E. affinis* does not occur in salinities above 15 and that it only occurs abundantly in salinities below 5 suggests that biotic factors are involved in pushing this species well below its preferred salinity of 12 (HEINLE, 1969). The distribution pattern in the Ems estuary is not unique, for BRADLEY (1975) found the same distribution in Chesapeake Bay. He suggests that competition with *A. tonsa* is the cause. BAKKER *et al.* (1977) also explain the seasonal distribution of *E. affinis* in Lake Veere and the Western Schelde, which shows the same trends as in the Ems estuary, by competition with *A. tonsa*. LONSDALE *et al.* (1979) have shown that *A. tonsa* can prey on nauplii of other species. While competition between these species and inter-specific predation may form part of the explanation of the observed distribution, predation by species other than copepods might be involved as well. Predation, even if the predation pressure on both species was equal, would favour the survival of *A. tonsa* over *E. affinis*. *E. affinis* carry their eggs in paired egg-sacs until the nauplii hatch (which has the disadvantage of slowing them down when they are trying to avoid predators), whereas *A. tonsa* drop their eggs shortly after extrusion. Predation on egg-carrying females of *E. affinis* so also entails the loss of the current batch of eggs. When reproductive females of *A. tonsa* are eaten, the eggs already laid can still contribute to the propagation of the species.

During periods of lower predation pressure, on the other hand, carrying the eggs around in egg-sacs is advantageous in that it enhances survival of the eggs: the eggs are kept from settling in/on the sediment with its high numbers of potential predators. Moreover, the viability of *A. tonsa* eggs in mud is only about 5 days at 17.5°C (UYE & FLEMINGER, 1976). Possibly, hydrogen sulfide plays a role here. This may explain why *A. tonsa* can become abundant in summer: then the development time of eggs is only 2 days (UYE & FLEMINGER, 1976), and predation pressure is so high that more *E. affinis* eggs are lost through predation on adult females than *A. tonsa* eggs are lost to benthic predators. *A. tonsa* is known to exhibit a near-linear temperature/respiration relation (CONOVER, 1956). Egg production may be susceptible to a similar relationship, and consequently temperature-related. The virtual disappearance of *A. tonsa* from the Ems estuary in

winter may so be caused by a decrease in egg production at low temperatures combined with a reduction in survival-until-hatching of the few eggs laid, due to the long development times. That *E. affinis* is abundant in winter and spring, more so than *A. bifilosa*, which is very closely related to *A. tonsa* and also produces single eggs, may indicate that it is advantageous to keep the eggs in egg-sacs.

Of the mysids, *Neomysis integer* has a pronounced abundance peak in June, due to reproduction, in the lower salinity reaches, with a maximum in salinities from 5 to 10. This species was rarely found at salinities above 25. The other common species, *Mesopodopsis slabberi*, appears to be indifferent to salinity, at least during the summer. Then it is found all over the estuary, with an abundance peak in September. The data indicate that there are at least two reproduction peaks: one in May and one in September. The catches of larval mysids during these months also show peaks. MAUCHLINE (1971) has shown that *N. integer* in Scottish waters has at least two generations: one in May, produced by the surviving winter generation and a second in September-October, produced by the May generation. The abundance peaks of *M. slabberi* may have the same cause. The data show that the occurrence of *M. slabberi* after September is restricted to high salinities, possibly indicating a migratory tendency towards the outer part of the estuary, which is deeper and, during this time of the year, warmer. VAN DER BAAN & HOLTHUIS (1971) confirm the existence of a migration towards deeper, warmer water in late autumn, originally postulated by HOLTHUIS (1954). The catches of the other mysid species were too irregular to construct a reliable distribution table.

Of the meroplankton in the Ems estuary, the cirripede larvae are numerically the most important. From June until October they often occur in densities of over 1000 per m^3 in salinities above 15. In salinities below 15 their occurrence is much more irregular. This probably has to do with most of the species present not being very tolerant to reduced salinities. Part of the cause may also be the lack of suitable hard substrate, which is very pronounced in the inner part of the Ems estuary, restricting the number of adults and hence the number of larvae locally produced. The number of cyprids may have been underestimated, due to their tendency to settle immediately on any hard substrate they encounter; in this case parts of our sampling gear or glassware.

The polychaete larvae again form a very heterogenous group, consisting of a large number of species that would merit a separate study. As a group they show a clearly marked abundance maximum in April, which is concentrated in the salinities between 15 and 25. A second, smaller peak can be seen in late summer in the higher salinities above 25. Representatives of this group are not common at salinities below 10.

This study being the first quantitative zooplankton study in the Ems estuary, it is not possible to compare abundances with other data from the literature. KÜHL & MANN (1968) did not enumerate separate species of calanoid copepods but did mention the existence of two abundance maxima of the group as a whole: one in the river Ems proper at 0-5 S and another, less pronounced, in the area around the island of Borkum in the outer part of the estuary. This agrees well with the results of this study, since their data are based on catches made during May and October. The distribution in their catches of the mysids *N. integer* and *M. slabberi* is consistent with our findings, especially the increase in density of *M. slabberi* towards sea in autumn. They mention finding the other four species also found during our investigation. STOCK & DE VOS (1960) give a list of the calanoid species they found in the area. Their findings agree very well with ours as to the species found, but not at all as to relative abundance of the different species. This is probably because they had to rely on summer samples only, whereas we were able to sample for a number of years in all seasons.

A major decrease does seem to have occurred in abundance of Appendicularia in the estuary during the last 25 to 30 years, because we never found any *Oikopleura dioica* or *Fritillaria borealis*, whereas KÜHL & MANN (1968) found *O. dioica* in large numbers. Possibly the reason for this change is the increase in turbidity in the estuary (DE JONGE, 1983).

5. REFERENCES

BAAN, S. M. VAN DER & L. B. HOLTHUIS, 1971. Seasonal occurrence of Mysidacea in the surface plankton of the southern North Sea near the "Texel" lightship.—Neth. J. Sea Res. **5**: 227-239.

BAKKER, C. & N. DE PAUW, 1975. Comparison of plankton assemblages of identical salinity ranges

in estuarine tidal, and stagnant environments II. Zooplankton.—Neth. J. Sea Res. **9:** 145-165.

BAKKER, C., W.J. PHAFF, M. VAN EWIJK-ROSIER & N. DE PAUW, 1977. Copepod biomass in an estuarine and a stagnant brackish environment of the S.W. Netherlands.—Hydrobiologica **52:** 3-13.

BARETTA, J. W., 1981. The zooplankton of the Ems estuary: quantitative data. In: N. DANKERS, H. KÜHL & W. J. WOLFF (eds.). Invertebrates of the Wadden Sea. Balkema, Rotterdam: 145-153.

BARLOW, J. P., 1955. Physical and biological processes determining the distribution of zooplankton in a tidal estuary.—Biol. Bull. **109:** 211-225.

BRADLEY, B. P., 1975. The anomalous influence of salinity on temperature tolerances of summer and winter populations of the copepod *Eurytemora affinis*.—Biol. Bull. **148:** 26-34.

CONOVER, R. J., 1956. Oceanography of Long Island Sound, 1952-1954.—Bull. Bingham oceanogr. Coll. **15:** 156-233.

DORRESTEIN, R., 1960. Einige klimatologigische und hydrologische Daten für das Ems-Estuarium.—Verh. K. ned. geol.—mijnb. Genoot. Geol. Serie 19, Symposium Ems-Estuarium (Nordsee): 39-42.

GEHRINGER, J.W., 1962. The Gulf III and other modern high-speed plankton samplers.—Rapp. P.—v. Réun. Cons. perm. int. Explor. Mer **153:** 19-22.

GORDON, D. C. & J. W. BARETTA, 1982. A preliminary comparison of two turbid coastal ecosystems: the Dollard (Netherlands-FRG) and the Cumberland Basin (Canada).—Hydrobiol. Bull. **16:** 255-267.

GUNTER, G., 1961. Some relations of estuarine organisms to salinity.—Limnol. Oceanogr. **6:** 182-190.

HEINLE, D. R., 1969. Culture of calanoid copepods in synthetic seawater.—J. Fish. Res. Bd Can. **26:** 150-153.

HELDER, W. & P. RUARDIJ, 1982. A one-dimensional mixing and flushing model of the Ems-Dollard estuary: calculation of time scales at different river discharges.—Neth. J. Sea Res. **15:** 293-312.

HICKEL, W., 1975. The mesozooplankton in the Wadden Sea of Sylt (North Sea).—Helgoländer wiss. Meeresunters. **27:** 254-262.

HOLTHUIS, L. B., 1954. Mysidacea. In: L. F. DE BEAUFORT. Veranderingen in de flora en fauna van de Zuiderzee (thans IJsselmeer), na afsluiting in 1932. Ned. Dierkundige Vereniging, Den Helder: 213-219.

JEFFRIES, H. P., 1962. Copepod indicator species in estuaries.—Ecology **43:** 730-733.

JONGE, V. N. DE, 1983. Relations between annual dredging activities, suspended matter concentrations and the development of the tidal regime in the Ems estuary.—Can. J. Fish. Aquat. Sci. **40** (Suppl. 1): 289-300.

JONGE, V. N. DE & L. A. BOUWMAN, 1977. A simple density separation technique for quantitative isolation of meiobenthos using the colloidal silica Ludox-TM.—Mar. Biol. **42:** 143-148.

KETCHUM, B. H., 1954. Relation between circulation and planktonic populations in estuaries.—Ecology **35:** 191-200.

KÜHL, H. & H. MANN, 1968. Über das Zooplankton der unteren Ems.—Veröff. Inst. Meeresforsch. Bremerhaven **11:** 119-136.

LONSDALE, D. J., D. R. HEINLE & C. SIEGFRIED, 1979. Carnivorous feeding behavior of the adult calanoid copepod *Acartia tonsa* Dana.—J. exp. mar. Biol. Ecol. **36:** 235-248.

MAUCHLINE, J., 1971. Seasonal occurrence of Mysids (Crustaceae) and social behaviour.—J. mar. biol. Ass. U.K. **51:** 809-825.

REDEKE, H. C., 1932. Über den jetzigen Stand unserer Kenntnisse der Flora und Fauna des Brackwassers.—Verh. Internat. Ver. Limnol. **6:** 46-61.

——, 1934. On the occurrence of two pelagic copepods, *Acartia bifilosa* and *Acartia tonsa*, in the brackish waters of the Netherlands.—J. Cons. Internat. Expl. Mer **9:** 39-43.

ROGERS, H. M., 1940. Occurrence and retention of plankton within the estuary.—J. Fish. Res. Bd Can. **5:** 164-171.

RUARDIJ, P., 1981. Een ééndimensionaal model van de transportprocessen in het Eems-Dollard oecosysteem.—Boede Publ. en Versl. 3-1981: 1-37.

SOKAL, R.R. & F.J. ROHLF, 1981. Biometry. Freeman, San Francisco: 1-858.

SPLUNDER, M. VAN, 1976. Verspreiding van het zoöplankton in het Eems-Dollard estuarium.—BOVA Publ. en Versl. 2-1976: 1-47.

STOCK, J. H. & A. P. C. DE VOS, 1960. Einige wirbellose Tiergruppen des Dollart-Ems Estuarium.—Verh. K. ned. geol.—mijnb. Genoot. Geol. Serie 19, Symposium Ems-estuarium (Nordsee): 203-220.

UYE, S. & A. FLEMINGER, 1976. Effects of various environmental factors on egg development of several species of *Acartia* in Southern California.—Mar. Biol. **38:** 253-262.

VAUPEL-KLEIN, J. C. VON & R. E. WEBER, 1975. Distribution of *Eurytemora affinis* (Copepoda: Calanoida) in relation to salinity: field and laboratory observations.—Neth. J. Sea Res. **9:** 297-310.

WIBAUT-ISEBREE MOENS, N. L., 1954. Plankton. In: L. F. DE BEAUFORT. Veranderingen in de flora en fauna van de Zuiderzee (thans IJsselmeer), na de afsluiting in 1932.—Ned. Dierkundige Vereniging, Den Helder: 90-155.

(received 6 May 1987; revised 12 February 1988)

Netherlands Journal of Sea Research
22 (1): 83-90 (1988)

IMPACT OF TAIL-NIPPING ON MORTALITY, GROWTH AND REPRODUCTION OF *ARENICOLA MARINA**

MAGDA J.N. BERGMAN[1], HENK W. VAN DER VEER[1] and LESZEK KARCZMARSKI[2]
[1]*Netherlands Institute for Sea Research, P.O. Box 59, 1790 AB Den Burg Texel, The Netherlands*
[2]*Academy of Agriculture, Szczecin, Poland*

ABSTRACT

The impact of predation by amputation of regenerating body parts (tail tips) of the lugworm *Arenicola marina* on species mortality, growth and reproduction has been studied under laboratory conditions by the artificial removal of tail tips at different frequencies. The loss of body weight by amputation was not compensated for by an increased growth. Within a wide range of amputation frequencies, total growth (body growth + amount of tail tip amputated) and reproduction of the lugworm were not affected. Also, both egg development and amount of energy stored in reproduction remained the same. Only at the highest frequency of amputation (once a week) did total growth decrease in the course of time, resulting even in a loss of body weight. The amount of energy stored in reproduction was also significantly less at the highest rate of amputation. Lugworms appeared to be unable to sustain this high level of amputation and the anaerobic sediment conditions in the cuvettes suggest a reduced pumping activity and food intake. Mortality in this group was also higher than in the other groups. The consequences of tail-nipping by flatfish for *A. marina* in the field situation are discussed.

1. INTRODUCTION

The estuarine Wadden Sea is an important nursery area for a number of fish species, *e.g.* the commercially important plaice *Pleuronectes platessa* L. (ZIJLSTRA, 1972; KUIPERS, 1977; VAN DER VEER, 1986). Stomach content analysis of plaice carried out by KUIPERS (1977) and DE VLAS (1979a) showed that food items mainly consist of regenerating body parts of macrobenthic organisms living in the tidal flats. Siphons of the tellin *Macoma balthica* (L.) and tail tips of the lugworm *Arenicola marina* (L.) were frequently found and may be the main food item for several months (KUIPERS, 1977; DE VLAS, 1979a).

Estimates of predation pressure of plaice on the macrobenthic fauna suggest that this predation of regenerating body parts might have an impact on the prey populations (DE VLAS, 1979a; KUIPERS *et al.*, 1986). In the Balgzand tidal flat area lugworms are tail-nipped on average about once per week during the spring-summer season (DE VLAS, 1979a), and about 10 to 30% of the annual production of *A. marina* is removed by this predation (DE VLAS, 1979b; KUIPERS *et al.*, 1986). This means that the lugworm might have to regenerate an amount equal to a complete tail within 6 months (KUIPERS *et al.*, 1986). Juvenile lugworms can have more than 100 tail segments (DE VLAS, 1979b). Since neoformation of tail segments does not occur (DE VLAS, 1979b) and because the lugworm dies when only a few tail segments are left (DE VLAS, 1979a), a considerable mortality might be induced. It is unknown, however, whether this loss will affect not only growth but also the reproduction capacity of *A. marina* by delaying the development or reducing the amount of spawning products.

This paper is one in a series dealing with fish-benthos interactions and presents the results of laboratory experiments carried out with lugworms to investigate the impact of artificial tail-nipping on mortality, growth and reproduction.

**Publication no. 25 of the project "Ecological Research of the North Sea and Wadden Sea" (EON).*

Acknowledgement.—Thanks are due to Henri Etcheber for analysing the carbon content of the eggs, to T. Kuip and R. Lakeman for technical assistance and to J.J. Beukema, J. de Vlas, P.A.W.J. de Wilde and J.J. Zijlstra for critical reading of the manuscript.

2. MATERIAL AND METHODS

To house the lugworms and to separate them from the sediment without injuring their tails, PVC cuvettes were constructed, similar to those described by DE VLAS (1979b). Each cuvette contains an amount of sediment with a surface area of 1.5 x 22.0 cm and a depth of 38 cm and has a front side that can be removed. This block of sediment proved to be sufficient for the lugworms to construct a J-shaped living tube. The worms were introduced by simply placing them on top of the sediment, and normally they burrowed immediately. To remove the worm, the front side of the cuvette was taken off. The cuvettes were placed in 2 rows in 3 asbestos-concrete containers. The containers were kept in running seawater (salinity about 25 to 30), in which an artificial tidal regime was applied with low water for 3 h twice a day.

Once a week about 2 to 3 g of deep-frozen spinach pulp was introduced in each cuvette to maintain a sufficient food content in the sediment, as in the experiments of DE VLAS (1979b). The water temperature was recorded once a day and adjusted to that of the nearby Wadden Sea. Every week all worms were removed from their cuvettes, some were amputated and all were placed on top of the sediment again. Tail-cropping was simulated by removing part of the tail by gently pulling the tail tip of a worm. In most cases the tail autotomized at the border of the nearest segment.

Lugworms in the range of 3 to 4 g wet weight were collected by hand in a tidal flat area near the island of Texel. Before the introduction of the worms in the cuvettes, they were dried between blotting paper and their wet weight was measured. Some worms were dried at 60°C for 2 days and burnt at 520°C for 2 h to estimate the relationship between wet and weight-ash-free dry weight (AFDW) at the beginning of the experiment. The lugworms were introduced in the cuvettes on 23 March 1987. The first artificial amputation was performed on 30 March and the last on 19 July. The lugworms were divided into 4 groups, each consisting of about 50 to 60 animals, with a different frequency of amputation:

— series 0: control group, no amputation
— series 1/4: amputation once a month
— series 1/2: amputation once every two weeks
— series 1/1: amputation once a week

The maximal number of amputations in the experiment was based on the actual predation frequency found on the tidal flats of Balgzand (DE VLAS, 1979a, 1979b). Half the lugworms were killed on 31 May and the remaining part on July 26. During the experiment, all tail tips removed were dried at 60°C for 2 days, weighed, and burnt at 520°C for 2 h. The loss of weight was considered to represent the AFDW.

At the end of the experiment, all worms were opened carefully and the coelomic fluid was collected in a Petri dish. At a magnification of 160, the fluid was inspected for the presence of sexual products, and so the animals were classified into males and females. In each female, the diameters of about 100 oocytes were measured at a magnification of 320 along straight lines to obtain random samples.

To collect the oocytes, the coelomic fluid of the females killed on July 26 was filtered with Whatmann glass microfibre filters GF/F (porosity 0.4 to 0.8 μm) to estimate the AFDW of the reproductive organs. Filtering was done with a Nalgene vacuum hand gauge pump at 10 to 15 cm Hg pressure. AFDW was determined by drying the filters for 1 day at 60°C, weighing, burning for 2 h at 520°C and weighing again. To get an indication of the carbon content of the AFDW of the oocytes, some filters were crushed and subsamples were analysed according to the wet oxidation method described by STRICKLAND & PARSONS (1972).

3. RESULTS

Temperature conditions during the experiment showed a close correspondence with the field situation (Fig. 1). Only during March was the water temperature in the containers too high, due to technical problems with the cooling equipment.

At the start of the experiment AFDW of the lugworms was related with wet weight according to:

$$D = 0.117xW - 0.02 \; (n = 66;\ r = 0.98;\ p < 0.05)$$

in which D is AFDW (g) and W is wet weight (g).

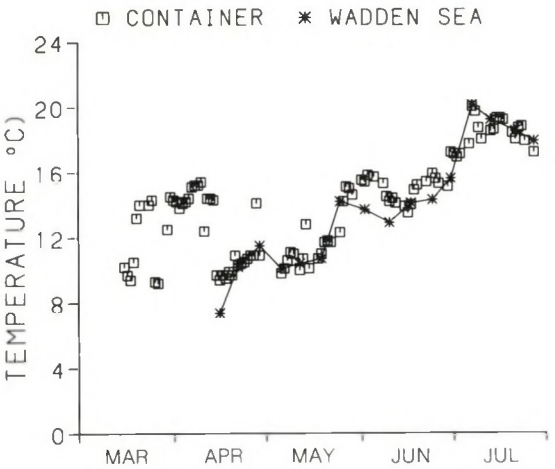

Fig. 1. Temperature conditions (°C) in the containers and in the Wadden Sea (Marsdiep inlet) in the course of the experiment.

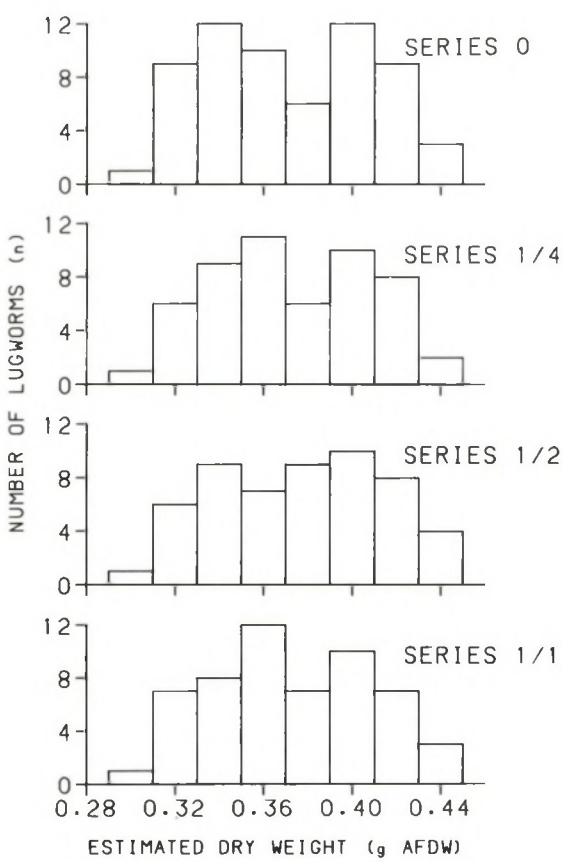

Fig. 2. Frequency distribution of individual weights (g AFDW) of *A. marina* at the beginning of the experiment. For explanation see text.

Based on this relation the individual AFDW of the lugworms at the beginning of the experiment was estimated (Fig. 2). Initial values of mean body weights of the worms were about the same in all series, 0.38 g AFDW.

Table 1 gives the relation between initial body weight and respectively body growth and amount of tail tip amputated in each series during the experiment. Because no significant relations were found, the mean values of all worms per series can be compared directly without correcting for individual differences in initial body weight.

With a higher frequency of amputation, the amount of tail removed also increased (Fig. 3). The total amount amputated during the first part of the experiment was about the same as during the second period. In the group amputated once a week (series 1/1) in total about 0.10 g AFDW was removed in 4 months, *i.e.* about 25% of the initial weight. In this group of most heavily amputated worms some extra mortality occurred (Fig. 4).

Fig. 5 shows the mean body growth (g AFDW) in the course of the experiment, estimated as the difference in body weight between the end and the beginning of the experiment. The worms of series 0 and 1/4 showed a near-similar body growth. The lugworms of series 1/2 also had a positive body growth, be it a lower one. The worms of series 1/1 showed the lowest body growth, and even a negative growth over the entire period. During the second part of the experiment, in all series body growth was lower than in the first period, even in the control group.

With respect to total growth, defined as the sum of body growth and loss due to amputation, (Fig. 6), the series 0, 1/4 and 1/2 showed a rather similar pattern, which means that predation apparently did not stimulate growth. Total growth of the most heavily amputated group of lugworms (series 1/1) was lower than in the other groups.

The development of oocytes is given in Fig. 7. At the beginning of the experiment hardly any oocytes could be found. Halfway, development had not yet started, although lots of small eggs could be found in the coelomic fluid. In all series a strong increase in diameter was observed during the second part of the experiment, without a significant difference between the various series.

The total biomass of oocytes at the end of the experiment is presented in Table 2. As in body weight and growth, a significant difference in

TABLE 1

Relation according to $y = aX + b$, between X = estimated initial body weight of *Arenicola marina* in March (in g AFDW) and y = resp.: (1) body growth, (2) amount of tail tips amputated and (1 + 2) total growth during various periods.

			a	*b*	*r*	*N*	*p*
Series 0							
	May	body growth	0.02	0.18	0.01	15	n.s.
	July	body growth	0.28	−0.02	0.14	20	n.s.
Series 1/4							
	May	body growth	0.16	−0.03	−0.01	15	n.s.
		amputation	−0.37	0.03	−0.36	15	n.s.
		total growth	−0.06	0.19	−0.03	15	n.s.
	July	body growth	−0.73	0.47	−0.32	20	n.s.
		amputation	0.66	0.04	0.02	20	n.s.
		total growth	−0.73	0.51	−0.31	20	n.s.
Series 1/2							
	May	body growth	0.13	0.06	0.05	20	n.s.
		amputation	0.12	0.03	0.07	20	n.s.
		total growth	0.14	0.09	0.06	20	n.s.
	July	body growth	−0.50	0.35	−0.20	17	n.s.
		amputation	0.07	0.02	−0.03	17	n.s.
		total growth	0.14	−0.09	0.06	17	n.s.
Series 1/1							
	May	body growth	−0.43	0.12	−0.14	19	n.s.
		amputation	0.34	−0.03	0.37	19	n.s.
		total growth	−0.09	0.09	−0.03	19	n.s.
	July	body growth	−0.43	0.12	−0.14	17	n.s.
		amputation	0.12	0.01	0.35	17	n.s.
		total growth	−0.09	0.09	−0.02	17	n.s.

total oocyte weight (t-test; $p < 0.05$) was found between the worms of series 1/1 (0.021 g AFDW) and those in the other series (0.052 to 0.059 g AFDW). Results of the wet oxidation revealed that about 66% of this AFDW consisted of organic carbon (Table 3).

4. DISCUSSION

4.1. EXPERIMENTAL RESULTS

De Vlas (1979b) already showed that tail-nipping on lugworms in the field by predatory fish, such as plaice, could be imitated under laboratory conditions. However, from his experiments it was unclear to what extent quantitative differences in predation pressure could be brought about by differences in frequency only. The present experiments show that although the tail tips were amputated by hand, the differences in the amount of tail tip removed indeed depend mainly on the frequency of amputation.

The results further suggest that the loss of body weight by artificial tail-nipping was not compensated for by an increased growth, with the possible exception of the lowest rate of amputation (once per month). In all groups of amputated lugworms total growth was almost the same or less than the total growth in the control series, whereas the relative distribution over am-

TABLE 2

Mean values and 95% confidence limits of oocytes biomass of individual *A. marina* at the end of the amputation experiment (g AFDW)

	oocyte biomass (g AFDW)
serie 0	0.052 ± 0.02
serie 1/4	0.059 ± 0.02
serie 1/2	0.054 ± 0.03
serie 1/1	0.021 ± 0.02

TABLE 3

Organic carbon content (mgC) of eggs of 3 lugworms *A. marina* in series 0 at the end of the experiment

worm	*weight of eggs*		*total org C.*	*orgC/AFDW*
	dry(mg)	*AFDW (mg)*	*(mgC)*	*(%)*
1	91.2	57.3	39.4	68.8
2	63.1	59.9	35.7	59.6
3	117.5	31.8	22.4.	70.3

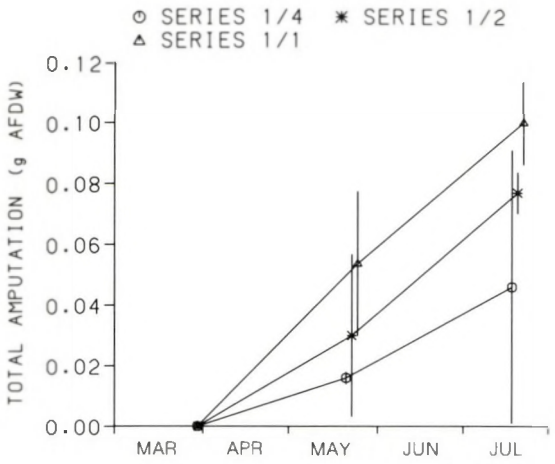

Fig. 3. Mean total weight (g AFDW) with 95% confidence limits of tail tips removed per worm during the experiment. For explanation see text.

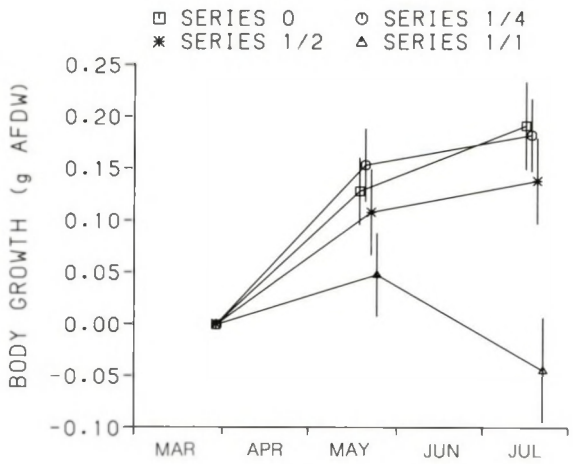

Fig. 5. Mean body growth (g AFDW) with 95% confidence limits of lugworms during the experiment. For explanation see text.

putation and body growth varied between the series.

The results of the experiment indicate that up to a frequency of once every other week (series 1/2), *A. marina* can sustain the impact of tail-nipping fairly well. Mortality and total growth remained the same, as did gamete production and total reproduction capacity, measured as the amount of AFDW stored in reproduction. This development of the oocytes corresponded with that reported by DE WILDE & BERGHUIS (1979b). However, the AFDW stored in ripe oocytes is, with 60 mg in relation to a mean weight of the worms of 380 + 220 = 600 mg, lower than found by DE WILDE & BERGHUIS (1979b) on the basis of wet weight (25%).

However, at higher amputation levels, as demonstrated by the amputation frequency of once a week, tail-nipping seems to have adverse effects on the worms. Mortality was much higher and the black sediment in the cuvettes of the surviving worms —which points to an increased FeS formation— suggested a lower (pumping) activity and hence food intake. The normal functioning of the worms appeared to be affected, which was also suggested by the reduced total growth, and

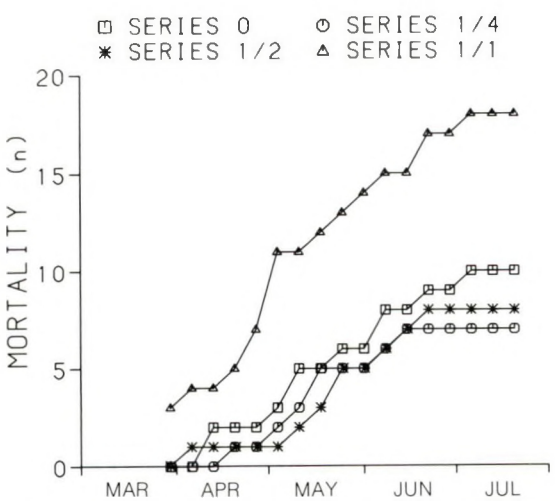

Fig. 4. Total mortality among 50 to 60 lugworms in the containers during the experiment. For explanation see text.

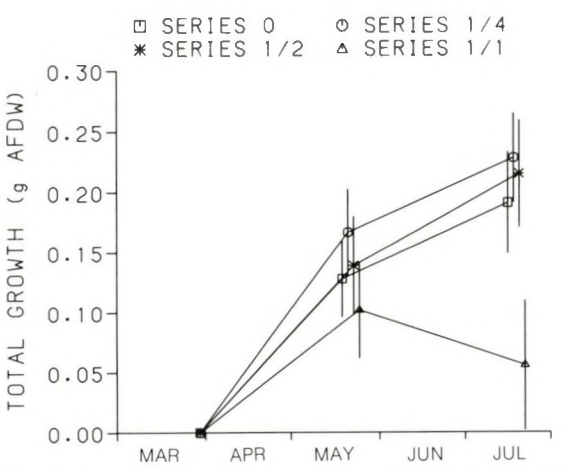

Fig. 6. Mean total growth (= body growth + amount of tail tip amputated) in g AFDW with 95% confidence limits of lugworms during the experiment. For explanation see text.

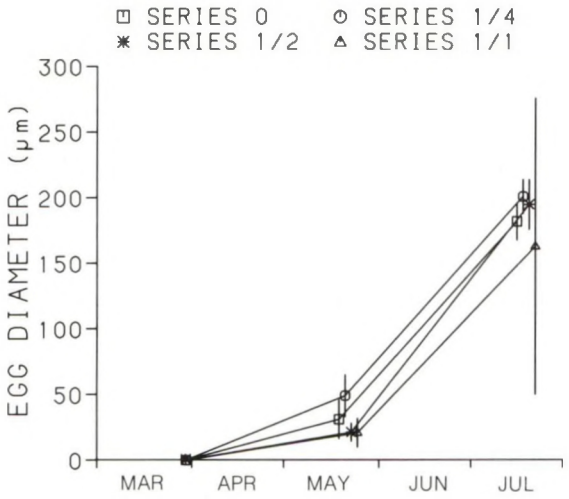

Fig. 7. Development of oocyte diameter (μm) of lugworms during the experiment. For explanation see text.

even negative growth when gamete production had started, and the reduction of the reproductive capacity by about 60%. However, the development of individual oocytes remained about the same, which means that the total number had decreased.

4.2. COMPARISON WITH THE FIELD SITUATION

In the field tail-nipping by flatfish, mainly plaice, is the most important source of predation on lugworms (KUIPERS, 1977; DE VLAS, 1979a, 1979b). The impact of this predation on the worms will to a large extent depend on the predation frequency and possibly the feeding conditions, since growth appears to be food-limited in the field (DE WILDE & BERGHUIS, 1979a). In a large tidal flat system in the western Wadden Sea, Balgzand, a detailed analysis has been made on the food intake of flatfish (KUIPERS, 1977; DE VLAS, 1979a) and the effects of tail-nipping on the production of lugworms (DE VLAS, 1979b). With information on the population parameters of the lugworms at the same locations (BEUKEMA & DE VLAS, 1979), a compilation of body growth and predation in the field can be made (Table 4).

Given the densities of lugworms and the total amount of predation by flatfish per m^2, it means that depending on the location each worm will have been preyed on between 2.3 and 4.1 times per month during the April to July period (4). The amount of biomass removed by this predation in the field will have ranged from 9 to 20 mg AFDW per worm per month between April and July (7), compared with 46 to 100 mg AFDW per worm, or about 12.5 to 25 mg AFDW per month during the experiment. This means that the amount of tail tip removed by predation in the field falls within the range of, or is slightly lower than, the biomass amputated in the experiment. The predation pressure in the experimental set-up thus reflected the field situation fairly well. This is true in particular for series 1/2 , whereas in series 1/1 even a higher predation pressure has been applied than is likely to occur on Balgzand.

If food conditions are reflected in the ultimate body growth of the worms, the following can be concluded about the food conditions in the field compared with those applied in the experimental

TABLE 4

Compilation of data on growth and predation (mg AFDW) of *Arenicola marina* at 3 locations on the Balgzand tidal flat area (see DE VLAS, 1979a), based on ref. I: BEUKEMA & DE VLAS (1979); ref. II: DE VLAS (1979a); ref. III: DE VLAS (1979b). The whole period of predation has been estimated at about 6.5 months per year (according to DE VLAS, 1979a).

	Unit	*Transect*			*Ref.*
		3	*4*	*5*	
(1) mean density	$(n \cdot m^{-2})$	15	25	30	III
(2) consumption of tail tips by plaice	$(n \cdot m^{-2} \cdot y^{-1})$	203	573	494	II
by flounder		14	47	85	
total		217	620	579	
(3) amputations per worm [(2)/(1)]	$(n \cdot y^{-1})$	14.5	24.8	19.3	
(4) amputations per worm per month	$(n \cdot mo^{-1})$	2.2	3.8	3.0	
(5) predation of tail tips	$(mg \cdot m^{-2} \cdot y^{-1})$	1695	2971	1684	II
(6) predation of tail tips per worm [(5)/(1)]	$(mg \cdot y^{-1})$	113	119	56	
(7) predation of tail tips per worm per month	$(mg \cdot mo^{-1})$	17.4	18.3	8.6	
(8) body growth per worm during April - July	$(mg \cdot mo^{-1})$	194	341	188	I
(9) predation/total growth during April - July	(%)	26	18	15	

situation. Between April and the end of July, individual body growth of adult worms in the field varied from 188 to 341 mg AFDW (BEUKEMA & DE VLAS, 1979), which means that together with the biomass of tail tips removed by predation (between 34 and 73 mg AFDW), total growth amounted to about 222 to 414 mg AFDW. Expressed as proportion of total growth, between 15 and 26% of body growth will have been removed by amputation (Table 4). In the experiment total growth varied between 191 and 228 mg AFDW per worm, except for the ones most severely preyed on, which showed a growth of only 50 mg AFDW. The percentage of tail biomass amputated varied between the series from respectively 20, 36 to 178% of the total growth. Therefore, maximum total growth of the worms in the experiment appeared to have been lower than the total growth observed in the field. At part of Balgzand (transects 3 and 5 in DE VLAS, 1979a), total growth was about the same as in the experiment. The higher total growth at transect 4 suggests the presence of more favourable food conditions for these worms in the field than were applied in the laboratory.

4.3. IMPACT ON POPULATION PARAMETERS OF *A. MARINA* IN THE WADDEN SEA

At present, owing to lack of data, no clear conclusions can be drawn about the impact of predation on the *A. marina* population in the Wadden Sea.

Because a lugworm is thought to die when fewer than 3 to 5 tail segments are left (DE VLAS, 1979b), mortality in lugworms will depend on the total amount of segments removed during the season and the initial number of segments present in spring, when predation starts as soon as juvenile plaice have immigrated (KUIPERS, 1977). The initial number of segments present in spring will be the result of the predation in previous seasons. Therefore, the lifetime of a lugworm will be strongly related to this predation pressure.

In the experiments an increased mortality was only observed in the series most heavily preyed on. However, these experiments lasted only 4 months. In the field at Balgzand lower predation rates occur over a longer period, but even this pressure is thought to result in mortality (DE VLAS, 1979b; KUIPERS *et al.*, 1986). DE VLAS (1979b) found a decrease in the number of tail segments by predation of between 14 and 22 during one season. Because the initial number of tail segments is limited to between 70 and 120 (DE VLAS, 1979b), most tail segments will be removed by predation within a few seasons. As neoformation of segments does not occur (DE VLAS, 1979b), the worms are bound to die after a few seasons.

The predation on tail tips will depend upon the yearclass strength of plaice, and variations in plaice abundance will have a direct effect on the mortality rate and hence the age-composition of the lugworm population. At the present level of plaice abundance, the stable population of *A. marina* on Balgzand suggests that recruitment of juveniles seems to be large enough to compensate for the loss by mortality, which in total appears to be about 22% a year (BEUKEMA & DE VLAS, 1979). The existence of *A. marina* in other parts of the Wadden Sea (BEUKEMA *et al.*, 1978) suggests a similar situation for these populations. It is unclear at what level of flatfish predation a situation of over-exploitation of the *A. marina* population will be created.

5. REFERENCES

BEUKEMA, J.J., W. DE BRUIN & J.J.M. JANSEN, 1978. Biomass and species richness of the macrobenthic animals living on the tidal flats of the Dutch Wadden Sea: long-term changes during a period with mild winters.—Neth. J. Sea Res. **12:** 58-77.

BEUKEMA, J.J. & J. DE VLAS, 1979. Population parameters of the lugworm *Arenicola marina* living on tidal flats in the Dutch Wadden Sea.—Neth. J. Sea Res. **13:** 331-353.

KUIPERS, B.R., 1977. On the ecology of juvenile plaice on a tidal flat in the Wadden Sea.—Neth. J. Sea Res. **11:** 56-91.

KUIPERS, B.R., H.W. VAN DER VEER & J.J. ZIJLSTRA, 1986. Interaction between juvenile plaice (*Pleuronectes platessa*) and benthos in a tidal flat area.—Coun. Meet. int. Coun. Explor. Sea C.M.-ICES/L 3: 1-8.

STRICKLAND, J.H.D. & T.R. PARSONS, 1972. A practical handbook of seawater analysis.—J. Fish. Res. Bd Can. **167:** 1-310.

VEER, H.W. VAN DER, 1986. Immigration, settlement and density-dependent mortality of a larval and early post-larval O-group plaice (*Pleuronectes platessa*) population in the western Wadden Sea.—Mar. Ecol. Prog. Ser. **29:** 223-236.

VLAS, J. DE, 1979a. Annual food intake by plaice and flounder in a tidal flat area in the Dutch Wadden Sea with special reference to consumption of regenerating parts of macrobenthic prey.—Neth. J. Sea Res. **13:** 117-153.

——, 1979b. Secondary production by tail regeneration in a tidal flat population of lugworms (*Arenicola marina*) cropped by flatfish.—Neth J. Sea Res. **13:** 362-393.

WILDE, P.A.W.J. DE & E.M. BERGHUIS, 1979a. Laboratory experiments on growth of juvenile lugworms, *Arenicola marina*.—Neth. J. Sea Res. **13:** 487-502.

——, 1979b. Spawning and gamete production in *Arenicola marina* in the Netherlands, Wadden Sea.—Neth. J. Sa Res. **13:** 503-511.

ZIJLSTRA, J.J., 1972. On the importance of the Waddensea as a nursery area in relation to the conservation of the southern North Sea fishery resources.—Symp. zool. Soc. Lond. **29:** 233-258.

(received 16 December 1987; revised 10 February 1988)

Netherlands Journal of Sea Research
22 (3): 185-198 (1988)

TIDAL AND RESIDUAL FLOWS IN THE WESTERN DUTCH WADDEN SEA II: AN ANALYTICAL MODEL TO STUDY THE CONSTANT FLOW BETWEEN CONNECTED TIDAL BASINS*

H. RIDDERINKHOF

Netherlands Institute for Sea Research, P.O.Box 59, 1790 AB Den Burg, Texel, The Netherlands

ABSTRACT

In a one-dimensional analytical model the origin of constant flows between connected tidal basins, as well as the origin of the associated residual levels, is examined. Linearized shallow water equations are used to describe the propagation and damping of a tidal wave in schematized (uniform width and depth) connected basins. Analytical expressions are derived for the tidal stress terms, including the contribution of the non-linear bottom-friction term, which serve as the forcing functions in the equations for the mean field. It is shown that in a first approximation the residual levels in the tidal inlets, which give boundary conditions for the tidally-averaged equations, are dependent on the tidal velocities in the inlet because of a "Bernoulli effect". The model shows that in general differences between the fluctuating water levels at the inlets influence the residual flow more than morphological differences between two connected basins. The tidally-driven mass transport in the western Dutch Wadden Sea, directed southwards from the Vlie basin towards the Marsdiep basin, can be explained from the larger water-level amplitude at the inlet of the Vlie basin.

1. INTRODUCTION

In a preceding paper on tidal and residual flows in the western Dutch Wadden Sea, in which results from a detailed two-dimensional numerical model were discussed, it has been shown that the tidally-driven mean flows in this area can be subdivided into a large-scale part, the constant flow between connected tidal basins, and a small-scale part, the isolated residual eddies (RIDDERINKHOF, 1988). The boundaries with the open sea of this numerical model are located outside the region of influence of the tidal inlets in the adjacent, relatively deep, North Sea (Fig. 1). In contrast to most modelling studies on residual flows (*e.g.* PRANDLE, 1978), in which boundary conditions often directly induce a constant flow through the region under interest, no residual levels are prescribed on the boundaries of this numerical model. So the computed large-scale residual flow between the different tidal basins is internally driven by the tide.

The magnitude of the mean transport, 900 m^3s^{-1}, between the two major Wadden Sea basins, the Vlie and Marsdiep basins, is only about one percent of the transport amplitude in the inlets. However, this tide-induced constant flow can play an important role when for instance the composition or flushing time scale of water masses in the Marsdiep basin is considered. For comparison, the average supply of fresh water from the IJsselmeer is about 450 m^3s^{-1}. To gain more insight into the origin of this large-scale residual flow as well as of the associated residual elevations, a one-dimensional analytical model has been developed. This model is used to examine how the tidal mean field is influenced by morphological asymmetries between the two basins as well as by the influence of differences between the fluctuating water levels at the two inlets. A comparable analytical study on mass transport induced by tidal asymmetries at the inlets of a tidal canal was performed by VAN DE KREEKE & DEAN (1975). Studies on the effect of inlet asymmetries on the tide induced flow are presented in VAN DE KREEKE (1976) and VAN DE KREEKE & COTTER (1974).

Acknowledgements.—I am grateful to L.R.M. Maas for his interest and discussions during the set up of the analytical model.

Publication no. 22 of the project "Ecological Research North Sea and Wadden Sea" (EON)

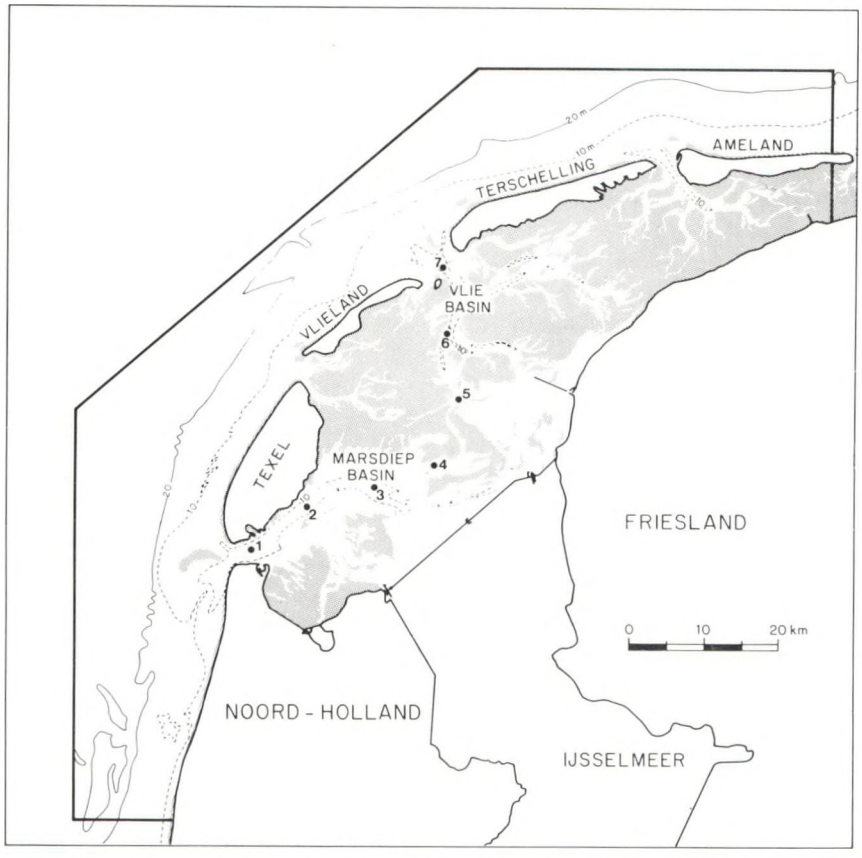

Fig. 1. Map of the western Dutch Wadden Sea showing some isobaths (10 m, 20 m), emersing tidal flats and the location of the boundaries of the numerical model (RIDDERINKHOF, 1988). Results in the gridpoints 1 to 7 are used in Fig. 4.

2. DESCRIPTION OF THE ANALYTICAL MODEL

In schematizing the western Wadden Sea only the two main basins, the Marsdiep and the Vlie basins, have been considered. Fig. 2 shows the schematization of the two-dimensional reality of these basins in a one-dimensional system. Either basin is schematized as a tidal channel with a constant width and depth. The chosen value of the morphological parameters of these channels is discussed in section 3.2. The transition between the tidal basins and the open sea, the in and outflow areas of the basins, is schematized as a funnel-shaped area with a length short compared with the basin length and the tidal wave length. From hereon the boundary between this inflow area and the tidal channels is referred to as the inlet of the channels. For this model the basic shallow water equations read:

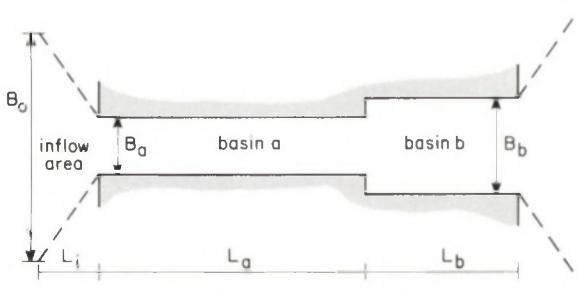

Fig. 2. Schematization of the tidal basins and adjacent inflow regions. Basin a represents the schematized Marsdiep basin and basin b represents the schematized Vlie basin.

$$\frac{\partial Q}{\partial t} + \frac{\partial}{\partial x}\left(\frac{Q^2}{BD}\right) + gBD\frac{\partial \zeta}{\partial x} + \frac{k\,Q|Q|}{BD^2} = 0 \qquad (1)$$

$$\frac{\partial Q}{\partial x} + B\frac{\partial \zeta}{\partial t} = 0 \qquad (2)$$

in which:
Q volume transport
D total water depth $H + \zeta$
H mean water depth
B width
ζ water elevation relative to the mean water depth
k bottom-friction coefficient.

Compared to the governing equations in the numerical model (RIDDERINKHOF, 1988), the Coriolis and horizontal turbulent viscosity terms are neglected. The equations are written in terms of the volume transport, Q, to have non-linear terms only in the momentum equation. These basic equations have to be linearized to find analytical expressions for the tidal water levels and volume transports. Using the method of LORENTZ (1926) to reduce the quadratic bottom-friction term, in which in a tidal period the energy dissipation of a single harmonic tidal constituent due to the linearized bottom friction term equals the energy dissipation due to the non-linear term, and assuming the amplitude of the fluctuating water levels to be much less than the mean water depth ($\zeta << H$), the following set of linear tidal equations can be deduced:

$$\frac{\partial Q}{\partial t} + gBH\frac{\partial \zeta}{\partial x} + \frac{\lambda_1 Q}{H} = 0 \tag{3}$$

$$\frac{\partial Q}{\partial x} + B\frac{\partial \zeta}{\partial t} = 0 \tag{4}$$

in which:

$$\lambda_1 = \frac{8k}{3\pi}\frac{|Q_m|}{BH} \tag{5}$$

where ($|Q_m|/BH$) represents a characteristic value of the tidal velocity amplitude in the area.

To find the equations which describe the tidal mean flow and elevations the basic equations (1) and (2) have to be averaged over a tidal cycle. In this averaging procedure it is assumed that:

$$Q = Q_0 + Q_1; \quad \overline{Q_1} = 0; \quad Q_0 << Q_1 \tag{6}$$

$$\zeta = \zeta_0 + \zeta_1; \quad \overline{\zeta_1} = 0; \quad \zeta_0 << \zeta_1 << H \tag{7}$$

in which:

Q_0, ζ_0 = residual components
Q_1, ζ_1 = tidal components

$$\overline{a} = \frac{1}{T}\int_{-T/2}^{T/2} a\,dt, \qquad T = \text{tidal period}$$

In this averaging procedure especially the linearization of the bottom-friction term needs care. Therefore the reduction of this term is discussed in detail. HEAPS (1978), using the method of HUNTER (1975) with complex variables, showed that use of (6) in the numerator of the quadratic friction term and averaging over a tidal period yields (see appendix A):

$$\frac{\overline{kQ|Q|}}{B(H+\zeta)^2} = \frac{\overline{2k|Q_1|Q_0}}{B(H+\zeta)^2} + \frac{\overline{kQ_1|Q_1|}}{B(H+\zeta)^2} \tag{8}$$

The assumption of a tidal motion associated with a single harmonic constituent together with condition (7) gives a further simplification of the first term in the right-hand side of eq. (8):

$$\frac{\overline{2k|Q_1|Q_0}}{B(H+\zeta)^2} = \frac{\lambda_0 Q_0}{H} \tag{9}$$

in which, analogous to eq. (6), the residual friction coefficient is dependent on the average tidal velocity amplitude:

$$\lambda_0 = \frac{4k}{\pi}\frac{|Q_m|}{BH} = 1.5\lambda_1 \tag{10}$$

Equation (10) shows that the term that is linearly dependent on the mean transport requires an increased friction coefficient. The numerator in the second term at the right-hand side of eq. (8) can be linearized by expanding $Q_1|Q_1|$ in a Fourier series. Retaining only the first term of this series gives:

$$\frac{\overline{kQ_1|Q_1|}}{B(H+\zeta)^2} = \frac{8}{3\pi}\frac{\overline{kQ_1}}{B(H+\zeta)^2} = \frac{\overline{\lambda_1 Q_1}}{(H+\zeta)} \tag{11}$$

in which the same expression as in eq. (5) is used for the friction coefficient. Expanding the denominator in the last term of eq. (11) and substituting condition (7) subsequently gives:

$$\frac{\overline{\lambda_1 Q_1}}{(H+\zeta)} = \frac{\overline{\lambda_1 Q_1}}{H} - \frac{\overline{\lambda_1 Q_1 \zeta_1}}{H^2} \tag{12}$$

Combining eqs. (8), (9), (11) and (12) together with conditions (6) and (7) finally gives the tidally-averaged linearized bottom-friction term:

$$\frac{\overline{kQ|Q|}}{B(H+\zeta)^2} = \frac{\lambda_0 Q_0}{H} - \frac{\overline{\lambda_1 Q_1 \zeta_1}}{H^2} \tag{13}$$

Equation (13) gives the required form of a term linear in the mean transport and a term quadratic in tidal quantities. It is of interest to note that an analysis exactly parallelling the above may be carried out working in terms of depth mean currents (u_1 and u_0) rather than volume transports. As a result it can be shown that in eq. (13) Q_1 is replaced by u_1 and Q_0 by u_0. In both cases the second term on the right-hand side of eq. (13) can be interpreted as a frictional effect acting on the Stokes drift, here expressed as a Stokes transport ($\overline{Q\zeta/H}$) and as a Stokes velocity ($\overline{u\zeta/H}$) when depth mean currents are used. Another method to linearize the bottom friction term is followed by VAN DE KREEKE & DEAN (1975). Their result is equal to eq. (13) if λ_1 in the first term on the right hand side of (13) is replaced by λ_0. This stems from a different treatment of the factor $kQ|Q|$ in the basic expression. The coefficient λ_1 is found when the procedure is started with the linearization of $kQ|Q|$ to $\lambda_1 Q$ before substituting (6). An increased coefficient, λ_0, is found when the procedure is started with substituting (6), as is shown above. Here the latter procedure is followed because it is analogous to the treatment of the other terms in eqs. (1) and (2).

Returning to the basic equations (1) and (2), making use of the inequalities in (6) and (7), substituting eq. (13) and assuming small non-linear advection we finally find the following set of equations for the mean field:

$$\overline{\frac{\partial}{\partial x}\left(\frac{Q_1^2}{BH}\right)} + \overline{gB\frac{\partial}{\partial x}\left(\frac{\zeta_1^2}{2}\right)} + gBH\frac{\partial \zeta_0}{\partial x} + \frac{\lambda_0 Q_0}{H} - \overline{\frac{\lambda_1 Q_1 \zeta_1}{H^2}} = 0 \qquad (14)$$

$$\frac{\partial Q_0}{\partial x} = 0 \qquad (15)$$

The first two terms of the momentum equation (eq. 14) are the well-known tidal stress terms (NIHOUL & RONDAY, 1976), which, together with the last term that originates from the non-linear bottom friction, are the forcing terms for the mean state. This total tidal stress must be balanced by a residual water-level gradient and/or a bottom-friction term caused by a residual transport (in the case of open basins). To derive expressions for the mean field, the linearized tidal equations (3 and 4) are used to determine the tidal water levels and volume transports which subsequently give analytical expressions for the forcing terms in eq. (14). After integrating eq. (14) the residual water levels in the interior of both basins can be expressed as a function of the tidal stresses, the residual flow (Q_0) and two integration constants. These integration constants can only be determined when the residual level is known at two positions, presumably the boundaries with the open sea. As these boundary conditions are not known *a priori*, but are in fact part of the problem of finding the tidal mean state, the schematized model area was extended over a relatively short distance to the open sea. To circumvent the "open boundary" problem for the tidal mean state it is now assumed that at the seaward boundaries of the inflow area the residual levels are not influenced by the tidal flows in the basins. A difference between the residual levels at both seaward boundaries can therefore only be caused by the tidal flows in the open sea and has to be interpreted as an external forcing. As such an externally forced pressure gradient is absent in the numerical model simulations (RIDDERINKHOF, 1988), it is also neglected here. So, when the tidal stresses in the inflow area are known, the residual level at both inlets can be computed and subsequently used to determine the internally-driven mean field in both basins.

3. RESULTS FOR THE TIDAL AND TIDAL MEAN FIELD

3.1. INFLOW AREA

The length of the funnel-shaped inflow area can be assumed to be much smaller than the tidal basin length. Having now two horizontal length scales over which variables may vary, it seems appropriate to

TABLE 1

Scales and non-dimensional parameters in the analytical model.

$B = B_A b'$	B_A = width basin a
$H = H_A h'$	H_A = depth basin a
$x = L_i x_i' + L_A x'$	L_A = length basin a, L_i = length inflow area
$\zeta = Z_A \zeta'$	Z_A = tidal amplitude at $x = -L$ ($x' = -1$)
$t = t'/\sigma$	σ = frequency tidal wave
$q = <Q> q'$	$<Q> = B_A L_A Z_A \sigma$
$\lambda_1 = \sigma H_A \lambda'_1$	λ_1 = linearized bottom friction coefficient
$k = k' / L_A$	$k = \frac{\sigma}{\sqrt{gH_\alpha}}$ = wave number
$\zeta_0 = <\zeta_0> \zeta_0'$	$<\zeta_0> = Z_A^2 H_A^{-1}$
$q_0 = <q> q_0'$	$<q_0> = <Q>\ Z_A\ H_A^{-1}$
$\lambda_0 = \sigma H_A \lambda_0'$	$\lambda_0' = 1.5\lambda_1'$

apply a multiple scale expansion (MAAS *et al.*, 1987) which in a first approximation simplifies the governing equations for the inflow area. Table 1 lists the introduced scaling and non-dimensional parameters. A consequence of using two horizontal coordinates is that the $\partial/\partial x$ operator reads:

$$\frac{\partial}{\partial x} = L_A^{-1}\left(\frac{\partial}{\partial x'} + \epsilon^{-1}\frac{\partial}{\partial x_i'}\right), \quad \epsilon = \frac{L_i}{L_A} << 1 \tag{16}$$

Using (16) and scaling (3) and (4) according to Table 1, the dimensionless form of the linear tidal equations (3 and 4) (dropping primes), is

$$\epsilon\frac{\partial q}{\partial t} + \epsilon\frac{bh}{k^2}\frac{\partial \zeta}{\partial x} + \frac{bh}{k^2}\frac{\partial \zeta}{\partial x_i} + \epsilon\frac{\lambda_1 q}{h} = 0 \tag{17}$$

$$\epsilon\frac{\partial q}{\partial x} + \frac{\partial q}{\partial x_i} + \epsilon\, b\frac{\partial \zeta}{\partial t} = 0 \tag{18}$$

Expanding the dependent variables in (17) and (18) in a perturbation series (using ϵ as a small parameter) yields at zeroth order for the tidal field in the inflow area

$$\frac{\partial \zeta}{\partial x_i} = 0, \quad \frac{\partial q}{\partial x_i} = 0 \tag{19}$$

Thus on the relatively small length scale of the inflow area the tidal wave propagates in a first approximation as if it has a rigid upper surface. The same procedure is followed to determine the governing equations for the mean field in the inflow area. Using the governing equations for the mean field (14) and (15), extending the set of non-dimensional parameters with non-dimensional variables for the tidal mean variables, ζ_0' and q_0' (Table 1), expanding these variables in a perturbation series, and substituting (16) yield at zeroth order for the mean field in the inflow area (dropping primes)

$$\overline{\frac{\partial}{\partial x_i}\frac{q_1^2}{bh}} + \overline{\frac{b}{k^2}\frac{\partial \zeta_1^2}{\partial x_i}} + \frac{bh}{k^2}\frac{\partial \zeta_0}{\partial x_i} = 0 \tag{20}$$

$$\frac{\partial q_0}{\partial x_i} = 0 \tag{21}$$

Using (19), eq. (20) can be further simplified

$$\overline{\frac{q_1^2}{h}\frac{\partial}{\partial x_i}b^{-1}} + \frac{bh}{k^2}\frac{\partial \zeta_0}{\partial x_i} = 0 \tag{22}$$

To find the required expression for the residual levels at the transition between the tidal channel and the inflow area eq. (22) has to be integrated. Taking the residual level at the seaward end of the inflow area as a boundary condition ($\zeta_0 = 0$) and assuming a fast decrease of the inflow width in this region ($B_A << B_0$, Fig. 2) yields the following expression for the residual level at the open boundary of the tidal channel

$$\zeta_0 = \overline{-q_1^2}\,\frac{k^2}{2bh} \quad \left(= -\frac{\overline{Q_1^2}}{2gB^2D^2} = -\frac{\overline{u_1^2}}{2g}\right) \tag{23}$$

Substitution of the relevant scales gives the term in brackets in (23). The resulting drop in the residual water level in a tidal inlet, about 2.5 cm for $u = 1$ ms^{-1}, can be interpreted as a Bernoulli effect caused by a fast reduction of the inflow section over a relatively short distance. This phenomenon can be recognized in the numerical model (RIDDERINKHOF, 1988) as well as in the analysis of observations (RIJKSWATERSTAAT, 1987).

3.2. SCHEMATIZED BASINS

3.2.1. TIDAL FLOWS AND WATER LEVELS

Of course the "rigid lid" approximation of the tidal flow in the inflow area cannot be used to describe the

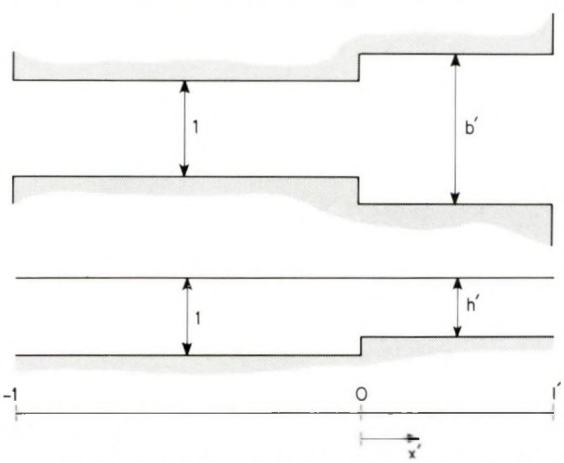

Fig. 3. Schematization of the tidal basins in non-dimensional parameters. The upper part shows a plan view of both basins and the lower part shows the longitudinal cross-section.

tidal field in the interior of the two basins. To determine the tidal stresses an analytical model has been developed. This model has to represent the tidal transports and water elevations as reasonably as can be done by approximating the two-dimensional reality of our numerical model to a one-dimensional system. Choosing the boundary between the two channels as the origin for the non-dimensional x-coordinate (Fig. 3) and omitting hereafter the accents for the non-dimensional variables results in the following sets of tidal equations:

$-1<x<0$ basin a $b=h=1$

$$\frac{\partial q}{\partial t}+\frac{1}{k^2}\frac{\partial \zeta}{\partial x}+\lambda_1 q=0 \qquad (24)$$

$$\frac{\partial q}{\partial x}+\frac{\partial \zeta}{\partial t}=0 \qquad (25)$$

$0<x<l$ basin b

$$\frac{\partial q}{\partial t}+\frac{bh}{k^2}\frac{\partial \zeta}{\partial x}+\frac{\lambda_1 q}{h}=0 \qquad (26)$$

$$\frac{\partial q}{\partial x}+b\frac{\partial \zeta}{\partial t}=0 \qquad (27)$$

Combining the momentum and continuity equation and substituting (*c.c* means the complex conjugate function):

$-1<x<0$

$$\zeta_A(x,t)=\zeta_A(x)\,e^{it}+c.c$$

$$\zeta_A(x)=A\,e^{i\tau_A x}+B\,e^{-i\tau_A x}$$

$$q_A(x,t)=q_A(x)\,e^{it}+c.c \qquad (28)$$

$0<x<l$

$$\zeta_B(x,t)=\zeta_B(x)\,e^{it}+c.c$$

$$\zeta_B(x)=C\,e^{i\tau_B x}+D\,e^{-i\tau_B x}$$

$$q_B(x,t)=q_B(x)\,e^{it}+c.c \qquad (29)$$

in which A, B, C and D are complex integration constants, we find for τ and q:

$-1<x<0$

$$\tau_A^2=k^2(1-\lambda i) \qquad (30)$$

$$q_A(x)=\frac{i}{\tau_A^2}\frac{\partial \zeta_A}{\partial x} \qquad (31)$$

$0<x<l$

$$\tau_B^2=\frac{k^2}{h}\left(1-\frac{\lambda}{h}i\right) \qquad (32)$$

$$q_B(x)=\frac{bi}{\tau_B^2}\frac{\partial \zeta_B}{\partial x} \qquad (33)$$

To find the complete solution of the propagation and damping of the tidal wave in both basins we need to impose 4 boundary conditions:

$$\begin{aligned}
&1)\ x=-1 && \zeta_A(-1,t)=e^{it}+c.c\\
&2)\ x=l && \zeta_B(l,t)=Z\,e^{i(t+\varphi)}+c.c\\
&3)\ x=0 && \zeta_A(0,t)=\zeta_B(0,t)\\
&4)\ x=0 && q_A(0,t)=q_B(0,t)
\end{aligned} \qquad (34)$$

The first two boundary conditions represent the fluctuating water levels at both inlets, which can differ both in amplitude and phase. Boundary conditions 3) and 4) at $x=0$ guarantee the continuity of sea level and volume transport at the boundary between the two basins. Condition 4) implies that partial reflection of the tidal wave at the transition between the two basins is neglected. Substituting these boundary conditions yields:

$$C=\frac{(\cos\tau_A+i\gamma\sin\tau_A)Ze^{i\varphi}-e^{-i\tau_B l}}{2i(\cos\tau_A\sin(\tau_B l)+\gamma\sin\tau_A\cos(\tau_B l))}$$

$$D=\frac{(-\cos\tau_A+i\gamma\sin\tau_A)Ze^{i\varphi}+e^{i\tau_B l}}{2i(\cos\tau_A\sin(\tau_B l)+\gamma\sin\tau_A\cos(\tau_B l))}$$

$$A=\frac{1}{2}((C+D)+\gamma(C-D))$$

$$B=\frac{1}{2}((C+D)+\gamma(C-D))$$

$$\gamma=b\tau_A/\tau_B \qquad (35)$$

In both basins $Q(x,t)$ and $\zeta(x,t)$ can now be computed depending on the choice of tidal and morphological parameters. The combination of parameters which appears to give reasonable results with regard to the observed amplitudes and phases

TABLE 2

Parameters and coefficients as used in the schematization of the Wadden Sea basins. H_A, B_A and λ_1 were tuned according to the conditions given in the text.

$L_A = 40 \cdot 10^3$m	$L_B = 20 \cdot 10^3$m	($l' = 0.5$)
$H_A = 4.5$ m	$H_B = 3.00$ m	($h' = 0.66$)
$B_A = 15 \cdot 10^3$m	$B_B = 24 \cdot 10^3$m	($b' = 1.6$)
$Z_A = 0.70$ m	$Z_B = 0.86$ m	($z' = 1.23$)
$\sigma = 1.4 \cdot 10^{-4}$s^{-1}	$\varphi = -0.63$	
$g = 9.81$ ms^{-2}	$\lambda_1 = 2.0 \cdot 10^{-3}$.ms^{-1}	

of transport in both basins is listed in Table 2. Global characteristics of the topography in the Marsdiep and Vlie basins show a significant depth (h=0.66) and length difference (l=0.5) between the two. The width ratio chosen (b=1.6), in combination with the length ratio, is in agreement with the known small difference between the total surface area of the Vlie and Marsdiep basins (ZIMMERMAN, 1976).

In tuning the analytical model, the morphological ratios (h, b, l) and the length of basin a, (L_A), as well as the tidal boundary conditions (Z,φ), well known from observed data, were kept constant. The friction coefficient, λ_1, and depth scale of basin a, H_A, which determine the damping and the phase speed of the tidal wave, have to meet the following requirements: 1) the boundary at $x=0$ should coincide with a transport amplitude minimum 2) the amplitude of the tidal velocities in both inlets should be approximately equal. The first requirement ensures that the incoming tidal waves meet at the transition between the two basins, in the prototype resulting in the formation of tidal watersheds. The second requirement concerning the velocity ratios in the inlets, which equal the

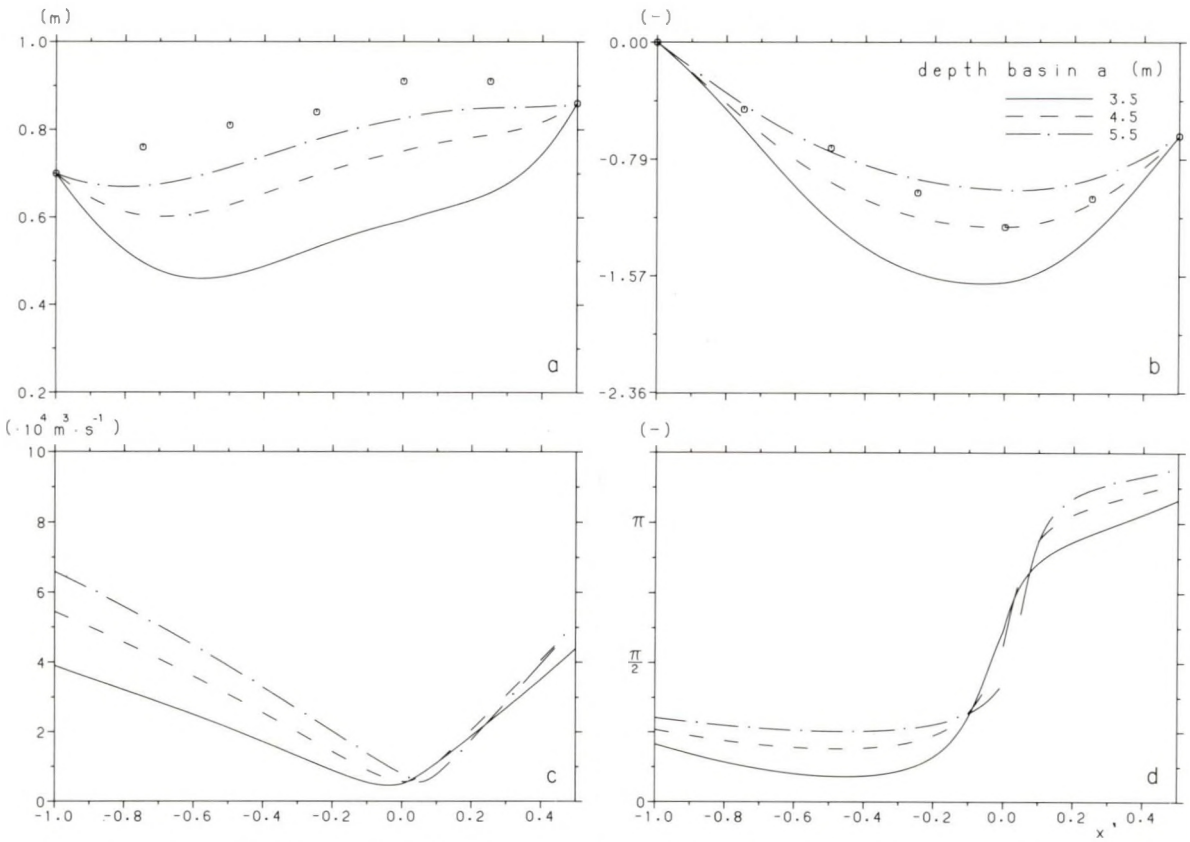

Fig. 4. Water level and transport amplitudes and phases dependent on the depth of basin a, as a function of the non-dimensional x'- coordinate. For comparison results in corresponding grid points in the numerical model are shown (O O O). The grid points 1 to 7 in the numerical model correspond with resp. x'=−1.0, −0.75, −0.50, −0.25, 0., 0.25, 0.50 in the analytical model.

(a) Phase of tidal sea level relative to the tidal sea level at x'=−1 (-)

(b) Amplitude of tidal sea level (m)

(c) Phase of volume transport relative to the tidal sea level at x'=−1 (-)

(d) Amplitude of volume transports (10^4m^3.s^{-1})

transport ratios because of the width and depth ratio chosen, follows from observations and numerical model results (RIDDERINKHOF, 1988). This is an important requirement as it influences the tidal stress ratio at both open boundaries as well as the residual level boundary conditions for the mean state. Furthermore, this condition justifies the assumption that the bottom friction coefficient, being dependent on a representative value of the tidal velocity amplitude according to eq. (5), does not differ in the two basins. Finally, the width of basin a was varied to tune the transport amplitudes in the two inlets. The final outcome of this tuning was a value of $2 \cdot 10^{-3}$ ms^{-1} for the friction coefficient, λ_1, 4.5 m for the depth scale, H_A, and $15 \cdot 10^3$m for the width scale, B_A. Fig. 4a to d gives the resulting amplitudes and phases of the fluctuating water levels and volume transports in both channels. For some positions Fig. 4a and b shows results in corresponding gridpoints of the numerical model. The position of these gridpoints is indicated in Fig. 1. The influence of changing the depth scale is also given in these figures.

Although it is not shown here, changing the bottom friction coefficient or length of basin a yields comparable results, in which an increasing depth scale corresponds with a decreasing length or bottom-friction coefficient.

The major effect of changing the depth scale is the increase/decrease in the phase speed of the tidal wave. With respect to the transport amplitudes this results in a shift of the transport minimum while the ratio of the amplitudes in both inlets is adapted to the associated changing "effective" basin length. The depth scale chosen, 4.5 m, is close to the mean depth in the Marsdiep basin, 4.3 m, and appears to give the most reasonable results in terms of the conditions stated before.

Of course, compared to the observations and numerical model results the analytical model can only meet qualitative requirements. For instance the schematization of a morphologically irregular area into a basin with a uniform depth leads to a relatively too strong damping of the tidal wave near the inlets, resulting in a decreasing water-level amplitude (see Fig. 4a), which cannot be recognized in the numerical model results. However, keeping in mind the rather crude schematization, this model can serve as a basis for a qualitative study of the mean field.

3.2.2. THE TIDAL MEAN FIELD

The set of non-dimensional equations for the mean field, based on eqs. (14 and 15), reads:

$-1 < x < 0 \qquad b = h = 1$

$$\overline{2q_1 \frac{\partial q_1}{\partial x}} + \frac{1}{k^2} \overline{\zeta_1 \frac{\partial \zeta_1}{\partial x}} + \frac{1}{k^2} \frac{\partial \zeta_0}{\partial x} + \lambda_0 q_0 - \lambda_1 \overline{q_1 \zeta_1} = 0 \tag{36}$$

$$\frac{\partial q_0}{\partial x} = 0 \tag{37}$$

$0 < x < l$

$$\frac{2}{bh} \overline{q_1 \frac{\partial q_1}{\partial x}} + \frac{b}{k^2} \overline{\zeta_1 \frac{\partial \zeta_1}{\partial x}} + \frac{bh}{k^2} \frac{\partial \zeta_0}{\partial x} + \frac{\lambda_0 q_0}{h} - \frac{\lambda_1 \overline{q_1 \zeta_1}}{h^2} = 0 \tag{38}$$

$$\frac{\partial q_0}{\partial x} = 0 \tag{39}$$

Making use of eqs. (24 to 27) the last term in eqs. (36) and (38) can be expressed as a function of the first two terms:

$$-1 < x < 0 \qquad \lambda_1 \overline{q_1 \zeta_1} = -\frac{1}{k^2} \overline{\zeta_1 \frac{\partial \zeta_1}{\partial x}} + \overline{q_1 \frac{\partial q_1}{\partial x}} \tag{40}$$

$$0 < x < l \qquad \frac{\lambda_1 \overline{q_1 \zeta_1}}{h^2} = -\frac{b}{k^2} \overline{\zeta_1 \frac{\partial \zeta_1}{\partial x}} + \frac{1}{bh} \overline{q_1 \frac{\partial q_1}{\partial x}} \tag{41}$$

so that the tidal stress term, T_{xx}, can be written as:

$$-1 < x < 0 \qquad T_{xx_A} = \frac{2}{k^2} \overline{\zeta_1 \frac{\partial \zeta_1}{\partial x}} + \overline{q_1 \frac{\partial q_1}{\partial x}} \tag{42}$$

$$0 < x < l \qquad T_{xx_B} = \frac{2b}{k^2} \overline{\zeta_1 \frac{\partial \zeta_1}{\partial x}} + \frac{1}{bh} \overline{q_1 \frac{\partial q_1}{\partial x}} \tag{43}$$

These expressions for the tidal stress show that the Stokes part of the tidally-averaged bottom friction increases the contribution of the water-level component to the total tidal stress while the contribution of the transport component decreases.

Substituting (42) and (43) in (36) and (38) and integrating yields:

$$-1 < x < 0 \qquad \int T_{xx_A} dx + \frac{1}{k^2} \zeta_0 + \lambda_0 q_0 x = A \tag{44}$$

$$q_0 = \text{constant}$$

$$0<x<l \quad \int T_{xx_B} dx + \frac{bh}{k^2}\zeta_0 + \frac{\lambda_0 q_0}{h}x = B \qquad (45)$$

$$q_0 = \text{constant}$$

in which A and B are integration constants. In these equations (44 and 45) the tidal stress terms can be computed by substitution of eqs. (28) and (29). For instance averaging and integrating of the water-level components gives a simple expression:

$$\overline{\zeta_1 \frac{\partial \zeta_1}{\partial x}} = \zeta_1^* \frac{\partial \zeta_1}{\partial x} + \zeta_1 \frac{\partial \zeta_1^*}{\partial x} \qquad (46)$$

$$\int \overline{\zeta_1 \frac{\partial \zeta_1}{\partial x}} dx = \zeta_1 \zeta_1^* = |\zeta_1|^2 \qquad (47)$$

where an asterisk indicates the complex conjugate and ($|\ |$) the tidal amplitude. The transport component of the tidal stress can be simplified in an analogous way.

Again we need 4 boundary conditions to be able to find the solution of this set of equations:

1) $x=-1 \quad \zeta_0 = Z_{0_{-1}}$

2) $x=l \quad \zeta_0 = Z_{0_l}$

3) $x=0 \quad \zeta_{0_A} = \zeta_{0_B}$

4) $x=0 \quad q_{0_A} = q_{0_B}$ (48)

Conditions 1) and 2) impose a residual level at both inlets. These are a function of the tidal transports and can be computed by employing eqs. (31) and (33). The conditions 3) and 4) guarantee the continuity of residual level and residual flow at the connection of the two basins.

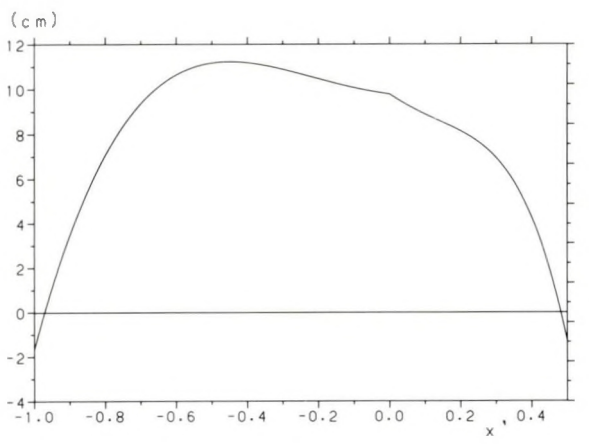

Fig. 5. Residual water elevation in the schematized tidal channels (cm) as a function of the non-dimensional x-coordinate.

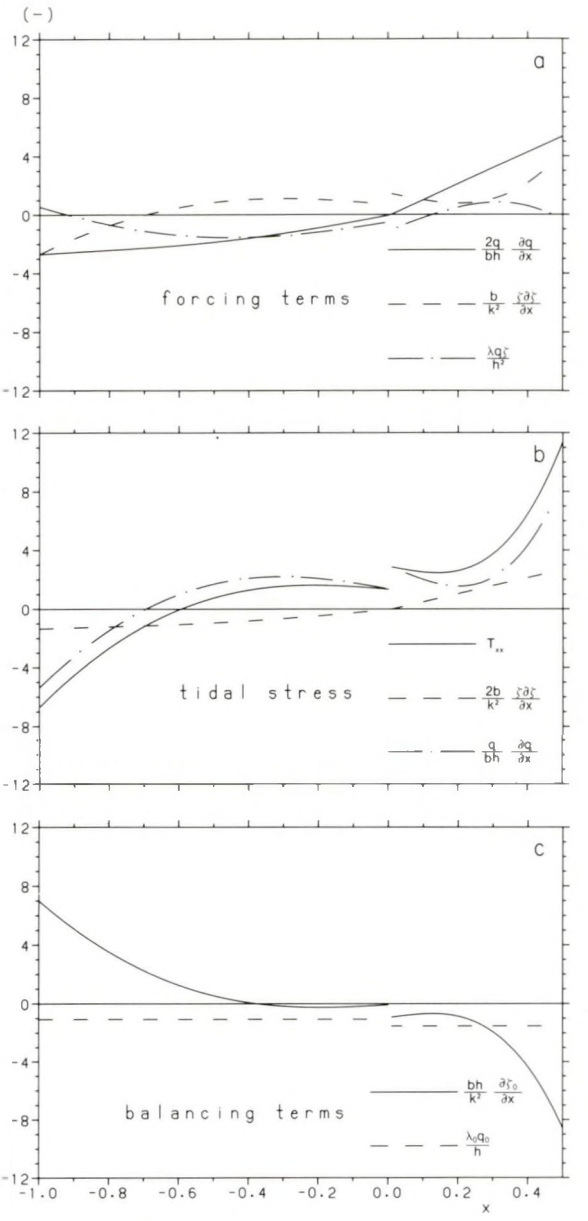

Fig. 6. Non-dimensional magnitude of the terms in eqs. (36), (38), (42) and (43) as a function of the non-dimensional x-coordinate. (a) Forcing terms in eqs. (36) and (38). (b) Composing terms of tidal stress and total tidal stress, eqs. (42) and (43). (c) Terms associated with tidal mean variables in eqs. (36) and (38).

Substitution of these conditions yields:

$$q_0 = \frac{1}{\lambda_0 + \frac{\lambda_0^I}{bh^2}} \left\{ \frac{Z_{0_{-1}} - Z_{0_I}}{k^2} + \int_0^{-1} T_{xx_A}\, dx + \frac{1}{bh\,I} \int^0 T_{xx_B} dx \right\} \quad (49)$$

This equation shows that a residual flow between two basins will be generated whenever the integrated tidal stress and/or the difference in residual levels between the two open boundaries differ from zero. Note that, because of the chosen morphological differences between the two basins, no direct integration between $x=-1$ and $x=I$ can be performed. After computing the boundary conditions and the tidal stresses with the tidal model the tidal mean field can be determined. Substitution of the typical Wadden Sea values (Table 1) leads to a residual transport (Q_0) of about 3 percent of the tidal transport amplitude in the inlets while computations with the numerical model resulted in a ratio of about 1 percent. In both models the residual flow is directed from the Vlie basin into the Marsdiep basin. The computed residual levels are shown in Fig. 5. Although the analytical model overestimates the residual levels in the interior of the basins compared with the numerical model results (fig. 9c in RIDDERINKHOF (1988)), this picture clearly shows the same strong increase in residual levels from the inlets to the middle of the basins. Fig. 6a gives the non-dimensional magnitude of the forcing terms in eqs. (36) and (38) as a function of the position in the basins. It shows that the relative importance of these three terms is approximately equal. Fig. 6b gives the magnitude of the total tidal stress as well as the magnitude of both components, defined according to eqs. (42) and (43). This figure clearly shows that the water-level component is more important than the transport component. The magnitude of the counterbalancing terms, associated with tidal mean variables, is shown in Fig. 6c.

4. DISCUSSION

Before examining the influence of morphological asymmetries and asymmetrical boundary conditions on the residual flow, attention is paid to the sensitivity of the analytical model to the schematization of the morphology of the Wadden Sea and to the bottom friction parameter. As in the tidal model, the boundary conditions for the tidal fluctuations, $z=1.23$ and $\varphi=-0.63$, and the depth and width ratio between the two basins, $h=0.66$ and $b=1.6$, were kept constant, as these are well known from the observed data. The influence of changing the depth scale or bottom coefficient on the residual flow as a function of the length ratio between the two basins is shown in Fig. 7a and b, where the percentage of the residual transport compared with the tidal transport amplitude at the inlet of basin a is given on the vertical axis. Both figures show that the magnitude of the residual flow is only slightly sensitive to a variation in these parameters, while the direction of this flow does not change. As in the tidal model, a comparison of Fig. 7a with 7b shows that varying the depth scale of basin a or the bottom-friction coefficient gives qualitatively the same results: a greater depth corresponding with a smaller friction coefficient.

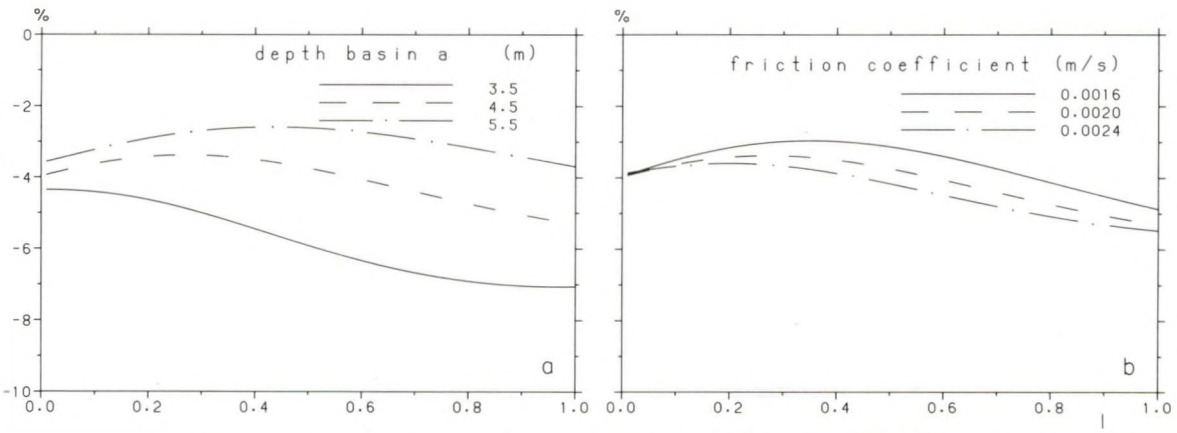

Fig. 7. Ratio between residual transport and tidal transport amplitude at the inlet of basin a (%) as a function of the length ratio between the two basins. (a) Influence chosen depth scale of basin a. (b) Influence bottom-friction coefficient.

Internal tidally-driven residual volume transports between connected basins can only exist when there are asymmetries between the two basins. These asymmetries are either of a morphological nature, *i.e.* length, width or depth differences, or of a tidal nature, *i.e.* amplitude or phase differences between the fluctuating water levels at the two inlets. The analytical model for constant morphological scales (Table 1) is used to examine the relative contribution of both asymmetries to the residual flow.

4.1. TIDAL ASYMMETRIES

To illustrate the consequences of different water-level boundary conditions at both inlets it is assumed that there are no morphological differences between the two basins ($h = b = 1$). This schematization is equal to a model of a single channel with different water-level boundary conditions at both ends. Making use of eq. (47) eq. (49) can now be simplified as:

$$q_0 = \frac{1}{\lambda_0(1+l)} \left\{ \frac{Z_{0_{-1}} - Z_{0_l} + 2|\zeta|^2_{-1} - 2|\zeta|^2_l}{k^2} + |q|^2_{-1} - |q|^2_l \right\} \quad (50)$$

which shows that a difference in tidal amplitude of the transport and/or water levels between the two inlets induces a residual flow towards the lowest amplitude. The difference in residual level, connected with a transport amplitude difference by the Bernouilli effect (eq. (22)), acts in the opposite direction. Using eq. (23) the residual pressure gradient term can be written as:

$$\frac{Z_{0_{-1}} - Z_{0_l}}{k^2} = -\frac{1}{2}(\overline{q^2_{-1}} - \overline{q^2_l}) = \frac{1}{4}(|q|^2_{-1} - |q|^2_l) \quad (51)$$

which shows that the magnitude of the residual flow is only reduced by the counterbalancing residual level gradient, but its sign is not reversed. Using eq. (31) the transport component of the tidal stress in eq. (50) can be written as a function of the differences in amplitude (Z) and phase (φ) of the water-level boundary conditions

$$|q|^2_{-1} - |q|^2_1 = F(Z^2 - 1) + G\,Z\sin\varphi \quad (52)$$

where the real parameters F and G can be expressed as (* means complex conjugate):

$$F = (PP^* - QQ^*), \quad G = \frac{(PQ^* - QP^*)}{2i} \quad (53)$$

with:

$$P = \frac{2}{\tau e^{-i\tau(1+l)} - \tau e^{i\tau(1+l)}},$$

$$Q = \frac{e^{i\tau(1+l)} + e^{-i\tau(1+l)}}{\tau e^{-i\tau(1+l)} - \tau e^{i\tau(1+l)}} \quad (54)$$

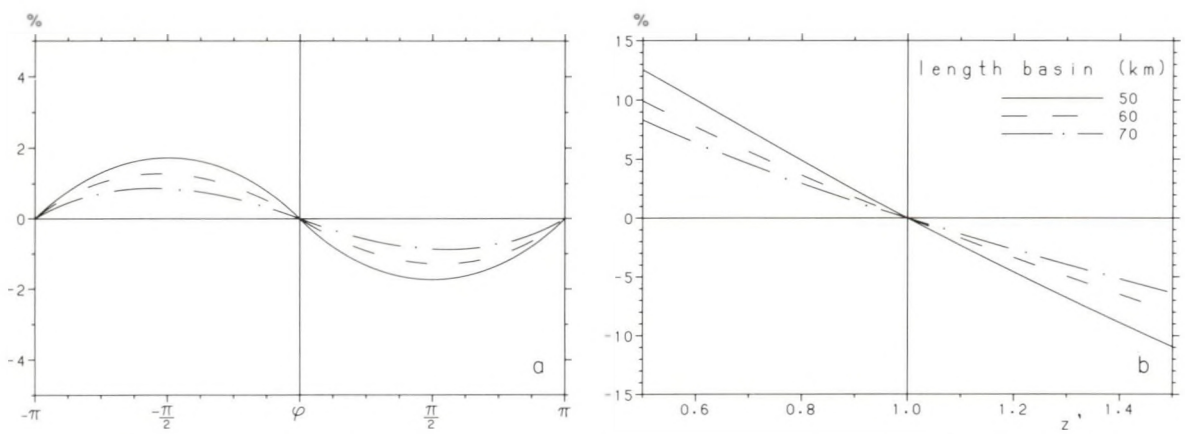

Fig. 8. Effects of differences in the fluctuating water levels at the open boundaries of a single channel. 8a. Ratio between residual transport and tidal transport amplitude at the inlet where the tidal wave enters first as a function of phase differences (%). 8b. Ratio between residual transport and tidal transport amplitude at the inlet of basin a as a function of amplitude differences (%).

Finally substituting eqs. (51) and (53) in eq. (50) yields

$$q_0 = \frac{1}{\lambda_0(1+l)} \left[\left(\frac{3}{4}F - \frac{2}{k^2} \right) (Z^2-1) + \frac{3}{4} G Z \sin\varphi \right] \qquad (55)$$

which demonstrates the independent effects of differences in amplitude and in phases of the water-level boundary conditions. A comparable study on mass transport induced by different water-level boundary conditions at both ends of a single canal has been performed by VAN DE KREEKE & DEAN (1975). Their final equation for the residual flow is equal to eq. (55) with respect to the effects of phase and amplitude differences on the direction of the residual flow. Minor differences stem from the contribution of the internally-driven residual pressure gradient and the increased friction coefficient for the residual flow in the final equation here presented (55). Both adjustments reduce the magnitude of the residual volume transport compared with the results of VAN DE KREEKE & DEAN.

In Fig. 8a and b the ratio between residual transport and the tidal transport amplitude at the inlet of the basin where the tidal wave enters first, basin a for positive phases and basin b for negative phases, is shown as a function of a phase difference ($z=1$, Fig. 8a), or an amplitude difference at the inlets ($\varphi=0$, Fig. 8b) and the total length of both basins (mind the different scales of the vertical axes in Fig. 8a and b). Fig. 8a shows that a phase difference results in a residual flow that is directed from the basin where the tidal wave first enters towards the other basin. The magnitude of the residual flow at a given phase difference depends strongly on the total length of both basins. The total length determines the ratio between the distances from the inlets and the position at which the transport amplitude has a minimum. The ratio in tidal transport amplitude in both inlets is related to this length ratio and results in a residual flow directed towards the lowest transport amplitude. The magnitude of the residual flow, caused by the transport component of the tidal stress, therefore strongly depends on the total length of a basin. A difference in the amplitude of the water-level fluctuations at the boundaries, Fig. 8b, directly imposes a tidal stress force in the model by the water-level component as well as the transport component, resulting in a residual flow towards the lowest water-level amplitude. The dependence of the magnitude of the tidal stress gradient on the length of both basins is reflected in the magnitude of this residual flow. A comparison of Fig. 8a with Fig. 8b shows that the residual flow is larger in the case of amplitude differences than in the case of phase differences. This is caused by the relatively small influence of the transport component in the total tidal stress.

4.2. MORPHOLOGICAL ASYMMETRIES

Assuming the water-level boundary conditions at both inlets to be equal ($z=1$, $\varphi=0$), the influence of morphological differences on the residual flow can be examined. In Fig. 9a the influence of a depth difference is illustrated. In the prototype the boundary between the two basins is located at the position where the transport amplitude has its minimum. Thus the length ratio is a function of the phase speed ratio of the tidal waves in both basins. This ratio is proportional to the square of the depth ratio ($l=\sqrt{h}$) in the case of zero bottom friction, and in a first approximation proportional to the depth ratio ($l=h$) in the case of strong, depth-dependent bottom friction

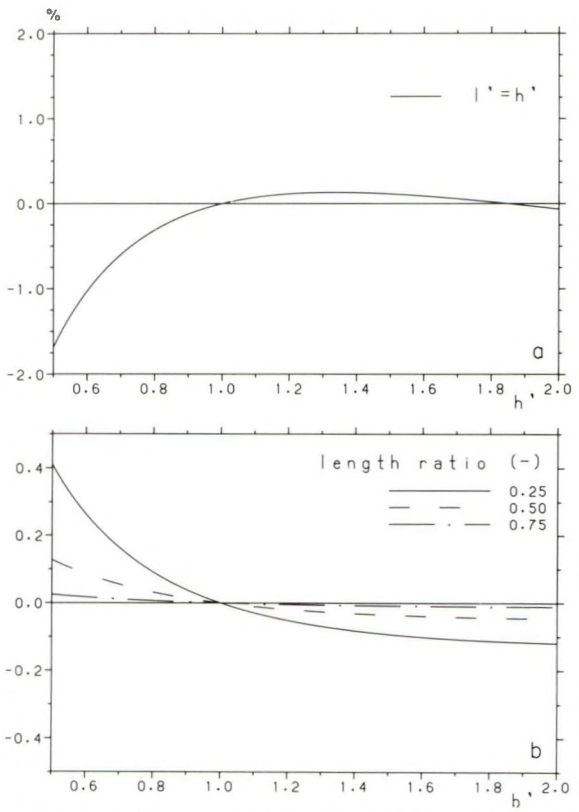

Fig. 9. Ratio between residual transport and tidal transport amplitude at the inlet of basin a (%) as a function of morphological asymmetries between connected tidal basins. 9a. Influence depth and associated length ratio (l'=h') between the two basins. 9b. Influence width ratio for different length ratios.

($\lambda >> \sigma$, eqs. 30 and 32). Hence by using the transport amplitude minimum as a criterion the length ratio is linearly dependent on the depth ratio. The latter ratio is used in Fig. 9a. It shows that a depth difference in general induces a residual flow towards the deeper basin. However, the magnitude of this residual flow is small (mind tne difference between Figs 8 and 9 in the scale of the vertical axes) compared with the residual flow caused by tidal asymmetries.

The influence of a width ratio at different length ratios is illustrated in Fig. 9b. Because of the boundary condition at the connection between the two basins (continuity of transports), a width ratio primarily influences the magnitude of the tidal velocities at both sides of this connection. The increased velocity in the narrower basin reduces the tidal stress force on this side of the connection, resulting in a residual flow towards the narrow basin. Fig. 9b shows that the magnitude of this residual flow is very small when the transition between the two basins is located near a transport minimum of the tidal flow ($l'=0.75$).

5. CONCLUSIONS

The analyses with the analytical model show that in general asymmetries in morphology and boundary tides between basins induce a residual flow between the two. In a single channel this residual flow is directed towards the inlet where, in the case of phase differences, the tidal wave enters last, or, in the case of amplitude differences, towards the inlet with the lowest water-level amplitude. When morphological differences are considered, a residual flow is induced towards the deeper and/or narrower part.

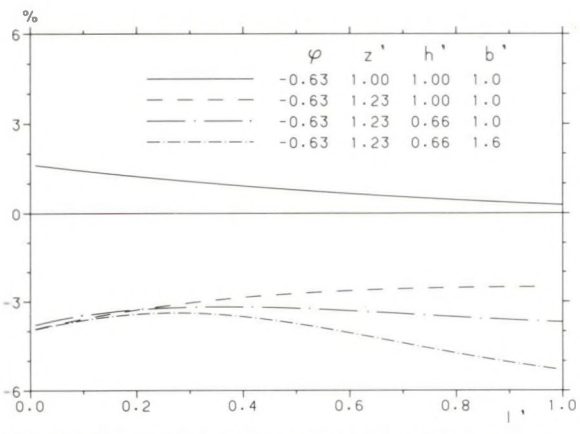

Fig. 10. Influence of different combinations of tidal and morphological asymmetries on the ratio between residual transport and tidal transport amplitude at the inlet of basin a (Marsdiep basin), as a function of the length ratio between the Vlie and Marsdiep basins. In reality the length ratio is approximately 0.5.

In Fig. 10 the consequences of a combination of these asymmetries are summarized for a schematization of the connected Marsdiep and Vlie basins. For different combinations of asymmetries the ratio between the residual transport and the tidal transport amplitude at the inlet of the Marsdiep basin is given as a function of the length ratio. In reality the length ratio is approximately 0.5. For this length ratio Fig. 10 shows that the amplitude difference of the water-level boundary conditions is the most important factor that causes the residual flow to be directed from the Vlie basin towards the Marsdiep basin.

Summarizing it can be concluded that the difference in water-level amplitude at the inlets as well as the depth and width ratio between the two basins directs the residual flow from the Vlie basin towards the Marsdiep basin, whereas phase differences direct the flow in the opposite direction. The combined effect of morphological differences and differences in water-level amplitude at the inlets appears to be larger than the effect of phase differences.

6. REFERENCES

DRONKERS, J.J., 1964. Tidal computations in rivers and coastal waters. Wiley, New York.

HEAPS, N.S., 1978. Linearized vertically integrated equations for residual circulation in coastal seas.—Dt. hydrogr. Z. **31:** 147-169.

HUNTER, J.R., 1975. A note on quadratic friction in the presence of tides.—Estuar. coast. mar. Sci. **3:** 473-475.

KREEKE, J. VAN DE, 1976. Increasing the mean current in coastal channels.—J. Waterw. Harb. Coast. Eng. Div. ASCE **102:** WW2: 223-234.

KREEKE, J. VAN DE & D.C. COTTER, 1974. Tide-induced mass transport in lagoon-inlet systems.—Proc. XIV Conf. Coast Eng. Copenhagen, Denmark: 2290-2301.

KREEKE, J. VAN DE & R.G. DEAN, 1975. Tide induced mass transport in lagoons.—J. Waterw. Harb. Coast. Eng. Div. ASCE **101:** WW4: 393-403.

LORENTZ, H.A., 1926. Verslag Staatscommissie Zuiderzee 1918-1926. Den Haag.

MAAS, L.R.M., J.T.F. ZIMMERMAN & N.M. TEMME, 1986. On the exact shape of the horizontal profile of a topographically rectified tidal flow.—Geophys. Astrophys. Fluid Dyn. **38:** 105-129.

NIHOUL, J.C.J. & F.C. RONDAY, 1975. The influence of the "tidal stress" on the residual circulation.—Tellus **27:** 484-489.

PRANDLE, D., 1978. Residual flows and elevations in the Southern North Sea.—Proc. R. Soc. Lond. (A) **359:** 189-228.

RIDDERINKHOF, H., 1988. Tidal and residual flows in the western Dutch Wadden Sea. I: Numerical model results.—Neth. J. Sea Res. **22:** 1-21.

RIJKSWATERSTAAT, 1986. Getijatlas van Nederland 1986.
ZIMMERMAN, J.T.F., 1976. Mixing and flushing of tidal embayments in the western Dutch Wadden Sea, I: Distribution of salinity and calculation of mixing time scales.—Neth. J. Sea Res. **10:** 149-191.

(received 23-12-1988; revised 2-5-1988)

APPENDIX Linearization of $Q|Q|$

The method of HUNTER (1975) and HEAPS (1978) is followed to average the numerator of the quadratic friction term. Substituting

$$Q = Q_0 + Q_1 \; ; \quad Q_0 << Q_1 \tag{A1}$$

gives:

$$\overline{Q|Q|} = \overline{(Q_0 + Q_1)|Q_0 + Q_1|}$$

$$= \overline{(Q_0 + Q_1)\sqrt{|(Q_0 + Q_1)\,(Q_0^* + Q_1^*)|}} \tag{A2}$$

where the asterisk denotes a complex conjugate. Neglecting terms of order Q_0^2 under the square root sign and expanding this equals:

$$\overline{(Q_0 + Q_1)|Q_1|\;\left\{1 + \frac{Q_0 Q_1^* + Q_0^* Q_1}{2|Q_1|^2}\right\}}$$

$$= \frac{\overline{3}}{2}\overline{|Q_1|Q_0} + \overline{\frac{Q_1^2 Q_0^*}{2|Q_1|}} + \overline{Q_1|Q_1|} \tag{A3}$$

Finally substituting:

$$Q_1 = A_1 + iA_2 \; ; \quad Q_0 = B_1 + iB_2 \tag{A4}$$

in (A3) and choosing axes such that $A_2 = 0$ and $B_2 = 0$ gives the following expression for one-dimensional motion:

$$\overline{Q|Q|} = \overline{2|Q_1|Q_0} + \overline{Q_1|Q_1|}$$

ENHANCED BENTHIC-PELAGIC COUPLING IN THE WESTERN WADDEN SEA MODEL*

"An inprovement of the EMOWAD-I model"

J.W. BARETTA and P. RUARDIJ

Netherlands Institute for Sea Research, P.O. Box 59, 1790 AB Den Burg, Texel, The Netherlands

ABSTRACT

A time-dependent mathematical ecosystem model of the western Wadden Sea has been developed. Its surface area of 1415 km^2 is subdivided into 12 spatial compartments, the bulk exchange coefficients having been calculated using a hydrodynamical model with a cell size of 500 x 500 m.

The ecosystem model contains 22 biological state variables, ranging from primary producers to carnivores. In addition, it allows for tracing detrital pathways by incorporating 14 detrital state variables with bio-availabilities ranging from days to years.

With the closure of the Zuiderzee in 1932 the western Wadden Sea acquired an extensive sublittoral area, which harbours large amounts of benthic subtidal suspension feeders. Moreover, the area has been exploited for culturing *Mytilus edulis*, further enhancing their density. The demands of this functional group on the pelagic system have consequences for the biological structure and the functioning of the system as a whole. These consequences are studied by comparing the annual carbon fluxes through the system in the model which includes a fully functional subtidal community with those calculated using the model with a reduced subtidal community.

Nutrient regeneration from the benthic system, and phytoplankton settling are indicated as being crucial to the functioning of the system.

1. INTRODUCTION

Total estuarine productivity is the result of a balance between autotrophy and heterotrophy, and import and export of organic matter (SIBERT & NAIMAN, 1979).

The subject of this study is to establish the role of the subtidal community of the western Wadden Sea in determining the balance between autotrophy and heterotrophy and import and export of organic carbon. To do this, the first step is to quantify the performance of the whole system.

A more or less reliable indication of the productivity of an open estuarine system such as the western Wadden Sea can only be given when the interplay between geomorphology, circulation and biological processes is taken into account. At this time the only practical way of investigating this interplay and its effects on the total system performance is by means of a mathematical ecosystem model which takes these aspects into account. A model including these features has been constructed for the Ems estuary (BARETTA & RUARDIJ, 1988), and it has now been adapted to the western Wadden Sea. The model results are summarized in the form of annual carbon budgets which show the contribution of the various processes to the system carbon turnover and hence the balance we mentioned before.

In shallow areas, measurements using sediment traps have shown that 25-60% of the primary production sinks down to the bottom (ZEITSCHEL, 1979). This does not take into account the effect of benthic suspension feeders filtering large amounts of organic matter from the overlying water column and depositing faeces and pseudofaeces into the sediment. In particular with systems such as the western Wadden Sea, where the mussel, *Mytilus edulis*, is cultured on a large scale, a large fraction of the pelagic primary production may be expected to be transferred to the sediment. The resultant biological activity in the benthic system would generate a considerable nutrient feedback into the watercolumn. The nutrient flux from the sediment can be more than twice the rate demanded by the observed primary production (ROWE *et al.*, 1975; DAVIES, 1975; ROWE & SMITH, 1977 and HARGRAVE & CONNOLLY, 1978) calculated that the release of nutrients from the sediments may make up between 30 and 100% of the nutrient requirements of the phytoplankton in the euphotic zone. The implication of this is that in shallow-water ecosystems nutrient regeneration from the bottom keeps pace with primary production and

*Contribution number 19 of the Ecologisch Onderzoek Noordzee en Waddenzee (EON).

that the primary producers depend very little on pelagic regenerative processes (ROWE & SMITH, 1977; ZEITSCHEL, 1979).

The benthic flora and fauna, as well as the chemistry, of the tidal flats in the western Wadden Sea have been studied extensively, also with a view to establish the interaction between the benthic and the pelagic system (*cf.* WOLFF, 1983). The benthic system in the subtidal area, however, has attracted surprisingly little attention, even though the surface of the subtidal area (753 km^2) in the western Wadden Sea is more than half the total surface (1415 km^2).

There are some data on subtidal macrobenthos biomass (DEKKER, 1987) but to our knowledge there are no experimental data of organic matter and nutrient cycling in the subtidal region. A simulation model has been used in which the subtidal benthic system has been constructed with the same state variables as the intertidal submodel — except for the primary producers. The model of the subtidal region has been calibrated with data from the intertidal benthic system. The model results will be presented in the form of annual carbon flow budgets.

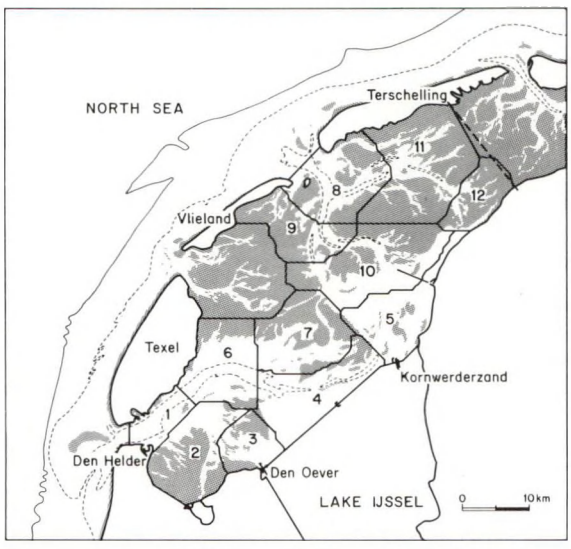

Fig. 1. Map of the western Wadden Sea with the model compartments.

1.1. SITE DESCRIPTION

The western Wadden Sea has a surface area of 1415 km^2 (Fig. 1) and is part of the Wadden Sea which extends along the northern coast of the Netherlands and the Federal Republic of Germany and also a large part of the west coast of Denmark.

The area has had its current shape only since the closure of the former Zuiderzee by a dike in 1932. This has caused an increase in the tidal amplitude and large-scale shifts in the areas where erosion or sedimentation occurs (EISMA & WOLFF, 1980). The subtidal area (753 km^2) is extensively used for culturing the mussel *Mytilus edulis*, with an annual harvest of about 10,000 metric tons (VERWEY, 1981). Also there occur large banks of "wild" mussels, together with high standing stocks of other suspensions feeders such as *Mya arenaria* (Dekker, pers. comm.).

1.2. MODEL DESCRIPTION

The western Wadden Sea has been notionally divided into 12 spatial compartments to enable the inclusion into the model of lateral transport processes. The exchange coefficients between the compartments have been calculated using a hydrodynamical model of the area with a grid size of 500x500 m (RIDDERINKHOF, 1988). This water movement model has been developed using the special-purpose modelling package WAQUA of Rijkswaterstaat, the department of public works. The biological processes in the model (uptake, respiration, excretion/egestion, growth and mortality) are based on experimentally derived physiological parameters of the different state variables. This carbon flow model is used to calculate a carbon budget for the whole system. More details on the model structure are given in BARETTA & RUARDIJ (1987).

2. METHODS

To quantify the role of the subtidal community in this system we have adapted a mathematical ecosystem simulation model, originally developed for the Ems estuary (BOEDE, 1985; BARETTA & RUARDIJ, 1988). Since this estuary does not possess a large subtidal area, the Ems model did not incorporate the subtidal community.

The model of the western Wadden Sea includes submodels which describe the transport processes, both of dissolved substances and of particulate material and the dynamics of the pelagic, as well as the benthic and epibenthic state variables in the intertidal. It has been extended with a further submodel describing the dynamics of the subtidal community. Preliminary analysis of this model (EON, 1988) has shown the subtidal submodel to severely underestimate the standing stock of subtidal macrobenthos. This was caused in the model by an almost continuous food-limitation, because the watervolume allowed for suspension feeders (a watercolumn of 20 cm deep) with a lenght of the tidal excursion) was depleted of edible particles by

repeated filtering. Though this watervolume is a considerable fraction of the tidally-averaged compartment volume (20-50%), it apparently cannot supply the benthic system with sufficient particulates to maintain benthic biomass at the observed levels. Due to the low simulated benthic biomass, the contribution of the subtidal community to the total carbon flow in the model was almost negligible.

The assumption in the model was that as far as transport processes are concerned, phytoplankton behaves as a dissolved substance. In other words, it is subject to diffusive and advective exchange and there is no vertical concentration gradient.

However, under conditions of nutrient stress phytoplankton has a tendency to settle to the bottom (SMAYDA, 1970, 1971) and also, on each tidal cycle, around slack water, the concentration of chlorophyll-*a* near the bottom tends to be much higher than near the surface (TENORE, 1977) which indicates a general settling tendency of phytoplankton. The model results from simulations with phytoplankton homogeneously distributed over the water column showed that the subtidal fauna was so severely food-limited that the model supported much too low subtidal standing stocks. We therefore extended the pelagic submodel with a mechanism which caused a fraction of the phytoplankton — dependent on the prevailing nutrient limitation — to be subjected to the same transport processes that operate on non-living particulate matter, such as silt and detritus. This results in a non-homogeneous distribution of phytoplankton over the vertical, with increased concentrations near the bottom.

The model was run for a period of one year (1986) with the correct forcing functions (light, temperature, fresh water discharges, tidal effects and boundary conditions) for that year, once with phytoplankton homogeneously distributed across the vertical (the EMOWAD-I version) and once with the phytoplankton settling mechanism included. The model results for 1986 have been validated with field data, where available (*cf.* EON, 1988).

3. RESULTS

The carbon budgets for the western Wadden Sea, as calculated from the ecosystem model are given in Table 1, both including and excluding the phytoplankton settling mechanisms.

These results differ strongly from each other. The annual carbon budget of the simulation with phytoplankton settling (Table 1) is higher than that without, but it is surprising that the increase in pelagic primary production ($127 \cdot 10^6$ kg C) to a large extent compensates for the increase of consumption/mineralization in the subtidal region ($175 \cdot 10^6$ kg C). This increase is entirely due to increased pelagic primary production, since the benthic primary production is stable ($53\text{-}54 \cdot 10^6$ kg C) in both runs. The increase in pelagic production is caused by increased nutrient regeneration in the subtidal region. Thus, in the model, the subtidal system is nearly self supporting, the difference between the increase in primary production and the carbon uptake by the subtidal community being made up by a decrease in the export to sea and a reduction in the pelagic uptake of organic carbon.

The additional consumption of phytoplankton in the subtidal region has only a slight impact on the consumption/mineralization in the pelagic, which decreases from $360 \cdot 10^6$ kg C to $342 \cdot 10^6$ kg C. The total annual carbon turn-over increases from $671 \cdot 10^6$ kg C in the run without phytoplankton settling to $821 \cdot 10^6$ kg C, an increase of $136 \cdot 10^6$ kg C. This exceeds the increase in primary production by $9 \cdot 10^6$ kg C.

The residual tidal current in the western Wadden Sea runs from the Vlie to the Marsdiep, thus causing a net import through the Vlie and a net export from the Marsdiep to the North Sea (RIDDERINKHOF, 1988). Though the transport processes themselves are unaffected by the activity level of the subtidal community, the amounts transported into and through the system are changed by it. Both with and without phytoplankton settling the western Wadden

TABLE 1

Comparison of some model results between simulation runs with and without phytoplankton settling.

import/production (10^3 *tonne C·y*$^{-1}$)	*phytoplankton settling*				*export/consumption*
	with	*without*	*with*	*without*	
Input IJsselmeer	133	133	146	165	Output North Sea
Pelagic prim. prod.	610	483	342	360	pelagic consumption
Benthic prim. prod.	53	54	109	112	intertidal consumption
From carbon pool	25	15	192	17	subtidal consumption
			32	31	buried
total	821	685	821	685	

Sea is a system which exports organic carbon to the North Sea. The annual export is $165 \cdot 10^6$ kg C without, and $146 \cdot 10^6$ kg C with phytoplankton settling. This reduction in export, across the boundary between compartment 1 and the North Sea (the Marsdiep), occurs even while the import across the boundary between compartment 8 and the North Sea (the Vliestroom) increases from $38 \cdot 10^6$ kg C to $53 \cdot 10^6$ kg C. The decrease in this import/export asymmetry in the model run with phytoplankton settling is caused by diffusive exchange, due to the slightly lower concentrations of particulate organic carbon in the pelagic in this case. In view of the fact that the eutrophic IJsselmeer also brings $133 \cdot 10^6$ kg C into the system annually, the western Wadden Sea only has a small export surplus of $13 \cdot 10^6$ kg C.

The budgets in Table 1 give the total carbon flows for the whole western Wadden Sea. To allow comparisons with other carbon budgets, which usually are calculated in g $C \cdot m^{-2} \cdot y^{-1}$, we converted our results to the same units (Table 2, 3 and 4). In Tables 2-4 we use the results from the model version with the phytoplankton settling mechanism to compare with other budget calculations since the biomass and, hence, the activity of the subtidal community is far too small in the model version without phytoplankton settling. Tidal and subtidal areas do not add up to the total area since the channel area, something of a submerged desert, is not included.

The major sources of organic carbon according to the budget calculated from the model are pelagic primary production and import from the IJsselmeer; according to the budget calculated by DE WILDE & BEUKEMA (1984) (W&B in the tables) import from the North Sea is the largest source, closely followed by pelagic primary production. On pelagic mineralization both budgets agree rather well.

Though the consumption/mineralization in the subtidal community is much larger than in the intertidal (Table 1), this might be misleading, because the surface area of the intertidal is much smaller (452 km^2) than the subtidal area (753 km^2). In Table 3 the results for the intertidal are given per m^2 and in Table 4 those of the subtidal. Comparing these, it is clear that consumption/mineralization in the intertidal area (240 g $C \cdot m^{-2} \cdot y^{-1}$) is slightly smaller than in the subtidal region (295 g $C \cdot m^{-2} \cdot y^{-1}$). In this comparison the amount of carbon in the intertidal that is fossilized is not included, since it is not utilised.

In the pelagic zone, the carbon flows through micro-organisms, the primary producers, microzooplankton and bacterioplankton, completely dwarf the carbon flow through the meso- and macrozooplankton in both budgets (Table 2). The only other considerable sources or sinks of particulate carbon are the transport flows from the IJsselmeer and to or from the North Sea.

In the intertidal (Table 3) macrobenthic organisms account for 27% of the consumption/mineralization compared to 35% in the subtidal (Table 4).

TABLE 2

Comparison between some pelagic process rates estimated by DE WILDE & BEUKEMA(1984) and model results.

pelagic system rates	*gC·m⁻³·y⁻¹*	
tidally averaged volume: 4664·10⁶ m³	*model*	*W&B*
pelagic primary production	130.70	45.49
consumption by microplankton and bacteria	72.10	77.00
consumption by zooplankton	1.15	3.00
import of POC from IJsselmeer	12.22	19.71
import of POC from the North Sea	−46.34	50.04

TABLE 3

Comparison between some intertidal process rates estimated by DE WILDE & BEUKEMA(1984) and model results

intertidal system rates	*gC·m⁻²·y⁻¹*	
surface area: 452·10⁶ m²	*model*	*W&B*
production by:		
phytobenthos	117.5	155.0
annual consumption/mineralization by:		
aerobic bacteria + meio- + phyto-benthos	104.0	260.0
macrobenthos	65.8	63.0
anaerobic bacteria	69.9	80.0
buried	69.9	—

TABLE 4

Comparison between some subtidal process rates estimated by DE WILDE & BEUKEMA (1984) and model results.

subtidal system rates	*gC·m⁻²y⁻¹*	
surface area: 753·10⁶ m²	*model*	*W&B*
annual consumption/mineralization by:		
aerobic bacteria + meiobenthos	102.7	?
macrobenthos	89.3	100.0
anaerobic bacteria	103.1	?

The model results, as well as field data (*cf.* VOSJAN, 1987), show that in the pelagic zone of the western Wadden Sea no anaerobic mineralization is found, because oxygen consumption and oxygen production are in balance and, generally, no anoxic conditions occur.

In the intertidal sediments, aerobic mineralization dominates over anaerobic mineralization because of the *in-situ* production of oxygen by phytobenthos and the regular exposure to the air. In the subtidal sediments, however, anaerobic mineralization clearly dominates aerobic mineralization. Here, all oxygen must be supplied by the overlying water. The

contribution of anaerobic decomposers, mainly sulphate reducers, in the subtidal community thus rises to 62% of the total mineralization by micro-organisms, making this the largest subtidal carbon flow. This model result is in line with a recent estimate by VOSJAN (1987) of 100-200 g $C \cdot m^{-2} \cdot y^{-1}$ being mineralized by sulphate reducers in the Wadden Sea.

4. DISCUSSION

There are two major differences in Table 2 between the model budget and that of DE WILDE & BEUKEMA (1984). The first discrepancy is the higher primary production in the model. This discrepancy diminishes to some extent when we convert the gross production value as calculated in the model to the net production value by subtracting exudate production (22 g $C \cdot m^{-3}$).

There are two possible explanations for this discrepancy. The first one is that benthic primary production in the model, as well as the field measurements, are underestimates. The method used by CADÉE & HEGEMAN (1974), CADÉE (1980) in the western Wadden Sea and by COLIJN & DE JONGE (1984) in the Ems estuary, whose field observations have been used to calibrate the model, probably underestimates the benthic primary production. Though the degree to which the field experiments result in low estimates of benthic primary production is difficult to quantify, it probably should be a factor of 1.5-3.5 (REVSBECK *et al.*, 1981; LINDEBOOM & DE BREE, 1982). A higher benthic primary production would result in a higher uptake of nutrients by microphytobenthos and hence to a lower release of nutrients from the sediment. This, in turn would cause a lower nutrient concentration in the water column and the pelagic primary production calculated by the model would be more strongly nutrient-limited and hence lower.

Another explanation could be that nitrogen is not included in the model, while it is known from field observations (HELDER, 1974) that in summer the nitrogen concentration (NH_4^+: and NO_3^-) becomes limiting for phytoplankton which would depress primary production.

The second discrepancy is that our model calculations indicate an export of POC to the North Sea, whereas other authors calculate an import of POC into the Western Wadden Sea (POSTMA, 1961; DE JONGE & POSTMA, 1974 and CADÉE, 1980). Import is caused by the ebb/flood asymmetry in the tidal current velocities (POSTMA, 1954; POSTMA, 1961 and POSTMA, 1967) which causes a net transport of particulates in a landward direction, counteracting the seaward transport by advection and diffusion processes. This mechanism is included in the model by letting particulate detritus be transported in an identical way as suspended sediment (BARETTA & RUARDIJ, 1988). Since almost all the suspended sediment in the western Wadden Sea originates from the North Sea (EISMA, 1981), the implication is that since the concentrations of suspended sediment in the system do not diminish, the amounts sedimenting out in the Wadden Sea must be made up for by import from the North Sea. The same principle also is thought valid for particulate detritus. The IJsselmeer is a considerable source of this material, however, and thus detritus sedimented in the Wadden Sea is not derived exclusively from the North Sea but from the IJsselmeer as well. The net sedimentation rate of suspended sediment in the model is the same as used in the Ems model (BARETTA & RUARDIJ, 1988). This rate has been estimated from field observations on the average deposition in the Dollard (DE SMET & WIGGERS, 1960; REENDERS & VAN DER MEULEN, 1972). EISMA (1981) estimated the total deposition in the whole Wadden Sea (Dutch + Danish + German) at $3 \cdot 10^9$ $kg \cdot y^{-1}$ where our model calculations arrive at a deposition of $0.5 \cdot 10^9$ $kg \cdot y^{-1}$ for the western part of the Dutch Wadden Sea. Since the total surface area of the Wadden Sea, including the barrier islands, is $\pm$ 10 000 km^2, this would seem to indicate that the import of suspended sediment in the model is too high rather than too low, and consequently, the import of particulate organic detritus which is driven by the same mechanisms as import of suspended sediment is not likely to have been underestimated. The particulate transport model acts in such a way that any differences in the carbon content of suspended matter in adjacent (spatial) compartments are minimized by tidally driven mixing and exchange. The carbon content of suspended matter is roughly equivalent to the POC concentration in the water column. The POC concentration is mainly determined by the primary production, since the major source of POC is dead phytoplankton. As long as primary production is higher in the estuary than at sea there will be a POC concentration gradient which may be steeper than the corresponding concentration gradient of suspended matter. In the model such a gradient indeed occurs and this leads to an export instead of an import of particulate organic carbon (BARETTA & RUARDIJ, 1987).

The steepness of this gradient in the model may be overestimated due to a too high primary production, which would lead to an overestimate of POC export. However, since a model run without nutrient regeneration (resulting in much lower primary production) still indicates an export of POC, the POC-gradient between the estuary and the North Sea apparently is not decisive in determining the direction of net transport of POC. It seems likely, therefore, that there is an export of POC from the western Wad-

den Sea to the North Sea.

As CADÉE (1984) has pointed out, the calculations that led to the conclusion that the western Wadden Sea imported POC were based on assumptions that may not be justified. Of course, the same may be said about the assumptions that are part and parcel of the model structure, but the calculation of the transport fluxes in our model is based on a validated hydrodynamical model. Earlier calculations of the carbon budget of the western Wadden Sea had to do without such a model. Secondly, earlier budget calculations also had to use data from different years, whereas our model calculations were performed with data on the boundary conditions and forcing functions from the year 1986 only.

The least-known part of the western Wadden Sea is the subtidal area, which is shown by the model to be a very vital part of the whole system. It is recommended that future work on the western Wadden Sea focus in on the subtidal area to test the validity of the model results.

5. REFERENCES

BOEDE, 1985. Biological Research Ems-Dollard Estuary. Rijkswaterstaat Communications. 40: 182 pp.

BARETTA, J.W. & P. RUARDIJ, 1987. Evaluation of the Ems estuary ecosystem model.—Continental Shelf Res. **7:** 1471-1476

——,1988. Tidal flat estuaries. Simulation and analysis of the Ems estuary. Ecological studies no. 71. Springer, Berlin, Heidelberg, New York 353 pp.

CADÉE, G.C., 1980. Reappraisal of the production and import of organic carbon in the western Wadden Sea. Neth. J. Sea Res. **14:** 305- 322.

——, 1984. Has input of organic matter into the western part of the dutch Wadden Sea increased during the last decade? In: R.W.P.M. LAANE & W.J. WOLFF. The role of organic matter in the Wadden Sea. Netherlands Institute for Sea Research Publication Series. 10-1984: 71-82.

CADÉE, G.C. & J. HEGEMAN, 1974. Primary production of benthic microflora living on tidal flats in the Dutch Wadden Sea.—Neth. J. Sea Res. **8:** 250-291.

COLIJN, F. & V.N. DE JONGE, 1984. The primary production of microphytobenthos in the Ems-Dollard Estuary.—Mar. Ecol. Progr. Ser. **14:** 185-196.

DAVIES, J.M., 1975. Energy flow through the benthos in a Scottish Sea Loch.—Mar. Biol. **31:** 353-362.

DEKKER, R., 1987. The importance of the subtidal macrobenthos as food source for the Wadden Sea ecosystem. In: S. TONGAARD & S. ASBRIK. Proceedings of the 5th International Wadden Sea Symposium Esbjerg, Denmark Sept. 29th-Oct. 3, 1986.

EISMA, D., 1981. Supply and deposition of suspended matter in the North Sea.—Spec. Publs. int. Ass. Sediment **5:** 415-428.

EISMA, D. & W.J. WOLFF, 1980. The development of the westernmost part of the Wadden Sea in historical times. In: K.S. DIJKEMA, H.-E. REINECK & W.J. WOLFF. Geomorphology of the Wadden Sea area. Balkema, Rotterdam: 95-103.

EON, 1988. Ecosysteemmodel van de Wadden Sea.—NIOZ-Rapport 1988 - 1: 1-88.

HARGRAVE, B.T. & G.F. CONNOLLY, 1978. A device to collect supernatant water for measurement of the flux of dissolved compounds across sediment surface.—Limnol. Oceanogr. **23:** 1005-1010.

HELDER, W., 1974. The cycle of dissolved inorganic nitrogen compounds in the Dutch Wadden Sea.—Neth. J. Sea Res. **8:** 154-173.

JONGE, V.N. DE & H. POSTMA, 1974. Phosphorus compounds in the Dutch Wadden Sea.—Neth. J. Sea Res. **8:** 139-153.

LINDEBOOM, H.J. & B.H.H. DE BREE, 1982. Daily production and consumption in an eelgrass (Zostera marina) community in saline Lake Grevelingen: discrepancies between the O_2 and ^{14}C-method.—Neth. J. Sea Res. **16:** 362-379.

POSTMA, H., 1954. Hydrography of the Dutch Wadden Sea.—Arch. néerl. Zool. **10:** 405-511.

——, 1961. Transport and accumulation of suspended matter in the Dutch Wadden Sea.—Neth. J. Sea Res. **1:** 148-190.

——, 1967. Sediment transport and sedimentation in the estuarine environment. In: G.H. LAUFF. Estuaries. Amer. Ass Advancement Sci. Washington DC: 158-184.

REENDERS, R. & D.H. VAN DER MEULEN, 1972. De ontwikkeling van de Dollard over de periode 1952-1969/'70. Rijkswaterstaat, directie Groningen, afdeling Studiedienst, nota 72.1 met 14 bijlagen: 23 pp.

REVSBECK, N.P., B.B. JØRGENSEN & O. BROX, 1981. Primary production of microalgae in sediments by oxygen microprofile, $H^{14}CO_3^-$ fixation and oxygen exchange in sediments by oxygen microprofile. Limnol. Oceanogr. **26:** 717-730.

RIDDERINKHOF, H., 1988. Tidal and residual flows in the western Wadden Sea. Part I: Numerical model results. Neth. J. Sea Res. **22:** 1-21.

ROWE, G.T., C.H. CLIFFORD, K.L. SMITH JR. & P.L. HAMILTON, 1975. Benthic nutrient regeneration and its coupling to primary productivity in coastal waters. Nature **255:** 215-217.

ROWE, G.T. & K.L. SMITH JR., 1977. Benthopelagic coupling in the Mid-Antlantic Bight. In: B.C. COULL. Ecology of Marine Benthos. Univ. of South Carolina Press, Columbia: 55-65.

SIBERT, J.R. & R.J. NAIMAN, 1979. The role of detritus and the nature of estuarine ecosystems. In: K.R. TENORE & B.C. COULL. Marine Benthic Dynamics, Univ. of South Carolina Press, Colombia: 311-323.

SMAYDA, T.J., 1970. The suspension and sinking of phytoplankton in the sea.—Ocean. Mar. Biol. Ann. Rev. **8:** 353-414.

SMAYDA, T.J., 1971. Normal and accelerated sinking of phytoplankton in the sea.—Mar. Geol. **11:** 105-122.

SMET, L.A.H. DE & A.J. WIGGERS, 1960. Einige bemerkungen über die Herkunft und die Sedimentationsgeschwindigkeit der Dollart-ablagerungen.—Verh. Kon. Ned. geol.-mijnb. Genootsch. XIX, 129-133.

STROO, D., 1986. A method for validation. NIOZ Interne Verslagen EON 1986-1: 35 pp.

TENORE, K.R., 1977. Food chain pathways in detrital feeding benthic communities: A review, with new observation on sediment resuspension and detrital recycling. In: B.C. COULL. Ecology of marine benthos. University of South Carolina Press, Columbia: 37-54.

VERWEY, J., 1981. The blue mussel *Mytilus edulis*. In: N. DANKERS, H. KWHL & W.J. WOLFF. Invertebrates of the Wadden Sea. Balkema, Rotterdam: 114-115.

VOSJAN, J.H., 1987. A sketchy outline of the fate of organic matter in the dutch Wadden Sea.—Hydrobiol. Bull. 21(1), in press.

WILDE, P.A.W.J. DE & J.J. BEUKEMA, 1984. The role of zoobenthos in consumption of organic matter in the Wadden Sea. In: R.W.P.M. LAANE & W.J. WOLFF. The role of organic matter in the Wadden Sea. Netherlands Institute for Sea Research Publication Series. 10-1984: 145-158.

WOLFF, W.J. 1983. Ecology of the Wadden Sea. Reports of the Wadden Sea working group. Balkema, Rotterdam, Vols. 1-13.

ZEITSCHEL, B., 1979. Sediment-water nutrient dynamics. In: K.R. TENORE & B.C. COULL. Marine benthic dynamics. University of South Carolina Press, Columbia: 195-218.

EUTROPHICATION OF THE DUTCH WADDEN SEA
EXTERNAL NUTRIENT LOADINGS OF THE MARSDIEP AND VLIESTROOM BASINS

HENK W. VAN DER VEER, WIM VAN RAAPHORST & MAGDA J.N. BERGMAN

Netherlands Institute for Sea Research P.O. Box 59, 1790 AB Den Burg Texel, The Netherlands

ABSTRACT

The increasing P and N content in the two main tidal basins in the western Dutch Wadden Sea, the Marsdiep and the Vliestroom basins, has been reconstructed from the 50s onwards. The area is enriched with nutrients by two sources both originating from the river Rhine, one being the discharge from Lake IJssel and the other the exchange with the coastal zone of the North Sea. Due to a buffering by Lake IJssel for about 15-20 years, the eutrophication of the western Wadden Sea showed a time lag compared with the continuously increasing nutrient concentrations in the river Rhine and the coastal zone of the North Sea. At present, the primary production in the area still seems to be not fully nutrient limited in summer, while loadings have already been decreasing in recent years. So far, no severe, negative effects on the ecosystem have been reported. Some remarks are made on the eutrophication in other parts of the Dutch Wadden Sea in relation to the hydrographic characteristics of these areas.

1. INTRODUCTION

During the last decades fresh surface waters in western Europe have been enriched considerably with nutrients from land run-off as well as from industrial and domestic waste water discharges. In the Netherlands this has resulted in a dramatic increase in nutrient concentrations in the main surface waters (ANON., 1980). Serious effects such as nuisance causing blooms of blue- green algae and transparencies of less than 30 cm in formerly clear waters have been observed (ANON., 1980).

Freshwater run-offs are finally discharged in the marine environment and here, particularly in the coastal zone, eutrophication may also be expected. Part of the Dutch coastal zone, consists of estuarine areas, the main one being the Wadden Sea, which is a nursery area for a number of commercially important fish species such as plaice (ZIJLSTRA, 1972; KUIPERS, 1978; VAN DER VEER, 1986) and a resting area for wading birds (for a review see SMIT & WOLFF, 1983).

Although the nutrient cycling of the Dutch Wadden Sea has been the subject of extensive studies (POSTMA, 1954, 1966, 1985; DUURSMA, 1961; VAN BENNEKOM *et al.*, 1974; HELDER, 1974; DE JONGE & POSTMA, 1974 RUTGERS VAN DER LOEFF, 1980), a review of the general trend in the nutrient concentrations in the area has never been compiled. The enormous freshwater discharge by Lake IJssel in the western part of the Wadden Sea is expected to enrich especially this estuarine area with nutrients. In recent years an increasing amount of information has become available on effects of eutrophication on primary as well as on secondary production in this area (BEUKEMA & CADÉE, 1986; CADÉE, 1986).

This paper describes the eutrophication of the two main tidal basins in the western part of the Dutch Wadden Sea, the Marsdiep and the Vliestroom basins. Eutrophication may be defined confirming to POSTMA (1985): "an enrichment with nutrients or organic matter". The ecological effects of an increased loading with nutrients are left out in this definition. Attention is paid mainly to P and N, because at least in the past these nutrients seemed to limit primary production (CADÉE & HEGEMAN, 1974) and the concentrations of both of these nutrients have increased considerably in inland waters during the last few decades. Besides giving a review of the nutrient concentrations in the area and of the loadings by the main sources, an attempt has been made to compare the importance of the coastal zone of the North Sea and the discharge from Lake IJssel as sources of P and N. Finally, some remarks are made on the effects of eutrophication on the ecosystem.

This paper forms a baseline study for a review of the eutrophication of the Dutch Wadden Sea, which will be presented at the VIth International Wadden Sea Symposium at Sylt, October 1988.

Acknowledgement.—Thanks are due to G.C. Cadée for critical reading of the manuscript.

2. MATERIAL AND METHODS

Fig. 1 shows the location of the sampling stations in the western part of the Dutch Wadden Sea (henceforth called western Wadden Sea), together with the main nutrient source, the river Rhine,

feeding the Wadden Sea via the coastal zone of the North Sea and via discharge from Lake IJssel. The synopsis of the development of the eutrophication of the western Wadden Sea has been based upon a compilation of published and unpublished data. In case of lack of data, an attempt has been made to reconstruct the missing data.

Figure 1. The western part of the Wadden Sea (shaded), together with Lake IJssel (3), the coastal zone of the North Sea and the two main rivers feeding the western Wadden Sea indirectly, the rivers Rhine (1) and IJssel (2)

2.1. THE RIVERS RHINE AND IJSSEL

All information concerning flows and concentrations of N and P components of the rivers Rhine and IJssel were obtained from the annual reports of the International Rhine Commission, Koblenz, and from the quarterly reports on the water quality of the Dutch waters as published by Rijkswaterstaat, Rijks Instituut voor Zuivering van Afvalwater, (RIZA) Lelystad. However, before 1972 total-N and total-P concentrations were not determined regularly. Therefore the total-N values had to be estimated. The ratio $(NH_4^+ + NO_3^-)$/total-N, in river IJssel was approximately 0.75 during the period 1972-1985 (Fig. 2). This ratio has also been assumed in the Rhine and the IJssel for the period 1954-1972. Total-P has been estimated from the ratio ortho-P/total-P. Around 1960 (Postma, unpubl.) and in the early 70s, this ratio in the IJssel was about the same, 0.40 (Fig. 2). This value has also been adopted for the intervening years. The uncertainty introduced by this assumption is roughly estimated at 10%. From the 70s onwards, these ratios have seemed to increase to values of approximately 0.90.

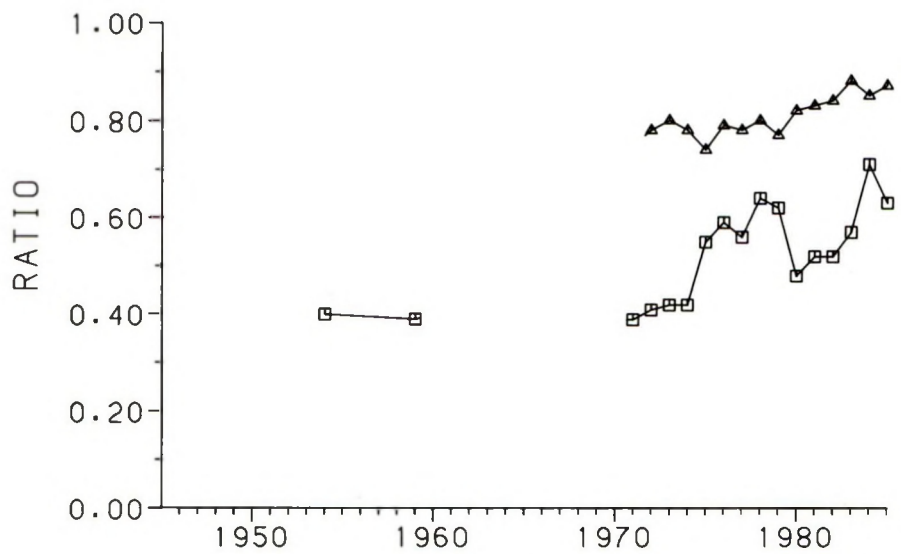

Figure 2. Ratio between the concentration of $(NH_4^+ + NO_3^-)$/total-N (△) and of ortho-P/total-P (□) in river IJssel from 1955 onwards

2.2. DISCHARGE OF LAKE IJSSEL

Data on the monthly discharges of fresh water from Lake IJssel into the Wadden Sea were obtained from Rijkswaterstaat Directie Zuiderzeewerken, Lelystad. Data on the concentrations of N and P components near the sluices (location Y1 and Y2) were published in the quarterly reports of RIZA from 1972 onwards. Ortho-P and total-P were measured from 1949 to 1951 by POSTMA (1954), in 1957 by DUURSMA (1961), in 1958-1959 by POSTMA (1967 and unpubl.) and during 1967 to 1970 by DE KLOET (1971). Data concerning N components were determined in 1957 (NH_4^+) by DUURSMA (1961), in 1960-1962 (NH_4^+, $N0_3^-$, total-N) by POSTMA (1966), from 1966-1972 near Andijk (total-N) by the Rijkswaterstaat, in 1971-1972 (NH_4^+, $N0_3^-$) by HELDER (1974). Based on the ratio between the concentrations at Andijk and near the sluices in 1972-1985, data of total-N from near Andijk (Governmental Water Company, unpublished) for the period 1966- 1972 were converted into concentrations near the sluices by multiplying by 0.90. The possible error in this factor is about 20%. Missing data of total-N for the period before 1966 were estimated by extrapolation from measured ratios between total-N and total-P in later years (Table 1). Overall, this results in a level of uncertainty in the reconstructed data of approximately 35%.

TABLE 1

Ratios between total-N and total-P in the northern part of Lake IJssel for a number of years, extrapolated from measurements in the intervening years (for further explanation see text)

	quarter			
	1	*2*	*3*	*4*
1949-1951	25	35	25	25
1958-1959			25	
1960-1962	25	35	35	35
1966-1967	22	22	22	22
1970-1971	20	23.5	15	18

2.3. THE COASTAL ZONE OF THE NORTH SEA

Nutrient data for the coastal zone of the North Sea were obtained from the quarterly reports of RIZA for a location off Calantsoog (C2 and C4) from 1973 onwards. Ortho-P has been measured from 1973 onwards. Older data were only available for the period 1949-1951 (POSTMA, 1954) and 1958-1959 (DUURSMA, 1961) near lightvessel Texel. It was assumed that at this location the concentrations were 1.3 times lower than those at C2 and C4 (DE WIT *et al.*, 1982). The uncertainty in this conversion is approximately 25%. For total-P, data were available only for the period 1975-1982. Based on the ratio ortho-P/total-P during this period, the ratio for the other years was estimated and missing data for total-P were calculated (Table 2). The ratios for the period 1949-1959 could only be calculated very roughly. Data about NH_4^+ and NO_3^- were available from 1975 onwards from the quarterly reports of the RIZA and for the period 1960-1962 (POSTMA, 1966) near lightvessel Texel. For N, the concentrations at this station were estimated to be 1.7 times lower than those at C2 and C4 (DE WIT *et al.*, 1982), with an uncertainty of 25%. Total-N was only measured in 1960-1962 (POSTMA, 1966) and between 1975-1982 (RIZA). Based on the ratio ($NH_4^+ + NO_3^-$)/total-N during these years the ratio has been extrapolated for the years 1983-1985 (Table 3) from which total-N could be estimated. For the period before 1960 and between 1962- 1973 total-N was estimated in a similar way (Table 4). The final level of uncertainty in the reconstructed data is in the order of 50%.

TABLE 2

Ratios between ortho-P and total-P in the coastal zone of the North Sea (C2 and C4), extrapolated from measurements in the intervening years (for further explanation see text)

	quarter			
	1	*2*	*3*	*4*
1949-1951	0.50	0.25	0.25	0.50
1958-1959	0.50	0.25	0.25	0.50
1973	0.30	0.30	0.30	0.50
1983-1985	0.40	0.25	0.55	0.55

TABLE 3

Ratios between ($NH_4^+ + NO_3^-$) and total-N in the coastal zone of the North Sea (C2 and C4), extrapolated from measurements in the period 1975-1982 (for further explanation see text)

	quarter			
	1	*2*	*3*	*4*
1983-1985	0.70	0.35	0.35	0.70

TABLE 4

Ratios between total-N and total-P in the coastal zone of the North Sea (C2 and C4), extrapolated from measurements in the intervening years (for further explanation see text)

	quarter			
	1	*2*	*3*	*4*
1949-1951	8	8	5.5	5.5
1958-1959	8	8	5.5	5.5
1960-1962	8	8	5.5	5.5
1973	8	8	5.5	5.5

2.4. THE WESTERN WADDEN SEA

Data on nutrient concentrations in the western Wadden Sea are available from 1972 onwards from the quarterly reports of the RIZA. Older data of P components are available for the period 1970-1971 (ortho-P) by De JONGE & POSTMA (1974), and for the period 1949-1951 (ortho-P and total-P) by POSTMA (1954). N components are presented for 1970-1971 (NH_4^+ and NO_3^-) measured by HELDER (1974), for 1960-1962 (NH_4^+, NO_3^- and total-N) by POSTMA (1966). Based on the ratios between total-N and total-P in these years (Table 5) missing data on total-N and total-P were reconstructed, with an estimated error of approximately 40%.

TABLE 5

Ratios between total-N and total-P in the western Wadden Sea, extrapolated from measurements in the intervening years (for further explanation see text)

	quarter			
	1	*2*	*3*	*4*
1949-1951	15	15	12.5	12.5
1960-1962	15	15	12.5	12.5
1970-1971	15	15	12.5	12.5

3. RESULTS

3.1. THE RIVERS RHINE AND IJSSEL

The concentrations of nutrients in the rivers Rhine and IJssel are multiplied by the water flows to calculate the yearly mean loadings. Both total-P (Fig. 3) and total-N (Fig. 4) showed a continuous increase from 1954 onwards. In 1981, the loadings had increased 5-7 times for total-P and 2-3 times for total-N, compared with 1954. Ortho-P and NO_3^- did even show a stronger increase. From 1981 to 1985, mean loadings decreased by about 20 - 30%. This was not caused by differences in river flow but was merely due to reduced nutrient concentrations.

3.2. DISCHARGE OF LAKE IJSSEL

The discharge from Lake IJssel into the Wadden Sea is given in Fig. 5. From 1950 until 1981 there was an increase in total-P from 0.03 $kg.s^{-1}$ to 0.16 $kg.s^{-1}$, and in total-N from 0.8 to 2. 3 $kg.s^{-1}$. From 1981, the discharge of total-N has stabilized, while total-P showed a little decrease at a similar amount of fresh water discharged through the sluices during that period (1981-1985). The increase in the nutrient

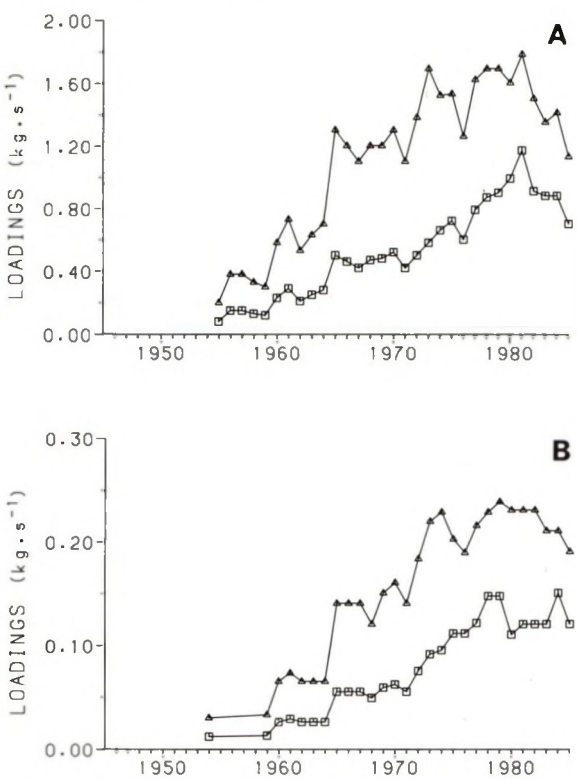

Figure 3. Loadings of ortho-P (□) and total-P (△) ($kg{\cdot}sec^{-1}$) A: the river Rhine near Lobith; B: the river IJssel near Kampen

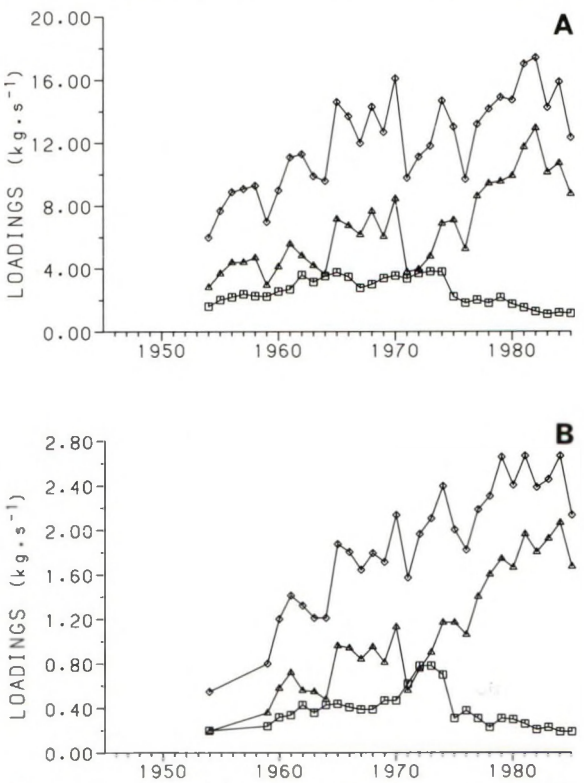

Figure 4. Loadings of total-N (◇), NO_3^- (△) and NH_4^+ (□) in $kg{\cdot}sec^{-1}$ A: the river Rhine near Lobith; B: the river IJssel near Kampen

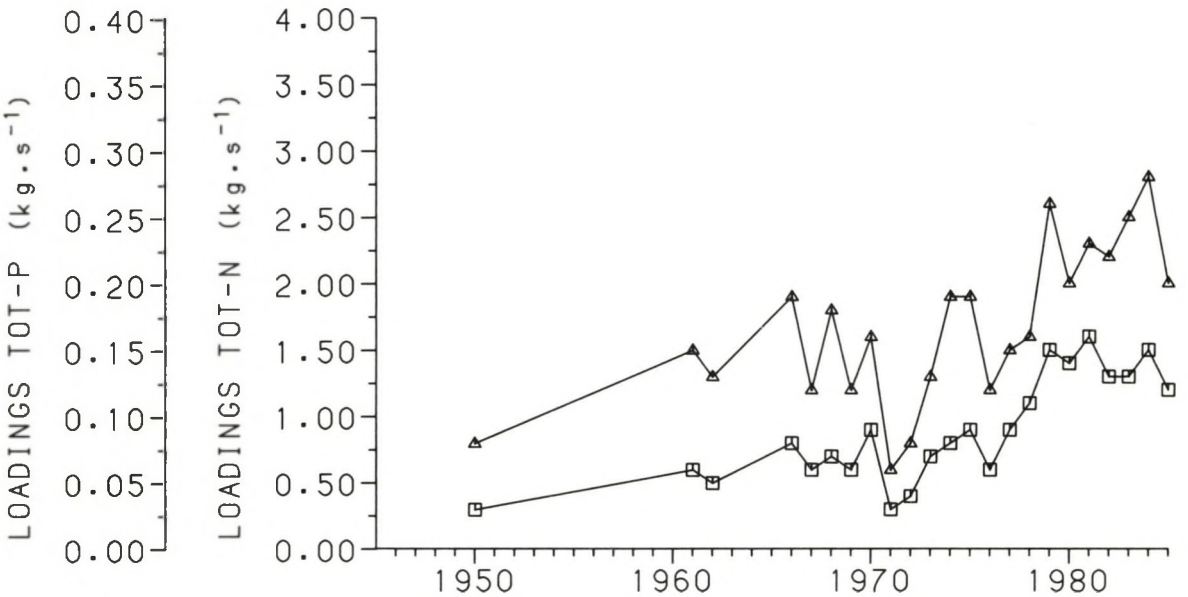

Figure 5. Loadings of total-P (□) and total-N (△) in the discharges of Lake IJssel (kg·sec^{-1})

loadings in the discharges mainly took place from 1970 onwards, which is in contradiction with the situation at the inflow of the lake, the river IJssel (see Figs 3 and 4).

3.3. THE COASTAL ZONE OF THE NORTH SEA

Fig. 6 shows the nutrient concentrations in the coastal zone of the North Sea in the first and third quarter of the year. Since only few data were available and most had to be reconstructed the overall level of uncertainty is high. Most likely seems a continuous increase in both the concentrations of total-P and total-N from 1950 onwards until 1980 and a stabilization hereafter. From 1950 to 1985 total-P increased by approximately a factor of 7 and total-N by approximately a factor of 5. The other quarters of the year showed a similar pattern. Based on annual mean concentrations, total-P and total-N have increased by approximately about a factor of 4 during the period 1950 to 1985.

3.4. THE WESTERN WADDEN SEA

The nutrient concentrations in the western Wadden Sea are presented in Figs 7 and 8 for the first quarter of the year, and in Figs 9 and 10 for the third quarter. The differences in concentrations between the various locations seemed to be rather small compared with the variations in time. In general, the pattern showed to be about the same in the whole area, with lowest concentrations near the tidal inlets of the area, especially in the Vliestroom. The increase in the concentrations of P components from 1950 onwards seemed to be much larger than that of the N components. In the third quarter the N components hardly showed any increase at all. A main part of the increase in nutrient concentrations took place between about 1970 and 1980. During the last few years concentrations have seemed to drop somewhat. Between 1950 and 1980, ortho-P and total-P increased respectively by a factor of 5-6 and 3-6 in the first and third quarters. For N, the increase was much lower and depended on the season: in the first quarter about 2 times, in the third quarter hardly any increase at all. The general trend during the other quarters of the year is the same: a large increase between 1970 and 1980, followed by a small decrease in the most recent years.

4. DISCUSSION

Recently, POSTMA (1985) reviewed the eutrophication of Dutch inshore and some coastal waters (Ems-estuary). However, he did not present a detailed analysis of the increase in nutrient loadings and concentrations. Due to the strong influence of the river Rhine in the western Wadden Sea, it was expected that this area would be more affected by an increased loading with nutrients then the eastern part of the Wadden Sea. Inflow of fresh water from the Rhine takes place in two ways, but in neither way occurs directly. One source is the discharge of Lake IJssel, which to a great extent is fed by fresh water from the

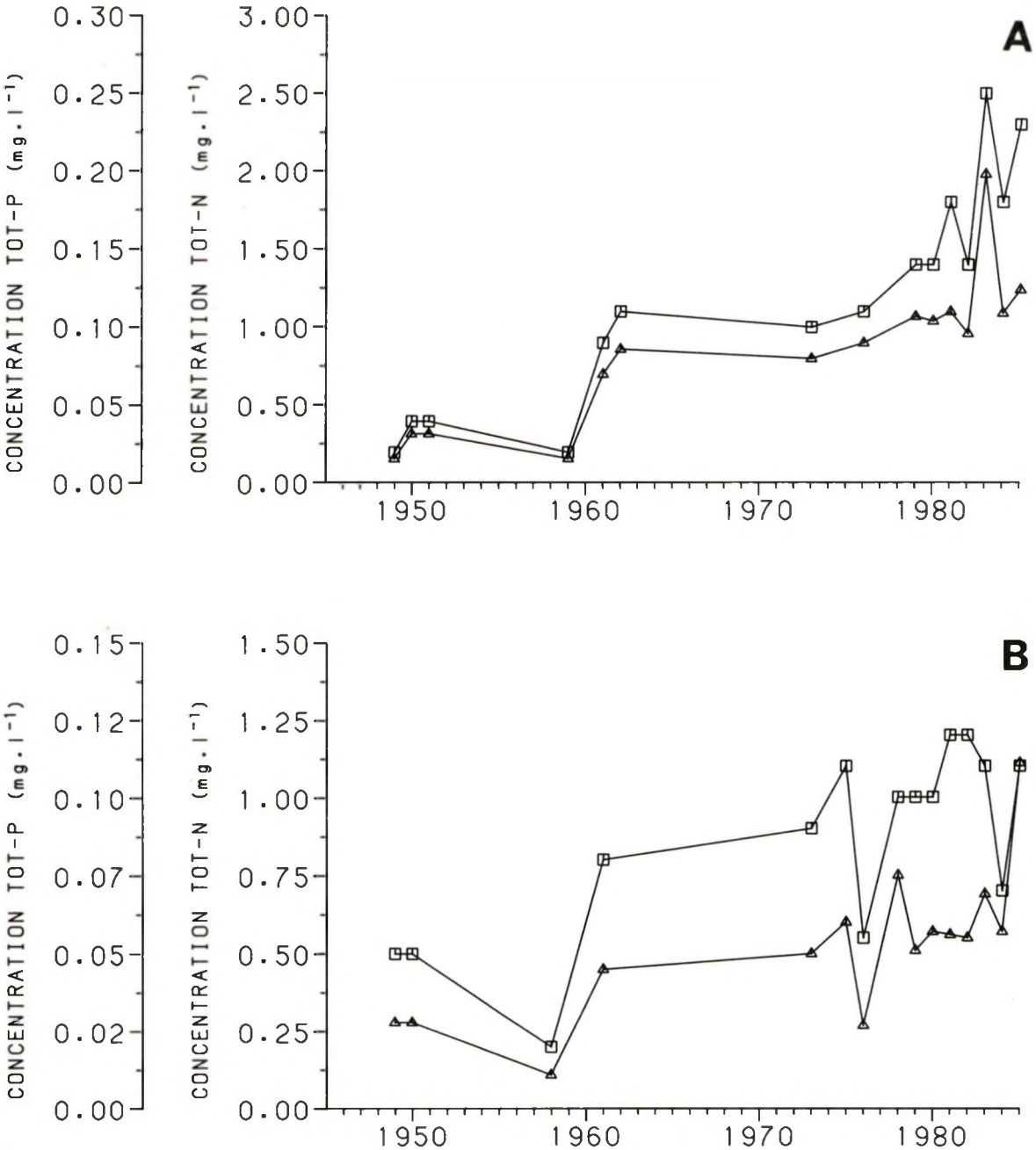

Figure 6. Concentrations of total-N (□) and total-P (△) in the coastal zone of the North Sea near Callantsoog ($mg \cdot l^{-1}$)
A: first quarter; B: third quarter

river IJssel, a branch of the Rhine. The other source is the import of saline coastal water through the tidal inlets which also consists partly of fresh water from the Rhine transported along the coastal zone (VAN BENNEKOM *et al.*, 1974 ZIMMERMAN, 1976).

The reconstruction of the nutrient concentrations in the area and the loadings of the main sources is hampered by lack of data especially from the past. Therefore, a partial reconstruction has been made by interpolation and extrapolation of the missing observations. This procedure result in uncertainties in the order of 30 to 50%. Particularly the data of the period before 1970 should be treated with some reservation. A comparison of the nutrient loadings

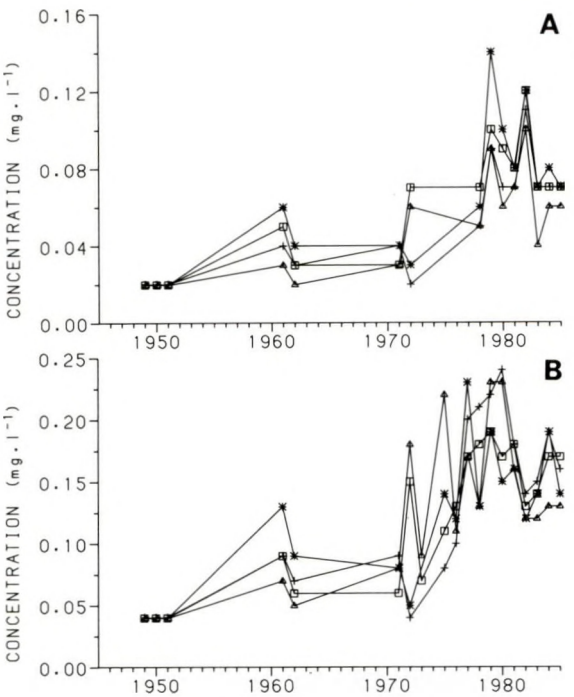

Figure 7. Concentrations of P components ($mg \cdot l^{-1}$) in the western Dutch Wadden Sea: Marsdiep inlet (□), Vliestroom inlet (△), Blauwe Slenk (✚) and Doove Balg (✳) during the first quarter A: ortho-P; B: total-P

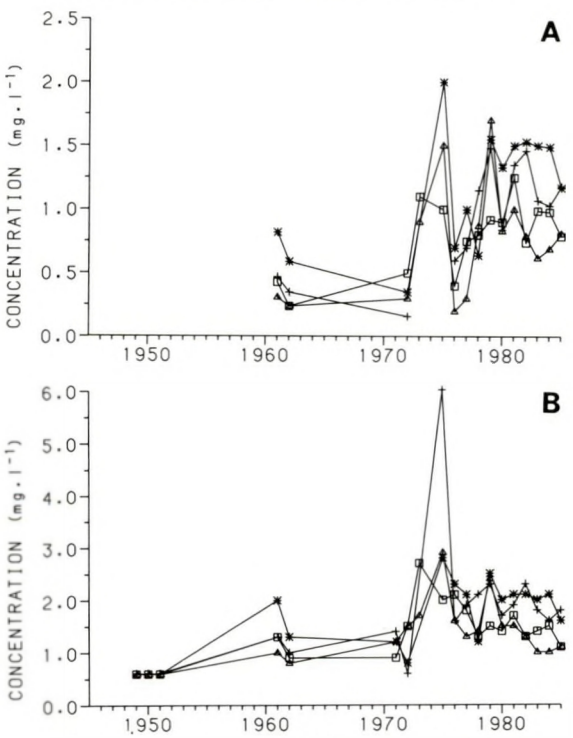

Figure 8. Concentrations of N components ($mg \cdot l^{-1}$) in the western Dutch Wadden Sea: Marsdiep inlet (□), Vliestroom inlet (△), Blauwe Slenk (✚) and Doove Balg (✳) during the first quarter A NO_3^-; B total-N

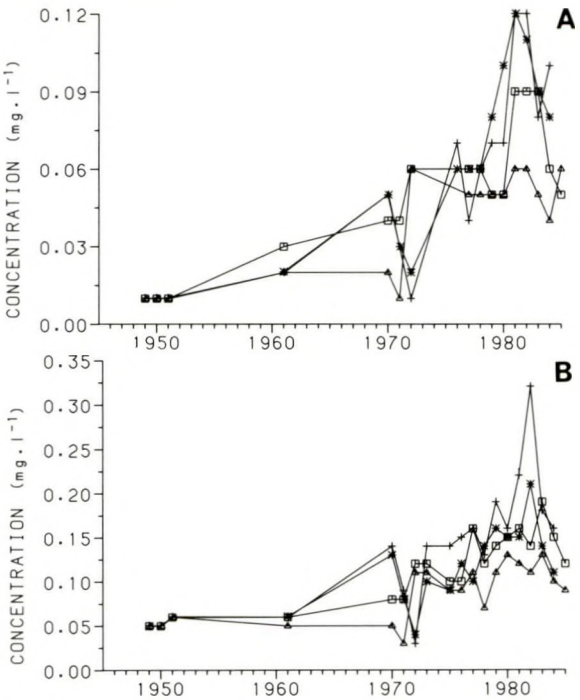

Figure 9. Concentrations of P components ($mg \cdot l^{-1}$) in the western Dutch Wadden Sea: Marsdiep inlet (□), Vliestroom inlet (△), Blauwe Slenk (✚) and Doove Balg (✳) during the third quarter A ortho-P; B total-P

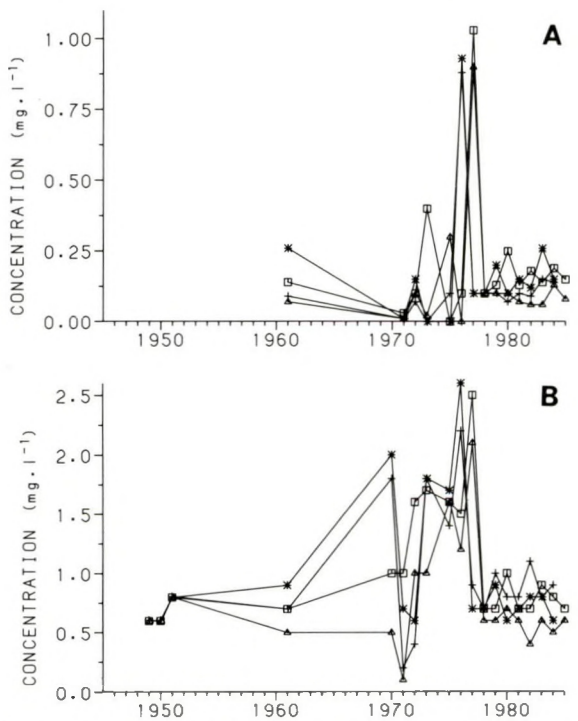

Figure 10. Concentrations of P components ($mg \cdot l^{-1}$) in the western Dutch Wadden Sea Marsdiep: inlet (□), Vliestroom inlet (△), Blauwe Slenk (✚) and Doove Balg (✳) during the third quarter A: NO_3^-; B: total-N

from the sources with the resulting concentrations in the western Wadden Sea reveals some striking facts. Although rather strong year-to- year fluctuations in nutrient concentrations and loadings occurred, clear trends can be observed.

The increase in the nutrient content of the Rhine seemed to be a rather continuous process during the period 1950-1980, followed by a slight decrease in recent years. The same pattern could be observed in the coastal zone of the North Sea, which is directly enriched by inflow from the Rhine. The river IJssel, feeding Lake IJssel, showed a similar increase in nutrient loading in the course of time. However, in the discharge of Lake IJssel there seemed to be a time lag. Until about 1970 loadings remained the same, and an increase could only be observed between 1970 and 1980. This suggests that for at least 15-20 years, Lake IJssel acted as a trap for the nutrient loadings from the river IJssel. This pattern of nutrient concentrations in the discharge of Lake IJssel was also found in the western Wadden Sea. A similar time lag of at least 15 years could be observed before an increase in concentrations started around 1970. During the past 5 years even a decrease in nutrient concentrations occurred. The correspondence between the development of the nutrient levels in the western Wadden Sea and the nutrient discharges of Lake IJssel suggests that these loadings from Lake IJssel are the main nutrient source of the western Wadden Sea, rather than import from the coastal zone of the North Sea. This conclusion is in contradiction with the suggestions made by POSTMA (1954) and DE JONGE & POSTMA (1974), who stressed the importance of import from the coastal zone as a source of organic matter and associated P components. Reappraisal of their figures by CADÉE (1980) and DE WILDE & BEUKEMA (1984) resulted in about an equal importance of Lake IJssel and the coastal zone as sources of organic matter for the western Wadden Sea in the 80ties. However, all these conclusions are based on budget calculations made for only a few years. Due to the strong year-to-year fluctuations, their conclusions might be true for these years, but considering the long-term trends, it seems most likely that in general Lake IJssel is the main source of nutrients for the western Wadden Sea.

Hardly any measurements on nutrients and primary production were performed before 1965. This means that for most Dutch inshore and coastal waters the effect of increased nutrient levels on primary production cannot be followed over the whole period of eutrophication, as already stated by POSTMA (1985). However, because of the buffering of Lake IJssel, this situation does not hold for the western Wadden Sea. Here, eutrophication essentially started from about 1970 onwards, while the first measurements of primary production were already made during the period 1963-1966 (POSTMA & ROMMETS, 1970) and 1972-1973 (CADÉE & HEGEMAN, 1974). So, apart from methodical problems related to the measurements of production, the figures from POSTMA & ROMMETS (1970) and CADÉE & HEGEMAN (1974) may be considered as baseline levels. On the basis of their measurements of pelagic primary production CADÉE & HEGEMAN (1974) concluded that in spite of the high turbidity of the Wadden Sea, a nutrient limitation in summer could not be excluded in part of the area. In winter, nutrient limitation did not seem to occur in these years.

TABLE 6

Pelagic primary production in the western Dutch Wadden Sea ($gC \cdot m^{-2} \cdot y^{-1}$) as estimated by different authors from 1963 onwards. All measurements were done in deep gullies [1]: Marsdiep tidal inlet; [2]:inner part of the area

year	*production*	*reference*
1964-1966	120[1]—170[2]	POSTMA & ROMMETS, 1970
	92.5[1]—151.5[2]	CADÉE & HEGEMAN, 1974
1972-1973	150[1]—200[2]	CADÉE & HEGEMAN, 1974
		CADÉE & HEGEMAN, 1979
1974-1975	135[1]—145[2]	CADÉE & HEGEMAN, 1979
1981-1982	340[2]	CADÉE, 1986
1985	260[2]	CADÉE, 1986
1986	165[1]—303[2]	VELDHUIS *et al.*, 1988

In these areas an increased nutrient loading may have resulted in a lenghtening of the period of non-nutrient limitation and probably in an increased production. Although there are not enough monthly production figures, the above suggestion is strongly supported by annual production figures measured over a number of years (Table 6). Not only the data for the Marsdiep tidal inlet area (as reviewed by CADÉE, 1986) but also the production in other parts of the western Wadden Sea have increased from 100-150 $gC.m^{-2}.y^{-1}$ in 1970 to 165-300 in 1986. However, CADÉE (1986) mentioned a discrepancy between eutrophication and the timing in increase of primary production, but he considered ortho-P as indicator for the state of eutrophication instead of total-P. Although ortho-P did show an increase from 1950 onwards, total-P remained approximately constant. The increase in ortho-P therefore illustrated a shift between P components and a shift from P- limitation to most likely N-limitation at least during parts of the year (VELDHUIS *et al.*, 1988). The increase of ortho-P in the period 1950-1970 as observed by DE JONGE & POSTMA (1974) and mentioned by CADÉE (1986) therefore not necessarily means a severe increase in the amount of nutrients available for primary production. According to the present data such an increase most likely started after 1970, approximately at the

same time as the increase in primary production as observed by CADÉE (1986). The increased annual production indicates a narrowing of the period of nutrient limitation during the year, but still in the present situation VELDHUIS *et al.* (1988) suggest a nutrient limitation during the summer period. So although the area has become more eutrophic over the years, the western Wadden Sea still does not seem to be fully nutrient limited all year round.

The increase in annual primary production may have resulted in an enlarged food supply for the consumers over the year and may also have an impact on the functioning of the ecosystem as far as this increased food supply is not exported towards the North Sea. CADÉE & HEGEMAN (1986) suggest an increase in the Phaeocystis abundance and BEUKEMA & CADÉE (1986) found a doubling of both biomass and annual production of the macrozoobenthos living on the tidal flats in the western Wadden Sea during 1970-1984. An impact on the functioning of the ecosystem is difficult to detect. So far, severe negative effects of eutrophication have not been reported, and only low oxygen conditions seem to occur locally even over longer periods (TIJSSEN & VAN BENNEKOM, 1976; VAN DER VEER & BERGMAN, 1986).

Eutrophication of the western Wadden Sea seems to be determined by the loadings of Lake IJssel and because of the buffering of nutrients by the lake, eutrophication of the western Wadden Sea has been delayed for quite a long time, *i.e.* some 15 years compared to the sources of the nutrients, the river Rhine. It might be stated that other parts of the Dutch Wadden Sea with a freshwater run-off directly into the estuary, such as the Ems-Dollard estuary, may show a more continuous increase in nutrient concentrations from the 50s onwards. Areas without any significant input of fresh water will only be influenced by exchange with the coastal zone of the North Sea. These areas will also show a pattern of a continuous increase, though on a rather low level, because of the rather low loadings coming from the North Sea. To confirm these hypotheses a more detailed analysis of the nutrient concentrations in these areas is necessary.

5. REFERENCES

ANONYMOUS 1980. Ontwikkeling van grenswaarden voor doorzicht, chlorophyl, fosfaat en stikstof. Resultaten van de tweede eutrofiëringsenquete. Coördinatiecommisie uitvoering wet verontreiniging oppervlaktewateren, werkgroep VI. 48 pp.

BENNEKOM, A.J. VAN, E. KRIJGSMAN-VAN HARTINGSVELD, G.C.M. VAN DER VEER & H.F.J VAN, VOORST, 1974. The seasonal cycle of reactive silicate and suspended diatoms in the Dutch Wadden Sea.—Neth. J. Sea Res. **8:** 359-374.

BEUKEMA, J.J. & G.C. CADÉE, 1986. Zoobenthos responses to eutrophication of the Dutch Wadden Sea.—Ophelia **26:** 55-64.

CADÉE, G.C., 1980. Reappraisal of the production and import of organic carbon in the western Wadden Sea.—Neth. J. Sea Res. **14:** 305-322.

——, 1986. Increased phytoplankton primary production in the Marsdiep area (western Dutch Wadden Sea).—Neth. J. Sea Res. **20:** 285-290.

CADÉE, G.C. & J. HEGEMAN, 1974. Primary production of phytoplankton in the Dutch Wadden Sea.—Neth. J. Sea Res. **8:** 240-259.

——, 1979. Phytoplankton primary production, chlorophyll and composition in an inlet of the western Wadden Sea (Marsdiep).—Neth. J. Sea Res. **13:** 224-241.

——, 1986. Seasonal and annual variation in *Pheaocystis pouchetii* (Haptophyceae) in the westernmost inlet of the Wadden Sea during the 1973 to 1985 period.—Neth. J. Sea Res. **20:** 29-36.

DUURSMA, E.K., 1961. Dissolved organic carbon, nitrogen and phosphorus in the sea.—Neth. J. Sea Res. **1:** 1-148.

HELDER, W., 1974. The cycle of dissolved inorganic nitrogen compounds in the Dutch Wadden Sea.—Neth. J. Sea Res. **8:** 154-173.

JONGE, V.N. DE & H. POSTMA, 1974. Phosphorus compounds in the Dutch Wadden Sea.—Neth. J. Sea Res. **8:** 139-153.

KLOET, W.A. DE, 1971. Het eutrofiëringsproces in het IJsselmeergebied.—Meded. Hydrobiol. Ver. **5:** 23-28.

KUIPERS, B.R., 1978. Opname en gebruik van voedsel door de jonge schol (*Pleuronectes platessa* L.) in een getijdengebied. Thesis Universiteit van Amsterdam: 91 pp.

POSTMA, H., 1954. Hydrography of the Dutch Wadden Sea.—Archs. neerl. Zool. **10:** 405-511.

——, 1966. The cycle of nitrogen in the Wadden Sea and adjacent areas.—Neth. J. Sea Res. **3:** 186-221.

——, 1967. Observations in the hydrochemistry of the inland waters in the Netherlands. In: GOLTERMAN, H.L., CLYMO, R.S. Chemical environment in the aquatic habitat, Proc. IBP symp. KNAW: 30-38.

——, 1985. Eutrophication of Dutch coastal waters. Neth. J. Zool. **35:** 348-359.

POSTMA, H. & J.W. ROMMETS, 1970. Primary production in the Wadden Sea.—Neth. J. Sea Res. **1:** 148-190.

RUTGERS VAN DER LOEFF, M.M., 1980. Time variation in interstitial nutrient concentrations at an exposed subtidal station in the Dutch Wadden Sea.—Neth. J. Sea Res. **14:** 123-143.

SMIT, C.J. & W.J. WOLFF, 1983. Birds of the Wadden Sea. Final report of the section Birds of the Wadden Sea Working Group. In: WOLFF, W.J. Ecology of the Wadden Sea. A.A. Balkema Press Rotterdam, 6/1-6/308.

TIJSSEN, S.B. & A.J. VAN BENNEKOM, 1976. Lage zuurstofgehaltes in het water op het Balgzand.—H_2O **9:** 28-31.

VEER, H.W. VAN DER, 1986. Regulation of the population of 0-group plaice (*Pleuronectes platessa* L.) in the Wadden Sea. Thesis Rijksuniversiteit Groningen, 91 pp.

VEER, H.W. VAN DER & M.J.N. BERGMAN, 1986. Development of tidally related behaviour of a newly settled 0-group plaice (*Pleuronectes platessa*) population in the western Wadden Sea.—Mar. Ecol. Prog. Ser. **31:** 121-129.

VELDHUIS, M.J.W., F. COLIJN, L.A.H. VENEKAMP & L. VILLERIUS. Phytoplankton primary production and biomass in the western Wadden Sea (the Netherlands): a comparison with an ecosystem model.—Neth. J. Sea Res. **22:** 37-49.

WILDE, P.A.W.J. DE & J.J., BEUKEMA, 1984. The role of zoobenthos in the consumption of organic matter in the Dutch Wadden Sea. In: LAANE, R.W.P.M., WOLFF, W.J. The role of organic matter in the Wadden Sea. Proc. 4th Intern Wadden Sea Symp. Texel, 1-3 November 1983. Netherlands Institute for Sea Research, Publ. Ser. 10-1984: 145- 158.

WIT, J.A.W. DE, F.M. SCHOTEL & L.E.J. BEKKERS, 1982. De waterkwaliteit van de Waddenzee. Rijkswaterstaat/RIZA nota nr. 82-065: 67 pp.

ZIMMERMAN, J.T.F., 1976. Mixing and flushing of tidal embayments in the western Dutch Wadden Sea. Part I. Distribution of salinity and calculation of mixing time scales.—Neth. J. Sea Res. **10:** 149-191.

ZIJLSTRA, J.J., 1972. On the importance of the Waddensea as a nursery area in relation to the conservation of the southern North Sea fishery resources.—Symp. zool. Soc. London **29:** 233-258.

This paper not to be cited without prior reference to the author

International Council for the Exploration of the Sea

C.M.1987/L:10
Demersal Fish Committee
Ref. G and H

ABUNDANCE AND GROWTH OF 0-GROUP PLAICE (*PLEURONECTES PLATESSA* L.) IN RELATION TO FOOD ABUNDANCE IN A COASTAL NURSERY AREA*

MAGDA J.N. BERGMAN, AART STAM and HENK W. VAN DER VEER

Netherlands Institute for Sea Research P.O. Box 59, 1790 AB Den Burg, Texel, The Netherlands

ABSTRACT

After settling has completed in the western Wadden Sea in May, the abundance of 0-group plaice in a number of tidal flat areas appears to be positively related to the local abundance of macrobenthos, which points to the importance of food as a key factor in the process of larval settling. Growth rates of 0-group plaice at the various tidal flat areas also appear to be related to the abundance of macrobenthos. In some tidal flat areas the growth of plaice seems to be food limited. As a result of the combined relationship of both abundance and growth of plaice to food abundance, predation pressure by 0-group plaice will increase exponentially with increasing macrobenthic biomass.

1. INTRODUCTION

Since ZIJLSTRA (1972) pointed to the importance of the Wadden Sea as nursery area for a number of commercial fish species, much research has been carried out in the whole area, especially on juvenile plaice (*Pleuronectes platessa* L.). In the Dutch part, CREUTZBERG *et al.* (1978) and RIJNSDORP *et al.* (1985) studied the immigration of larvae from the North Sea through the tidal inlets. KUIPERS (1978) studied the population dynamics, food intake and food consumption of plaice at the tidal flats, and RAUCK & ZIJLSTRA (1978), ZIJLSTRA *et al.* (1982) and VAN DER VEER (1986) paid attention to the regulating mechanisms present in the nursery. The thesis of BERGHAHN (1984) forms an important contribution to the knowledge of plaice in the German part.

These studies and the results of the Demersal Young Fish Surveys carried out in the Dutch, German and Danish Wadden Sea, have shown that the Wadden Sea is the main nursery area of North Sea plaice. About 60% of the recruitment of juveniles to the adult parent stock in the North Sea originates from the Wadden Sea (ANONYMOUS, 1985).

From this point of view it is of interest to know whether juvenile plaice is using the nursery completely or only partly. In a previous paper the main factors determining the carrying capacity of the nursery for plaice and the actual use of it were outlined (VAN DER VEER & BERGMAN, 1987b).

One of the main factors will be the amount of food available for the juveniles. KUIPERS (1977), ZIJLSTRA *et al.* (1982) and VAN DER VEER (1986) argued that at least in their area of study, *i.e.* the Balgzand (a large tidal flat system in the western Wadden Sea), the growth of juveniles, both, 0, I and II groups, would be maximal and not food limited. Stomach content analysis of juvenile plaice by KUIPERS (1977) and de VLAS (1979a) revealed that important food items of juvenile plaice consisted of regenerating body parts of infaunal animals such as siphons of the tellinid *Macoma balthica* and tail tips of the lugworm *Arenicola marina*. At least at the tidal flats of the Balgzand this "grazing" by 0-group plaice would result in maximum possible growth, however, this is a relatively rich tidal flat area with macrozoobenthic biomass values of up to 16 $gC \cdot m^{-2}$ (BEUKEMA, 1976) and other parts of the Wadden Sea may be less productive.

This paper summarizes the first results of a study carried out in 1986 on abundance and growth of 0-group plaice at a number of other tidal flat systems in the western Wadden Sea, which at least differ with respect to the available amount of food for plaice: the macrobenthic infauna.

Acknowledgement.—Thanks are due to B. Bak, J.J. Beukema, W.J. Wolff and J.J. Zijlstra for critical reading of this manuscript.

* Publication no. 17 of the project Ecological Research of the North Sea and Wadden Sea (EON).

2. MATERIAL AND METHODS

The tidal flat systems selected for this study are located in the two main tidal basins of the western Wadden Sea, the Marsdiep and Vliestroom area (Fig. 1). These tidal flats were selected on the following criteria:

1. differences in bottom fauna abundance and composition (see BEUKEMA, 1976)
2. a regular distribution over the western Wadden Sea area, excluding exchange of individuals between the various sampling sites as much as possible
3. a sediment composition suitable for fishing with beam trawls, excluding extremely silty areas.

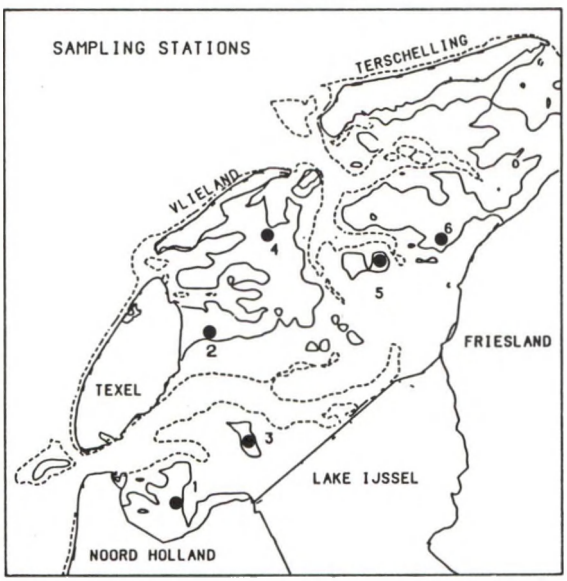

Fig. 1. Location of selected tidal flat systems in the western Wadden Sea. 1: Balgzand; 2: Wadden; 3: Lutjeswaard; 4: Vlielander wad; 5: Hendrik Tjaarsplaat; 6: Ballastplaat.

In this study also the Balgzand area is included to allow a comparison and link with published data about the Balgzand.

The selected tidal flats were visisted bimonthly throughout 1986. Fishing was done with a rubber dinghy and a 25 HP outboard motor for 3 hours around high water following KUIPERS (1977). The fishing gear consisted of a 2-m beam trawl with a 5x5 mm mesh size knotless nylon net. The distance of the hauls was registered by a meter-wheel fitted to the frame. At each location 2-3 hauls were made of at least 300 m. After sorting and measuring of the plaice in 5 mm size classes, numbers caught were corrected for net efficiency according to KUIPERS (1975) and converted into numbers per 1000 m^2. For each location the arithmetic mean abundance and mean length is presented.

In September 1986 a survey of the benthic infauna at all locations was carried out. Results of the meiofauna will be presented. Data on macrofaunal assemblage and sediment composition are not yet available. Instead, data from 1978 are used (BEUKEMA *et al.*, 1978).

3. RESULTS

3.1. ABUNDANCE

Fig. 2 shows the abundance of 0-group plaice at the various tidal flat areas through 1986. The tidal flats can be divided into two groups: one with low densities throughout the year: H. Tjaarsplaat, Wadden and Lutjeswaard; and another with high plaice densities: Vlielander wad, Balgzand and Ballastplaat.

Because of the differences in sampling dates, an index of year-class strenght had to be calculated, defined as the mean density in May after settlement has completed. This index has already been used previously (see ZIJLSTRA *et al.*, 1982; VAN DER VEER, 1986). The resulting indices for the various tidal flats are given in Table 1 and will reflect differences in abundance in the various areas even better than the data presented in Fig. 2.

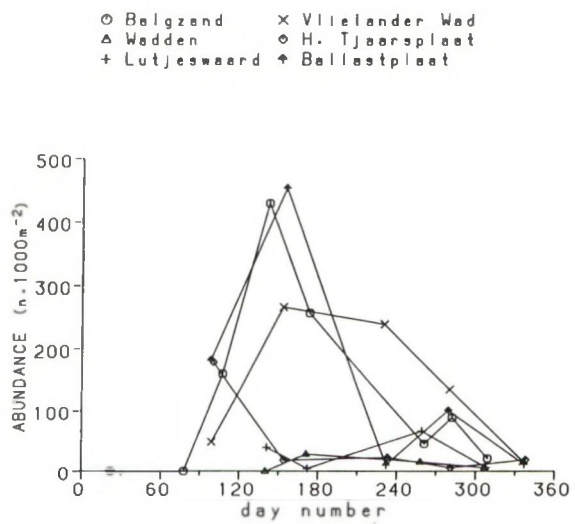

Fig. 2. Abundance of 0-group plaice ($n \cdot 1000m^{-2}$) at the various tidal flat areas in the western Wadden Sea in the course of 1986.

3.2. GROWTH

The mean length of 0-group plaice throughout 1986 is presented in Fig. 3. At the start of the growing season at June 1 when settlement of larvae has completed (VAN DER VEER, 1986), mean lengths differed between the tidal flats. Emigration of plaice to deeper

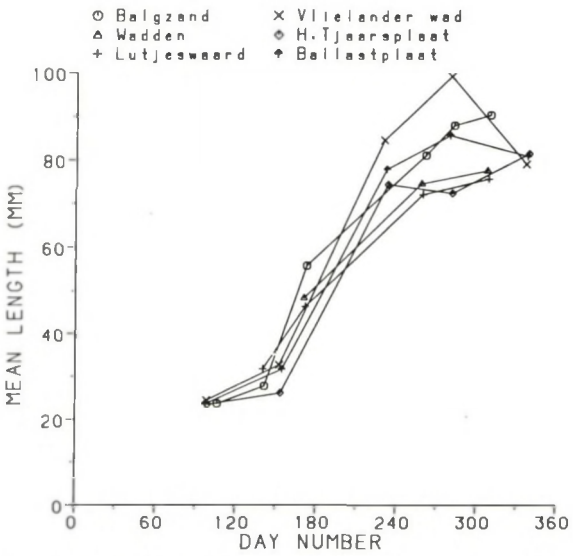

Fig. 3. Mean length of 0-group plaice (mm) at the various tidal flat areas in the western Wadden Sea in the course of 1986.

waters in autumn will depend on water temperature and does not start normally before the end of September. Therefore, the differences between mean length at day 270 (the end of September) and day 150 (June 1) has been taken as indication of the growth during the season. The values of all areas are given in Table 1. Again, two groups can be distinguished similar to the index of year-class strength.

At the tidal flats with low plaice densities (Wadden, Lutjeswaard and H. Tjaarsplaat), growth was lowest, between 39-44 mm. In the other areas (Balgzand, Ballastplaat and Vlielander wad) with high plaice densities, mean growth of plaice was stronger, up to 50-52 mm and even 62 mm at the Vlielander wad. These results suggest a positive relationship between density and growth. At tidal flats with higher densities plaice show a faster growth (Fig. 4; r_s = 0.77; $p < 0.10$). These variations will not be caused by possible differences in temperature regime over the year, because water temperatures at high water in the neighbourhood of the tidal flats showed a similar pattern (Fig. 5).

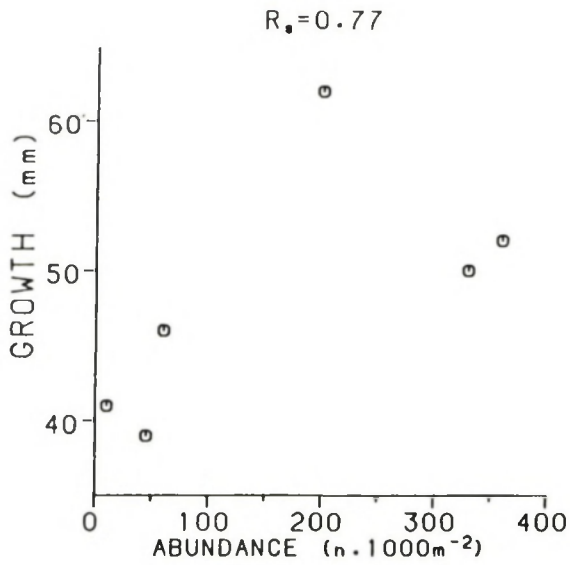

Fig 4. Relation between index of year-class strength of 0-group plaice (n·1000m^{-2}) and growth at a number of tidal flat areas in the western Wadden Sea in 1986.

3.3. FOOD ABUNDANCE

Macrobenthic surveys at the various tidal flats have been carried out by BEUKEMA *et al.* (1978) both in 1971/1972 and 1977. In Table 2 mean biomass values are presented for the two surveys. Although these surveys result in somewhat different total biomass values, these differences are rather small in comparison to differences between the areas. Lowest biomass was found at H. Tjaarsplaat (about 7 g as free dry weight.m^{-2}), while also Wadden and Lutjeswaard were rather poor (about 13 g AFDW.m^{-2}). High values were found at Ballastplaat, 34 g AFDW.m^{-2} and Balgzand 30 g

TABLE 1

Relation between year-class strength (n.1000 m^{-2}) of 0-group plaice in May, defined according to ZIJLSTRA *et al.*(1982) and growth (mm) during the season, based on mean length increase (mm) between June 1 and October 1. Between brackets resp. surface area fished and number of fishes measured.

	year-class index	*mean length at June 1*	*mean length at Oct. 1*	*growth*
Balgzand	330 (1100 m^2)	28 (483)	83 (97)	55
Wadden	10 (1250 m^2)	33 (17)	74 (15)	41
Lutjeswaard	45 (1550 m^2)	32 (48)	71 (62)	39
Vlielander wad	200 (950 m^2)	32 (215)	94 (67)	62
H. Tjaarsplaat	60 (850 m^2)	26 (497)	72 (15)	46
Ballastplaat	360 (1000 m^2)	32 (293)	84 (61)	52

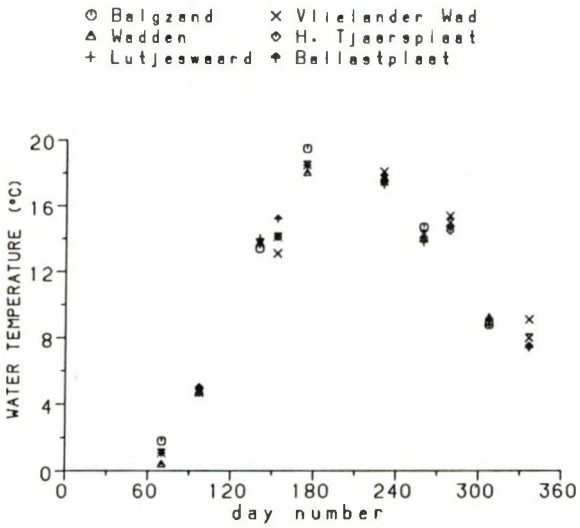

Fig. 5. Water temperature in the neighbourhood of the various tidal flat areas in the western Wadden Sea in the course of 1986.

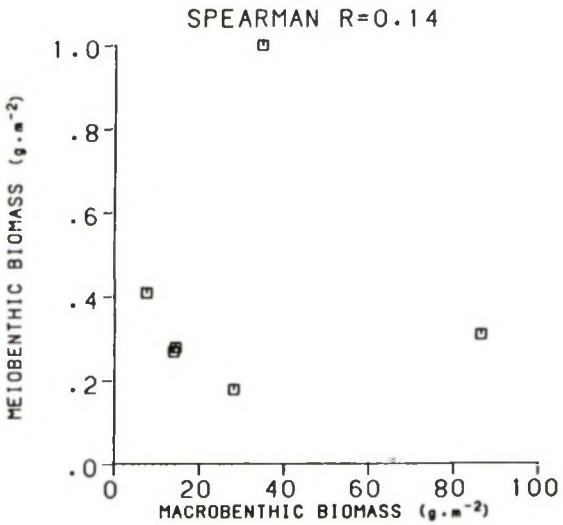

Fig. 6. Relation between macrobenthic biomass (g AFDW·m^{-2}) and meiobenthic biomass (g AFDW·m^{-2}) at the various tidal flat areas in the western Wadden Sea.

AFDW.m^{-2}, while Vlielander wad showed the highest biomass with on average 85 g AFDW.m^{-2}.

Meiobenthos has been less extensively surveyed. In September 1986 biomass values were at all tidal flats less than 1 g AFDW·m^{-2} (Table 3). Meiobenthic and macrobenthic biomass showed a different distribution pattern, and both groups were not related to each other (Fig. 6; r^s = 0.14; p > 10%).

TABLE 2

Mean biomass (g AFDW·m^{-2}) of macrobenthic infauna on the tidal flats in 1971/1972 and 1977 (according to BEUKEMA ET AL, 1978).

	Balgzand		*Wadden*		*Lutjes-waard*		*H. Tjaars-plaat*		*Vlielander wad*		*Ballast-plaat*	
	'71	'77	'71	'77	'71	'77	'71	'77	'72	'77	'71	'77
A. marina	6.10	14.50	1.31	0.82	3.66	0.04	1.53	0.00	36.23	10.43	8.30	11.92
N. hombergii	0.14	1.33	0.47	0.33	0.40	0.95	1.31	1.64	1.15	2.40	0.27	0.31
N. diversicolor	0.51	0.30	0.02				0.18		1.07	13.92	4.24	2.82
L. conchilega			0.04	0.16			0.53	5.35	5.13	41.49	0.22	
S. armiger	0.10	0.10	0.13	0.87	0.78	1.44	0.62	0.51	0.02		0.20	0.69
H. filiformis	0.38	1.56						0.02	0.38	0.02	2.09	4.82
Harmothoë spec		0.17		0.16						0.24	0.16	
Phyllodoce sp.	0.01	0.07		0.16						0.31	0.02	
E. longa	0.05	0.17									0.02	
Nerine spec					0.20	0.18			0.04	0.13		0.13
Pectiformis sp.										0.02		
Hydrobia ulvae				0.56							0.02	
M. balthica	4.10	3.66	0.27		0.16	0.51	1.98	0.71	3.26	3.86	13.88	11.34
E. edule		0.68	15.94	5.22		0.04	0.16		18.76	6.50	0.09	0.98
M. arenaria	11.05	11.45	0.73	0.07	7.66	3.73		0.07	6.39	11.63	1.75	4.82
T. tenuis								0.58				
T. fabula								0.09				
M. edulis					0.87	7.39				9.44	0.11	
total biomass												
g AFDW·m^{-2}	22.44	33.99	18.91	8.35	13.73	14.28	6.31	8.97	72.43	100.4	31.37	37.83
gC·m^{-2}	9.78	13.60	7.56	3.34	5.49	5.71	2.52	3.59	28.97	40.2	12.55	15.13

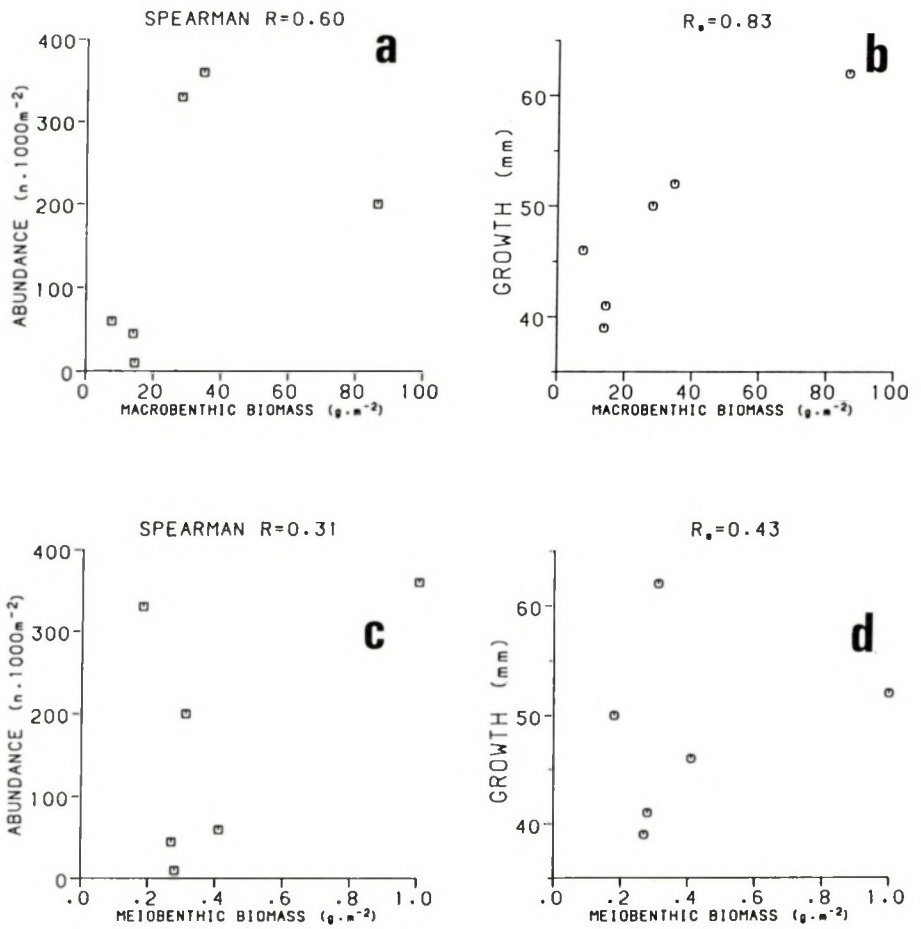

Fig. 7. Relations between abundance (n·1000m^{-2}) and growth (mm) of 0-group plaice and macro- and meiobenthic biomass (g AFDW·m^{-2}) at the various tidal flat areas in the western Wadden Sea. a: abundance of plaice and macrobenthic biomass; b: growth of plaice and macrobenthic biomass; c: abundance of plaice and meiobenthic biomass; d: growth of plaice and meiobenthic biomass.

TABLE 3

Mean biomass (g AFDW·m^{-2}) of meiobenthos on the tidal flats in September 1986 (pers. comm. van Dessel).

	biomass ($g \cdot m^{-2}$)
Balgzand	0.18
Wadden	0.28
Lutjeswaard	0.27
Vlielander wad	0.41
H. Tjaarsplaat	0.31
Ballastplaat	1.00

4. DISCUSSION

4.1. ABUNDANCE

About the larval immigration and the process of settling of plaice little is known (CREUTZBERG *et al.*, 1978; RIJNSDORP *et al.*, 1985). It is thought that larvae are transported passively by the tidal currents and enter the area during flood tide. At slack water the larvae sink down and during ebb tide they are either washed back or remain on the bottom (RIJNSDORP *et al.*, 1985). The key factor in the process of larval settling seems to be the search for food by the larvae. In an extensive study, CREUTZBERG *et al.* (1978) showed that under laboratory conditions hungry larvae always show a swimming behaviour and that demersal settling could only be induced by feeding of the larvae. This means that in the Wadden Sea, when

settling at slack tide in areas with suitable and enough food items, the larvae will stay and settle definitively. Otherwise, the hungry larvae are thought to enter the water column again during ebb tide and to be washed away. This mechanism will cause a concentration of settled plaice at suitable, rich areas and explains why settling plaice accumulate in areas with a high food supply. This is supported by the relation between macrobenthic biomass and abundance of plaice. However, due to the small amount of observations, the relation is not statistically significant (Fig. 7a; $r_s = 0.60$; $p > 0.10$).

4.2. GROWTH

The easiest way to compare growth of 0-group plaice at different tidal flats is to examine seasonal length increase. However, this requires that exchange between different populations is absent. Although absolute evidence cannot be obtained, all information suggests no or only minor movements of 0-group plaice at least until the end of the summer (see ZIJLSTRA *et al.*, 1982).

In relating growth with food abundance, only those food items should count that have been found in the stomachs of plaice. At present such detailed information is not available, so values for total biomass have been taken. Even then, growth of plaice appears to be positively related to the abundance of the macrobenthos (Fig. 7b; $r_s = 0.83$; $p < 0.05$) and shows a marked difference between the various locations. The meiobenthic food component may be less important, in view of the absence of a relationship between meiobenthic biomass and respectively abundance (Fig. 7c; $r_s = 0.31$; $p > 0.10$) and growth of plaice (Fig. 7d; $r_s = 0.43$; $p > 0.10$). Because of the higher production-biomass ratio, the production of the meiobenthos might be a more relevant estimate to compare with, but only the youngest stages of 0-group plaice, the just settled ones, will feed on it (PIHL, 1985). With increasing size of plaice, macrobenthic food items such as siphons of *Macoma balthica* and tail-tips of *Arenicola marina* become more important (KUIPERS, 1977; DE VLAS, 1979a).

As temperature conditions showed only minor differences between the various locations, the observed relation between available amount of food and growth rate of plaice suggests that food limitation of plaice occurs in parts of the Wadden Sea. In previous research, a comparison of growth in the laboratory under optimal food conditions with the field situation showed that in the Balgzand area growth of 0-group plaice would be optimal and only dependent on prevailing water temperature (ZIJLSTRA *et al.*, 1982 VAN DER VEER, 1986). The validity of the growth model has been demonstrated by ZIJLSTRA *et al.* (1982), who showed that also for plaice in some British bays growth differences between years could be fully explained by differences in water temperature. This means that growth at the Wadden, Lutjeswaard and H. Tjaarsplaat was limited by food. In this view, the growth rate at the Vlielander wad was too high and must be caused by an underestimation of the real water temperature.

Although in large parts of the Wadden Sea growth rates may be close to optimal and only regulated by temperature, the suggestion of RAUCK & ZIJLSTRA (1978) of a density-dependent growth in the nursery appears to be true for at least some parts of the area.

4.3 CONSQUENCES FOR THE NURSERY FUNCTION OF THE WADDEN SEA

In a previous paper VAN DER VEER & BERGMAN (1987b) presented the three main factors determining the actual use of the Wadden Sea as a nursery area:

1. Larval supply
2. Available amount of space and food
3. Suitable environmental conditions O_2 etc.)

The importance of larval supply is illustrated by the difference between the Marsdiep and Vliestroom tidal basin at the inlet as as been found in some years (RIJNSDORP *et al.*, 1985). Moreover, although food availability at Vlielander wad makes a much higher plaice population possible, actual densities are less than expected at least in 1986. This means that at the Vlielander wad larval supply was probably a limiting factor. The relation between amount of food available and abundance of 0-group plaice supports the view of CREUTZBERG *et al.* (1978) that the process of settling is determined by the search for food by the larvae: they accumulate in areas with a high food availability.

Once settled, the growth of plaice at the several locations also shows a relation to the available amount of food. This means that also predation pressure by plaice on the benthos will be related to the available amount of food. However, because the abundance of plaice shows also a relation to food abundance, the overall effect will be that predation pressure by plaice will show an exponential increase with food abundance instead of a linear one. Especially at high densities and high growth rates of plaice, this predation will affect the benthic prey populations, as has already been suggested in previous papers (DE VLAS, 1979a, b, 1985; KUIPERS *et al.*, 1986). However, the precise magnitude is unknown.

The consequence for the nursery function of the Wadden Sea is that the richer a tidal flat area is in terms of food, the more important the area will be as a nursery for plaice. In the past, especially these rich

areas have been the object of plans of embankment (Balgzand). This also means that in the future more attention should be paid especially to these rich areas, not only with respect to embankments but also with respect to the problems of euphrofication and cockle and mussel fisheries. Eutrophication of the area may have a positive effect on the amount of food available (BEUKEMA & CADÉE, 1986), but also a negative effect on the environmental conditions, causing especially low oxygen conditions (TIJSSEN & VAN BENNEKOM, 1976; VAN DER VEER & BERGMAN, 1986). Cockle and mussel seed fisheries on rich tidal flats will not only reduce the total amount of food available for 0-group plaice, but also destroy the remaining individuals (DE VLAS, 1987).

4.4. THE MODEL APPROACH

The results of this study stress the importance of the Wadden Sea as nursery area for plaice. At present a number of factors threaten this function: eutrophication, pollution, etc. However, possible effects of these threats are difficult to quantify. Not enough field information is available and such research is very time consuming and will last for years. Moreover, different factors may have antagonistic or synergistic effects.

An alternative approach might be to simulate these processes using a mathematical ecosystem model. For the Wadden Sea area such an ecosystem model has been made for the Ems-Dollard estuary, situated at the border of the Netherlands and Western Germany (BARETTA *et al.*, 1988). A few years ago it was decided to develop a similar ecosystem model for the westernmost part of the Wadden Sea. The structure of the biological aspects of this model should be identical to this Ems-Dollard model.

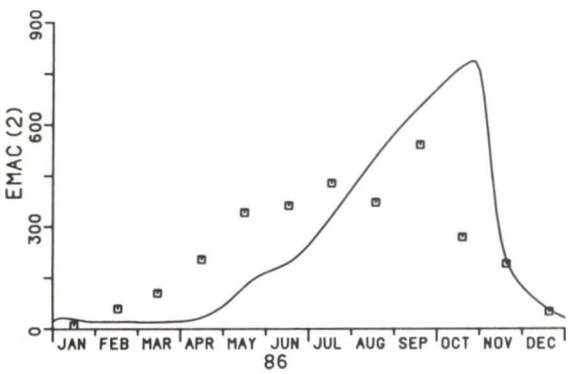

Fig. 8. Seasonal distribution of EMAC, the epibenthic predators (mgC·m^{-2}) in compartment 2; symbols refer to field data, line represents the results os simulation run.

In this ecosystem model 12 compartments are distinguished based on hydrographic and morphological differences. The model consists of four submodels: a transport model, a pelagic model, a benthic model and an epibenthic submodel. The transport model regulates the transport and exchange of the water masses with all dissolved components and the distribution of suspended matter together with sedimentation and resuspension between the compartments. The pelagic submodel describes the processes in the plankton and the sedimentation of detrital material to the benthic system. This benthic system is modelled in the benthic submodel, except for the epibenthic predators. The epibenthic submodel does not only describe the epibenthic predators, but also regulates the distribution of the predators over the compartments. Each compartments has two benthic and two epibenthic submodels, one to simulate the intertidal area and one to simulate the subtidal area. The model structure of the several submodels is identical in all compartments. Biological differences between compartments in simulation runs are only forced by different morphological and hydrographic conditions. All state variables and fluxes are expressed in carbon units, which means that for instance numerical responses of functional groups other than in changes of carbon are not modelled. At the end of the year the main results will be published. Already some parameter fitting, calibration and validation has taken place.

With this ecosystem model an attempt can be made to simulate and quantify the effects of various threats, for instance the effects of eutrophication on the Wadden Sea ecosystem and especially the growth conditions of predators. At present preliminary exercises are carried out to get insight in potential applications of the ecosystem model and especially to see what kind of requirements must be fulfilled before such "case-studies" can be carried our, if possible.

To give a brief impression of the present features of the model of the western Wadden Sea (EMOWAD), some results are presented for the epibenthic predators in the model and compared with field data for compartment no 2, the Balgzand area.

The epibenthic predators in the intertidal mainly consist of flatfishes (plaice and flounder) and crustaceans (shrimps and shore crabs). Their seasonal distribution is illustrated in Fig. 8. Some calibrations seems to be necessary to come to a good fit between the field situation and the results of the simulation run. More important than the biomass are the underlying fluxes. The predation pressure of the group on the various food items is the most important flux. In the field total predation is 6 gC·m^{-2}.y^{-1} (Table 4). Besides cannibalism (up to 20%) the main

TABLE 4

Epibenthic predators (EMAC) in compartment 2, a comparison of the field situation (Balgzand) with the results of the model simulation.

state variables ($mgC \cdot m^{-2} \cdot y^{-1}$)	*field*	*model*
EMAC	240	254
BBBM	5600	950
BSF	9000	4290
fluxes ($mgC \cdot m^{-2} \cdot y^{-1}$)		
total predation pressure of EMAC	6.1	7.1
on BBBM	3.0	1.3
on BSF	1.4	5.0
on meiofauna	0.4	0.1
cannibalism	1.1	0.3

food source for the epibenthic predators is the macrobenthos. Predation pressure on suspension feeders (BSF), *Mytilus edule*, *Cardium edule* and *Macoma balthica*, amounts to 1.4 $gC \cdot m^{-2} \cdot y^{-1}$ and on the other species (BBBM) some 3 $gC \cdot m^{-2} \cdot y^{-1}$. The model simulation results in roughly the same picture. Total predation is about the same as in the field. However, the share of the macrobenthic filterfeeders is too high and that of the deposit feeders too low. As a result the model simulates too low biomass values for suspension feeders: mean yearly values of 4 $gC \cdot m^{-2}$ compared with 9 $gC \cdot m^{-2}$ in the field. Nevertheless, the seasonal variation is rather well simulated (Fig. 9 and BEUKEMA, 1976).

Although at present the ecosystem model appears to be not ready for applications related with for instance the subject of this study, the preliminary results are hopeful and after a parameter check and validation of the model, the model approach might become a useful tool.

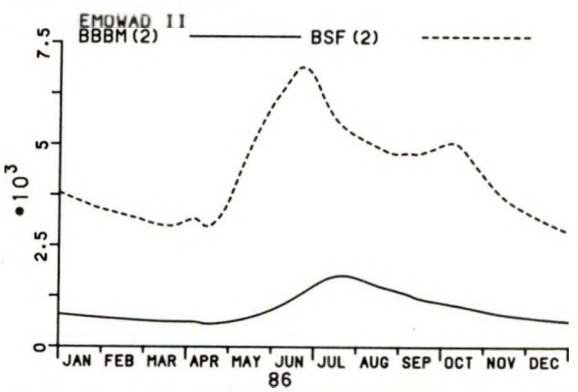

Fig. 9. Seasonal variation in macrobenthos in compartment 2 as simulated by the ecosystem model. BSF = suspension feeders; BBBM = deposit feeders ($mgC \cdot m^{-2}$).

5. REFERENCES

ANONYMOUS, 1985. Report of the 0-group North Sea Flatfish Working Group, IJmuiden 21-25 November 1983.—Coun. Meet. int. Coun. Explor. Sea C.M.-ICES/G:2.

BARETTA, J.W. & P. RUARDIJ, 1988. Tidal Flat Estuaries. Simulation and analysis of the Ems estuary.—Ecological Studies, Vol. 71. Springer-Verlag, Berlin: 1-353.

BERGHAHN, R., 1984. Zeitliche und räumliche Koexistenz ausgewählter Fisch- und Krebsarten im Wattenmeer unter Berücksichtigung von Räuber-Beute-Beziehungen und Nahrungskonkurrenz. Dissertation Universität Hamburg: 220 pp.

BEUKEMA, J.J., 1974. Biomass and species richness of macrobenthic animals living on the tidal flats of the Dutch Wadden Sea.—Neth. J. Sea Res. 10: 236-261.

BEUKEMA, J.J., W. DE BRUIN & J.J.M. JANSEN, 1978. Biomass and species richness of the macrobenthic animals living on the tidal flats of the Dutch Wadden Sea: long-term changes during a period with mild winters.—Neth. J. Sea Res. 12: 58-77.

BEUKEMA, J.J. & G.C. CADÉE, 1986. Zoobenthos responses to eutrophication of the Dutch Wadden Sea.—Ophelia 26: 55-64.

CREUTZBERG, F., A.TH.G.W. ELTINK & G.J. VAN NOORT, 1978. The migration of plaice larvae *Pleuronectes platessa* into the western Wadden Sea. In: MCLUSKY, D.S. & BERRY, A.J. (ed). Physiology and behaviour of marine organisms, Proceedings 12th European Marine Biological Symposium, Pergamon Press, New York: 243-252.

EDWARDS, R. & J.H. STEELE, 1968. The ecology of 0-group plaice and common dab at Loch Ewe. I. Population and food.—J. exp. mar. Biol. Ecol. 2: 215-238.

KUIPERS, B.R., 1975. On the efficiency of a two-meter beam trawl in juvenile plaice (*Pleuronectes platessa*).—Neth. J. Sea Res. 9: 69-85.

——, 1977. On the ecology of juvenile plaice on a tidal flat in the Wadden Sea.—Neth. J. Sea Res. 11: 59-91.

——, 1978. Opname en gebruik van voedsel door de jonge schol (Pleuronectes platessa L) in een getijdengebied. Thesis Universiteit van Amsterdam.

KUIPERS, B.R., H.W. VAN DER VEER & J.J. ZIJLSTRA, 1986. Interaction between juvenile plaice (*Pleuronectes platessa*) and benthos in a tidal flat area.—Coun. Meet. int. Coun. Explor. Sea C.M.-ICES/L: 3: 8 pp.

KUIPERS, B.R., P.A.W.J. DE WILDE & F. CREUTZBERG, 1981. Energy flow in a tidal flat ecosystem.—Mar. Ecol. Progr. Ser. 5: 215-221.

PIHL, L., 1985. Food selection and consumption of mobile epibenthic fauna in shallow marine waters.—Mar. Ecol. Progr. Ser. 22: 169-179.

RAUCK, G. & J.J. ZIJLSTRA, 1978. On the nursery aspects of the Wadden Sea for some commercial fish species and possible long-term changes.—Rapp. P.-v. Réun. Cons. perm. int. Explor. Mer 172: 226-275.

RIJNSDORP, A.D., M. VAN, STRALEN & H.W. VAN DER VEER, 1985. Selective tidal transport of North Sea plaice *Pleuronectes platessa* in coastal nursery areas.—Trans. Am. Fish. Soc. 114: 461- 470.

TIJSSEN, S.B. & A.J. VAN BENNEKOM, 1976. Lage zuurstofgehaltes in het water op het Balgzand. H_2O 9: 28-31.

VEER, H.W. VAN DER, 1986. Regulation of the population of 0-group plaice (*Pleuronectes platessa* L.) in the Wadden Sea. Thesis Rijksuniversiteit Groningen: 91 pp.

VEER, H.W. VAN DER & M.J.N. BERGMAN, 1986. Development of tidally related behaviour of a newly-settled 0-group plaice (*Pleuronectes platessa* L.) population in the western Wadden Sea.—Mar. Ecol. Progr. Ser. 31: 121-129.

——, 1987a. Predation by crustaceans on a newly-settled 0-group plaice (*Pleuronectes platessa* L.) population in the western Wadden Sea.—Mar. Ecol. Progr. Ser. 35: 203-215.

——, 1987b. The nursery function of the western Wadden sea. Proc. 5th Intern. Wadden Sea Symp. Esbjerg September 29-October 3 1986. In: TOUGAARD, S. & S. ASBIRK (eds.).—Fiskeri-og SØFORTMUSEET, SOLTVANDSAKVARIETS. BIOL. MEDD. 31: 123-145.

VLAS, J. DE, 1979a. Annual food intake by plaice and flounder in a tidal flat area in the Dutch Wadden Sea, with special reference to consumption of regenerating parts of macrobenthic prey.—Neth. J. Sea Res. 13: 117-153.

——, 1979b. Secondary production by tail regeneration in a tidal flat population of lugworms (*Arenicola marina*) cropped by flatfish.—Neth. J. Sea Res. 13: 362-393.

——, 1985. Secondary production by siphon regeneration in a tidal flat population of *Macoma balthica*.—Neth. J. Sea Res. 19: 147-164.

——, 1987. Effects of cockle fisheries on the macrobenthos in the Wadden Sea. Proc. 5th Intern. Wadden Sea Symp. Esbjerg September 29-October 3 1986. In: TOUGAARD, S. & S. ASBIRK (eds.).—Fiskeri- og SØFORTMUSEET, SOLTVANDSAKVARIETS. BIOL. MEDD. 31: 215-227.

ZIJLSTRA, J.J., 1972. On the importance of the Waddensea as a nursery area in relation to the conservation of the southern North Sea fishery resources.—Symp. zool. Soc. Lond. 29: 233-258.

ZIJLSTRA, J.J., R. DAPPER & J.IJ. WITTE, 1982. Settlement, growth and mortality of post-larval plaice (*Pleuronectes platessa* L.) in the western Wadden Sea.—Neth. J. Sea Res. 15: 250-272.

MEIOBENTHOS IN THE WESTERN PART OF THE DUTCH WADDEN SEA

BOPP VAN DESSEL

Netherlands Institute for Sea Research, P.O. Box 59, 1790 AB Den Burg Texel, The Netherlands.

ABSTRACT

In this study an inventory is presented of the meiofauna of the Marsdiep and Vlie basins in the western part of the Dutch Wadden Sea. At four permanent stations the seasonal distribution was examined and at 41 stations which were sampled only once the spatial distribution was examined. No clear seasonal pattern in biomass could be found. In the Vlie basin meiobenthic biomass was higher than in the Marsdiep basin. In the Vlie basin a negative correlation was found between meiofauna biomass and tidal depth. In the Marsdiep area the abundance of meiobenthos was similar in tidal, subtidal and deep water bottoms. The annual mean meiobenthic biomass on the tidal flats in the western Wadden Sea was 0.73 g DW·m^{-2} and in the subtidal and deep water zones 0.37 and 0.30 g DW·m^{-2} respectively.

1. INTRODUCTION

This study is part of the "Ecological Research Project North Sea and Wadden Sea" (EON, 1988). To check the outcome of model simulations on abundance and distribution of the meiofauna, information on the situation in the western Wadden Sea was needed.

Worldwide, several articles have been published on distribution (WARWICK, 1971, 1984; ELMGREN, 1976; GRAY, 1976), behaviour (BOUWMAN, 1978, 1981, 1983; WARWICK, 1981) and ecology (MCINTYRE, 1969 WARWICK, 1981; HEIP *et al.*, 1984, 1985) of the meiofauna in marine sediments, but observations on the benthic meiofauna in the western part of the Dutch Wadden Sea are restricted to the Balgzand tidal area (WITTE & ZIJLSTRA, 1984). In that paper the abundance and distribution of the most important meiobenthic groups in the western Wadden Sea were reported and their ecological importance was roughly estimated.

To study the seasonal distribution of these dominant meiobenthic groups samples were taken several times during the year at four stations representing different types of tidal flats. Also, one survey was made with sampling at a large number of stations throughout the western Wadden Sea to study the spatial distribution. Observations on the occurrence of meiobenthos in the sediment at different water depths were made and the abundance of meiofauna in relation to water depth was investigated.

2. MATERIAL AND METHODS

2.1 AREA OF STUDY

The western Wadden Sea is bounded by the islands of Texel, Vlieland and Terschelling, the watershed of Terschelling and the mainland (Fig. 1). It is an estuary consisting of tidal flats (32%), subtidal bottoms (53%) and gullies up to 23 meters deep (15%). Two main tidal basins connected by tidal channels are distinguished: the Marsdiep basin in the southwest and the Vlie basin in the northeast. Tidal range varies from 1.35 m at Den Helder to 1.85 m in the southeastern part (BEUKEMA, 1976). Salinity ranges from 32 ‰ between Vlieland and Terschelling to incidentically 14‰ at the outlets of Lake IJssel (ZIMMERMAN, 1976). The sediments have a predominantly sandy composition. Only along the mainland coast can silty parts be found (DE GLOPPER, 1967; MANUELS & ROMMETS, 1973).

2.2. SAMPLING

All cores were taken with a perspex tube (24 mm diameter, 10 cm deep). To estimate the representativity of the sampling, the results were compared of 10 samples of 3 cores (= 13,5 cm^2) and 10 samples of 6 cores (= 27 cm^2) taken at the same station. The numbers of nematodes counted in the samples ranged from $\bar{x} \pm$ 15% (6 cores) to $\bar{x} \pm$ 25% (3 cores). Nematode individual weights ranged from $\bar{x} \pm$ 22% (6 cores) to $\bar{x} \pm$ 28% (3 cores). Less abundant groups gave a much poorer confidence.

The seasonal fluctuations were studied at four permanent stations. At these stations six samples were collected, approximately 100 m apart. Each sample consisted of six cores. The samples were taken on 4 or 5 (depending on the station) different dates, during emergence of the tidal flat (Table 1).

All samples were preserved in a heated 4% formaline seawater solution (WITTE & ZIJLSTRA, 1984) and elutriated (UHLIG *et al.*, 1973). After elutriation no meiofauna was recovered in the separation funnel. The elutriated samples were stored in a 4% formaline seawater solution with rose bengal for several days. A subsample of 5% of the total volume of each

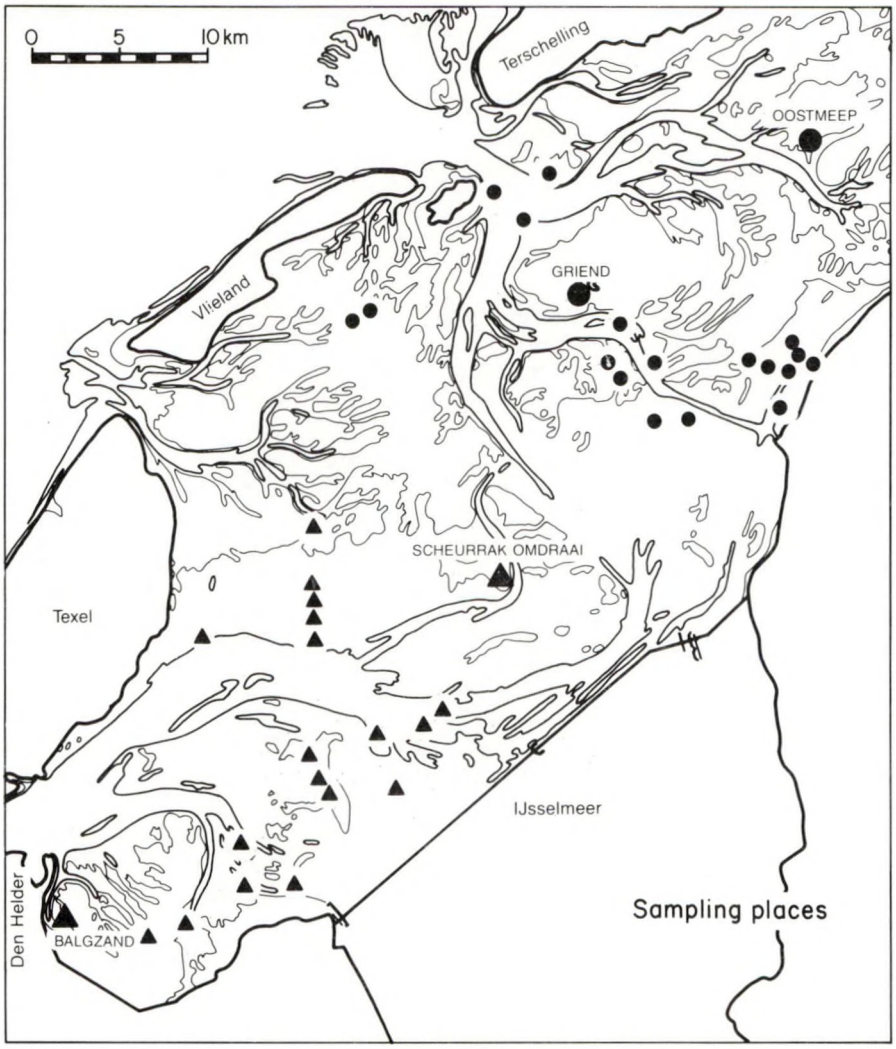

Fig. 1. Dutch western Wadden Sea with the sampling stations: Vlie basin: regularly visited (●), occasionally visited (•) Marsdiep basin: regularly visited (▲), occasionally visited (▲).

TABLE 1

Day and month of sampling at the four permanent stations

Station	*Sampling data 1986*				
Scheurrak-Omdraai	24/3	—	17/6	5/8	11/11
Griend	25/3	22/5	18/6	6/8	12/11
Oostmeep	26/3	21/5	29/6	7/8	13/11
Balgzand	9/4	—	12/6	19/8	19/11

sample was examined for meiofauna, using a dissection microscope (16x). Length and diameter of the nematodes was measured at a magnification of 40 times.

Only nematodes, annelids and harpacticoids were sorted out. Other taxonomic groups suffered substantial damage or loss of individuals by the elutriation, so these could not be counted adequately. The biomass of the nematodes was calculated by means of the formula of ANDRASSY (1956):

$$\text{dry weight(g)} = \frac{.25\ (\text{length (cm)} \times \text{width}^2\ \text{(cm)}) \times 1.13}{1.7}$$

For the other groups an average biomass value derived from the literature was assumed: 2.0 μg DW per harpacticoid and 1.55 μg DW per annelid (WITTE & ZIJLSTRA, 1984). For each station arithmetic means of numbers and biomass were calculated.

In October 1986 a survey was made in the western Wadden Sea, visiting 41 transects in a depth range from 0.5 above to 16.0 meter under MLT. All samples were taken with a boxcorer. On each transect sta-

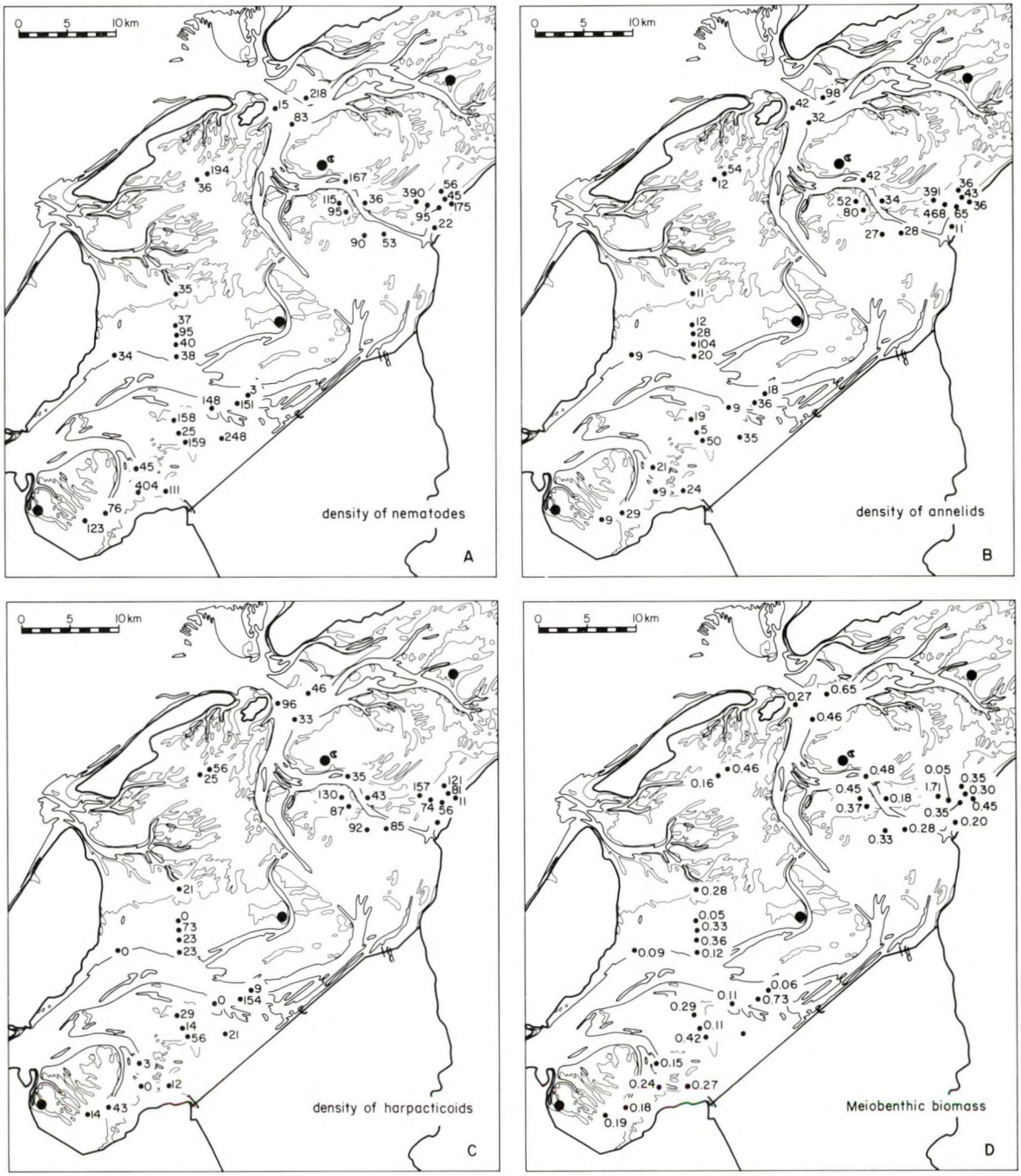

Fig. 2. The distribution of (A) nematodes ($n \cdot 10^4 \cdot m^{-2}$), (B) annelids ($n \cdot 10^2 \cdot m^{-2}$), (C) harpacticoids ($n \cdot 10^2 \cdot m^{-2}$) and (D) meiobenthos biomass (g $DW \cdot m^{-2}$) over the western Wadden Sea.

TABLE 2

Average October values for density and biomass of nematodes, annelids and harpacticoids at 45 stations in the western Wadden Sea. A separation of the stations is made by depth in tidal (above MLT), subtidal (MLT– –4m) and deeper (beneath –4 m MLT) stations.

Depth	*Group*	*Density* ($n \cdot 10^3 \cdot m^{-2}$)	*%*	*Biomass* ($g\ DW \cdot m^{-2}$)	*%*
Tidal	Nematodes	1635	89.9	0.30	49.2
	Annelids	106	5.8	0.16	26.2
	Harpacticoids	77	4.3	0.15	24.6
	TOTAL	1818		0.61	
Subtidal	Nematodes	1169	93.1	0.16	51.6
	Annelids	31	2.5	0.05	16.1
	Harpacticoids	56	4.5	0.10	32.2
	TOTAL	1256		0.31	
Deeper water sediment	Nematodes	774	91.5	0.12	48.0
	Annelids	26	3.1	0.04	16.0
	Harpacticoids	46	5.4	0.09	36.0
	TOTAL	846		0.25	

tions were sampled (consisting of 5 cores each, which were put together). The distance between the stations was 200 m. Per transect arithmetic means were calculated.

3. RESULTS AND DISCUSSION

The aim of this study was to gather quantitative information on meiofauna in the Dutch western Wadden Sea. In a short period an extended area had to be surveyed, so an easy separation technique was chosen. Such a separation technique (elutriation) and the sorting out of only the major taxonomic groups allows a quick processing of many samples. As a consequence the information on ecological diversity is restricted. Rare species were overlooked. Soft bodied taxa (*e.g.* Turbellaria) do not sustain the elutriation very well and cannot be studied properly by this method (McIntyre, 1969; Martens & Schockaert, 1986). Occasionally these taxa were found in the samples. In addition other meiofauna (ostracods), macrofauna (juvenile molluscs) and protozoan groups (foraminiferes, ciliates) were found, but only in small numbers. Therefore they were negligible in biomass and omitted in the measurements.

The 3 most important taxonomical groups of meiofauna in the western Wadden Sea are nematodes, annelids and harpacticoids. The distribution of these groups is shown in Fig. 2. The spatial distribution of the meiobenthos in the western part of the Wadden Sea is characterized by 2 features: the difference between tidal (+1.00 — 0.00 MLW), subtidal (MLW — –4.00 MLW) and deeper water regions (–4.00 — –20.00 MLW) (Table 2) and the differences between the western (Marsdiep) and eastern (Vliestroom) part (Table 3). Overall, meiofauna is most abundant in the tidal zone, but in the subtidal and deeper water sediments considerable amounts of meiofauna are present as well: respectively 50-100% and 30-100% of the meiofaunal biomass found in the tidal zone. This phenomenon is in agreement with other studies where meiobenthos was found down to several thousand of metres depth (McIntyre, 1969; Heip *et al.*, 1985).

TABLE 3

Mean biomass values of meiobenthos in October 1986 for the Marsdiep basin and Vlie basin ($g\ DW \cdot m^{-2}$).

	Tidal	*Subtidal*	*Deeper water*
Marsdiep basin	0.29	0.28	0.30
Vlie basin	0.85	0.42	0.31

Differences in meiobenthos biomass between tidal, subtidal and deeper water sediments (Table 3) are pronounced in the Vlie basin. In the Marsdiep basin biomass is lower, but the values are equal for the different depth zones. The higher values in the Vlie basin could be a matter of food supply, as organic matter and bacteria are present in higher quantities as well (van Duyl, 1988). Another possible explanation is a different species composition in the Marsdiep and Vliestroom area. This is, however, not investigated in this study.

At all depths in both basins the group of nematodes is the most dominant, contributing up to

90% of the meiobenthos numbers and 50% of the total meiobenthic biomass.

The individual weight of nematodes is variable, depending on time of the year, location and species composition (McIntyre, 1969; Heip *et al.*, 1984, 1985). It ranges at the four permanent stations from 0.1 to 0.3 μg DW·individual^{-1} (Fig. 3d). The annual average, 0.19 μg DW·nematode^{-1} for the four stations is low in comparison with Witte & Zijlstra (1984) (0.28 μg DW), but similar to other literature data, for instance Gray (1976) (0.25 μg DW) and Warwick (1971) (0.17 μg DW).

Based on the results of the repeated sampling at the four permanent stations, the seasonal variation was determined of the density of nematodes, annelids and harpacticoids, of the individual weights of nematodes and of nematode- and total meiobenthic biomass (Fig. 3a-f).

There is no clear seasonal pattern in the numbers of nematodes, annelids and harpacticoids. Nematode densities tend to be more abundant in summer, with lowest values in winter. That a seasonal variation in abundance of nematodes is seldom observed (McIntyre, 1969; Witte & Zijlstra, 1984) can probably be explained by the high number of species in this group. Because the interspecific variation of nematodes in size, lifetime and lifecycle, and in optimal environmental circumstances are large, the group of nematodes is a very heterogeneous one (McIntyre, 1969; Heip *et al.*, 1984, 1985).

Annelids more often show a seasonal pattern (Bouwman, 1978, 1981, 1983; Witte & Zijlstra, 1984), caused by juvenile polychaetes and oligochaetes contributing temporarily to the meiobenthos, when their size is between 50 and 1000 μm. In this study highest annelid numbers are found in summer.

The density of harpacticoids is much lower than the density of nematodes or annelids. The seasonal variation in harpacticoid numbers for the four stations show little parallelism. No evident seasonal differences are found, except for the very low values in April and May.

Comparing the results of Balgzand 1986 (this study) with the situation on Balgzand 1976 (Witte & Zijlstra, 1984) shows that the density of nematodes is about the same. But the individual weight is much lower, so that the total biomass of nematodes is about 50% less (Table 4). In 1986 more harpacticoids were found and fewer annelids. The total biomass in 1986 is 40% lower than in 1976. This can be a matter of different sampling locations or a consequence of the severe winters of 1984-1985 and 1985-1986. Some meiobenthic groups (nematodes, harpacticoids) are sensitive to frost and ice. The time needed for recovery may be up to 1.5 years (McIntyre, 1969). This period is marked by the predominance of small specimens. Incidental measurements in early spring 1987, after another very cold winter, tended to result in even lower biomass values on Balgzand (0.49 g DW·m^{-2}). Balgzand turned out to be the poorest of all four permanent stations: fewest and smallest nematodes, fewest annelids and the lowest total biomass.

Annual means for the western Wadden Sea were calculated of the densities and biomasses of the 3 taxonomical groups, based on the data of the four permanent stations (Table 5). The mean annual meiobenthic biomass was 1.16 g DW·m^{-2}. This is 1.2 times the biomass at these four stations in October. For this month also an average biomass can be calculated based on all 45 sampling stations: 0.61 g DW·m^{-2}. If this value is multiplied by 1.2, a mean annual biomass for the western Wadden Sea of 0.73 g DW·m^{-2} is derived.

TABLE 4

Average densities and biomass of nematodes, annelids and harpacticoids on Balgzand in 1976 (Witte & Zijlstra, 1984) and 1986 (this study).

Group	Density ($n \cdot 10^3 \cdot m^{-2}$)	%	Biomass (g DW·m^{-2})	%
Balgzand 1976				
Nematodes	2127	86.7	0.60	53.1
Annelids	230	9.4	0.35	31.0
Harpacticoids	56	2.3	0.10	8.8
Other groups	41	1.7	0.08	7.1
TOTAL	2454		1.13	
Balgzand 1986				
Nematodes	1878	90.5	0.30	45.5
Annelids	103	5.0	0.16	24.2
Harpacticoids	95	4.6	0.20	30.3
TOTAL	2076		0.66	

TABLE 5

Average density and biomass of nematodes, annelids and harpacticoids at the four permanent stations.

Group	Density ($n \cdot 10^3 \cdot m^{-2}$)	%	Biomass (g DW·m^{-2})	%
Nematodes	3037	89.8	0.57	49.1
Annelids	236	7.0	0.37	31.9
Harpacticoids	110	3.3	0.22	19.0
TOTAL	3383		1.16	

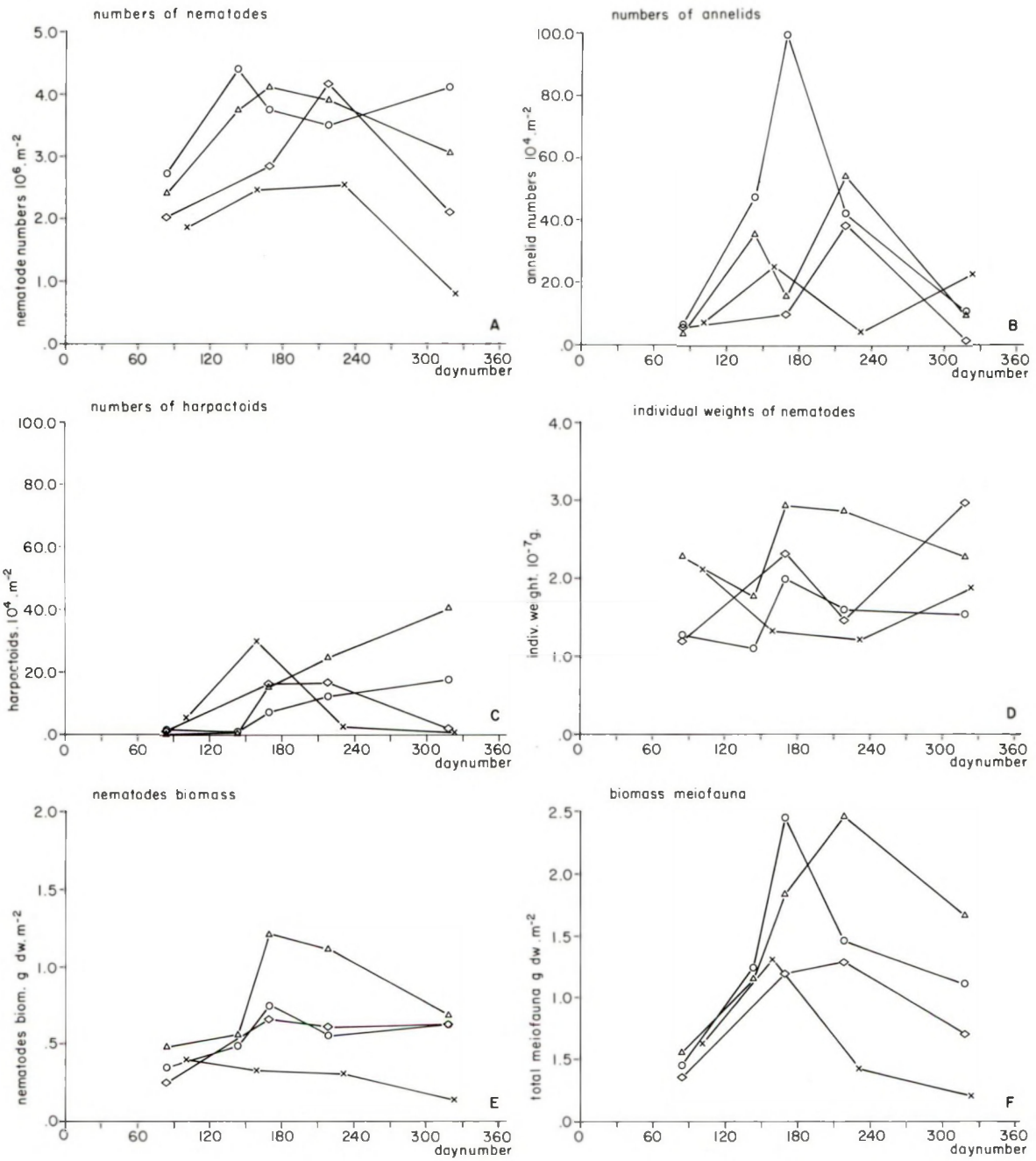

Fig. 3. Seasonal variations in the numbers of (A) nematodes ($n \cdot 10^6 \cdot m^{-2}$), (B) annelids ($n \cdot 10^4 \cdot m^{-2}$), (C) harpacticoids ($n \cdot 10^4 \cdot m^{-2}$) at four stations in the western Wadden Sea. Also the individual nematode weight (D) in 10^{-7}g, the total nematode biomass (E) in g $DW \cdot m^{-2}$ and total meiobenthic biomass (F) in g $DW \cdot m^{-2}$ are given.
Stations: Scheurrak Omdraai (◇), Griend (△), Oostmeep (o),Balgzand (x).

The role of the meiobenthos in the benthic system is manifold. Nematodes for instance absorb dissolved organic compounds, consume unicellular organisms, regenerate nutrients, excrete mucus, improve gas diffusion and serve as food for other organisms, including predators belonging to their own taxon (BOUWMAN, 1983). DE WILDE & BEUKEMA (1984) have estimated their role in the benthic system quantitatively. They calculated that meiobenthos consumes only 5% of the total imput of carbon to the benthic system. This estimate was based on the biomass values found at the Balgzand in 1976. The present study shows that the share of the meiobenthos is probably 3-4% of the total benthic consumption. So meiobenthos plays only a minor role in consumption and mineralisation, compared to macrobenthos, microbenthos and bacteria.

4. LITERATURE

ANDRASSY, I., 1956. Die Rauminhalts- und Gewichtsbestimmung der Fadenwürmer (Nematoden).—Acta. Zool. Hung. **11:** 1-5.

BEUKEMA, J.J., 1976. Biomass and species richness of the macrobenthic animals living on the tidal flats of the Dutch Wadden Sea.—Neth. J Sea Res. **10:** 236-261.

BOUWMAN, 1978. Investigations on nematodes in the Ems-Dollard estuary.—Annls. Soc. Zool. Belg. **108:**.103-105.

——, 1981. A survey of nematodes from the Ems estuary. Part 1 Systematics.—Zool. JB (syst) **108:** 335-385.

——, 1983. Systematics, ecology and feeding biology of estuarine nematodes.—BOEDE Publ. en Versl. **3:** 173 pp.

DUYL, F.C. VAN & A.J. KOP, 1988. Temporal and lateral fluctuations in production and biomass of bacterioplankton in the western Dutch Wadden Sea.—Neth. J. Sea Res. **22:** 51-68.

ELMGREN, R., 1976. Baltic benthos communities and the role of the meiofauna.—Cortr. Askö. Lab. Univ. Stockholm **14:** 1-31.

EON, 1988. Ecosysteemmodel van de westelijke Waddenzee.—NIOZ rapport **1988-1:** 1-88.

GLOPPER, R.J. DE, 1967. Over de bodemgesteldheid van het waddengebied.—Van Zee tot Land **43:** 1-67.

GRAY, J.S., 1976. The fauna of the polluted river Tees estuary.—Estuar. Coast. Mar. Sci. **4:** 65-76.

HEIP, C., R. HERMAN & M. VINK, 1984. Variability and productivity of meiobenthos in the Southern Bight of the North Sea.—Rapp. P.-v. Réun. Cons. perm. int. Explor. Mer **183:** 51-56.

HEIP, C., M. VINK & G. VRANKEN, 1985. The ecology of marine nematodes.—Oceanogr. Mar. Biol. Ann. Rev. **23:** 399- 489.

MANUELS, M.V. & J.W. ROMMETS, 1973. Metingen van zoutgehalte, temperatuur, zwevend materiaal in de Waddenzee, april 1970-oktober 1972.—NIOZ intern rapport 1973-6.

MARTENS, P.M. & E.R. SCHOKAERT, 1986. The importance of turbellarians in the marine meiobenthos, a review.— Hydrobiologica **132:** 295-303.

MCINTYRE, A.D., 1969. Ecology of marine meiobenthos.—Biol. Rev. **44:** 245-290.

UHLIG, G., H. THIEL & J.S. GRAY, 1973. The quantitative separation of meiofauna.—Helgol. wiss. Meeresunters. **25:** 173-195.

WARWICK, R.M., 1971. Nematode associations in the Exe estuary.— J. mar. biol. Ass. UK **51:** 439-454.

——, 1981. Survival strategies of meiofauna. In: N.V. JONES & W.J. WOLFF . Feeding and survival strategies of estuarine organisms.—Plenum New York: 39-52.

——, 1984. Species size distribution in marine benthic communities.—Oecologia **6:** 176-190.

WILDE, P.A.W.J. DE & J.J. BEUKEMA, 1984. The role of the zoobenthos in the consumption of organic matter in the Dutch Wadden Sea.—Neth. Inst. Sea Res.—Publ. Ser. **10-1984:** 145- 158.

WITTE, J.Y. & J.J. ZIJLSTRA, 1984. The meiofauna of a tidal flat in the western part of the Wadden Sea and its role in the benthic ecosystem.—Mar. Ecol. Progr. Ser. **14:** 129-138.

ZIMMERMAN, J.T.F., 1976. Mixing and flushing of tidal embayments in the Western Dutch Wadden Sea, Part 1.—Neth. J. Sea Res. **10:** 149-191.

ERRATA

-The first three lines of the contents have to be replaced by:

H.J. Lindeboom. Preface
H.J. Lindeboom, W. van Raaphorst, H. Ridderinkhof & H.W. van der Veer. Ecosystem of the western Wadden Sea, a summary.....II-XII

-The page numbers of the paper by Bergman et al., in the contents, have to be: 123-131.

CONTENTS

Printed by ARTIGRAFICA Den Helder